



UNIVERSITAT DE
BARCELONA

Correction of point mutations at the endogenous *locus* of the mammalian *dihydrofolate reductase* gene using polypurine reverse hoogsteen hairpins

Anna Solé Ferré

ADVERTIMENT. La consulta d'aquesta tesi queda condicionada a l'acceptació de les següents condicions d'ús: La difusió d'aquesta tesi per mitjà del servei TDX (www.tdx.cat) i a través del Dipòsit Digital de la UB (diposit.ub.edu) ha estat autoritzada pels titulars dels drets de propietat intel·lectual únicament per a usos privats emmarcats en activitats d'investigació i docència. No s'autoritza la seva reproducció amb finalitats de lucre ni la seva difusió i posada a disposició des d'un lloc aliè al servei TDX ni al Dipòsit Digital de la UB. No s'autoritza la presentació del seu contingut en una finestra o marc aliè a TDX o al Dipòsit Digital de la UB (framing). Aquesta reserva de drets afecta tant al resum de presentació de la tesi com als seus continguts. En la utilització o cita de parts de la tesi és obligat indicar el nom de la persona autora.

ADVERTENCIA. La consulta de esta tesis queda condicionada a la aceptación de las siguientes condiciones de uso: La difusión de esta tesis por medio del servicio TDR (www.tdx.cat) y a través del Repositorio Digital de la UB (diposit.ub.edu) ha sido autorizada por los titulares de los derechos de propiedad intelectual únicamente para usos privados enmarcados en actividades de investigación y docencia. No se autoriza su reproducción con finalidades de lucro ni su difusión y puesta a disposición desde un sitio ajeno al servicio TDR o al Repositorio Digital de la UB. No se autoriza la presentación de su contenido en una ventana o marco ajeno a TDR o al Repositorio Digital de la UB (framing). Esta reserva de derechos afecta tanto al resumen de presentación de la tesis como a sus contenidos. En la utilización o cita de partes de la tesis es obligado indicar el nombre de la persona autora.

WARNING. On having consulted this thesis you're accepting the following use conditions: Spreading this thesis by the TDX (www.tdx.cat) service and by the UB Digital Repository (diposit.ub.edu) has been authorized by the titular of the intellectual property rights only for private uses placed in investigation and teaching activities. Reproduction with lucrative aims is not authorized nor its spreading and availability from a site foreign to the TDX service or to the UB Digital Repository. Introducing its content in a window or frame foreign to the TDX service or to the UB Digital Repository is not authorized (framing). Those rights affect to the presentation summary of the thesis as well as to its contents. In the using or citation of parts of the thesis it's obliged to indicate the name of the author.



UNIVERSITAT DE
BARCELONA

FACULTAT DE FARMÀCIA

DEPARTAMENT DE BIOQUÍMICA I BIOLOGIA MOLECULAR

Programa de doctorat en Biotecnologia

**CORRECTION OF POINT MUTATIONS AT THE ENDOGENOUS *LOCUS* OF THE
MAMMALIAN *DIHYDROFOLATE REDUCTASE* GENE USING POLYPURINE
REVERSE HOOGSTEEN HAIRPINS**

ANNA SOLÉ FERRÉ

Barcelona, 2015



UNIVERSITAT DE
BARCELONA

FACULTAT DE FARMÀCIA

DEPARTAMENT DE BIOQUÍMICA I BIOLOGIA MOLECULAR

Programa de doctorat en Biotecnologia

**CORRECTION OF POINT MUTATIONS AT THE ENDOGENOUS *LOCUS* OF THE
MAMMALIAN *DIHYDROFOLATE REDUCTASE* GENE USING POLYPURINE
REVERSE HOOGSTEEN HAIRPINS**

Memòria presentada per Anna Solé Ferré per optar al títol de Doctor per la
Universitat de Barcelona

Dr. Carlos J. Ciudad Gómez

Director

Dra. Verónica Noé Mata

Directora

ANNA SOLÉ FERRÉ

Barcelona, 2015

No sóc de les persones que diu que van néixer sabent que volia fer un doctorat i dedicar-se al món de la investigació, sinó més aviat van ser les diferents circumstàncies les que m'hi van empènyer.

Tot va començar un dia que vaig sentir per casualitat les paraules “treball dirigit” que em van cridar l'atenció. Directa cap al departament de Bioquímica i Biologia Molecular a descobrir el nou camí que m'esperava. Primer un treball dirigit, després un altre, després beques de col·laboració, després un màster...i fins arribar al doctorat!

A vegades m'he preguntat què és exactament el que em va fer continuar amb la recerca, després de totes les frustracions i patacades que et va donant a canvi, i ara sé que una bona part de la culpa la té la gent que he tingut al costat durant tot aquest llarg trajecte.

Així que, primer de tot, m'agradaria agrair a la Vero i al Carles per ser els principals culpables de què ara mateix estigui escrivint aquestes paraules. M'heu ajudat a créixer com a investigadora i com a persona. Encara recordo el primer moment en què vaig trepitjar el departament, una veu que va dir: Tu ets l'Anna! (Carles, encara avui no sé com sabies que era jo!). Gràcies per trobar sempre un costat positiu als resultats desesperançadors, per ajudar-me a buscar colònies invisibles als ulls humans, per tenir sempre tots els experiments controlats, i per ensenyar-me tècniques insòlites! A tu Vero, gràcies per fer-me costat en moments difícils, per posar “ordre i mètode” sempre que ha calgut, i per asseure't amb mi a la “poyata” quan no me'n sortia! No oblidaré tampoc les anècdotes en congressos i les classes de bioquímica!

A la resta de culpables del laboratori, per fer-me aixecar cada dia amb il·lusió per anar a treballar! Sou un exemple a seguir. La Carlota, la primera que em va fer descobrir el treball de “poyata”, gràcies per la paciència! La Núria, per la serenitat en fer les coses i les explicacions! La Laura, per totes les hores dins i fora del laboratori, sempre disposada a ajudar amb el que calgui i a prendre la iniciativa quan es necessita. No canviïs ni deixis que et canviïn!! La Claudia, per la teva energia i ganes de lluitar per allò que vols, ets molt especial! Xenius, la nova espècie humanoide! Gràcies per ser allí sempre que calia, sobretot per desconectar i fer una mica el boig, i per totes les tardes de reflexions profundes sobre la vida tot fent una “oferta”, ets única!

A tots els treballs dirigits i màsters, de tothom se n’aprenen petites coses i sou el futur del laboratori! Estela, Cris, Àlex, Isabel... Ànims i endavant!! Gizem, thank you for your Turkish classes! Gorusuruz!

A la Xana i a l’Albert, que tot i no sé del mateix laboratori, ja en formeu part! Albert, gràcies per poder comptar amb tu sempre, i per l’aportació artística de la tesi, gràcies per la portada!!

Gràcies a tots els integrants del departament de Bioquímica i biologia molecular. Pocs de vosaltres us heu escapat d’haver-me d’ajudar en algun moment!

A la família i amics, per interessar-vos pel que feia al laboratori i intentar entendre’m quan us ho explicava, però sobretot per ajuda-me a desconectar!

ABBREVIATIONS

Abbreviations

-GHT	Without glycine, hypoxanthine, thymidine
10-CHO-THF	10-Formyltetrahydrofolate
³² P	Phosphorus-32
5-CH ₃ -THF	5-methyltetrahydrofolate
5,10-CH ₂ -THF	5,10-Methylenetetrahydrofolate
A	Adenine
Abbreviations	
ABC	ATP-binding cassette
ADA	Adenosine deaminase
AGO	Argonaute
AICARFT	Phosphoribosylaminoimidazolecarboxamide formyltransferase
AKR1C1	Aldo-Keto Reductase Family 1
AP site	Abasic site (Apurinic/Apyrimidinic site)
APRT	Adenine phosphoribosyltransferase
ATM	Ataxia telangiectasia mutated protein
ATP	Adenosine triphosphate
ATR	Ataxia telangiectasia and Rad3-related protein
BCL-2	B-cell lymphoma 2
BER	Base excision repair
BLAST	Basic Local Alignment Search Tool
bp	base pair
C	Cytosine
cAMP	cyclic adenosine monophosphate
Cas9	CRISPR associated protein 9
CD	Circular Dichroism
cdk2	Cyclin-dependent kinase 2
cDNA	Complementary DNA
CDS2	CDP-diacylglycerol synthase (phosphatidate cytidyltransferase) 2
CF	Cystic fibrosis
CFTR	Cystic fibrosis transmembrane conductance regulator
cGMP	guanosine monophosphate
CHO	Chinese hamster ovary
Ci, μ ci	Curies, Microcuries

CRISPR	Clustered regularly interspaced short palindromic repeats
DCP2	mRNA-decapping enzyme 2
DEPC	Diethylpyrocarbonate
DHF	Dihydrofolate
DHFR	Dihydrofolate reductase
DKK1	Dikkopf homolog 1
DMSO	Dimethyl sulfoxide
DNA	Deoxyribonucleic acid
dNTPs	Deoxynucleotide triphosphates
DOTAP	N-[1-(2,3-Dioleoyloxy)propyl]-N,N,N-trimethylammonium methyl-sulfate
DSB	Double-strand break
dsDNA	double-stranded DNA
dTMP	Deoxythymidine monophosphate
dUMP	Deoxyuridine monophosphate
EEF1A1	eukaryotic translation elongation factor 1 alpha 1
EMSA	Electrophoretic mobility shift assay
FPGS	Folylpolyglutamate synthetase
FR	Folate receptor
FRET	Fluorescence resonance energy transfer melting curves
G	Guanine
G4	G-quadruplex
GARFT	Glycinamide ribonucleotide formyltransferase
GAT	Gene augmentation therapy
GFP	Green fluorescent protein
Hb	Hemoglobin
HBB	beta-globin
HBS	HEPES Buffered Saline
HDR	Homology directed repair
HEXA	Hexosaminidase A
HIV	Human immunodeficiency virus
HR	Homologous recombination
HSPC159	Galectin-related protein
IMP	Inosine monophosphate
IMPDH	Inosine-5'-monophosphate dehydrogenase
iPSC	Induced pluripotent stem cell
Kb	Kilobase

KDa	Kilodalton
LDR-PPRH	Long-distance-repair-PPRH
MDM2	E3 ubiquitin protein ligase
miRNA / miR	microRNA
MMR	Mismatch repair
mRNA	Messenger ribonucleic acid
mTOR	Mammalian target of rapamycin (serine/threonine kinase)
MTX	Methotrexate
MYC	Myelocytomatosis viral oncogene homolog
MYST3	MYST histone acetyltransferase (monocytic leukemia) 3
NER	Nucleotide excision repair
NHEJ	Non homologous end joining
NMD	Nonsense mediated decay
nt	Nucleotide
ODN	Oligodeoxynucleotide
PCR	Polymerase chain reaction
PKC α	Protein kinase C alpha
PNA	Peptide nucleic acids
PPRH	PolyPurine Reverse Hoogsteen hairpin
PTO	Phosphorotioate
RFC	Reduced folate carrier
RISC	RNA-induced silencing complexes
RNA	Ribonucleic acid
RNase	Ribonuclease
RO	Repair oligonucleotide
ROS	Reactive oxygen species
RT	Reverse transcriptase
RVD	Repeat-variable diresidues
S100A4	S100 calcium binding protein A4
SCA	Sickle-cell anemia
SDR-PPRH	Short-distance-repair-PPRH
siRNA	Small interfering RNA
SLC4A4	Sodium bicarbonate cotransporter 1
SNP	Single nucleotide polymorphism
ssDNA	single-stranded DNA
ssO/ssODN	single-stranded oligonucleotide

T	Thymine
TALEN	Transcription activator-like effector nuclease
TBE	Tris-borate-EDTA
TDS	Thermal difference spectra
TE	Tris-EDTA
TFBO	Bifunctional triple-helix-forming oligonucleotides
TFO	Triplex forming oligonucleotide
THF	Tetrahydrofolate
Tm	Melting temperature
TOP1	Topoisomerase (DNA) I
TRBP	TAR RNA binding protein
TS	Thymidylate synthase
UGT1A	UDP glucuronosyltransferase 1 family, polypeptide A complex locus
UTR	Untranslated region
UV	Ultraviolet
WC	Watson-Crick
ZFN	Zinc finger nuclease

INDEX

1.3.1. Methotrexate	39
1.3.1.1. MTX resistance mechanisms and prevention	40
1.3.2. Micro RNAs (miRNAs)	42
2. Objectives	47
3. Materials and Methods	51
3.1. Materials	53
3.1.1. Cell lines	53
3.1.2. Culture media	54
3.1.3. Dihydrofolate reductase minigene	54
3.1.4. PPRHs and oligonucleotides for binding assays	55
3.1.5. Repair- PPRHs	56
3.1.6. PPRHs and oligonucleotides for structure characterization of PPRHs	59
3.1.7. Oligonucleotides for miRNA-mRNA interactions	60
3.2. Methods	61
3.2.1. Transfection and selection	61
3.2.2. Enzymatic activity assay	62
3.2.3. UV absorption measurements	63
3.2.4. Fluorescence measurements	64
3.2.5. Electrophoretic mobility shift assay (EMSA)	64
4. Results	67
4.1. Article I: Repair of Single-Point Mutations by Polypurine Reverse Hoogsteen Hairpins	69
4.1.1. Additional results to Article I	87

4.1.1.1. Binding assays between duplexes and hairpins at different temperatures	87
4.1.1.2. Negative and positive controls	88
4.1.1.3. Gradient of decreasing concentration of hairpins	89
4.1.1.4. A specific oligonucleotide can bind to the displaced polypurine strand at 37°C	90
4.1.1.5. Strand displacement using a single hairpin and posterior binding of a specific oligonucleotide	91
4.1.1.6. G4-E2rep used as a negative control	92
4.2. Article II: Correction of single point mutations at the endogenous <i>locus</i> of the <i>dihydrofolate reductase</i> gene in mammalian cells using Polypurine Reverse Hoogsteen hairpins	93
4.2.1. Additional results to Article II	127
4.2.1.1. Study of the ability of PPRHs to form a D-loop	127
4.3. Article III: Polypurine reverse Hoogsteen Hairpin motifs can form triplexes with their target sequences even under conditions of folding into G-quadruplexes	129
4.4. Article IV: Validation of miRNA-mRNA interactions by electrophoretic mobility shift assays	165
5. Discussion	175
5.1. Repair-PPRHs	177
5.1.1. Repair-PPRHs in an endogenous <i>locus</i>	180
5.1.2. G-quadruplex	184

5.2. miRNAs	186
6. Conclusions	189
Bibliography	193
Appendixes	217
Article V: Improved Design of PPRHs for Gene Silencing	219
Article VI: Effect of Polypurine Reverse Hoogsteen Hairpins on Relevant Cancer Target Genes in Different Human Cell Lines	233

PRESENTATION

This work is focused on the study of Polypurine Reverse Hoogsteen (PPRH) hairpins and their ability as gene correction tools.

The repair of a point mutation at its endogenous gene *locus* has been the focus of many researchers during the past decades by using various approaches such as gene replacement, gene augmentation therapy (GAT) and different repair oligonucleotides. Cystic fibrosis, sickle-cell anemia and Tay-Sachs disease are some examples of the high number of disorders caused by a single-point mutation. In this work we present an alternative repair methodology using PPRH molecules, that although first developed in our laboratory as a gene-silencing tool, we hypothesized that they could also be applied as a gene correction tool.

PPRHs are double-stranded DNA molecules formed by two antiparallel homopurine domains linked by a 5-thymidine loop, which form intramolecular reverse Hoogsteen bonds. PPRHs have been described to effectively bind to the dsDNA forming a triplex structure (Coma et al., 2005), and have been designed against either the template or the coding strand of the dsDNA (de Almagro et al., 2009, de Almagro et al., 2011a).

Taking advantage of the ability of PPRHs to form a triplex structure with the pyrimidine strand of the dsDNA, in the present work we wanted to explore the ability of PPRHs to correct point mutations. First of all, we studied the *in vitro* conditions for PPRHs to bind to dsDNA and to maintain it in an open conformation by binding assays. Then, we designed different repair-PPRHs by adding to the PPRH core a repair tail complementary to the mutated region of the DNA except for the nucleotide to be corrected. These repair-PPRHs were used in mammalian cells to repair a point mutation in a *dihydrofolate reductase (dhfr)* plasmid.

Finally, those results led us to further demonstrate the correction capability of repair-PPRHs in different mutant cell lines containing single point mutations in the endogenous *dhfr* gene. In addition, we developed improved Long-distance-repair-PPRHs (LDR-PPRHs) to correct mutations that are very distant with respect to the DNA target where the PPRH core binds.

Considering the possible high proportion of guanines in a PPRH sequence, an *in vitro* characterization of these molecules was carried out to study the effect of these guanines in the formation of secondary structures, such as G-quadruplex.

The triplex conformation formed by repair-PPRHs with their pyrimidine target sequences was also studied even when repair-PPRHs folded in a G-quadruplex structure instead of a hairpin.

As a second part of this thesis, we developed a new application of the electrophoretic mobility shift assay (EMSA) technique, to demonstrate the binding between miRNAs and their target sequences.

For over two decades, research in our laboratory has been focused on the pharmacogenomic study of methotrexate (MTX) resistance in cancer chemotherapy upon inhibition of DHFR. Beside gene amplification, our research group has shown that many genes are involved in this mechanism. In this direction, cellular genes and micro-RNAs such as miR-224 and its target genes SLC4A4, CDS2 and HSPC159 were identified to play an important role in the resistance to MTX in colon cancer cells (Mencia et al., 2011). For this reason, miR-224 was chosen to show in a direct and specific manner, its ability to bind to the SLC4A4 target gene, thus setting up the EMSA as a simple and useful method to validate the interaction between a miRNA and a specific mRNA target.

1. INTRODUCTION

1.1. POINT MUTATIONS IN THE DNA

Mutations are a natural process that alters the DNA and are constantly taking place in the genome. It is estimated that tens of thousands of changes happen daily in the DNA of a human cell (Jackson and Bartek, 2009). Not all the mutations result in functional impairment, but in some cases, small changes in the DNA sequence can provoke an enormous impact on an entire living being. Therefore, these mutations need to be reversed by the DNA repair machinery that fixes DNA damage such as mismatched nucleotides, DNA cross-links, bulky adducts and splicing broken DNA strands back together.

Depending on the cells affected, mutations can be classified in two groups: inherited mutations, when they affect germ cells, and the alteration can often be passed on to offspring; and acquired mutations, that can spontaneously arise during the life of an organism in somatic cells. In the later, mutations can result from normal metabolic activities including DNA replication errors, spontaneous lesions such as depurination and deamination of the DNA, and the generation of reactive oxygen species (ROS), but can also result from environmental factors such as physical or chemical mutagens (Lodish et al., 2004, Luch, 2005, Bernstein et al., 2013) (Figure 1).

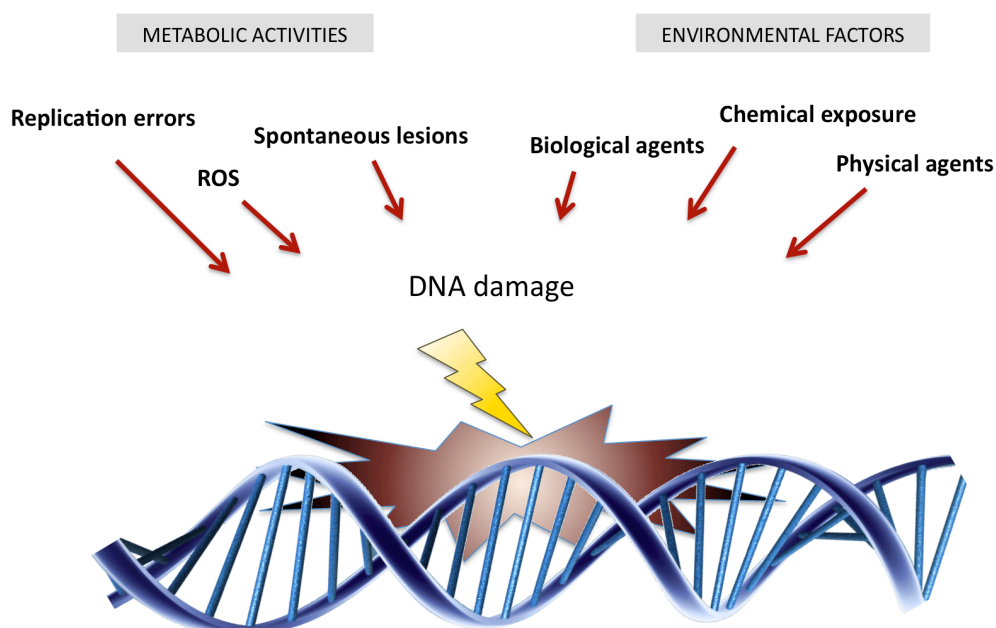


Figure 1. Causes of DNA damage.

In the present thesis we will focus on point mutations and their possible effects at the molecular level. Point mutations are a type of mutations that typically refer to an alteration of a single or a few adjacent base pairs in a DNA sequence. They usually take place during DNA replication (Kunkel, 2004), although other endogenous and exogenous agents can be implicated (Bernstein et al., 2013). Some point mutations are beneficial or have no effect. Polymorphisms for instance, are mutations that do not cause any functional damage in general under basal conditions. Nonetheless, these alterations can also be detrimental for gene function at various levels. If the mutation occurs in the promoter region of a gene, the expression of this gene may be altered. If the alteration is caused in a coding region, the activity may change and in the case of insertions or deletions, the whole peptide can be modified, since a frameshift is produced. In addition, if the mutated base pair is found near or in the intron-exon junction, it can result in a splicing alteration of the mRNA.

1.1.1. Classification of point mutations

Point mutations can be categorized in different groups:

1.1.1.1. Substitutions

It is the most common point mutation, and consists on a replacement of a base and its partner in the complementary DNA strand with another. Nucleotides can be substituted through transition between two pyrimidine or purine bases, or transversion between a purine and a pyrimidine. Since many amino acids are encoded by more than a single genetic codon (64 different codons specify 20 amino acids), a substitution in exon regions of the DNA can lead to synonymous mutations, when the amino acid is not modified, which it is very common when the mutation is located in the third nucleotide of the codon. These are also frequently called silent mutations, although transcription, splicing, mRNA transport, or translation can be altered in some cases (Table 1).

According to the consequence that the replacement will provoke, substitutions can be categorized in:

- *Nonsense mutations*: They result in a change of an amino acid codon into a premature stop codon that will produce a truncated protein and thus nonfunctional most of the times. Depending on the location of the mutation within the coding region of the gene, the functional consequences can be extremely different.

- *Missense mutations*: These mutations cause a change of an amino acid codon by another. If the mutated amino acid maintains the same properties as the wild type, it is called conservative mutation. Otherwise, if the properties change, the mutation is considered as non-conservative, and the protein can lose its function.

	Wild type	Substitution			
		Synonymous	Nonsense	Missense	
				Conservative	Non-conservative
DNA level	TTC	TTT	ATC	TCC	TGC
mRNA level	AAG	AAA	UAG	AGG	ACG
Protein level	Lys	Lys	STOP	Arg	Thr

Table 1. Example of the different types of substitutions.

1.1.1.2. Insertions and deletions

Insertions result from a mutation in which extra base pairs are inserted in a specific site of the DNA sequence. Deletions are mutations in which specific base pairs are lost or deleted (Table 2).

Both insertions and deletions can cause frameshift mutations when the number of altered nucleotides is not a multiple of three. In this case, every triplet downstream from the mutation will be incorrectly grouped into inaccurate codons, and read in erroneous frames. These types of mutations can also result in a premature translation termination (nonsense).

	Wild type DNA sequence	Insertion	Deletion
DNA level	TTC TCG AGT	TTC GTC GAG	TTC TGA GTA
mRNA level	AAG AGC UCA	AAG CAG CUC	AAG ACU CAU
Protein level	Lys Ser Ser	Lys Gln Leu	Lys Thr His

Table 2. Representation of an insertion and a deletion of one nucleotide.

1.1.2. DNA repair machinery

DNA damage may lead towards a large variety of lesions, including mismatches, chemical adducts or single- and double-strand breaks (DSBs). Therefore, different repair pathways have evolved, each focused on a particular type of lesion.

If DNA damage affects terminally differentiated cells, DNA damage repair will ensure the integrity of the transcribed genome. However, if DNA damage occurs in dividing cells, “cell cycle checkpoints” will detect the damage by sensor proteins, and by means of different protein complexes, signal transducers and effector proteins. These effector proteins will lead to the repair of DNA or will temporarily stop the proliferating cells in their cell cycle progression to provide enough time to the DNA repair machinery to act (Figure 2). Some of these important cell cycle checkpoint proteins are ataxia telangiectasa mutated (ATM) and ATM and Rad3 related (ATR), that act as signal transducers. In response to DNA damage in G1, for example, these proteins will phosphorylate p53 that acts as a transcription factor for p21, leading to an inhibition of both cyclinE/Cdk2 and cyclinA/Cdk2 complexes, and therefore an inhibition of G1/S transition, thus preventing the synthesis of damaged DNA (Canman et al., 1998, Banin et al., 1998, Tibbetts et al., 1999, Li et al., 1994). However, the specific pathway that will be activated is determined by the type of DNA damage.

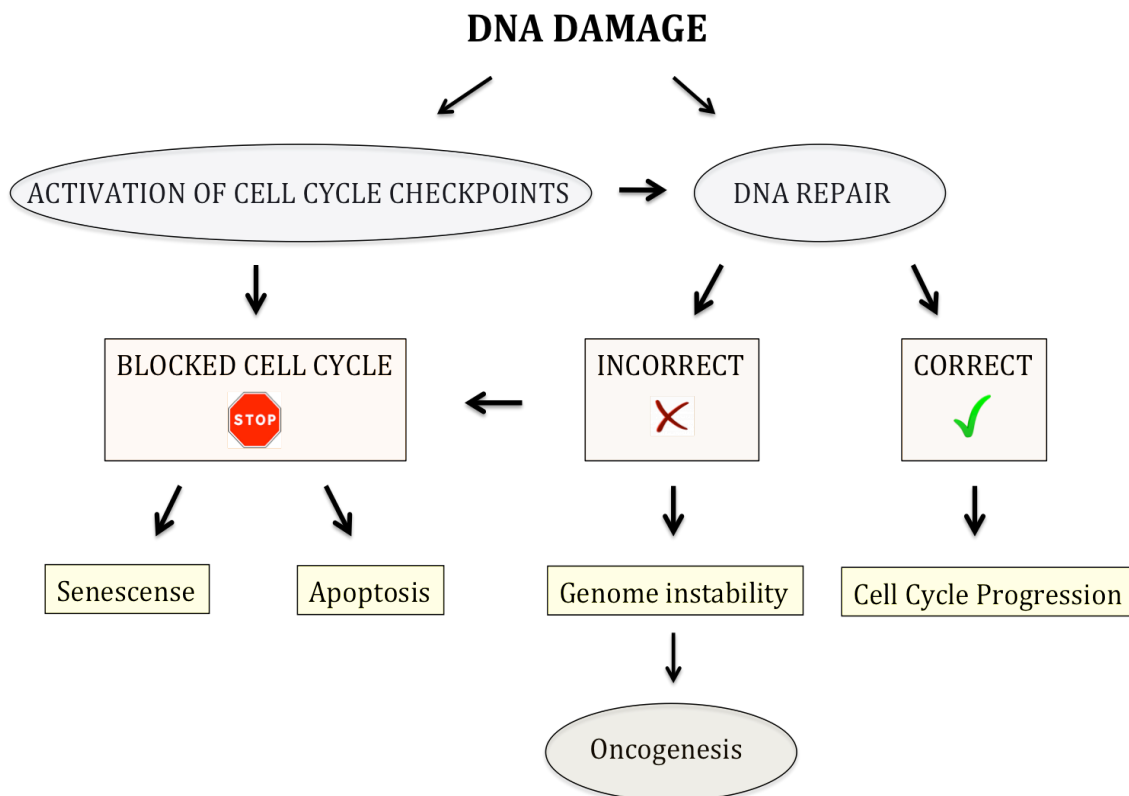


Figure 2. Scheme of DNA damage response pathways. Adapted from (Houtgraaf et al., 2006).

When repair processes fail and DNA damage cannot be repaired, cells may become senescent or can be conducted to programmed cell death or apoptosis. Apoptosis is conducted by different protein factors such as the anti-apoptotic protein Bcl-2, inhibited directly or indirectly by p53 (Miyashita and Reed, 1995). If any of these processes do not work properly, there may be an unregulated cell division that can lead to the formation of a tumor, which could become cancerous (Figure 2).

DNA damage checkpoints can halt cell proliferation, but the repair machinery is required to prevent the transduction of mutations to daughter cells. DNA-damage-signaling and DNA repair are believed to be linked and operate collectively (Verkade et al., 1999, Martinho et al., 1998). As mentioned before, since there is a wide diversity of possible lesions, a large variety of DNA repair mechanisms have

evolved, such as direct reversal repair, base excision repair (BER), nucleotide excision repair (NER), mismatch repair (MMR) and DSB repair (Figure 3).

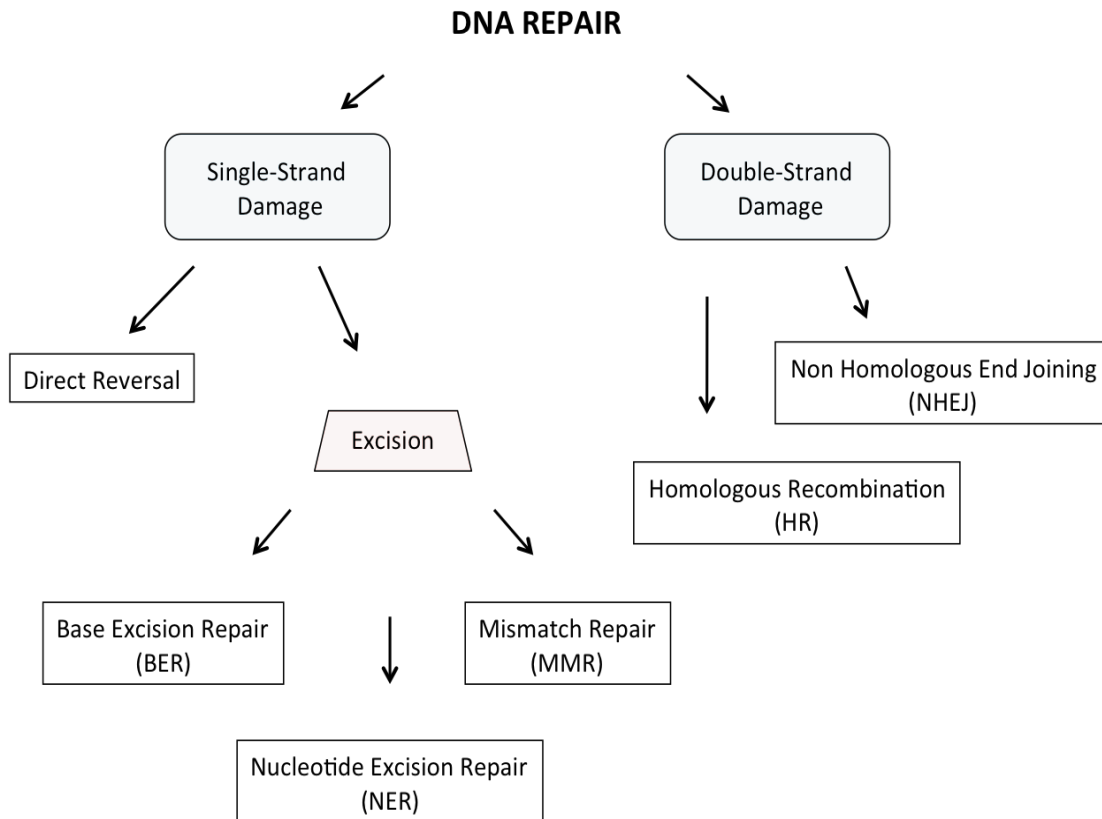


Figure 3. Scheme of DNA repair responses.

1.1.2.1. Direct reversal repair of DNA damage

Most DNA damage can be repaired by the removal of the mutated bases followed by resynthesis of the excised region. However, in some cases DNA damage can be corrected by the direct reversal repair, in which specific proteins repair the damaged area, without the requirement of nucleases, DNA polymerases or reference DNA templates. This repair mechanism mainly corrects pyrimidine dimers resulting from the action of the ultraviolet (UV) light and alkylated guanine residues, resulting from methylation or ethylation at the O⁶ position of the purine ring (Margison and Santibanez-Koref, 2002).

1.1.2.2. Excision repair mechanisms

In general, these mechanisms work by the removal of altered bases or nucleotides and the re-synthesis of the removed area, using different strategies:

Base excision repair (BER): Consists on the identification of bases that have been damaged, and their replacement by the corrected nucleotides, using the complementary strand of the DNA as a template. The altered DNA base is first identified and removed by DNA glycosylases, creating an “Abasic Site” or “AP site”. Subsequently, an AP-endonuclease will remove the phosphate ribose moiety of the AP site, leaving a gap of one nucleotide that is immediately filled by a DNA polymerase and sealed by ligase. Some examples of DNA lesions repaired by BER include abasic sites, 8-Oxoguanines, single-strand breaks or the presence of an uracil, mainly caused by physical and chemical agents such as X-rays, oxygen radicals and alkylating agents as well as spontaneous reactions (for review see (Memisoglu and Samson, 2000)).

Nucleotide excision repair (NER): NER mechanism is similar to BER, and they share some molecular elements. However, NER detects a wide variety of damages based on the structure integrity of the DNA double helix. When distortion in the DNA is detected with the assistance of damage surveillance protein complexes like XPC–RAD23B (Bergink et al., 2012), a specific endonuclease excises the damage region of the strand and its surrounding neighbors. Later, DNA polymerase and DNA ligase will fill and seal the small gap left. NER is particularly important after the action of polycyclic aromatic hydrocarbons and UV light, that results in bulky adducts such as thymine dimers and 6,4-photoproducts (Hess et al., 1997).

Mismatch repair (MMR): Incorrect bases are incorporated to the DNA during replication at an estimated rate of 10^{-7} to 10^{-8} (Kunkel, 2004). Base mismatches can also be caused by base deamination, oxidation and methylation (Christmann et al., 2003). MMR system detects and removes these mismatched bases in the newly replicated strand, which is has not yet been methylated (in prokaryotes) or

contains single-strand breaks (in eukaryotes) and can be easily distinguished from the parental strand. MutS and MutL bind to the mismatched base, and together with a helicase and an exonuclease, direct the cleavage of the incorrect base-pairing region, which is then re-synthesized by DNA polymerase and sealed by ligase.

Double-strand break (DSB) repair: DNA DSBs are especially hazardous to the cell because they are potent inducers of genotoxic effects and cell death (Lips and Kaina, 2001). They are basically caused by physical and chemical agents such as X-rays and anti-tumor agents. Repair of DSB damage involves two main possible mechanisms, called nonhomologous end joining (NHEJ) and homologous recombination (HR). Whereas NHEJ appears to be important in all phases of the cell cycle, HR is most critical during the late S and G2 phases (Rothkamm et al., 2003).

- **NHEJ** is a principal pathway of DSB repair in mammalian cells. It occurs by splicing between the ends of the truncated fragments of the duplex (Barnes, 2001), meaning that it does not require a homology template sequence. The action of NHEJ mechanism can result in deletions and inversions in the DNA, since there is not a quality control of the homologous bases.

- **HR** is a template-directed process in which the damage chromosome uses a homologous undamaged DNA molecule to ensure proper repair (Sonoda et al., 2001). HR starts with resection by helicases and nucleases of the double strand breakage to produce single-stranded DNA (ssDNA), which is a scaffold for assembly of Rad51 filament (RecA in prokaryotes). Rad51 promotes the homology search and catalyzes exchange of the DNA strand with the undamaged molecule (Baumann and West, 1998). HR can also repair single-strand DNA gaps and interstrand cross-links, and it is exploited in many strategies for gene targeting and correction of point mutations.

1.1.3. Relationship of point mutations to diseases

A large number of characterized genetic disorders are associated to a mutation in a single gene. Cystic fibrosis, sickle-cell anemia and Tay–Sachs are some examples of the most common diseases caused by a point mutation in one gene, and for this reason are described below. There are currently several ongoing research studies, but there is still no definitive treatment for these diseases (Bender and Douthitt Seibe, 2003, Kaback and Desnick, 2011, Moskowitz et al., 2008).

1.1.3.1. Cystic fibrosis (CF)

It is the most common autosomal recessive disorder in Caucasians (1 in about 2000). The disease is caused by mutations in the gene encoding the CF transmembrane conductance regulator (CFTR), an ATP-binding cassette (ABC) transporter that function as a ligand-gated anion channel. Its mutation results in dysfunction of the CFTR anion channel in epithelial cells (Moskowitz et al., 2008). This dysfunction causes abnormalities in fluid and electrolyte transport in exocrine epithelia, which result in hyperviscous mucus production, infections, and inflammation in the lungs of patients with CF. In addition, exocrine pancreas, sweat glands, intestine, male genital tract, and hepatobiliary system can also be affected, resulting in a complex multisystem disease (Kerem et al., 1989, Lubamba et al., 2012, Moskowitz et al., 2008, Quinton, 1990). The most common mutation corresponds to F508del-CFTR, a deletion of three nucleotides which results in the loss of a phenylalanine residue at position 508 of the putative product of the CF gene (Kerem et al., 1989). However, 2001 mutations are currently listed in this CFTR mutation database: <http://www.genet.sickkids.on.ca/cftr/> (Table 3).

Statistics by mutation type:

Mutation Type	Count	Frequency %
Missense	794	39.68
Frameshift	313	15.64
Splicing	228	11.39
Nonsense	167	8.35
In frame in/del	39	1.95
Large in/del	52	2.60
Promoter	15	0.75
Sequence variation	269	13.44
Unknown	124	6.20

Table 3. Type and frequency of mutations causing cystic fibrosis disease. Obtained from <http://www.genet.sickkids.on.ca/cftr/>.

1.1.3.2. Sickle-cell anemia

Sickle cell anemia is a group of disorders that affects hemoglobin, resulting in a mutant β -globin, predominantly hemoglobin S (Hb S). Hb S results from a single nucleotide alteration in the β -globin gene (HBB), changing the sixth amino acid in the β -hemoglobin chain from glutamic acid to valine (Glu6Val). Other forms of sickle cell disease result from the coinheritance of Hb S with other abnormal β -globin chain variants, the most common forms being sickle-hemoglobin C disease (Hb C) and two types of sickle β -thalassemia (Table 4). Hb S has a lower affinity to oxygen than regular Hb resulting in red blood cells more adherent and fragile. Sickle-cell disease is characterized by acute and chronic pain and organ damage, as a consequence of tissue ischemia (Bender and Douthitt Seibe, 2003)

DNA Change	Nucleotide	Protein Acid Change	Amino	Hb Variant	Reference Sequences
c.20A>T		Glu6Val (p.Glu7Val)		Hb S	
c.19G>A		Glu6Lys (p.Glu7Lys)		Hb C	
c.79G>A		Glu26Lys (p.Glu27Lys)		Hb E	NM_000518.4 NP_000509.1
c.364G>C		Glu121Gln (p.Glu122Gln)		Hb D-Punjab	
c.364G>A		Glu121Lys (p.Glu122Lys)		Hb O-Arab	

Table 4. Some of the HBB pathogenic variants. Obtained from (Bender and Douthitt Seibe, 2003).

1.1.3.3. Tay-Sachs disease

Tay-Sachs disease is an autosomal recessive disorder caused by a mutation in the α subunit of the hexosaminidase A (HEXA) gene. The six most common mutations comprehend three null alleles, the p.Gly269Ser allele; associated with the adult-onset form of HEXA deficiency, and two pseudodeficiency alleles; associated with reduced degradation of the synthetic substrate but not with neurologic disease (Table 5).

Gene	Mutations Detected	Allele Status
	c.1274_1277dupTATC	Null
	c.1421+1G>C	Null
	c.1073+1G>A	Null
HEXA	p.Gly269Ser	Adult onset
	p.Arg247Trp	Pseudo-deficiency
	p.Arg249Trp	Pseudo-deficiency

Table 5. The six most common mutations causing Tay-Sachs disease. Adapted from (Kaback and Desnick, 2011, Scott et al., 2010)

Tay-Sachs is a progressive neurodegenerative disorder caused by intralysosomal storage of the GM2 ganglioside, associated with progressive weakness, loss of motor skills, decreased attentiveness, and increased startle response (Kaback and Desnick, 2011).

1.1.3.4. Other diseases caused by point mutations

Many other genetic disorders are caused by genetic point mutations such as color blindness (Weitz et al., 1992), haemochromatosis (Klingler et al., 2000), haemophilia (Giannelli et al., 1990), phenylketonuria, polycystic kidney disease (Lee et al., 2010), and Fabry disease (Sakuraba et al., 1990).

Point mutations in proto-oncogenes or tumor-suppressor genes can contribute to cancer development, since they encode for proteins that play a key role in controlling cell growth and proliferation (Lodish et al., 2004).

1.1.4. Strategies to correct point mutations

Gene augmentation therapy (GAT) is one of the most studied strategies to treat diseases caused by point mutations; it consists in introducing a copy of the wild type gene in the affected cells to obtain the functional protein in sufficient amounts to restore the normal phenotype. This strategy is especially available for recessive diseases, since the mutated gene does not interfere with the normal product, and the amount of this product does not need a rigorous regulation to recover a normal phenotype. However, it presents some drawbacks, as random gene integration in the genome, and the loss of endogenous regulator elements of the gene. As an alternative, a different philosophy for gene repair was developed to correct point mutations in their endogenous *loci* using different types of oligonucleotides. These strategies consisted in targeting the genomic DNA with an oligonucleotide complementary to the DNA sequence, except for the nucleotide to be corrected. In the last years, different approaches have emerged in this direction:

1.1.4.1. Chimeric RNA-DNA oligonucleotides

Chimeric RNA-DNA oligonucleotides were first described in 1996 (Yoon et al., 1996). The main objective of these molecules is to activate intrinsic repair mechanisms to correct single point mutations *in situ*. The design of these oligonucleotides arose from the results obtained by Kotani et al., which suggested that an oligonucleotide comprising both an RNA and a DNA sequences bound to genomic DNA more efficiently than an oligonucleotide exclusively formed of DNA (Kotani and Kmiec, 1994). The original chimeric consisted of two complementary domains, one composed by 25 DNA nucleotides flanking the site of mutations with the exception of a single mismatched nucleotide located at the center, and the other one composed by an RNA/DNA hybrid strand with two regions of 10 2'-O-methylated oligoribonucleotides flanking both ends of a 5' DNA nucleotide stretch. These two domains were linked by a loop of 5 thymines in each end, allowing a double-hairpin structure folding (Figure 4).

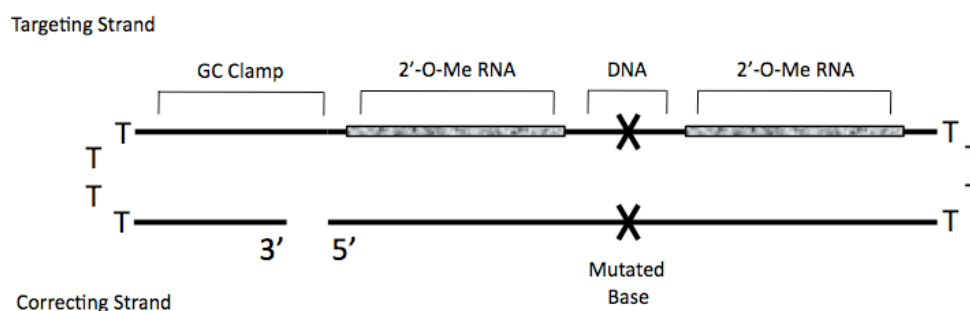


Figure 4. Structure of a chimeric RNA-DNA oligonucleotide

A 5bp guanine-cytosine clamp present in each domain, the modified RNA residues and the hairpin structure were designed to improve the resistance of these chimeras to degradation. When chimeric and DNA domains were studied separately, it was proved that the DNA domain induced gene correction, while the chimeric domain stabilized the molecule (Gamper et al., 2000).

Chimeric oligonucleotides have been studied, both in cellular and animal models, to correct point mutations in genes such as *alkaline phosphatase* (Kren et al., 1997, Yoon et al., 1996), *β -globin* (Cole-Strauss et al., 1996, Liu et al., 2002a, Xiang et al., 1997), *coagulation factor IX* (Bandyopadhyay et al., 1999, Kren et al., 1998), *UDP-glucuronosyltransferase* (Kren et al., 1999), *tyrosinase* (Alexeev et al., 2000, Alexeev and Yoon, 1998) *dystrophin* (Bartlett et al., 2000, Bertoni and Rando, 2002, Rando et al., 2000), *apolipoprotein E2* (Tagalakis et al., 2001) and *CFTR channel* (de Semir et al., 2003).

The use of chimeric RNA-DNA oligonucleotides presents some limitations such as the low reproducibility of the experiments (Diaz-Font et al., 2003, Manzano et al., 2003, Taubes, 2002) and the non-permanent effect (Tagalakis et al., 2002).

1.1.4.2. Single-stranded oligonucleotides (ssOs)

First evidences that a ssO was able to correct a point mutation were provided in 1988 when it was demonstrated that a 20-mer oligonucleotide could repair a point mutation in the yeast *cytochrome c* gene (Moerschell et al., 1988).

SsOs used to repair point mutations consist in short sequences ranging from 20 to 60 nucleotides in length that contain, in a central position, the wild base of the gene to be repaired. Chemical modifications were added to these oligonucleotides such as phosphorothioates (PTO) linkages (Agarwal et al., 2003, Lu et al., 2003b), 2'-O-methyl uracil (Igoucheva et al., 2001) or locked nucleic acids (Andrieu-Soler et al., 2005) to protect them from nucleolytic degradation, although some of these modifications could affect the repair frequency (Yin et al., 2005).

The first studies using these oligonucleotides were performed to correct point mutations in reporter genes, or genes conferring resistance to antibiotics. This methodology facilitated the study of the mechanism involved, since the selection of the repaired colonies was simple. Therefore, single-stranded oligonucleotides have been designed to repair a point mutation in the β -*galactosidase* gene in nuclear extracts, or in an episomal and chromosomal form in mammalian cells (Igoucheva et al., 2001), to repair point mutations in the *neomycin resistance* gene and in β -*galactosidase* in protein extracts from mitochondria (Kren et al., 2003) and in *GFP* stably transfected in HeLa cells (Yin et al., 2005).

SsOs have also been used to correct genes involved in different diseases, such as α -*D-glucosidase*, responsible for Pompe disease, caused by the accumulation of glycogen (Lu et al., 2003a).

Furthermore, 45-mer oligonucleotides were used to correct a point mutation in *tyrosine kinase* in albino rat melanocytes (Alexeev et al., 2002), and subsequently, an oligonucleotide was designed to introduce a point mutation in *keratin 17* in mice (Fan and Yoon, 2003).

Several works have been reported using *in vivo* ssO-directed gene modification in mice. The correction of an *rd1* point mutation in mutant mice was proved (Andrieu-Soler et al., 2007), although the frequency of repair remained insufficient. ssOs have also shown to correct a *mdx5cv* splice site mutation in the

dystrophin gene, but since muscle cells are multinucleated, the correction of a single nucleus may not be sufficient to protect the entire fiber (Bertoni et al., 2005). Hence, frequencies of ssO-mediated gene repair are still variable and often very low (Aarts et al., 2006, Hu et al., 2005, Igoucheva et al., 2001, Kenner et al., 2002, Nickerson and Colledge, 2003, Pierce et al., 2003).

1.1.4.3. Bifunctional triple-helix-forming oligonucleotides (TFBO)

Bifunctional triple-helix-forming oligonucleotides were first described in 1999 (Chan et al., 1999, Culver et al., 1999), and are formed by two domains:

- Repair domain; consisting of a single- or double-stranded sequence of 20 to 60 nucleotides of length. This sequence is complementary to the DNA target except for the position to be corrected, usually located in a central position of the repair domain.
- TFO domain; formed by a triplex-forming oligonucleotide ranging from 10 to 30 nucleotides of length, that is able to bind to an homopurine/homopyrimidine DNA sequence to form a triple helix structure.

Both domains are connected through a linker, thus providing some flexibility to the repair domain. At first it was thought that the covalently union between both domains was an essential requirement (Chan et al., 1999, Culver et al., 1999). Subsequently, it was shown that depending on the repair mechanism used, the influence of this parameter differed. Therefore, both domains used separately also demonstrated to be efficient (Datta et al., 2001).

TFOs alone can introduce alterations in the genome through two different mechanisms, either by inducing errors to the target region by themselves due to the high binding affinity (Wang et al., 1996, Vasquez et al., 2000) or by triggering a mutagen such as psoralen or chlorambucil (Havre et al., 1993, Wang and Glazer, 1995, Belousov et al., 1997, Majumdar et al., 1998).

The first TFBOs were designed to repair a point mutation present in the *supF* reporter gene (Chan et al., 1999), at a repair frequency ranging between 0.17% (single-stranded TFBO) and 0.68% (double-stranded TFBO) using a bacterial

system, which decreased to 0.036% and 0.014% respectively, when the same TFBOs were used to repair the *supF* gene in COS-7 cells. TFBOs were also used to repair point mutations in other genes such as adenosine deaminase (*ADA*) or *p53* (Culver et al., 1999).

One of the most important limitations of TFBOs was the low frequency of repair. For this reason new molecules were designed, formed by a repair domain linked to a PNA domain (Rogers et al., 2002).

1.1.4.4. Peptide nucleic acids (PNAs)

To increase the frequencies of correction, modifications in the backbone of the nucleic acid were introduced. PNAs are synthetic polymers that mimic DNA, but replacing the entire negatively charged sugar-phosphate backbone of DNA with a repeated N-(2-aminoethyl)-glycine units linked by peptide bonds (Egholm et al., 1993, Nielsen et al., 1991). PNAs show a high binding affinity and strength to DNA or RNA through Watson-Crick base pairing, although a mismatch in a PNA/DNA duplex is much more destabilizing than a mismatch in a DNA/DNA duplex (Nielsen, 2004). Due to its uncharged polyamide backbone, PNA can hybridize to negatively charged DNA or RNA without electrostatic repulsion, but this characteristic also represents an awkward in solubility and cellular uptake. Several approaches for correction of point mutations by different types of PNAs have emerged: Pseudocomplementary PNAs (pc-PNA) containing diaminopurine-thiouracil base pairs (Demidov et al., 1993, Lohse et al., 1999, Lonkar et al., 2009), bifunctional PNA-DNA conjugates (bis-PNAs) (Chin et al., 2008, Rogers et al., 2002), “tail-clamp” PNAs (tc-PNAs) composed of a short (hexamer) homopyrimidine triplex forming domain and a (decamer) mixed sequence duplex forming extension (Bentin et al., 2003, Kaihatsu et al., 2003), and single-stranded oligodeoxynucleotides composed of peptide nucleic acid bases (PNA-ssODNs) (Kayali et al., 2010, Nik-Ahd and Bertoni, 2014).

1.1.4.5. Site-specific nucleases

Programmable endonucleases such as zinc-finger nucleases (ZFN), transcription activator-like effector nucleases (TALENs) and Clustered Regulatory Interspaced Short Palindromic Repeats (CRISPR)/CRISPR-associated 9 (Cas9), are artificial proteins composed of a sequence specific DNA-binding domain fused to a nuclease, that are able to provoke double strand breaks (DSBs) in the genome, thus stimulating the cellular DNA repair-mechanisms, including error-prone NHEJ, in the absence of a homologous DNA template, and HR, in the presence of a synthetic repair template (Wyman and Kanaar, 2006) (Figure 5). These site-specific nucleases have shown to edit DNA to disrupt, introduce, invert, or delete genes (Carroll, 2014). Although to a lesser extent, these tools are also being studied to correct point mutations (Carroll, 2014, Ochiai, 2015).

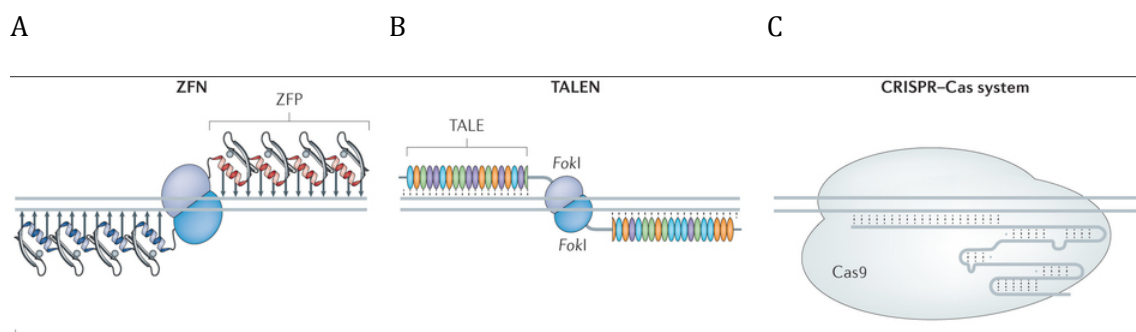


Figure 5. Site-Specific nucleases structure scheme. (A) ZFN, (B) TALEN and (C) CRISPR-Cas9 (Yin et al., 2014a).

Zinc-finger nucleases

ZFN have been used as a tool for genome editing since 2005. ZFN are custom-designed artificial endonucleases formed by two domains: A Cys₂-His₂ zinc finger DNA-binding domain and a nuclease domain from the FokI restriction enzyme, responsible for the catalytic cleavage. When two ZFNs form a dimer, the nuclease becomes active (Miller et al., 2007, Szczepek et al., 2007) and therefore, able to induced sequence-specific cleavage at a genomic *locus*, resulting on a double-strand break (DSB) (Kim et al., 1996, Porteus and Carroll, 2005) (Figure 5a). ZFNs

are currently the only nuclease-mediated genetic editing tool being applied to clinical trials (www.clinicaltrials.gov), to knockout the *chemokine (C-C motif) receptor 5 (CCR5)* gene in CD4+ T cells conferring resistance to HIV-1 (Perez et al., 2008). The disruption of *CXCR4* could be an alternative for HIV treatment (Voit et al., 2013). It has also been reported the use of ZFNs to target *TAP2* in human iPSCs for vaccination therapy (Haruta et al., 2013), and to correct the globin imbalance in α -thalassemia (Wang et al., 2012). Other studies have demonstrated that genome editing of single-base pairs are also a fact using ZFNs with donor plasmids (Urnov et al., 2005) or ssODNs (Chen et al., 2011, Soldner et al., 2011). Some examples are the restoration of the expression of *IL2R γ* in X-linked severe combined immune deficiency patients (Urnov et al., 2005), the repair of a Glu342Lys mutation in *α_1 -antitrypsin (A1AT)* by using a combination of ZFNs and *piggyBac* technology (Yusa et al., 2011a, Yusa et al., 2011b) or the correction of the sickle cell anemia mutation in *β -globin* in human iPS cells (Sebastiano et al., 2011). This technology is also seen applicable to create a targeted codon modification in *RPS6KA3* encoding for kinase RSK2, implicated in different mental and skeletal disorders, and in cancer (Chen et al., 2011), or to generate isogenic pluripotent stem cells that differ at susceptibility variants for Parkinson's disease by modifying the *α -synuclein* gene in single base pairs (Soldner et al., 2011).

TALENs

TALENs have emerged as an alternative to ZFNs for genome editing (Boch et al., 2009, Moscou and Bogdanove, 2009). These artificial restriction enzymes are formed by an unspecific FokI domain fused to a TAL effector DNA-binding domain, which is a naturally protein secreted by the pathogenic *Xanthomonas* bacteria, commonly located in plant cells (Boch and Bonas, 2010). The DNA-binding domain contains two highly variable aminoacids called repeat-variable diresidues (RVDs) out of 33-35 that are strongly conserved. RVDs are very related with the specificity of the nucleotide recognition (Deng et al., 2012, Mak et al., 2012) (Figure 5b). TALENs are typically used for gene disruption (Carlson et al., 2012, Li et al., 2012, Mussolino et al., 2011, Wood et al., 2011) and gene addition (Hockemeyer et al., 2011, Zu et al., 2013), but also for single-base pair genome editing. For example, to

identify an intergenic mutation upstream of *mitotic checkpoint serine/threonine kinase (BUB1B)* gene causing the mosaic variegated aneuploidy syndrome (Ochiai et al., 2014), or to establish disease models by provoking, for instance, a 2bp substitution in *v-akt murine thymoma viral oncogene homolog 2 (AKT2)* (Ding et al., 2013), which is implicated in the regulation of insulin sensitivity. TALENs have also been used to introduce specific mutations in *CCR5* (Yang et al., 2013), *paired-like homeobox 2b (PHOX2B)* and *protein kinase, AMP-activated, gamma 2 non-catalytic subunit (PRKAG2)* (Miyaoka et al., 2014), and to correct a mutation of the *HBB* gene (Sun and Zhao, 2014).

CRISPR/Cas

The CRISPR/Cas system provides bacterial and archaeal immunity against foreign DNA by using RNAs to direct cleavage of the DNA (Wiedenheft et al., 2012). In 2012, the type II CRISPR system was adapted for genome editing (Jinek et al., 2012), and in a few years it has achieved great successes in this field (Figure 5c). A tracrRNA-crRNA chimeric single-guide (sgRNA) has been developed (Mali et al., 2013), which is able to recruit the Cas9 nuclease, responsible for introducing site-specific DSBs in target DNA (Jinek et al., 2012, Wiedenheft et al., 2012). Cas9 protein requires a “seed” sequence within the sgRNA and a protospacer adjacent motif (PAM) (Doudna and Charpentier, 2014). By re-designing the sgRNA, almost any DNA sequence can be targeted. CRISPR/Cas system has been shown to be efficient in a variety of organisms by changing the DNA sequence at specific a *locus*. A mutation in the *Crygc* gene was corrected in mouse embryos by using the homologous chromosome as a template (Wu et al., 2013). With the aid of an exogenous DNA template, CRISPR/Cas succeeded to correct a mutation in *dystrophin*, although only partially corrected mosaic mice was achieved (Long et al., 2014). A controversial study has been recently conducted in human embryos to modify *β-globin*, but a high number of off-target effects were observed (Liang et al., 2015). In somatic cells, various works have also been reported, such as the correction of *fumarylacetoacetate hydrolase (FAH)*, responsible for the hereditary type I tyrosinemia (Yin et al., 2014b), the disruption of *proprotein convertase subtilisin/kexin type 9 (PCSK9)* (Ding et al., 2014), or the treatment of hepatitis B

virus (HBV) infection by modeling chronic HBV infection in mouse livers with expression vectors, to be further targeted and disrupted (Lin et al., 2014). In *ex vivo* experiments, iPSCs were used to tackle the β -thalassemia disorder, selecting for a co-integrated antibiotic resistance cassette to identify the modified genes (Xie et al., 2014), and to correct mutations in *dystrophin* causing Duchenne muscular dystrophy (Li et al., 2015, Ousterout et al., 2015). CRISPR/Cas has also demonstrated to be efficient in targeting the *CFTR locus* together with a template for homology-directed repair and a puromycin resistance cassette, in primary somatic stem cells (Liao et al., 2015), and in treating human immunodeficiency virus (HIV) infection following two approaches, by targeting the HIV-1 long terminal repeats (LTRs) in infected primary CD4⁺ T-cells (Liao et al., 2015), and by modulating chemokine receptor 5 (CCR5), a co-receptor needed for HIV-1 T-cell infection (Mandal et al., 2014).

1.2. PPRHS AS AN ALTERNATIVE TOOL FOR GENE THERAPY

Polypurine Reverse Hoogsteen (PPRH) hairpins are non-modified double stranded DNA molecules developed in our laboratory (Coma et al., 2005). PPRHs are formed by two homopurine antiparallel domains linked by a five-thymidine loop. The two homopurine domains are able to fold in a hairpin structure by intramolecular Reverse Hoogsteen bonds. Since purines have the capacity to form a Watson Crick bond with a pyrimidine, at the same time as they can form a Reverse Hoogsteen bond with another purine (Figure 6a and b), PPRHs are able to bind to a third polypyrimidine strand forming a triplex structure (Figure 6c).

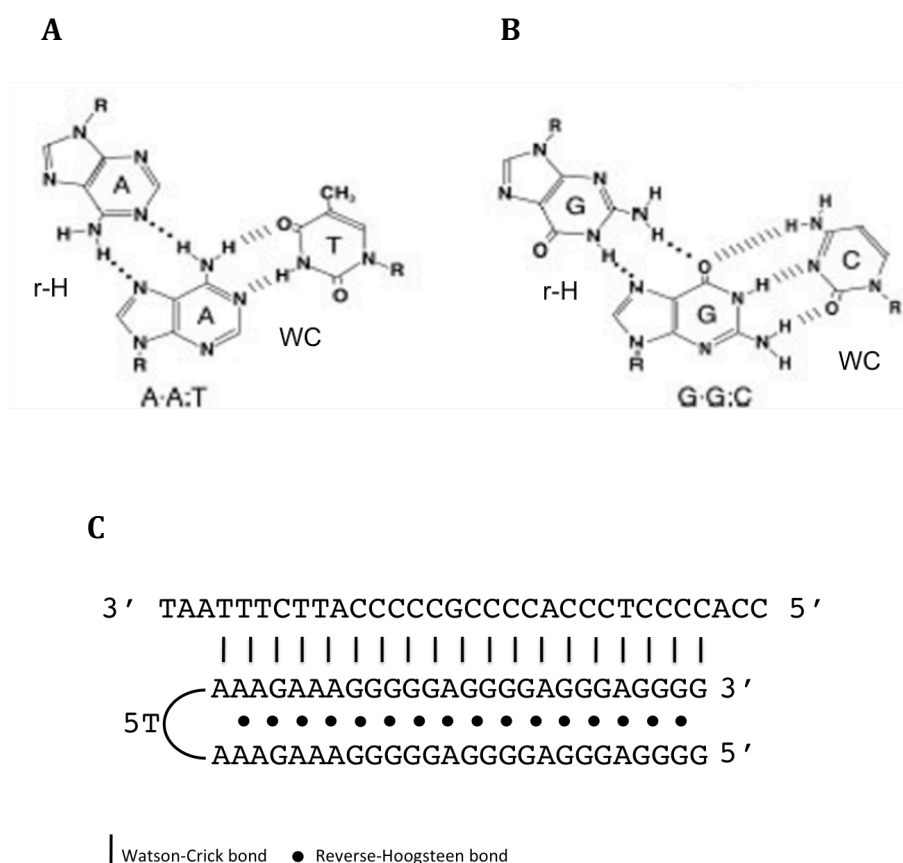


Figure 6. Formation of Watson-Crick (WC) and reverse Hoogsteen bonds (r-H) between two adenines (A) and two guanines (B). Schematic representation of the triplex formed upon PPRH binding to the target sequence (C).

PPRHs were first described for gene silencing (de Almagro et al., 2009, de Almagro et al., 2011a, Rodriguez et al., 2013, Villalobos et al., 2015, Villalobos et al., 2014), and were classified in either template-PPRHs that bind to the template DNA strand (de Almagro et al., 2009), or Coding-PPRHs binding to the coding DNA strand (de Almagro et al., 2011a). PPRHs are an inexpensive tool to decrease gene expression that shows high stability and low immunogenicity properties without the need for chemical modifications (Villalobos et al., 2014). In our group, PPRHs have been used successfully to target different genes including DHFR, survivin, BCL-2, TOP1, mTOR, MDM2 and MYC (de Almagro et al., 2009, de Almagro et al., 2011a, Rodriguez et al., 2013, Villalobos et al., 2015). The design and usage of these molecules have been gradually improved in terms of specificity, affinity and efficacy. For example, the polypyrimidine sequences found in the genome are not always pure stretches and present purine interruptions. In the past, we found that using adenines in both domains of the PPRH sequence, we could maintain the binding to the target sequence (Coma et al., 2005). Subsequently, it was shown that PPRHs including pyrimidine interruptions in their sequences instead of substituting the interruptions by adenines (Wild-Type-PPRHs), have a higher affinity to their target sequence, and therefore, they are meant to have less off-target effects (Rodriguez et al., 2015).

In the present thesis we used PPRH molecules to repair point mutations, using the *dihydrofolate reductase* gene as a model.

1.2.1. G-quadruplex

Nucleic acids present a high conformational flexibility that allows them to form different structures such as double helix, triplex, i-motifs; formed by cytosine-rich sequences, or G-quadruplex in which we are going to focus on.

Guanines have the ability to form Hoogsteen hydrogen bonds with other guanines, thus forming G-tetrads structures (Figure 7). These G-tetrads consist on a coplanar conformation where each guanine forms four hydrogen bonds. This arrangement forms a central cavity where a cation can be placed to stabilize the molecule.

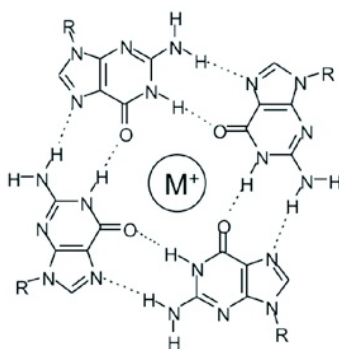


Figure 7. G-tetrad structure with a cation placed in the central cavity.

The stacking of two or more G-tetrads can lead to a four-stranded nucleic acid structure called G-quadruplex (G4) (Burge et al., 2006), held by loops arising from the nucleotides that are not involved themselves in the tetrads. G4 may be described as parallel or antiparallel depending on the direction of the strands, and can also be intramolecular or intermolecular when they are formed by a single DNA (or RNA) strand, or by two or four strands, respectively (Figure 8).

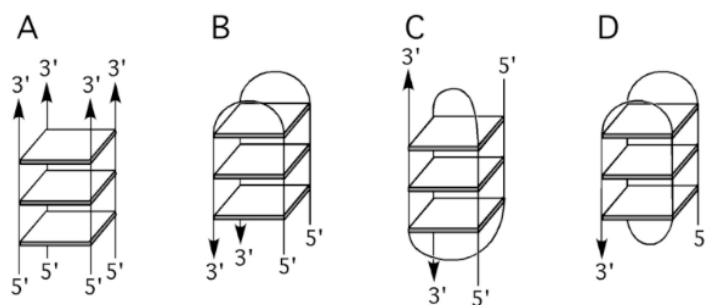


Figure 8. Some possible topologies for G-quadruplex structures. (A) Topologies constructed from four parallel strands, (B) from two strands that are non-crossing or (C) cross-over, and (D) from a single strand (P. Shing Ho and Megan Carter, 2011).

Therefore, G4 present a high polymorphism, and one sequence can lead to different quadruplex structures depending on the number of stacked G-tetrads, the polarity of the strands and the location and length of the loops.

The presence of consecutive guanines runs in a given sequence can impair its folding into a reverse Hoogsteen hairpin structure in favor of a guanine quadruplex (G4) structure, especially under physiological conditions. Differently from duplex or triplex structures, the stability of G4s depends on the nature of the cation present in solution; in particular they are strongly stabilized by the physiological relevant potassium ion. Therefore, it is important to take into consideration the possible high guanine content when designing a PPRH motif.

Various assays have been previously performed to study the binding of PPRHs to single or double stranded DNA (de Almagro et al., 2011a). Gel shift assays allowed to ascertain the binding of a PPRH oligonucleotide to its pyrimidine target, but not to prove triplex formation. A specific PPRH was found to bind its ssDNA target in a sequence specific manner more strongly than that achieved by the Watson-Crick bonds in dsDNA, supporting the formation of a triplex structure (Coma et al., 2005).

Our interest in this work is to study the secondary structures that PPRHs could form in the presence of a high amount of guanines, including G4, the stability of PPRH oligonucleotides, and the complexes they form with their pyrimidine target sequences such as triplex structures.

1.3. DIHYDROFOLATE REDUCTASE (DHFR)

Dihydrofolate reductase (DHFR) is a key enzyme in folate metabolism, especially in the *de novo* synthesis of the purine ring, thymidylate and glycine, and therefore, it is involved in DNA replication. DHFR catalyzes the reduction of dihydrofolate (DHT) to tetrahydrofolate (THF), which is a cofactor in the transfer of moncarbon groups, and participates in the formation of biologically active cofactors, such as 5,10-methylenetetrahydrofolate (5,10-CH₂-THF), 10-formyltetrahydrofolate (10-CHO-THF) and 5-methyltetrahydrofolate (5-CH₃-THF) (Figure 9).

- Thymidylate synthase (TS) catalyzes the conversion of deoxyuridine monophosphate (dUMP) to deoxythymidine monophosphate (dTMP), yielding DHF as a secondary product from the oxidation of 5,10-CH₂-THF, which in turn, is regenerated by the DHFR enzyme, thus reducing DHF to THF. dTMP is the first step for the *de novo* synthesis of pyrimidines (Olsen, 1991). The 5,10-CH₂-THF cofactor is regenerated from serine, which donates a carbon to THF to form 5,10-CH₂-THF and glycine, in a reaction mediated by serine hydroxymethyltransferase.
- In purine synthesis, 10-CHO-THF, obtained by the oxidation of 5,10-CH₂-THF, is used as a carbon donor (Gonen and Assaraf, 2012). 10-CHO-THF is regenerated through the reaction of THF with a formate molecule. Other enzymes involved in this pathway are glycinamide ribonucleotide formyltransferase (GARFT), responsible for the formation of the imidazole ring of purines, and phosphoribosylaminoimidazolecarboxamide formyltransferase (AICARFT), an enzyme that generates the inosine monophosphate (IMP) intermediary (Gonen and Assaraf, 2012).
- 5-CH₃-THF is a cofactor for the conversion of homocysteine to methionine catalyzed by methionine synthase (Nesher et al., 1991, Nesher et al., 1996). Methionine can be conjugated to a molecule of ATP, originating s-adenosyl methionine, which is involved in the synthesis of phospholipids and neurotransmitters, and in many important reactions of methylation of DNA and proteins (Fox and Stover, 2008).

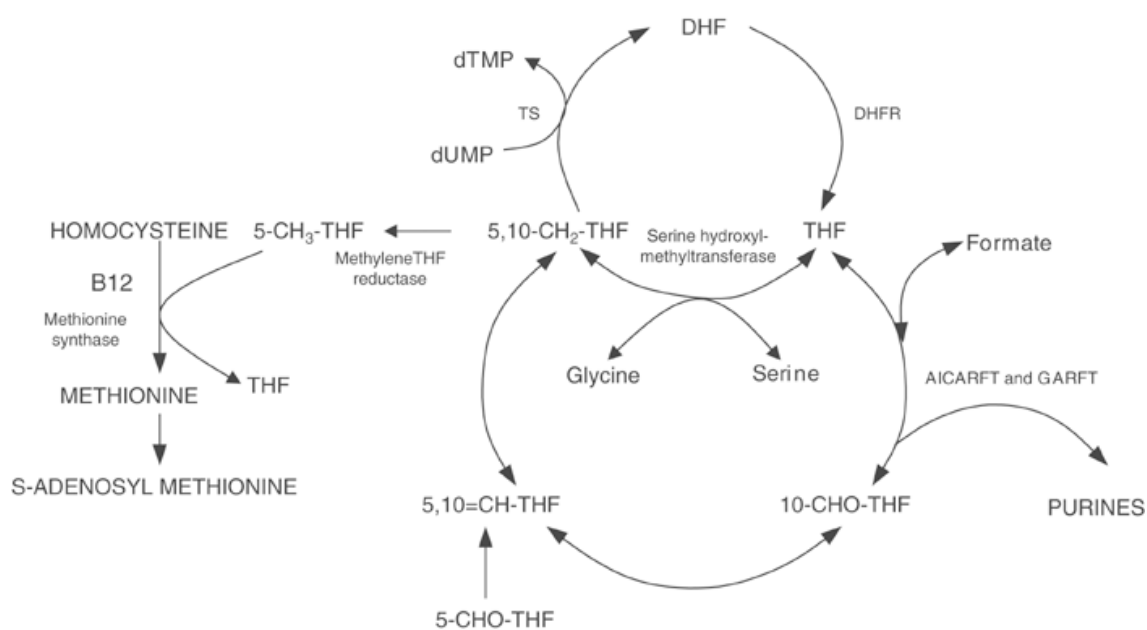


Figure 9. Scheme of metabolism of folates (Zhao and Goldman, 2003).

1.3.1. Methotrexate

Methotrexate (MTX or amethopterin) is a 4-amino 10-methyl analog of folic acid (Figure 10) that binds to the catalytic center of DHFR (Olsen, 1991), inhibiting the enzyme in a competitive and reversible manner, and thus interfering in the regeneration of tetrahydrofolate.

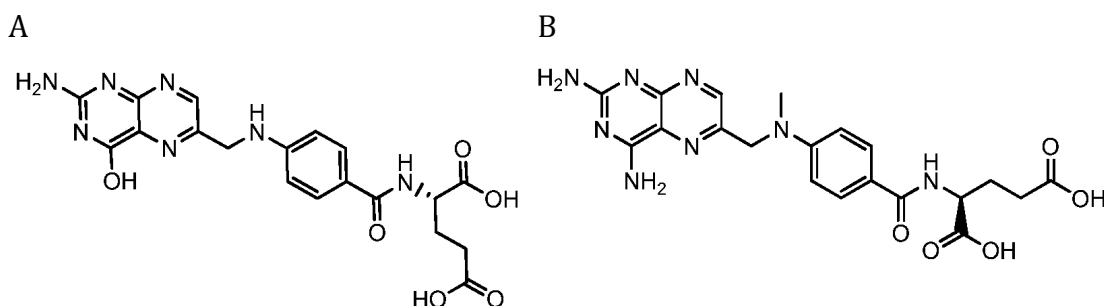


Figure 10. Structure of (A) folates and (B) Antifolate methotrexate (Garland et al., 2009).

MTX was one of the first antimetabolite drugs developed; it causes the inhibition of DNA synthesis that leads to cellular death. It has been used as a chemotherapeutic agent for over 50 years (Farber et al., 1956) in human malignancies such as infectious and inflammatory diseases, and cancer (Gonen and Assaraf, 2012) alone or in combination with other chemotherapeutic agents (Chu et al., 1996, Jolivet et al., 1983).

As folates, MTX is predominantly taken up into the cell via the reduced folate carrier protein (RFC). Once in the cytoplasm, MTX undergoes polyglutamylation by the sequential addition of multiple glutamate residues to the γ -carboxyl group catalyzed by folylpolyglutamate synthetase (FPGS) (Assaraf, 2007). Polyglutamylation ensures a metabolite with longer half-life that sustains and enhances target enzyme inhibition (Allegra et al., 1985, Allegra et al., 1987, Baggott et al., 1986). The main targets of polyglutamated MTX are DHFR, TS, and several enzymes involved in purine synthesis (Assaraf, 2007).

1.3.1.1. MTX resistance mechanisms and prevention

The efficacy of MTX is often compromised by the development of resistance in cancer cells (Hryniuk and Bertino, 1969), attributed to different mechanisms such as:

- Alterations in its target enzyme DHFR (Alt et al., 1978, Dicker et al., 1990, Srimatkandada et al., 1989, Yu and Melera, 1993). Mutations in the *dhfr* gene reduce the affinity of the DHFR protein to MTX, and therefore, enzyme inhibition by the drug.
- Decreased drug import into the cells by RFC (Dixon et al., 1994, Jansen et al., 1998, Roy et al., 1998, Sun et al., 2004, Zhao et al., 1999). Decreased levels of the RFC protein have been described in different neoplasias (Rots et al., 2000, Wettergren et al., 2005, Ifergan et al., 2003, Kastrup et al., 2008, Ferreri et al., 2004).
- Decreased polyglutamylation of MTX (Rhee et al., 1993, Roy et al., 1997) the mechanism by which folates and antifolates are retained into the cell. Some studies have suggested that this decrease could be due to point mutations in the FPGS (Liani et al., 2003).

- Amplification of the *dhfr* locus (Carman et al., 1984, Curt et al., 1984). This mechanism of resistance has been described in both cell lines (Noe and Ciudad, 1995, Selga et al., 2009) and in samples from patients with different neoplasias (Gonen and Assaraf, 2012).
- Increased MTX output due to the overexpression of different members of the ABC transporters family (Chen et al., 2002, Hooijberg et al., 2003).

To prevent MTX resistance, several approaches have been described:

- To modulate the levels of transporters responsible for the intracellular import of MTX, such as a combination therapy with either cAMP (Rothen et al., 2004) or cGMP (Stark and Assaraf, 2006) analogues, and a DNA methylation inhibitor (Worm et al., 2001), or the overexpression of the folate receptors (FR) FR α and FR β (Assaraf, 2007).
- To increase the lipophilicity of the MTX molecule to favor its uptake by passive diffusion across the cell membrane, for instance, by modifying the carboxyl groups of the glutamate molecule (Rahman and Stratton, 1998).
- To identify additional genes associated with drug response. Overexpression or underexpression of various genes has been described in different tumor cell lines resistant to MTX, and the modulation of these genes has been shown to sensitize cells to MTX: *IMPDH2*, *survivin*, *topoisomerase I*, *vimentin* (Penuelas et al., 2005a), *AKR1C1* (Selga et al., 2008b), *PKC α* , *enolase2*, *caveolin 1*, *E-cadherin* (Selga et al., 2008a), *DKK1* (Selga et al., 2009) and *S100A4* (Mencia et al., 2010) in colon cancer cells; *IMPDH* in osteosarcoma (Penuelas et al., 2005b); *UGT1A* (Selga et al., 2009, de Almagro et al., 2011b) in breast cancer cells; and *EEF1A1* in pancreatic cancer, osteosarcoma and leukemia cells (Selga et al., 2009).

It has also been observed the over- or underexpression of different miRNAs in MTX resistant cells when compared to sensitive cells. Incubation with MTX reduces the levels of miR-224, suggesting a possible mechanistic relation between MTX and miR-224, and that the underexpression of miR-224 could be involved in the initial steps of the resistance of MTX (Mencia et al., 2011).

1.3.2 Micro RNAs (miRNAs)

miRNAs are non-coding 22nt single-stranded RNAs that act at the post-transcriptional level as repressors of gene expression through the hybridization to specific sequences mainly in the 3'-UTR of their mRNA targets (Carrington and Ambros, 2003, Bartel, 2004). It has also been shown that miRNAs can bind to 5'-UTR (Lytle et al., 2007) and coding regions of the mRNA targets (Kloosterman et al., 2004). The effect of miRNAs is via mRNA destabilization (Eichhorn et al., 2014) or translational repression (Lee et al., 2015), although in recent studies, it has been demonstrated that under specific conditions, the binding between miRNA and its target can stimulate gene translation (Vasudevan et al., 2007).

miRNA genes are primarily transcribed by RNA polymerase II leading to a hundred nt long precursor called the primary-miRNA (pri-miRNA) (Lee et al., 2004). Once transcribed, pri-miRNA containing both a 5'-cap structure (7MGpppG) as well as a 3'-end poly(A) tail (Cai et al., 2004) folds in a hairpin structure. This molecule is then processed by RNase III Drosha associated to a double stranded-RNA-binding protein DGCR8, generating a ~70nt precursor miRNA (pre-miRNA) product, also structured as a hairpin, plus a 2nt overhang at the 3' end (Lee et al., 2003). Pre-miRNA is then recognized by the Ran-GTP-dependent transporter Exportin 5 and exported to cytoplasm by an active process (Yi et al., 2003), maintaining the stem-loop structure. In the cytoplasm, the RNase III enzyme Dicer associated to TRBP cleaves the stem-loop of the pre-miRNA generating a miRNA/miRNA* duplex of about 21nt, similar to a siRNA (Grishok et al., 2001, Hutvagner et al., 2001). One of the duplex strands will be the mature miRNA guide, selected according to thermodynamic properties. The other strand, miRNA*, can be degraded or selected as a functional product to play important biological roles (Bhayani et al., 2012). microRNAs are then associated to different proteins to form RNA-induced silencing complexes (RISC). These complexes are formed by the mature single-stranded miRNA molecule, AGO proteins and other proteins that act as regulatory or effector factors (Filipowicz et al., 2005, Sontheimer, 2005) (Figure 11).

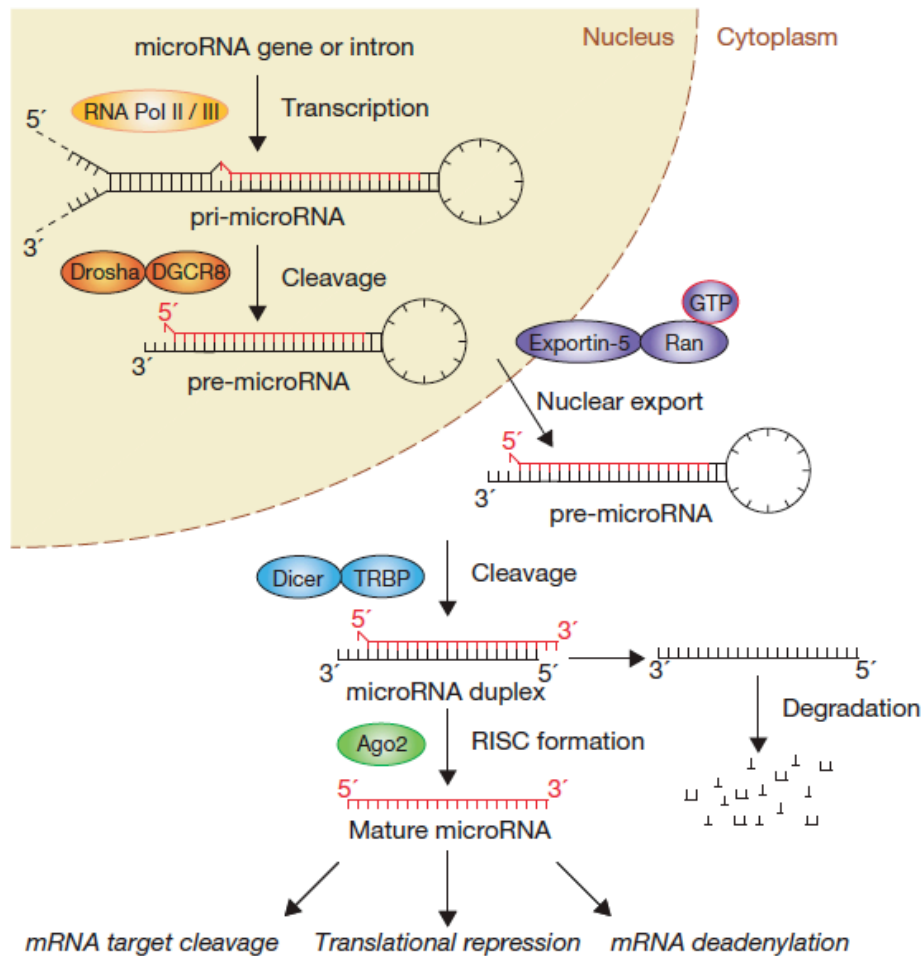


Figure 11. Many roads to maturity: microRNA biogenesis pathways and their regulation (Winter et al., 2009).

When microRNAs are totally complementary to the mRNA target, the RNase H catalytic domain of AGO proteins degrade the mRNA. In animals, the complementary region of miRNAs and their targets is formed by just 6-7nt, the seed sequence or seed region (Bartel, 2004), which is mainly situated at position 2-7 from the miRNA 5' end. Thus, the seed sequence has to be perfectly complementary to the miRNA, even though the remaining sequence does not match.

Different mechanisms have been attributed to the repression of gene expression by miRNAs:

- Translational repression, which can be divided into three steps:
 - Repression at the initiation step of the translation, for which the presence of the 5'-cap structure (7MGpppG) is necessary (Humphreys et al., 2005, Pillai et al., 2005), as well as the blockage of the association between the mRNA and the ribosomal 40S-subunit (Mathonnet et al., 2007).
 - Repression at post-initiation steps due to either slowed elongation or ribosome 'drop-off'.
 - Proteolysis: mRNA targets can be translated by active polysomes, but nascent polypeptides could be degraded by proteases (Nottrott et al., 2006).
- mRNA deadenylation, decapping and decay. Binding of miRNAs to their mRNA targets can lead to deadenylation and subsequently decay of the target mRNA sequence.

miRNAs are involved in many cellular processes such as development, proliferation, differentiation, cell fate determination, apoptosis, signal transduction, organ development, host-viral interactions and tumorigenesis (Huang et al., 2011). Therefore, it has become evident that miRNAs play a significant role in most of the developmental and pathological processes in animals. In addition, it has been shown that miRNAs are deeply involved in the progress of chemosensitivity or chemoresistance in various types of cancer (Ma et al., 2010, Migliore and Giordano, 2013). miRNA expression pattern varies in tumor cells when compared to normal cells of the same tissue, or between different subtypes of the same cancer, as well as in tumor cells that become resistant. Functional genomics has been very useful to study and characterize these variations in the expression patterns of miRNAs.

In this direction, miRNA microarrays of sensitive and MTX-resistant HT29 colon cancer cells were performed in our laboratory, and miR-224 was found to be greatly underexpressed in MTX-resistant cells. This result was also confirmed in Caco-2 colon cancer cells and in leukemia cells K562. miR-224 was functionally

validated by using an anti-miR, and a decreased in the MTX sensitivity in normal cells was observed, mimicking the resistant phenotype. Furthermore, using TargetScan 5.1 software and integrating the results with the data from expression microarrays previously performed, 7 genes were identified as possible targets for miR-224 that were also overexpressed in resistant cells. The overexpression of CDS2, DCP2, HSPC159, MYST3 and SLC4A4 was validated at the mRNA level by qRT-PCR, and viability assays shown an increased sensitivity to MTX when siRNA were used against SLC4A4 or incubation of PolyPurine Reverse Hoogsteen (PPRH) hairpins against CDS2 or HSPC159 was performed (Mencia et al., 2011).

Additionally, a SNP in the 3'-UTR region of DHFR mRNA conferring resistance to MTX has been described. This SNP prevents the recognition of the mRNA by miR-24, so that the inhibitory effect of this miRNA is lost, leading to the overexpression of DHFR, which allows the cell to overcome MTX-induced cytotoxic effect (Mishra et al., 2007).

2. OBJECTIVES

This work is divided in two main parts, one related with gene correction for gene therapy purposes, and a second part related with a methodology to study interactions between miRNAs and its mRNA targets.

Therefore, the major aims of this work were the following:

- I. To study and develop repair-PPRHs as a gene therapy tool.
 - To study the *in vitro* capacity of PPRHs to bind to the dsDNA to maintain it in an open conformation.
 - To design different repair-PPRHs to be tested in mammalian cells to repair a point mutation in a *dihydrofolate reductase (dhfr)* minigene.
 - To explore the capacity of repair-PPRHs to correct endogenous point mutations in different mammalian cell lines.
 - To analyze *in vitro* the possible formation of G4 structures when repair-PPRHs contain a high proportion of guanines, and to study the properties of triplex conformation formed by repair-PPRHs when bound to their target sequence.

- II. To study miRNA-mRNA interactions *in vitro*.
 - To validate electrophoretic mobility shift assays as a methodology to study the interaction of miRNA-mRNA.

3. MATERIALS AND METHODS

Materials and Methods are described within the articles presented in the “Results” section of this thesis. However, the specific materials used in this work are described in this section, as well as the special methodology.

3.1. Materials

3.1.1. Cell lines

In this work we have used Chinese Hamster Ovary (CHO) cells. The UA21 cell line derives from the K1 parental cell line, but conserving just one copy of the *dhfr* gene (Urlaub et al., 1983). An extended collection of mutant cell lines containing point mutations in the *dhfr* gene have been used in the repair experiments. All these mutations cause the deficiency in DHFR protein. The DG44 cell line is a deletion mutant of the *dhfr* gene. DG44-p11Mut cells are cells that initially lacked the *dhfr* gene and were stably transfected with a mutated *dhfr* plasmid (Table 1).

Cell line	Position	Alteration	Base changes	Coding change
DG44	-	Deletion of the <i>dhfr</i> gene	-	-
DG44-p11Mut	102 (exon 2)	Substitution	TAC > TAG	Amber in place
DA5	541 (exon 6)	Deletion (-G)	GAA > -AA	Opal at 584 in exon 6 (normal termination is at 562)
DA7	235 (exon 3)	Substitution	GAG > TAG	Amber in place
DU8	136 +1 (exon2/intron2)	Double substitution	G/gt > A/at	Exon 2 skipped Opal at 139
DF42	541 (exon 6)	Substitution	GAA > TAA	Ochre in place
DP12B	370 – 2 (intron 4)	Substitution	ag > tg	Exon 5 skipped Opal at 504
DI33A	493 (exon6)	Insertion (+G)	GGG / GGGG	Opal at 505

Table 1. Cell lines used in this work. DG44 (Urlaub et al., 1986); DG44-p11Mut (Sole et al., 2014); DA5 and DA7 (Carothers et al., 1993b); DU8 (Urlaub et al., 1989); DF42 (Carothers et al., 1986); DP12B (Carothers et al., 1993a) and DI33A (Carothers et al., 1993a, Chasin et al., 1990).

3.1.2. Culture media

All cell lines were grown in Ham's F12 medium supplemented with sodium bicarbonate (14mM, Applichem), Penicillin G sodium salt (100 U/mL, Sigma-Aldrich), streptomycin (100 mg/L, Sigma-Aldrich), containing 7% fetal bovine serum (FBS, GIBCO, Invitrogen). Cells were incubated at 37°C in a humidified 5% CO₂ atmosphere. Trypsinization to expand and harvest cells were performed using 0.05% trypsin (Sigma-Aldrich) in PBS 1X (154mM NaCl, 3.88mM H₂NaPO₄, 6.1mM HNaPO₄, pH 7.4).

A selective medium lacking hypoxanthine (-H), or lacking glycine, hypoxanthine, and thymidine (-GHT medium, GIBCO) the final products of DHFR activity, containing 7% of dialyzed fetal bovine serum (Invitrogen) was used to select for repaired cells. Dialysis of the serum was performed to eliminate the low molecular weight products such as hypoxanthine and thymidine, and it was carried out in PBS 1X at 4°C, renewing the solution each 2-3hr, with a total of 4 washes.

3.1.3. Dihydrofolate reductase minigene

The mutated *dhfr* minigene (p11Mut) was derived from the starting plasmid pDCH1P11 (Noe et al., 1999), containing the six exons of the hamster *dhfr* gene, intron 1, about 400bp of the 5'-flank, and the first of the three-polyadenylation sites in exon 6. The p11Mut construct (Figure 1) carries a nonsense mutation in exon 2, a stop codon, generated by PCR using the pDCH1P11 as a template and an oligonucleotide containing the desired mutation (G > C). The PCR fragment was digested with EcoRI and BamHI and cloned unidirectionally into pDCH1P11 digested with the same restriction enzymes. DNA sequencing was carried out to confirm the mutation.

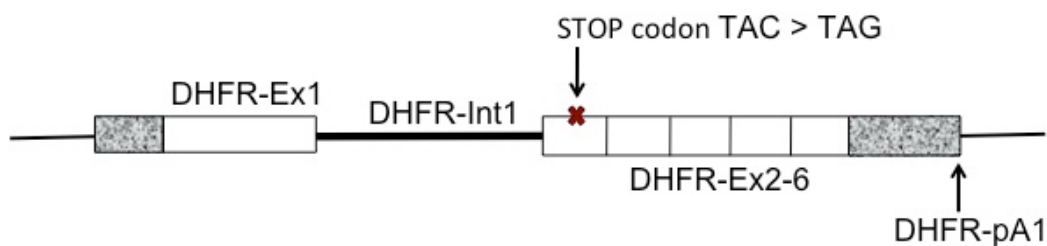


Figure 1. Mutated *dhfr* minigene p11Mut. White boxes represent exons, with shaded areas indicating the 5'-untranslated region. Black line represents intron 1. The arrows indicate polyadenylation site (pA1), and the nonsense mutation (red cross) in exon 2. Adapted from (Noe et al., 2003).

3.1.4. PPRHs and oligonucleotides for binding assays

The nomenclature of PPRHs and oligonucleotides is as follows:

- Hp: PPRH hairpin
- pPy: Polypyrimidine
- pPu: Polypurine
- RO: putative Repair Oligonucleotide

In the following table, the sequences of PPRHs and oligonucleotides used in the binding assays to study their *in vitro* characteristics are described (Table 2).

Name	Sequence (5' to 3')
	Sequences used <i>in vitro</i>
Hp13	GGAAAAGGAGGA-(T) ₅ -AGGAGGAAAAGG
pPy13	CCTTTTTCCTCCT
pPu13	AGGAGGAAAAGG
pPy25	TTGATGCCTTTTTCCTCCTGGACTT
pPu25	AAGTCCAGGAGGAAAAGGCATCAA
RO10	TTTTTCCTCC
pPy61	TCTTTCTGTTAGCCTTTCTTCTCATAGACTTAAAATTTAT

	ACTTGATGCCTTTTTTCCTCCT
pPu61	AGGAGGAAAAAGGCATCAAGTATAAATTTTAAGTCTATGA GAAGAAAGGCTAACAGAAAGA
Hp23	AGAAAGA <u>AAA</u> <u>AA</u> GGAAAGAAGAG-(T) ₅ - GAGAAGAAAGG <u>AAA</u> <u>AA</u> AGAAAGA
RO20	TAGACTTCAAATTTATACTT
p11Mut-pPy50	GAACGAATTCAAGTA G TTCCAAAGAATGACCACCACCTCCT CAGTGGAAAG
p11Mut-pPu50	CTTCCACTGAGGAGGTGGTGGTCATTCTTTGGAA C TACTTG AATTCGTTC

Table 2: The names and sequences of the PPRHs and ODNs are indicated. Mismatches in the PPRHs compared to their targets are in red and underlined. The nonsense mutation of p11Mut duplex is in blue and in bold.

3.1.5. Repair- PPRHs

Unmodified repair-PPRHs were designed according to the rules of Hoogsteen and Watson–Crick pairing. All repair-PPRHs contain a PPRH core linked to a repair tail. The sequences are listed in Table 3 and Table 4.

3.1.6. PPRHs and oligonucleotides for structure characterization of PPRHs

PPRHs and other oligonucleotides used to study the triplex formation of PPRHs with their target sequences are detailed in the following table (Table 5).

Name	Sequence (5' to 3')
HpE6	GAGAAGAAAGGCTAACAGAAAGA-(T) ₅ - AGAAAGACAATCGGAAAGAAGAG
Y6	GCAAGTATCTTTCTGTTAGCCTTTCTTCTCATAGAC
HpE6rep6	CATCAAGTATAAATTTGAAGTCTATGAGAAGAAAGGCTAACAGAAAGA- (T) ₅ -AGAAAGACAATCGGAAAGAAGAG
Y6rep6	TCTTTCTGTTAGCCTTTCTTCTCATAGACTTCAAATTTATACTTGATG
R6rep6	CATCAAGTATAAATTTGAAGTCTATGAGAAGAAAGGCTAACAGAAAGA
rep6	CATCAAGTATAAATTTGAAGTCTAT
HpE2	GGAGGAGGAGGAG-(T) ₅ -GAGGAGGAGGAGG
Y2	AAGAATGACCACCACCTCCTCAGTGGAAG
HpE2rep2	GGAGGAGGAGGAG-(T) ₅ - GAGGAGGAGGAGGTCATTCTTTGGAAGTACTTGAATTC
Y2rep 2	GAATTC AAGTAGTTCCAAAGAATGACCACCACCTCCTC
R2rep2	GAGGAGGAGGAGGTCATTCTTTGGAAGTACTTGAATTC
rep2	TCATTCTTTGGAAGTACTTGAATTC

Table 5. Sequences of PPRHs and other oligonucleotides used. HpE6rep6 and HpE2rep2 are composed of a PPRH motif (HpE6 and HpE2) and single stranded oligonucleotide extension (rep6 and rep2). R6rep6 and R2rep2 are the complementary sequences of Y6rep6 and Y2rep2, which are the pyrimidine target sequences.

3.1.7. Oligonucleotides for miRNA-mRNA interactions

The sequences of the molecules used for the validation of the miRNA-mRNA interactions are indicated in Table 6.

Molecule	Sequence
miR-224	3' UUGCCUUGGUGAUCACUGAAC 5'
SLC4A4 3'-UTR	5' AAGCUUUCUAUUGUGACUUU 3'
anti-miR-224	5' A*A*C*GGAAC*C*AC*T*AGT*GAC*T*T*G 3'
anti-miR-13MIS	5' <u>T</u> * <u>T</u> * <u>G</u> * <u>CCT</u> AC* <u>CAC</u> *T* <u>ACAC</u> * <u>T</u> * <u>G</u> * <u>A</u> * <u>A</u> *G 3'
SLC4A4 3'-UTR-MM	5' AAGCUUUCUAUUC <u>CACUGAAU</u> 3'

Table 6. Sequences of the RNA and DNA molecules used in the validation of the miRNA-mRNA interactions work. For antisense oligodeoxynucleotides, phosphorothioate-modified bonds are indicated as *. Mismatch bases are indicated as underlined nucleotides.

miR-224 is formed by an RNA sequence corresponding to the mature form of miRNA-224.

SLC4A4 3'-UTR consists on a 2'-mer RNA sequence of the 3'-UTR corresponding to SLC4A4 bearing the target site for miR-224.

Anti-miR-224 corresponds to the complementary sequence of the mature form of miR-224.

Anti-miR-224-13MIS is used as a negative control for anti-miR-224 since it contains 13 mismatches.

SLC4A4 3'-UTR-MM is used as a negative control 3'-UTR sequence for the SLC4A4 RNA, bearing 6 mismatches in the target site for miR-224.

3.2. Methods

3.2.1. Transfection and selection

Transfection of repair-PPRH was carried out using the calcium phosphate method (Wigler et al., 1979), which involved the addition of 250 mM CaCl₂ to the DNA complex. DNA/CaCl₂ solution was added drop wise to an equal volume of sterile twice-concentrated HEPES-buffered saline (2X HBS; 280mM NaCl, 50mM HEPES, and 1.5 mM sodium phosphate, pH-adjusted to 7.1). The calcium phosphate/DNA precipitate was allowed to form for 30 min at room temperature without agitation. A total amount of 200 µL of the mix was added per well directly to the 1.8 ml of growth medium containing the cells. After 5–6hr of incubation at 37°C, the medium was replaced and the cells were incubated for an additional 24hr. At that time, Ham's F-12 was changed to selective Ham's F-12 medium lacking hypoxanthine (-H medium), or lacking glycine, hypoxanthine, and thymidine (-GHT medium, GIBCO), to initiate the selection of repaired cells.

- DG44 cells were transfected with repair-PPRH/p11Mut complexes since the DG44 cell line is a deletion mutant of the *dhfr* gene.
- DG44-p11Mut cells were transfected with the different repair-PPRHs in the absence of plasmid, as the p11Mut target sequence was already stably transfected into the cells.
- All the endogenous mutated *dhfr* cell lines were also transfected with the repair-PPRH alone, since they already contain a point mutation at the endogenous level.

Different amounts of repair-PPRHs were used, ranging from 2 to 5µg per transfection.

Each assay was conducted a minimum of three times, and for each repair-PPRH that succeeded in repairing the point mutation, a minimum of three colonies from three different replicates were analyzed for DNA sequencing, and for DHFR levels of mRNA, protein, and activity.

In specific cases, transfection of repair-PPRH was also performed using 10µM of the cationic liposome DOTAP (N[1-(2,3-Dioleoyloxy)propyl]-N,N,N-trimethylammonium methyl-sulfate) (Biontech). A total amount of 200µL of a

Ham's F-12 medium solution containing the DOTAP/repair-PPRH complex was incubated for 20 min at room temperature without agitation and subsequently added per well directly to 800 μ L of growth medium containing the cells.

To calculate the frequency of correction, colonies were fixed with formaldehyde 2% (V/V), and stained by crystal violet 0.5% (P/V) (Sigma-Aldrich). Results are expressed by the number of colonies appearing in each well divided by the number of cells initially plated.

3.2.2. Enzymatic activity assay

DHFR activity of -GHT selected colonies was determined by an indirect method based on the incorporation of radioactive deoxyuridine into cellular DNA, which depends on the generation of tetrahydrofolate by DHFR from folate supplied in the medium. Tetrahydrofolate is used in the reductive methylation of deoxyuridylate to thymidylate (Figure 2). The latter is subsequently incorporated into DNA (Ciudad et al., 1988), which is then isolated by precipitation in ethanol at 66% (final concentration) (Noe et al., 1998).

Dishes (35 mm) were seeded with $3 \cdot 10^4$ or $1 \cdot 10^5$ *dhfr* negative or repaired cells in 1 ml of selective -GHT medium lacking glycine, hypoxanthine, and thymidine. After 16hr, 2 μ Ci of 6-[3 H] deoxyuridine (20mCi/mmol; Moravek Biochemicals) was added for 24hr. Cells were rinsed twice with phosphate-buffered saline (PBS 1X) and lysed in 100 μ l of 0.1% sodium dodecyl sulfate. The lysate was harvested in 31ET paper (Whatman) and washed three times with 66% cold ethanol containing 250mM NaCl, dried, and counted in a scintillation counter by adding 5 mL of Biogreen (Scharlau).

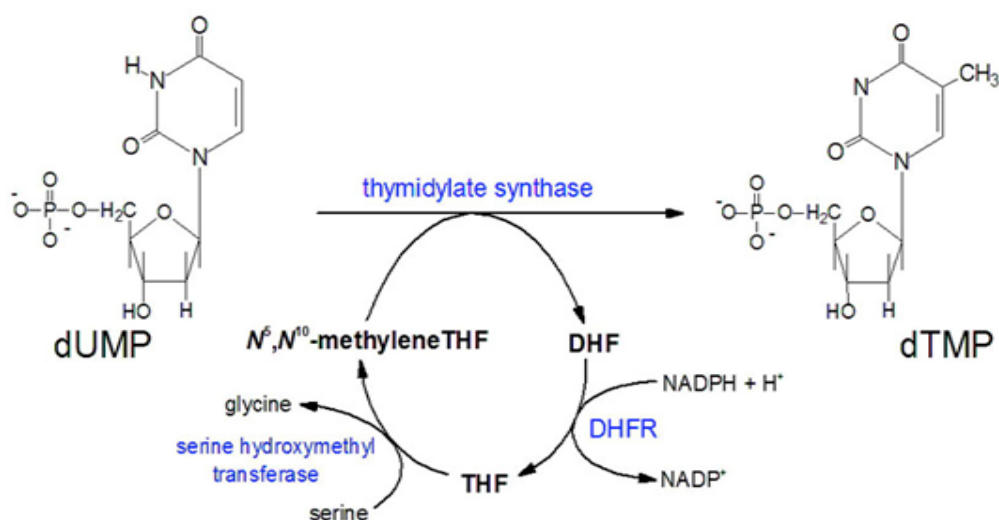


Figure 2. Thymidylate synthase catalyzes the conversion of deoxyuridine monophosphate (dUMP) to deoxythymidine monophosphate (dTMP), an essential component of DNA. Dihydrofolate reductase (DHFR) is the responsible to regenerate tetrahydrofolate (THF) from dihydrofolate (DHF), which is a product of the thymidylate synthase reaction.

3.2.3. UV absorption measurements

Oligonucleotides were dissolved in a 10 mM cacodylic acid buffer at pH 7.0 (adjusted with LiOH), containing 100 mM NaCl or 100 mM KCl, in the absence or in the presence of 10 mM MgCl₂. Oligonucleotide strand concentrations are indicated in figure legends (error on strand concentration was estimated to be about 10%). UV absorbance as a function of temperature was recorded on a XL spectrophotometer (Secomam) according to the following protocol: samples were heated at 92°C for 2 min, cooled from 95 to 5°C at a rate of 0.2°C min⁻¹, kept at 5°C for 10 min, and heated from 5 to 95°C at a rate of 0.2°Cmin⁻¹; the absorbance was recorded at 260, 295 nm and 335 nm. Temperature was varied with a circulating water bath and measured with an inert glass sensor immersed into a water-filled quartz cell; evaporation at high temperatures and condensation at low temperatures were prevented by a layer of mineral oil and by a dry airflow in the sample compartment, respectively. Melting profiles were corrected for baseline drifting (the absorbance at 335 nm was subtracted from the absorbance at 260

and 295 nm). We defined “temperature of thermal transition”, T_t , the first derivative of the absorbance as a function of the temperature. Thermal difference spectra (TDS) were obtained by subtracting the absorption spectrum at low temperature (5°C) from the absorption spectrum at high temperature (95°C); absorption spectra at low temperature were recorded after annealing the samples from 95 to 5°C at 0.2°C min⁻¹. Circular dichroism (CD) spectra were recorded on a JASCO-810 spectropolarimeter.

3.2.4. Fluorescence measurements

Fluorescence measurements were carried on an HpE6 oligonucleotide bearing a 6-carboxyfluorescein (FAM) at its 5' extremity and a Dabcyl quencher at its 3'-extremity. For melting experiments, FAM-HpE6-Dabcyl was dissolved in a 10 mM cacodylic acid buffer at pH 7.0 (adjusted with LiOH), containing 100 mM KCl and 10 mM MgCl₂, at 0.2 mM strand concentration, in the absence or in the presence of 2 mM Y6 oligonucleotide. FAM emission as a function of temperature was recorded on a SPEX Fluorolog (HORIBA Jobin Yvon) at an excitation wavelength of 470 nm and an emission wavelength of 520 nm; temperature was raised with a circulating water bath from 5 to 80°C at 1°C min⁻¹. FAM-HpE6-Dabcyl emission as a function of temperature was normalized between the minimum and the maximum of fluorescence; we defined “temperature of half-dissociation”, $T_{1/2}$, the temperature at which the normalized fluorescence was equal to 0.5.

3.2.5. Electrophoretic mobility shift assay (EMSA)

Single-stranded, double-stranded ODN and PPRHs (100 ng) were 5'-end-labeled with [γ -³²P]-ATP (Perkin Elmer) by T4 polynucleotide kinase (New England BioLabs) in a 10 μ l reaction mixture, according to the manufacturer's protocol. After incubation at 37°C for 1 hr, 15 μ l of TE buffer (1mM EDTA and 10mM Tris, pH 8.0) was added to the reaction mixture, which was subsequently filtered through a Sephadex G-25 spin-column (Pharmacia) to eliminate the unincorporated [γ -³²P]-

ATP. DNA-PPRH bindings were analyzed by incubating different radiolabeled PPRHs, dsDNA or ssDNA (20,000 cpm), in the presence or absence of unlabeled DNAs (10nM), in a buffer containing 10mM MgCl₂, 100mM NaCl, and 50mM HEPES, pH 7.2. Binding reactions (20μl) were incubated for 30min at 37°C before running the electrophoresis. Unspecific DNA (Salmon Sperm DNA or poly-dI:dC) was included in each sample. Electrophoresis was performed on a nondenaturing 12% polyacrylamide gels containing 10mM MgCl₂, 5% glycerol, and 50mM HEPES, pH 7.2. Gels were run for 3–4 hr at 220V (12V/cm) using a running buffer containing 10mM MgCl₂ and 50mM HEPES, pH 7.2, at 4°C, dried, and analyzed on a Storm 840 Phosphorimager (Molecular Dynamics). (Specific conditions detailed in Article III).

4. RESULTS

4.1 Article I

Repair of Single-Point Mutations by Polypurine Reverse Hoogsteen Hairpins

Anna Solé, Xenia Villalobos, Carlos J. Ciudad, and Véronique Noé

Hum Gene Ther Methods. 2014 Oct;25(5):288-302

Background: Polypurine Reverse Hoogsteen (PPRH) hairpins are non-modified molecules formed by two homopurine antiparallel domains linked by a five thymidine loop, that are able to fold as a hairpin structure by intramolecular Reverse Hoogsteen bonds. We have previously described the ability of PPRHs to bind to polypyrimidine stretches forming a triplex structure, and their capacity to decrease gene expression.

Objectives: To explore the necessary conditions to maintain the dsDNA in an open conformation for the subsequent binding of a given repair oligonucleotide, and the ability of PPRHs to repair a single-point mutation in mammalian cells, using the *dihydrofolate reductase (dhfr)* gene as a model.

Results: Different PPRHs were designed to study their ability to open a dsDNA target to allow for the subsequent binding of a putative repair oligonucleotide. Hence, various binding assays were carried out, using fragments of different lengths from the Chinese hamster *dhfr* gene combined with two PPRHs and two repair oligonucleotides.

Repair-PPRHs used in the repair experiments were also designed and studied for their ability to bind to their polypyrimidine target. Repair-PPRHs are formed by a Hoogsteen hairpin core, extended on one of its ends by an oligonucleotide tail, homologous to the point mutation region of the target, except for the position of the mutated nucleotide to be corrected.

These repair-PPRHs were tested in two different approaches at the cellular level. In the first approach, a mutated *dhfr* plasmid was previously incubated with the repair-PPRH and then transfected to DG44 cells, which are *dhfr* negative. In the

second approach the mutated plasmid was stably transfected in *dhfr* minus cells, obtaining the new DG44-p11mut cell line, and the repair-PPRH was then transfected alone. In both approaches, repair-PPRHs were able to correct a single-point nonsense mutation in a *dhfr* minigene. Furthermore, this methodology was successfully applied to repair a single-point mutation at the endogenous *dhfr* gene locus, using as a model the DA5 cell line with a deleted nucleotide in *dhfr* exon six.

Conclusions: We have shown that repair-PPRHs are able to repair a nonsense mutation in the *dhfr* gene, either in an extra chromosomal location or when the mutated plasmid is stably transfected into cells. First evidences of the capacity of repair-PPRHs to correct a point mutation at an endogenous locus were also observed.

Repair of Single-Point Mutations by Polypurine Reverse Hoogsteen Hairpins

Anna Solé, Xenia Villalobos, Carlos J. Ciudad, and Véronique Noé

Abstract

Polypurine reverse Hoogsteen hairpins (PPRHs) are formed by two intramolecularly bound antiparallel homopurine domains linked by a five-thymidine loop. One of the homopurine strands binds with antiparallel orientation by Watson–Crick bonds to the polypyrimidine target sequence, forming a triplex. We had previously reported the ability of PPRHs to effectively bind dsDNA displacing the fourth strand away from the newly formed triplex. The main goal of this work was to explore the possibility of repairing a point mutation in mammalian cells using PPRHs as tools. These repair-PPRHs contain different combinations of extended sequences of DNA with the corrected nucleotide to repair the point mutation. As a model we used the dihydrofolate reductase gene. On the one hand, we demonstrate *in vitro* that PPRHs bind specifically to their polypyrimidine target sequence, opening the two strands of the dsDNA, and allowing the binding of a given repair oligonucleotide to the displaced strand of the DNA. Subsequently, we show at a cellular level (Chinese ovary hamster cells) that repair-PPRHs are able to correct a single-point mutation in a dihydrofolate reductase minigene bearing a nonsense mutation, both in an extrachromosomal location and when the mutated plasmid was stably transfected into the cells. Finally, this methodology was successfully applied to repair a single-point mutation at the endogenous locus, using the DA5 cell line with a deleted nucleotide in exon six of the *dhfr* gene.

Introduction

A LARGE NUMBER of characterized genetic disorders are associated with a mutation in a single gene. Cystic fibrosis, sickle-cell anemia, Tay–Sachs disease, and different types of cancer are some examples of diseases caused by a point mutation. The repair of single-point mutations in a gene within its endogenous locus has been the focus of many researchers during the past decades. After all these efforts, still more methods are needed to improve gene correction. In this direction, an alternative method could be the usage of polypurine reverse Hoogsteen hairpins (PPRHs) that are formed by two antiparallel homopurine domains bound by reverse Hoogsteen bonds linked by a five-thymidine loop (Coma *et al.*, 2005). One of the homopurine strands binds with antiparallel orientation and high affinity, by Watson–Crick bonds, to the polypyrimidine target sequence displacing the fourth strand away from the newly formed triplex (Coma *et al.*, 2005).

We had previously described the design and usage of template-PPRHs that bind to the template DNA strand (de Almagro *et al.*, 2009), and coding-PPRHs binding to the coding DNA strand (de Almagro *et al.*, 2011), as a tool to decrease gene expression (Rodríguez *et al.*, 2013) that shows high stability and low immunogenicity properties without the

need for chemical modifications (Villalobos *et al.*, 2014). In this work we explored a new application for PPRHs: the repair of point mutations, an ambitious gene therapy strategy.

Correction of a single nucleotide can be achieved by gene replacement or by gene repair, the latter consisting of targeting the genomic DNA with different types of oligonucleotides. In the last years, different approaches have emerged to correct a point mutation at the DNA level without provoking double-strand breaks (DSB): chimeric RNA-DNA oligonucleotides, which were first designed by Kmiec's group (Yoon *et al.*, 1996); single-stranded oligonucleotides, studied for the first time in 1988 (Moerschell *et al.*, 1988); bifunctional triple-helix-forming oligonucleotides, formed by two domains, a triplex forming oligonucleotide (TFO) domain and a repair domain (Chan *et al.*, 1999; Culver *et al.*, 1999); and several approaches of peptide nucleic acids (PNA) (Nielsen *et al.*, 1991; Egholm *et al.*, 1993), bis-PNA (Rogers *et al.*, 2002; Chin *et al.*, 2008), tc-PNA (Bentin *et al.*, 2003; Kaihatsu *et al.*, 2003), pc-PNA (Lohse *et al.*, 1999) (Demidov *et al.*, 2002; Lonkar *et al.*, 2009), and more recently PNA- single-stranded oligodeoxynucleotides (ssODNs) (Kayali *et al.*, 2010; Nik-Ahd and Bertoni, 2014).

Other approaches for gene repair involving DSB would be the nuclease-based methods, as homing endonucleases

(Kleinstiver *et al.*, 2012), zinc-finger nucleases (Urnov *et al.*, 2005; Urnov *et al.*, 2010), TALENs (Wood *et al.*, 2011; Liu *et al.*, 2012; Joung and Sander 2013), or CRISPR (Wiedenheft *et al.*, 2012; Hruscha *et al.*, 2013). One of the major hurdles in gene correction is that site-specific homologous recombination (HR) in mammalian cells occurs at a very low frequency (Hanson and Sedivy, 1995), although it can be enhanced by site-specific damage (Wang *et al.*, 1988) and cleavage (Rouet *et al.*, 1994; Bibikova *et al.*, 2001). However, TFOs without DNA-damaging adducts and bis-PNAs have also been shown to stimulate HR in a site-specific manner (Rogers *et al.*, 2002; Knauert *et al.*, 2006) and to induce mutagenesis through a pathway dependent on nucleotide excision repair (NER) (Wang *et al.*, 1996; Bailey and Weeks 2000). Based on these observations, we hypothesized that PPRHS could be an additional methodology for gene repair, since they also form triple-helix structures and consequently could induce recombination. It is also known by using chimeric RNA/DNA oligonucleotides that the DNA repair machinery of the cells recognizes a helical distortion, and the DNA sequence of the chimera can be used as a template to correct the mismatched base (Cole-Strauss *et al.*, 1999). Thus, in this study we used PPRHS containing different combinations of extended sequences of DNA with the corrected nucleotide to repair a point mutation (repair-PPRHs).

As a model, we used the dihydrofolate reductase (*dhfr*) gene. We started analyzing *in vitro* the binding of regular PPRHS to their polypyrimidine target sequences, the opening of the two strands of the dsDNA, and the binding of a given oligonucleotide to the displaced strand of the DNA. Subsequently, we studied whether, at a cellular level (Chinese ovary hamster [CHO] cells), repair-PPRHs were able to correct a single-point mutation in three approaches: (1) in an extrachromosomal *dhfr* minigene bearing a nonsense mutation, (2) when the mutated *dhfr* plasmid was stably transfected into the cells, and (3) in a cell line containing a single-nucleotide deletion in the *dhfr* locus.

Materials and Methods

Oligodeoxynucleotides

Unmodified PPRHS and ODNs were designed according to the rules of Hoogsteen and Watson-Crick pairing, depending on the desired interaction. The repair-PPRHs used in the cellular transfections for repair purposes contained A's on the bases opposite to the purines interruptions in the polypyrimidine strand, thus conferring them an optimal binding to the DNA targets (de Almagro *et al.*, 2009). However, when correcting the point mutation at the endogenous locus in DA5 cells, the complementary bases to the target interruptions were used in the PPRH. Lyophilized oligonucleotides (Sigma-

TABLE 1. SEQUENCE OF PPRHS AND OLIGONUCLEOTIDES USED IN THE STUDY

Name	Sequence (5' to 3') Sequences used in vitro
Hp13	GGAAAAAGGAGGA-(T) ₅ -AGGAGGAAAAAGG
pPy13	CCTTTTTCCTCCT
pPu13	AGGAGGAAAAAGG
pPy25	TTGATGCCTTTTTCCTCCTGGACTT
pPu25	AAGTCCAGGAGGAAAAAGGCATCAA
RO10	TTTTTCCTCC
pPy61	TCTTTCTGTTAGCCTTTCTTCTCATAGACTTAAAATTTAT ACTTGATGCCTTTTTCCTCCT
pPu61	AGGAGGAAAAAGGCATCAAGTATAAATTTTAAGTCTATGA GAAGAAAGGC TAACAGAAAGA
Hp23	AGAAAGAAAAAGGAAAGAAGAG-(T) ₅ -GAGAAGAAAGG <u>AAAA</u> AGAAAGA
RO20	TAGACTTCAAATTTTATACTT
<i>Sequences used in in vitro and in cellular experiments</i>	
HpE2rep	GGAGGAGGAGGAG-(T) ₅ -GAGGAGGAGGAGGTCATTCTTTGGAAGTACTTGAATTC
HpE2link	GAATTC <u>CAAGTACTTCCAAAGTTTTTGGAGGAGGAGGAG-(T)₅-GAGGAGGAGGAGG</u>
HpE2link-ds	GAATTC <u>CAAGTACTTCCAAATTTTTTGGAGGAGGAGGAG-(T)₅-GAGGAGGAGGAGG</u>
RO18	TTGGAAGTACTTGAATTC
HpE2ext	CCAAAGAATGTGGAGGAGGAGGAG-(T) ₅ -GAGGAGGAGGAGG
RO24	CATTCTTTGGAAGTACTTGAATTC
dHpE2link-rep	CTTTGGAACTACTTGAATTCTTTTTGAATTC <u>CAAGTACTTCCAAAGTTTTTGGAGGAGGAGGAG-(T)₅-GAGGAGGAGGAGG</u>
p11Mut-pPy50	GAACGAATTCAAGTAGTTCCAAAGAATGACCACCACCTCCTCAGTGGAAAG
p11Mut-pPu50	CCTCCACTGAGGAGGTGGTGGTCATTCTTTGGAAGTACTTGAATTCGTTT
HpE2rep-NH	AAGAAGAAGAAGA-(T) ₅ -GAGGAGGAGGAGGTCATTCTTTGGAAGTACTTGAATTC
HpE2rep-WC	CCTCCTCCTCCTC-(T) ₅ -GAGGAGGAGGAGGTCATTCTTTGGAAGTACTTGAATTC
HpE6rep	CATCAAGTATAAATTTGAAGTCTATGAGAAGAAAGGCTAACAGAAAGA-(T) ₅ -AGA AAGACAATCGGAAAGAAGAG

PPRH, polypurine reverse Hoogsteen hairpins; ODNs, oligodeoxynucleotides.

The names and sequences of the PPRHS and ODNs are indicated. Mismatches in the PPRHS compared with their targets are underlined. The nonsense mutation is in bold, and the corresponding corrected nucleotide in the repair-PPRHs is in italic.

Aldrich) were dissolved in sterile and RNase-free TE (1 mM EDTA and 10 mM Tris-HCl, pH 8.0) to attain a stock solution of 1 mM, and maintained at -20°C . The sequences of PPRHs and ODNs are listed in Table 1.

Preparation of polypurine/polypyrimidine duplexes for binding assays

The target duplexes of the PPRHs were formed by mixing 25 μg of each single-stranded polypurine and polypyrimidine oligodeoxynucleotides in a 150 mM NaCl solution. After incubation at 90°C for 5 min, solutions were allowed to cool down slowly to room temperature. The target duplex Dup576 was prepared by PCR using dhfr-I1-Fw: TACTGGCTGGATTGGGTTAG and dhfr-E4-Rv: CGGAAGTCCCAACTATC as primers and p11Mut as the template. The duplexes were purified in a nondenaturing 20% polyacrylamide gel and quantified by absorbance at 260 nm at 25°C .

Oligodeoxynucleotide labeling

Single-stranded, double-stranded ODN and PPRHs (100 ng) were 5'-end-labeled with [γ - ^{32}P]-ATP (Perkin Elmer) by T4 polynucleotide kinase (New England BioLabs) in a 10 μl reaction mixture, according to the manufacturer's protocol. After incubation at 37°C for 1 hr, 15 μl of TE buffer (1 mM EDTA and 10 mM Tris, pH 8.0) was added to the reaction mixture, which was subsequently filtered through a Sephadex G-25 spin-column (Pharmacia) to eliminate the unincorporated [γ - ^{32}P]-ATP.

DNA-PPRH binding assays

Triplex formation was analyzed by incubating different radiolabeled PPRHs, dsDNA or ssDNA (20,000 cpm), in the presence or absence of unlabeled DNAs (10 nM), in a buffer containing 10 mM MgCl_2 , 100 mM NaCl, and 50 mM HEPES, pH 7.2. Binding reactions (20 μl) were incubated for 30 min at 37°C before running the electrophoresis. Unspecific DNA (Salmon Sperm DNA or poly-dI:dC) was included in each sample. Electrophoresis was performed on a nondenaturing 12% polyacrylamide gels containing 10 mM MgCl_2 , 5% glycerol, and 50 mM HEPES, pH 7.2. Gels were run for 3–4 hr at 220 V (12 V/cm) using a running buffer containing 10 mM MgCl_2 and 50 mM HEPES, pH 7.2, at 4°C , dried, and analyzed on a Storm 840 Phosphorimager (Molecular Dynamics).

Construction of a mutated dhfr minigene

The mutated *dhfr* minigene (p11Mut) was derived from the starting plasmid pDCH1P11 (Noe *et al.*, 1999), containing the six exons of the hamster *dhfr* gene, intron 1, about 400 bp of the 5'-flank, and the first of the three polyadenylation sites in exon 6. The p11Mut construct carries a nonsense mutation in exon 2, a stop codon, generated by PCR using the pDCH1P11 as a template and an oligonucleotide containing the desired mutation (G > C). The PCR fragment was digested with *EcoRI* and *BamHI* and cloned unidirectionally into pDCH1P11 digested with the same restriction enzymes. DNA sequencing was carried out to confirm the mutation.

Cell culture

DG44 CHO cells (Urlaub *et al.*, 1986), lacking the *dhfr* gene, were used as a recipient cell line in the transfection

experiments. The DG44-p11Mut cell line was obtained by transfecting the plasmid p11Mut into DG44 cells using the calcium phosphate method and by selection with 400 $\mu\text{g}/\text{ml}$ of Geneticin (Sigma-Aldrich). The presence of the plasmid in this cell line was confirmed by PCR. In parallel, DG44 cells were transfected with plasmid pDCH1P11, but this time the selection and the growth were performed in selective medium lacking hypoxanthine (–H), one of the final products of DHFR activity, containing 7% of dialyzed fetal bovine serum (Invitrogen) to generate the cell line DG44-p11, used as a positive control. DA5 cells were used to repair the single-point mutation at the genomic level. DA5 is a CHO cell line, containing a single copy of the *dhfr* genomic gene bearing an endogenous point mutation in the exon 6 (GAA/G > -AAG) causing a frameshift in the sequence. UA21 is a CHO cell line containing one wild-type copy of the *dhfr* gene, and it was used as a positive control. Cells were grown in Ham's F12 medium containing 7% fetal bovine serum (Invitrogen), and incubated at 37°C in a humidified 5% CO_2 atmosphere. For expansion and harvesting, cells were detached with 0.05% trypsin (Sigma).

PPRH/plasmid DNA binding before cellular transfection in DG44 cells

Three μg (0.9 pmol) of mutant pDCH1P11 plasmid (p11Mut) was incubated with a 233-fold molar excess of various PPRHs in a 10 μl final volume in the presence of binding buffer at 37°C for 2 hr. In experiments using additional repair oligonucleotides, the mix was heated to 90°C for 30 sec and annealed at room temperature. All control oligonucleotides were also subjected to the same heat-annealing protocol (Chan *et al.*, 1999).

Transfection and selection

Transfection of repair-PPRH/p11Mut complexes was carried out using the calcium phosphate method (Wigler *et al.*, 1979), which involved the addition of 250 mM CaCl_2 to the DNA complex. DNA/ CaCl_2 solution was added dropwise to an equal volume of sterile twice-concentrated HEPES-buffered saline ($2\times$ HBS; 280 mM NaCl, 50 mM HEPES, and 1.5 mM sodium phosphate, pH-adjusted to 7.1). The calcium phosphate/DNA precipitate was allowed to form for 30 min at room temperature without agitation. An amount of 200 μl of the mix was added per well directly to the 1.8 ml of growth medium containing the recipient cells (DG44). After 5–6 hr of incubation at 37°C , the medium was replaced and the cells were incubated for an additional 24 hr. At that time, Ham's F-12 was changed to selective Ham's F-12 medium lacking hypoxanthine (–H medium), to initiate the selection of repaired cells. In the case of DG44-p11Mut, cells were transfected with the different repair-PPRHs in the absence of plasmid, as the p11Mut target sequence was already stably transfected into the cells. DA5 were also transfected with the repair-PPRH alone, since this cell line already contains a point mutation at the endogenous level.

A total of 41 colonies were randomly selected and grown in selective medium (–H). Each assay was conducted a minimum of three times, and for each repair-PPRH that succeeded in repairing the point mutation, a minimum of three colonies from three different replicates were analyzed for DNA sequencing, and for DHFR levels of mRNA, protein, and activity.

mRNA analysis

After selecting and growing the colonies, total RNA from repaired cells was extracted using Tri Reagent (Life Technologies), according to the manufacturer's specifications. The amount of RNA was determined by measuring its absorbance (260 nm) at 25°C in a Nanodrop ND-1000 spectrophotometer (Thermo Scientific). cDNA was synthesized in a 20 μ l reaction mixture containing 500 ng of total RNA, 250 ng of random hexamers (Roche), 10 mM dithiothreitol, 20 units of RNasin (Promega), 0.5 mM of each dNTP (AppliChem), 4 μ l of buffer (5 \times), and 200 units of Moloney murine leukemia virus reverse transcriptase (RT) (Invitrogen). The reaction mixture was incubated at 37°C for 1 hr. An amount of 3 μ l of the cDNA mixture was used for PCR amplification by real time.

Real-time PCR. The reaction was performed using the ABIPrism 7000 Sequence Detection System (Applied Biosystems) in a final volume of 20 μ l, containing 3 μ l of cDNA, 2 \times SYBR Select Master Mix (Applied Biosystems, Life Technologies), 0.125 μ M of reverse and forward primers (Sigma-Aldrich), and H₂O. Adenine phosphoribosyltransferase (APRT) mRNA was used to normalize the results. The primer sequences were as follows: Dhfr2-Fw, 5'-AAG AACGGAGACCTCCCTG-3'; Dhfr2-Rv, 5'-CGGAACTG CCTCCAATATC-3'; Aprt-Fw, 5'-GCATGGCGGCAAG ATCGACT-3'; Aprt-Rv, 5'-GTTCTAAGGCGTCTTTCTGG-3'. PCR cycling conditions were 2 min at 50°C, 10 min denaturation at 95°C, followed by 40 cycles of 15 sec at 95°C and 1 min at 60°C, and fourth stage of 15 sec at 95°C, 20 sec at 60°C, and 15 sec at 95°C. The mRNA amount of the target gene, normalized to APRT, was given by the $\Delta\Delta C_T$ method, where C_T is the threshold cycle indicating the fractional cycle number at which the amount of amplified mRNA reached the threshold of fluorescence.

Western blot analysis

Cells were harvested by trypsinization and treated with lysis buffer (50 mM HEPES, 0.5M NaCl, 1.5 mM MgCl₂, 1 mM EGTA, 10% glycerol, 1% Triton X-100, pH 7.2), supplemented with protease inhibitor mixture (Sigma-Aldrich). Total extracts were maintained at 4°C for 1 hr with vortexing every 15 min. Cell debris was removed by centrifugation (10,000 $\times g$ for 10 min). Protein concentrations were determined by the Bio-Rad protein assay (based on the Bradford method, using bovine serum albumin as a standard; Sigma-Aldrich).

Total protein cell extracts (100 μ g) were electrophoresed on SDS-12% polyacrylamide gels, and transferred to a polyvinylidene difluoride membrane (Immobilon P; Millipore) using a semidry electroblotter. The membranes were probed with antibodies against DHFR (1:250 dilution) and tubulin (1:800 dilution; CP06; Calbiochem, Merck) to normalize the results. Signals were detected with HRP-conjugated antibodies: anti-rabbit (1:2500 dilution; P0399; Dako) for DHFR, anti-mouse (1:2500 dilution; sc-2005; Santa Cruz Biotechnology) for tubulin, and enhanced chemiluminescence using ECL Prime Western Blotting Detection Reagent, as recommended by the manufacturer (GE Healthcare). Tubulin and total protein loading were both used to normalize the results. Chemiluminescence was detected

with ImageQuant LAS 4000 Mini (GE Healthcare) and quantification was performed using the Image Quant 5.2 software.

DHFR activity

The method is based on the incorporation of radioactive deoxyuridine into cellular DNA, which depends on the generation of tetrahydrofolate by DHFR from folate supplied in the medium. Tetrahydrofolate is used in the reductive methylation of deoxyuridylate to thymidylate. The latter is subsequently incorporated into DNA, which is then isolated by a simple trichloroacetic acid precipitation procedure (Ciudad *et al.*, 1988).

Dishes (35 mm) were seeded with 3×10^4 *dhfr* negative or repaired cells in 1 ml of selective medium lacking glycine, hypoxanthine, and thymidine (-GHT). After 16 hr, 2 μ Ci of 6-[³H] deoxyuridine (20 mCi/mmol; Moravek Biochemicals) was added for 24 hr. Cells were rinsed twice with phosphate-buffered saline and lysed in 100 μ l of 0.1% sodium dodecyl sulfate. The lysate was harvested in 31ET paper (Whatman) and washed three times with 66% cold ethanol containing 250 mM NaCl, dried, and counted in a scintillation counter.

DNA sequencing

Total DNA was obtained using the Wizard Genomic DNA Purification Kit (Promega), according to the manufacturer's specifications. PCR was performed to amplify the specific region containing either the point mutation or the repaired nucleotide, using the Biotools DNA Polymerase (Biotools). The primer sequences were as follows: Dhfr2-Fw and Dhfr2-Rv for the DG44 and the DG44-p11Mut cell lines (as described in mRNA analysis), and Dhfr6-Fw (GTCATGTGTCTTCAATGGGTG) and Dhfr6-Rv (TCTAAAGCCAACACAAGTCCC) for the DA5 cell line. Sequencing was carried out by Macrogen.

Results

Before testing if repair-PPRHs were able to repair a point mutation in cells, we carried out different binding assays to explore the necessary conditions to open the double-stranded DNA target, using different combinations of PPRHs, for the subsequent binding of a putative repair oligonucleotide. To this aim, we used two assays: in the first one, we designed a simplified model using a fragment of the Chinese hamster *dhfr* gene, to study the potential of PPRHs to keep the dsDNA open. In the second, the repair-PPRHs to be used in DG44 cells were also studied for their ability to bind to the polypyrimidine target.

Design of PPRHs for binding assays

We searched for polypurine/polypyrimidine sequences within the Chinese hamster *dhfr* gene with a length ranging between 10 and 20 bases (Coma *et al.*, 2005). Two sequences located within exon 6, separated from each other by 25 nucleotides, were selected. One of them contains 13 contiguous purines/pyrimidines, and the other one contains 23 nucleotides taking into account three interruptions. Two PPRHs were designed against these sequences, Hp13 and Hp23, respectively. Two oligonucleotides were also designed to bind

to the displaced polypurine strand. All the sequences used in this study are listed in Table 1.

Binding assays

Three approaches were carried out to test the ability of PPRHs to bind to its target, displacing the polypurine strand of the dsDNA, and allowing the subsequent binding of a specific oligonucleotide to the displaced polypurine strand. This study was carried out by electrophoretic mobility shift assays.

In the first approach, all the oligonucleotides (PPRH, DNA duplex, and the specific oligonucleotide) had the same length of 13 nucleotides. The incubation of Hp13 with its radiolabeled polypurine/polypyrimidine dsDNA target (Dup13) resulted in the formation of two new bands, one corresponding to a triple helical structure between Hp13 and the polypyrimidine single strand of the duplex DNA, and the other corresponding to the displaced polypurine strand (Fig. 1, lane 3). Furthermore, the addition of a specific oligonucleotide with a sequence equivalent to the polypyrimidine single strand of the duplex (pPy13) resulted in the disap-

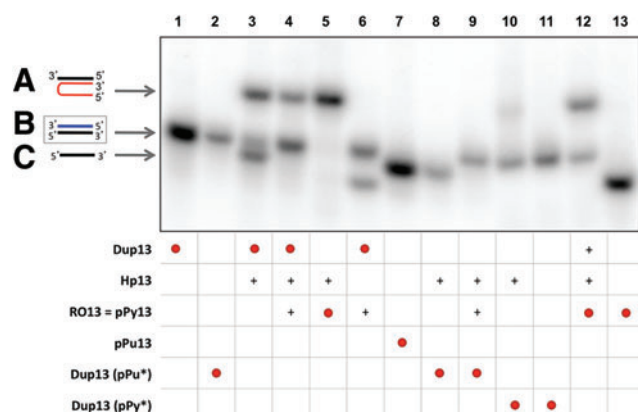


FIG. 1. Binding of PPRH to dsDNA. This binding occurs by triplex formation with the polypyrimidine strand, causing the displacement of the polypurine strand, allowing the binding of a specific oligonucleotide (RO13 or pPy13). Lane 1, labeled ^{32}P -polypurine/ ^{32}P -polypyrimidine duplex (Dup13) (1.2 nM); lane 2, ^{32}P -polypurine/polypyrimidine duplex (1.33 nM); lane 3, ^{32}P -Dup13 plus hairpin-13 (Hp13); lane 4, ^{32}P -Dup13 plus Hp13 and RO13; lane 5, ^{32}P -RO13 (13.14 nM) plus Hp13; lane 6, ^{32}P -Dup13 plus RO13; lane 7, ^{32}P -polypurine ssDNA (pPu13) (2.28 nM); lane 8, ^{32}P -polypurine/polypyrimidine duplex plus Hp13; lane 9, ^{32}P -polypurine/polypyrimidine duplex plus Hp13 and RO13; lane 10, polypurine/ ^{32}P -polypyrimidine duplex (12.6 nM) plus Hp13; lane 11, polypurine/ ^{32}P -polypyrimidine duplex; lane 12, ^{32}P -RO13 plus Hp13 and Dup13; lane 13, ^{32}P -RO13. All unlabeled species were used at 10 nM. Incubations were performed at 37°C for 30 min. As unspecific DNA, 1 μg of Salmon Sperm DNA was added. ssDNA targets, duplexes and triplexes are indicated by arrows. Labeled oligonucleotides are indicated as •. (+) indicate unlabelled oligonucleotides present in the reaction. (A) Triplex structure between the PPRH and the polypyrimidine strand (lanes 3, 4, 5, and 12). (B) Binding between the displaced polypurine strand and a specific polypyrimidine oligonucleotide (lanes 1, 2, 3, 4, 6, 9, 10, 11, and 12). (C) Displaced polypurine strand (lanes 3, 7, and 8). PPRH, polypurine reverse Hoogsteen hairpin. Color images available online at www.liebertpub.com/hgtb

pearance of the displaced polypurine strand, and an increase in the intensity of the duplex band, thus demonstrating that the specific oligonucleotide had bound to the polypurine strand, previously displaced by the PPRH. Proper controls were introduced to observe the mobility of the different single- and double-stranded DNAs, labeled either in the polypurine or polypyrimidine strand, or both.

In the second approach, the potency of Hp13 to open dsDNA was studied by increasing the length of the duplex dsDNA (Dup25). In this approach, the incubation of labeled Hp13 plus its Dup25 target originated a light-shifted band (Fig. 2, lane 4) of the same mobility as the triplex formed between Hp13 and its polypyrimidine ssDNA target (Fig. 2, lane 3). Once the strand displacement was observed, we performed the incubation of labeled Hp13 with Dup25 in the presence of a labeled specific polypyrimidine oligonucleotide RO10, corresponding to the complementary sequence of the polypurine strand of the duplex, which resulted in the appearance of three different bands in the electrophoresis (Fig. 2, lane 5). The lower one had the same mobility as RO10 (Fig. 2, lane 9) and the intermediate band corresponded to the binding

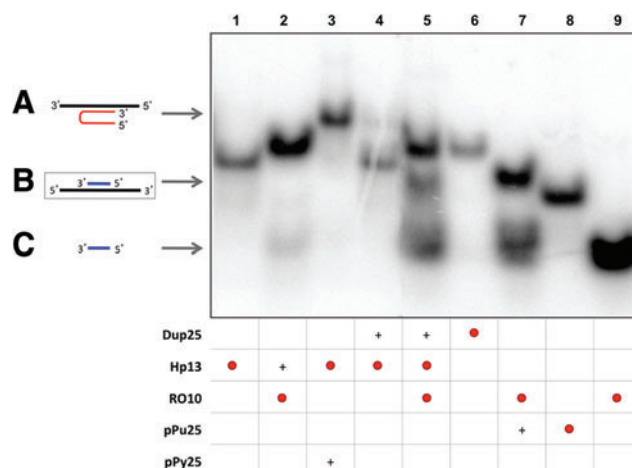


FIG. 2. Binding between the displaced polypurine strand of the duplex (pPu25) and a specific polypyrimidine oligonucleotide (RO10). Lane 1, labeled ^{32}P -Hp13 (2.9 nM); lane 2, specific polypyrimidine ^{32}P -oligonucleotide (RO10) (17.1 nM) plus Hp13; lane 3, ^{32}P -Hp13 plus polypyrimidine ssDNA (pPy25); lane 4, ^{32}P -Hp13 plus polypurine/polypyrimidine duplex (Dup25); lane 5, ^{32}P -Hp13 plus ^{32}P -RO10 plus Dup25; lane 6, ^{32}P -dup25 (3.7 nM); lane 7, ^{32}P -RO10 plus polypurine ssDNA (pPu25); lane 8, ^{32}P -pPu25 (3.2 nM); lane 9, ^{32}P -RO10. All unlabeled probes were used at 10 nM except for the Dup25 in lane 5, which was used at 1 μM to provide an excess of duplex to be bound by the PPRH and prevent that the PPRH would sequester RO, since RO10 is also complementary to the PPRH sequence. The whole mixture of all samples was heated at 50°C before binding reaction. Incubations were performed at 37°C for 30 min. An amount of 0.5 μg of poly-dI:dC was added to each sample. Oligonucleotides are indicated by arrows. Labeled oligonucleotides are indicated as •. (+) indicate unlabelled oligonucleotides present in the reaction. (A) Triplex structure between PPRH and polypyrimidine strand (lanes 3 and 4). (B) Binding between the displaced polypurine strand and a specific polypyrimidine oligonucleotide (lanes 5 and 7). (C) Repair-oligonucleotide (RO10) (lanes 2, 5, 7, and 9). Color images available online at www.liebertpub.com/hgtb

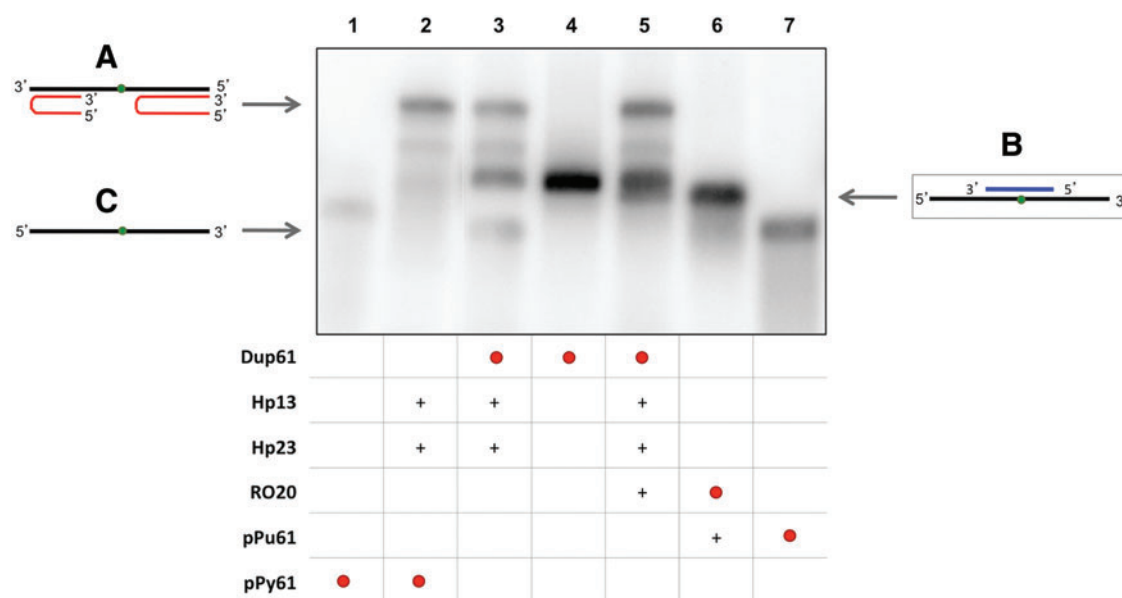


FIG. 3. Binding between the displaced polypurine strand of the duplex (pPu61) and a specific polypyrimidine oligonucleotide (RO20). Lane 1, labeled ^{32}P -polypyrimidine ssDNA (pPy61) (0.99 nM); lane 2, ^{32}P -pPy61 plus hairpin-13 (Hp13) and hairpin-23 (Hp23); lane 3, ^{32}P -polypurine/ ^{32}P -polypyrimidine dsDNA (Dup61) (0.19 nM) plus Hp13 and Hp23; lane 4, ^{32}P -Dup61 (pPu-61/pPy-61 duplex); lane 5, ^{32}P -Dup61 plus Hp13, Hp23 and RO20; lane 6, specific ^{32}P -RO20 (0.82 nM) plus polypurine ssDNA (pPu61); lane 7, ^{32}P -pPu61 (0.66 nM). The entire mixture of all samples was heated at 75°C before the binding reaction. Incubations were performed at 37°C for 30 min. An amount of 1 μg of poly-dI:dC was added to each sample. Oligonucleotides are indicated by arrows. Labeled oligonucleotides are indicated as •. (+) indicate unlabelled oligonucleotides present in the reaction. (A) Triplex structure between the two PPRHs and polypyrimidine strand (lanes 2, 3, and 5). (B) Binding between displaced the polypurine strand and a specific polypyrimidine oligonucleotide (lanes 5 and 6). (C) Displaced polypurine strand (lanes 3 and 7). Color images available online at www.liebertpub.com/hgtb

between pPu25 and RO10 (Fig. 2, lane 7), confirming that a specific polypyrimidine oligonucleotide was able to bind to a polypurine-displaced ssDNA strand, and the upper band was attributed to the binding between Hp13 and RO10 (Fig. 2, lane 2), as they have complementary sequences. The required controls were included to confirm the results.

The third approach was designed with an interruption in the duplex (61bp, Dup61) to simulate a point mutation. We incubated the labeled dsDNA duplex with both Hp13 and Hp23 either in the absence (Fig. 3, lane 3) or in the presence (Fig. 3, lane 5) of a longer specific oligonucleotide (RO20). As shown in Fig. 3, the band corresponding to pPu61 was shifted upward (compare lanes 3 and 5), originating a band of the same mobility as the binding between pPu61 and RO20 (lane 6), which indicated that RO20 was able to bind to polypurine ssDNA after the opening of the duplex. The two PPRHs were also incubated separately and at lower concentrations with the radiolabeled dsDNA. Hp23 alone and the combination of Hp13 and Hp23 were able to displace the polypurine strand even at 0.3 nM, while Hp13 alone was needed at least at 3 nM (data not shown). Unrelated competitors were unable to interfere with targets recognition (data not shown). In previous works, we had demonstrated the ability of PPRHs to bind to different concentrations of longer dsDNA sequences (152 and 227 bp) (Coma *et al.*, 2005).

Design of repair-PPRHs for cellular transfection in DG44 and DG44-p11Mut

To design the repair-PPRHs used in the repair experiments at the *dhfr* minigene level, we searched in the p11Mut

sequence for a polypyrimidine domain near to the stop codon introduced in the exon 2 of the *dhfr* plasmid. A sequence of 13 nucleotides downstream of the nonsense mutation was selected, containing two purine interruptions. We designed different repair-PPRHs, all containing the same Hoogsteen hairpin core, substituting the two interrupting pyrimidines for adenines (“A”) (de Almagro *et al.*, 2009). This core was extended on one of its ends with a 25 nt tail homologous to the point mutation region of the target, except for the position of the mutated nucleotide, which was corrected. The extended tails were added to provide the PPRHs with the ability to repair the point mutation and were either directly attached to the hairpin core (HpE2rep) (Fig. 4C), or connected through thymidine linkers of different extensions (5–7 nt) (HpE2link and HpE2link-ds).

As a negative control, we used a PPRH with an extension 2 nt shorter than the location of the mutated base in the DNA (HpE2ext). Some of these repair-PPRHs were used either alone or hybridized to a repair oligonucleotide (RO18 or RO24) complementary to the extended tail of the repair-PPRH. A last design (dHpE2link-rep) contained the repair oligonucleotide covalently bound to the extended tail of the repair-PPRH by a loop. As negative controls, we designed HpE2rep-NH, unable to form the intramolecular Hoogsteen bonds, and HpE2rep-WC, forming Watson-Crick bonds between the two domains of the hairpin core. To confirm the specificity of the sequences, all repair-PPRHs were subjected to BLAST analyses, using the sequence corresponding to the arm of the PPRH binding to the DNA plus the repair tail, with a total length ranging from 24 to 48 nucleotides. The *dhfr* gene target obtained an *E*-value of 3×10^{-9} , while the first

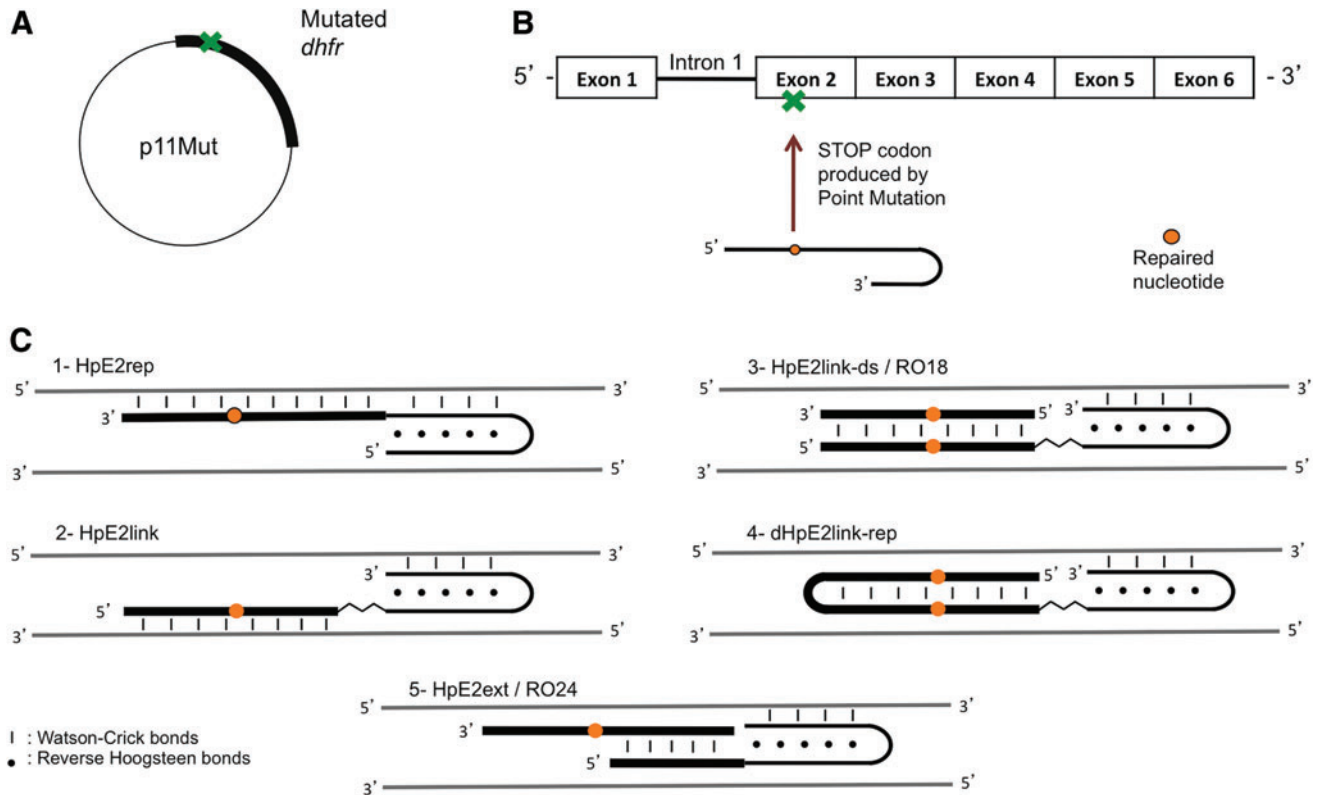


FIG. 4. Scheme of the p11Mut and the different PPRHs designs. (A) Scheme representing the p11Mut plasmid containing the nonsense mutation in the *dhfr* minigene. (B) The *dhfr* minigene contained the six exons of the hamster *dhfr* gene and its intron 1. The point mutation is localized in exon 2, where the repair-PPRHs are targeted. (C) Five repair-PPRHs were designed against the exon 2 of the *dhfr* gene. Two of them (HpE2rep and HpE2link) contained only a single extended sequence of DNA bearing the repaired nucleotide; HpE2link-ds/RO18 was complemented with an extra oligonucleotide hybridized to the extension of the repair-PPRH; dHpE2link-rep carried an oligonucleotide covalently bound to the extended tail by a loop, and the last repair-PPRH (HpE2ext/RO24) contained an extension tail until 2nt before the point mutation, and carried an extra oligonucleotide that did contain the repaired nucleotide. Color images available online at www.liebertpub.com/hgtb

unspecific target achieved an *E*-value of 0.68, thus showing high specificity of the repair-PPRH and minimizing the possible off-target effects. The sequences of the repair-PPRHs and ODNs are listed in Table 1.

Binding of repair-PPRHs for cellular transfection

The binding between the different repair-PPRHs and their target sequence was analyzed by labeling the double-stranded p11Mut target sequence. After incubation of the repair-PPRH with its dsDNA target (Dup50), a clear retarded band, corresponding to the triplex structure between four of the repair-PPRHs and the polypyrimidine strand, was observed (Fig. 5A, lanes 4, 6, 8, and 12). The binding of hairpin HpE2ext was not so clear, but it was definitively different from the probe alone and produced the strand displacement of the polypurine strand (pPu50). Strand displacement was also observed for HpE2rep and dHpE2link-rep (lanes 4 and 12). As controls, each repair-PPRH was also incubated with its labeled polypyrimidine single strand (pPy50), in the absence of the double-strand sequence target (lanes 5, 7, 9, 11, and 13), to confirm that the band with the lowest mobility corresponded to the triplex between Hp/pPy50 and that the band with the highest mobility corresponded to the displaced pPu50. HpE2Link-ds and HpE2ext carrying their repair oligonucleo-

tides RO18 and RO24, respectively, were also incubated with the p11Mut target, to confirm that the presence of the repair oligonucleotide did not affect the binding of the repair-PPRHs to their target (data not shown). Since genomic DNA is longer in length, we also performed binding assays with a dsDNA sequence of 576 bp with the repair-PPRHs target site centrally located. As it can be observed in Fig. 5B, the incubation of radiolabeled HpE2rep with its dsDNA target (Dup576) originated an upper band corresponding to the binding between the repair-PPRH and its polypyrimidine target.

Correction of a point mutation in DG44 cells

In an effort to demonstrate the ability of PPRHs to repair a point mutation in a cellular setting, 225,000 DG44 cells were seeded and transfected with repair-PPRHs plus p11Mut, previously incubated with each other to increase the likelihood of union and recognition of the specific sequence target. After transfection using calcium phosphate, cells were grown in selective medium (-H). Cell colonies were obtained with HpE2rep, HpE2link, and HpE2link-ds/RO18 (Table 1) at a repair frequency ranging between 1.5 and 1.7×10^{-3} (Fig. 8A). To calculate the repair frequency, the number of colonies appearing in each well were counted and divided by the number of cells initially plated. HpE2ext/

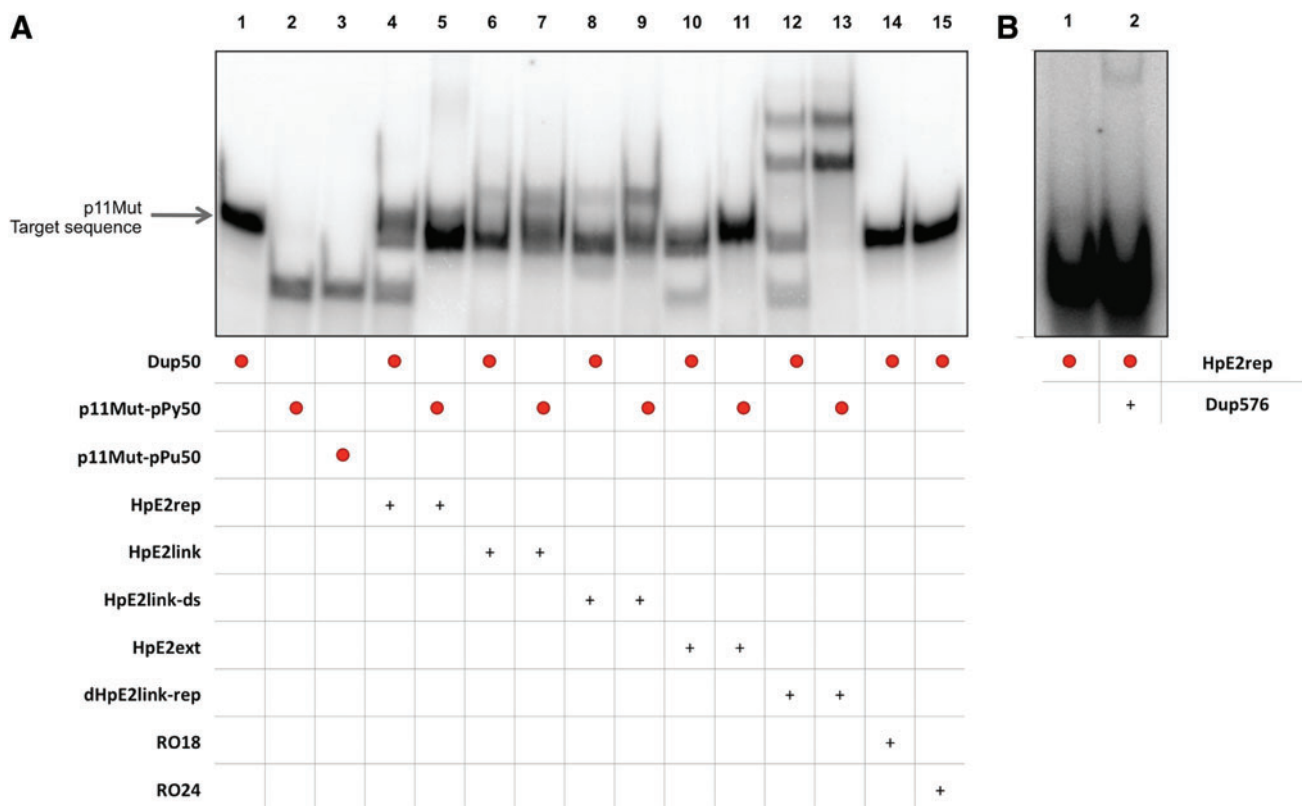


FIG. 5. Repair-PPRHs binding to their target sequence. **(A)** Binding between the radiolabeled dsDNA duplex (Dup50) and the different repair-PPRHs. Lane 1, labeled ^{32}P -polypurine/ ^{32}P -polypyrimidine dsDNA (Dup50) (0.67 nM); lane 2, ^{32}P -polypyrimidine ssDNA (pPy50) (0.27 nM); lane 3, ^{32}P -polypurine ssDNA (pPu50) (0.42 nM); lane 4, ^{32}P -Dup50 plus HpE2rep; lane 5, ^{32}P -pPy50 plus HpE2rep; lane 6, ^{32}P -Dup50 plus HpE2link; lane 7, ^{32}P -pPy50 plus HpE2link; lane 8, ^{32}P -Dup50 plus HpE2link-ds; lane 9, ^{32}P -pPy50 plus HpE2link-ds; lane 10, ^{32}P -Dup50 plus HpE2ext; lane 11, ^{32}P -pPy50 plus HpE2ext; lane 12, ^{32}P -Dup50 plus dHpE2link-rep; lane 13, ^{32}P -pPy50 plus dHpE2link-rep; lane 14, ^{32}P -Dup50 plus RO18; lane 15, ^{32}P -Dup50 plus RO24. **(B)** Binding of a longer dsDNA duplex (Dup576) and the radiolabeled HpE2rep. Lane 1, labeled ^{32}P -HpE2rep (0.35 nM); lane 2, ^{32}P -HpE2rep plus Dup576. (+) indicate unlabelled oligonucleotides present in the reaction. Color images available online at www.liebertpub.com/hgtb

RO24 did not succeed in correcting the point mutation, as no colonies survived in selective medium. As negative controls we used either HpE2ext without its hybridized repair oligonucleotide, which did not originate repaired colonies, or the repair oligonucleotides RO18 and RO24 alone that gave a very extremely low frequency of repair, in the order of 10^{-6} . HpE2rep-NH and HpE2rep-WC were also used as negative controls, and did not give rise to any repair colony. Spontaneous rate of correction was not observed in our assays. Repair of the sequence was confirmed by DNA sequencing.

DHFR mRNA analysis

Random surviving cell colonies resulting from independent experiments upon transfection of DG44 cells with PPRH/p11Mut were analyzed for DHFR mRNA levels. Because of the nonsense-mediated mRNA decay mechanism, by which mRNA bearing premature termination codons is selectively degraded, it was expected that DHFR mRNA encoded by p11Mut would be low and that repaired cell colonies would recover higher levels of mRNA. Indeed, the results confirmed in all cases higher levels of DHFR mRNA in repaired cell colonies than those in DG44-p11Mut. DHFR

mRNA levels in DG44 and DG44-p11 cells were used as negative and positive controls, respectively (Fig. 6A).

DHFR protein levels

Given that DHFR mRNA levels of repaired cells were recovered, we further explored the ability of the surviving cell colonies to produce DHFR protein. In all cases, the protein levels were restored. DG44-p11Mut and DG44 cells were used as negative controls, and DG44-p11 cells were used as a positive control (Fig. 6B and Fig. 9C.1).

Correction of a point mutation in DG44-p11Mut

Once we demonstrated that a point mutation was repaired in DG44 cells, we further examined if the same result could be achieved in DG44-p11Mut cells. The stable presence of p11Mut in these cells could represent an obstacle for the repair-PPRHs to recognize and bind to its target sequence, but on the other hand it would resemble more closely to the goal of repairing a point mutation of a gene in its endogenous locus. In total, 150,000 cells were seeded and transfected with the different repair-PPRHs, and then grown in $-H$ selective medium. HpE2rep, HpE2link, and dHpE2link-rep succeeded

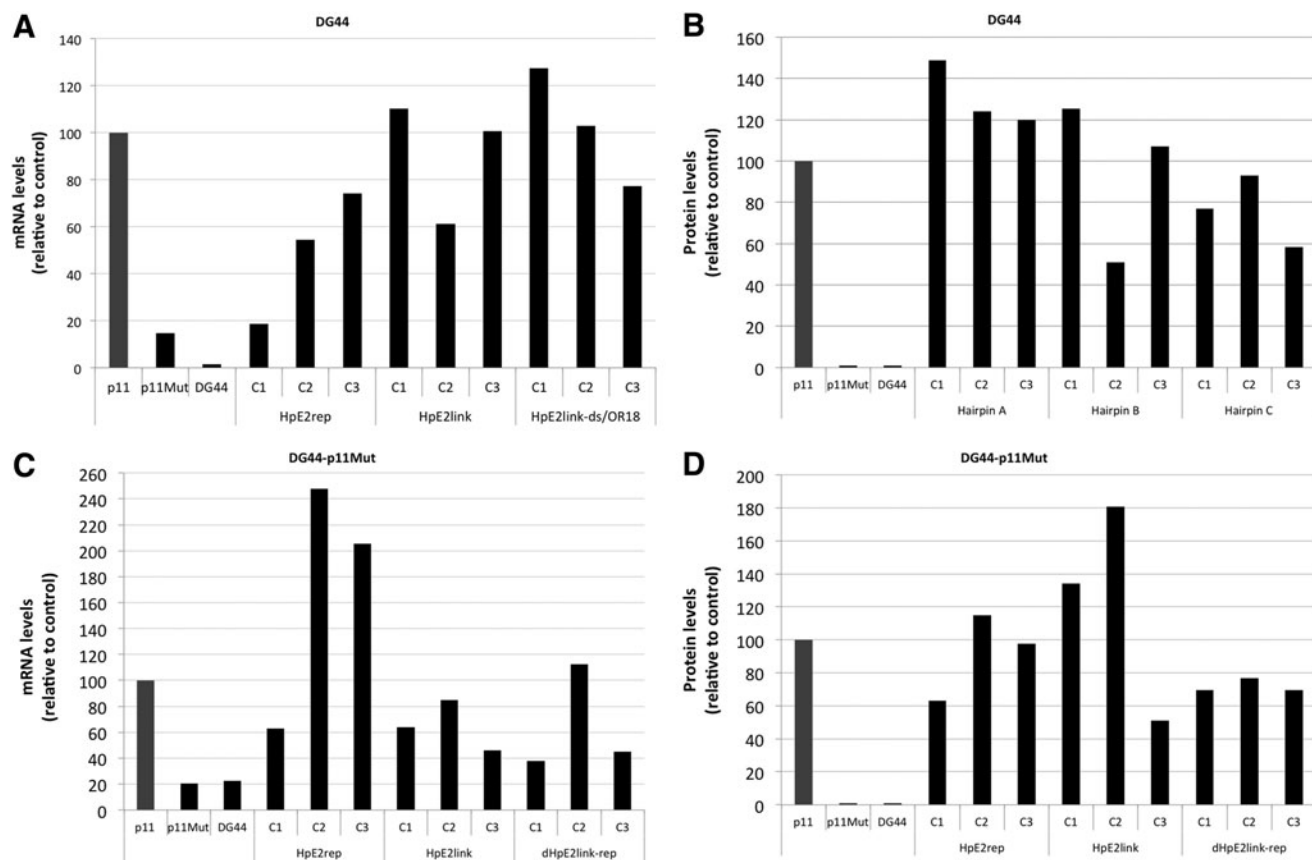


FIG. 6. Levels of DHFR mRNA and protein in repaired cells. **(A)** DHFR mRNA in repaired DG44 cells. RNA was extracted from repaired colonies of DG44 cells upon transfection with p11Mut and PPRHs. DHFR mRNA levels were determined using qRT-PCR and referred to the levels of endogenous APRT control. DHFR mRNA levels of the repaired colonies were referred to the mRNA levels of the positive control p11 (DG44-p11). **(B)** DHFR protein levels in repaired DG44 cells. Total protein extracts were obtained from the repaired DG44 colonies upon transfection with p11Mut and PPRHs and analyzed by Western blot. Protein levels were normalized using tubulin. Protein levels of the repaired colonies were referred to the protein levels of the positive control p11 (DG44-p11). **(C)** DHFR mRNA levels in repaired DG44-p11Mut cells. RNA was extracted from surviving DG44-p11Mut cell colonies upon transfection with PPRHs. DHFR mRNA levels were determined using qRT-PCR and referred to the levels of endogenous APRT control. DHFR mRNA levels of the repaired colonies were referred to the mRNA levels of the positive control p11 (DG44-p11). **(D)** DHFR protein levels in repaired DG44-p11Mut cells. Total protein extracts were obtained from DG44-p11Mut upon transfection with PPRHs and analyzed by Western blot. Protein levels were normalized using tubulin. Protein levels of the repaired colonies were referred to the protein levels of the positive control p11 (DG44-p11).

in correcting the point mutation with a frequency of about 1.5×10^{-3} (number of colonies/number of cells seeded) (Fig. 8A). The levels of DHFR mRNA and protein were determined in random surviving colonies. In all cases, repair-PPRHs achieved to recover DHFR mRNA levels compared with those in DG44-p11Mut (Fig. 6C). Regarding protein levels, all repair-PPRHs were able to produce DHFR (Fig. 6D and Fig. 9C.2), and the restored *dhfr* sequence was confirmed by DNA sequencing. HpE2ext, RO18, RO24, HpE2rep-NH, and HpE2rep-WC were used as negative controls. Whereas HpE2ext, HpE2rep-NH, HpE2rep-WC, and RO18 were unable to repair the point mutation, RO24 alone did achieve to correct it, although in a much lower efficiency (1.5×10^{-4}). Spontaneous corrections were not observed in our assays.

Correction of a point mutation at the endogenous locus

As a further step, we studied if repair-PPRHs were also able to repair a point mutation in an endogenous locus, using

the DA5 cell line bearing a deletion of a guanine in exon 6 of the *dhfr* gene. We selected a polypyrimidine sequence of 23 nucleotides downstream of the G deletion site, containing three purine interruptions in the target. We designed a repair-PPRH similar to HpE2rep, but in this case the interruptions were not substituted by adenines and the repair-PPRH contained three pyrimidines in the hairpin core, to minimize off-targets effects (Fig. 7A). In this approach, 150,000 cells were seeded and transfected with HpE6rep. After selecting cells in -H medium, surviving cell colonies were obtained at a frequency of 1×10^{-4} (Fig. 8A). The repair frequency was lower than in the other approaches, since in this case the repair of the point mutation was achieved at the endogenous locus and DA5 cells carry only one copy of the *dhfr* gene.

Six random cell colonies from different experiments were analyzed at DHFR mRNA and protein levels. mRNA levels of the repaired colonies were recovered compared with the negative control (DA5 cells) (Fig. 7B), and DHFR protein

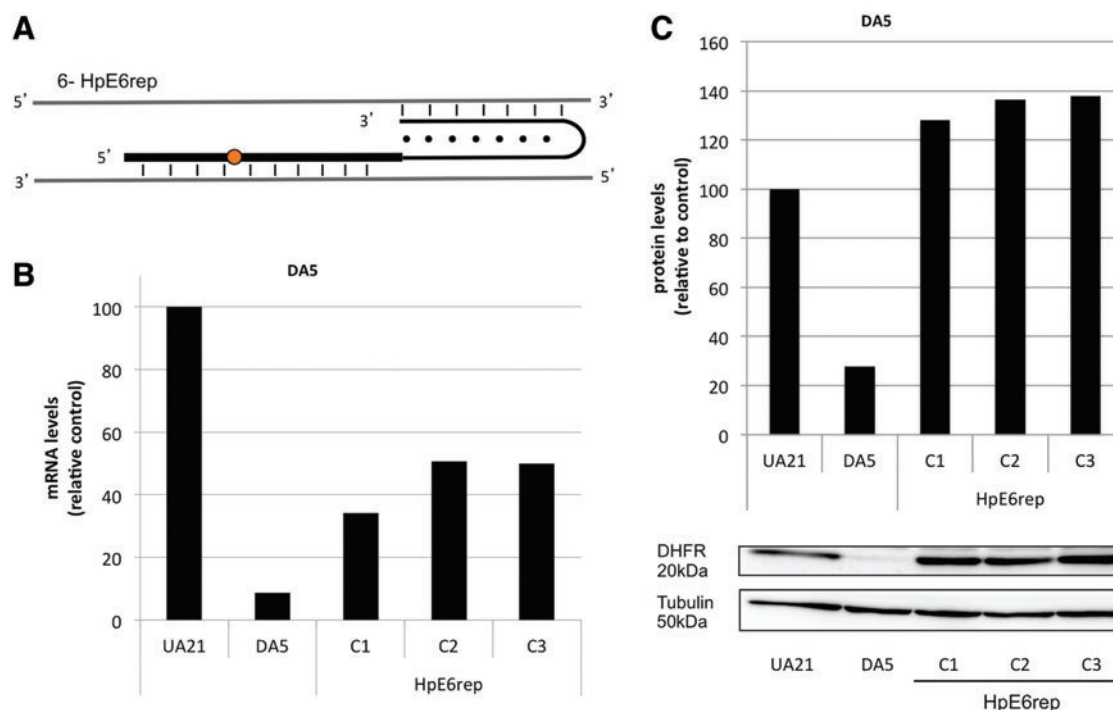


FIG. 7. Repair of a point mutation in an endogenous locus (DA5 cell line). (A) Scheme of HpE6rep. One repair-PPRH (HpE6rep) was designed against the exon 6 of the *dhfr* gene. HpE6rep contained a single extended sequence of DNA bearing the deleted nucleotide, and three pyrimidine interruptions in the hairpin core complementary to the target sequence. (B) DHFR mRNA levels in repaired DA5 cells. RNA was extracted from surviving DA5 cell colonies upon transfection with HpE6rep. DHFR mRNA levels were determined using qRT-PCR and were normalized to APRT. DHFR mRNA levels of the repaired colonies were referred to the positive control UA21. (C) DHFR protein levels in repaired DA5 cells. Total protein extracts were obtained from surviving DA5 cell colonies upon transfection with HpE6rep. Western blots were performed with 100 μ g of total extracts and were normalized to tubulin levels. Protein levels of the repaired colonies were referred to the protein levels of the positive control UA21. A representative image of the Western analyses is shown. Color images available online at www.liebertpub.com/hgtp

was restored in all cell colonies (Fig. 7C). In this approach, the point mutation could not activate NMD, since it is localized in the last exon of the *dhfr* gene and there is no downstream exon-exon junction (Maquat 2005; Neu-Yilik *et al.*, 2011). Thus, negative control DA5 can show a very low level of DHFR protein. The *dhfr* DNA of these cells was also sequenced to verify the restoration/introduction of the guanine.

Since the human recombinase Rad51 has been shown to stimulate the formation of the D-loop via Rad51-mediated strand invasion (Papaioannou *et al.*, 2012), it is required for triplex helix-induced recombination (Gupta *et al.*, 1997; Datta *et al.*, 2001), and it is a central player in HR (Krejci *et al.*, 2012) as a strand-exchange protein, we performed different assays with DA5 cells in the presence of Rad51. Following the same protocol, 150,000 cells were seeded and transfected with HpE6rep plus the Rad51 plasmid. The results showed a frequency of repair of 10^{-3} , which represents an increase of 10-fold compared with the transfection of HpE6rep alone (Fig. 8A).

DHFR activity

Although the repaired colonies had been selected in DHFR selective medium (-H), we wanted to corroborate that the DHFR protein present in those colonies showed DHFR activity. Thus, we selected a representation of one

repaired colony recovered from each of the approaches using the different PPRHs. These cells were incubated with 6- 3 H deoxyuridine that was incorporated into DNA. The degree of incorporation depended on the rate-limiting enzyme DHFR when the cells were grown in selective -GHT medium. As it can be observed in Fig. 8B, the repaired cells showed a high degree of DHFR activity compared with the negative control cells DG44, DG44-p11Mut, or DA5.

DNA sequencing

The presence of the corrected nucleotide, containing the same sequence as pDCH1P11 or UA21, using the three cell lines approaches (DG44, DG44-p11Mut, and DA5), was confirmed by DNA sequencing in randomly selected colonies. In all cases, the point mutation was corrected, thus demonstrating the effectiveness of the repair-PPRHs (Fig. 9A). The two-purine interruptions in the hairpin core (HpE2) did not cause a change in the DNA sequence of the target in the repaired colonies (data not shown).

Effect of aphidicolin and hydroxyurea incubation on gene repair by repair-PPRHs

We incubated two cell lines (DG44 and DG44-p11Mut) with 2 mM of hydroxyurea (HU) or 5 μ g/ml of aphidicolin

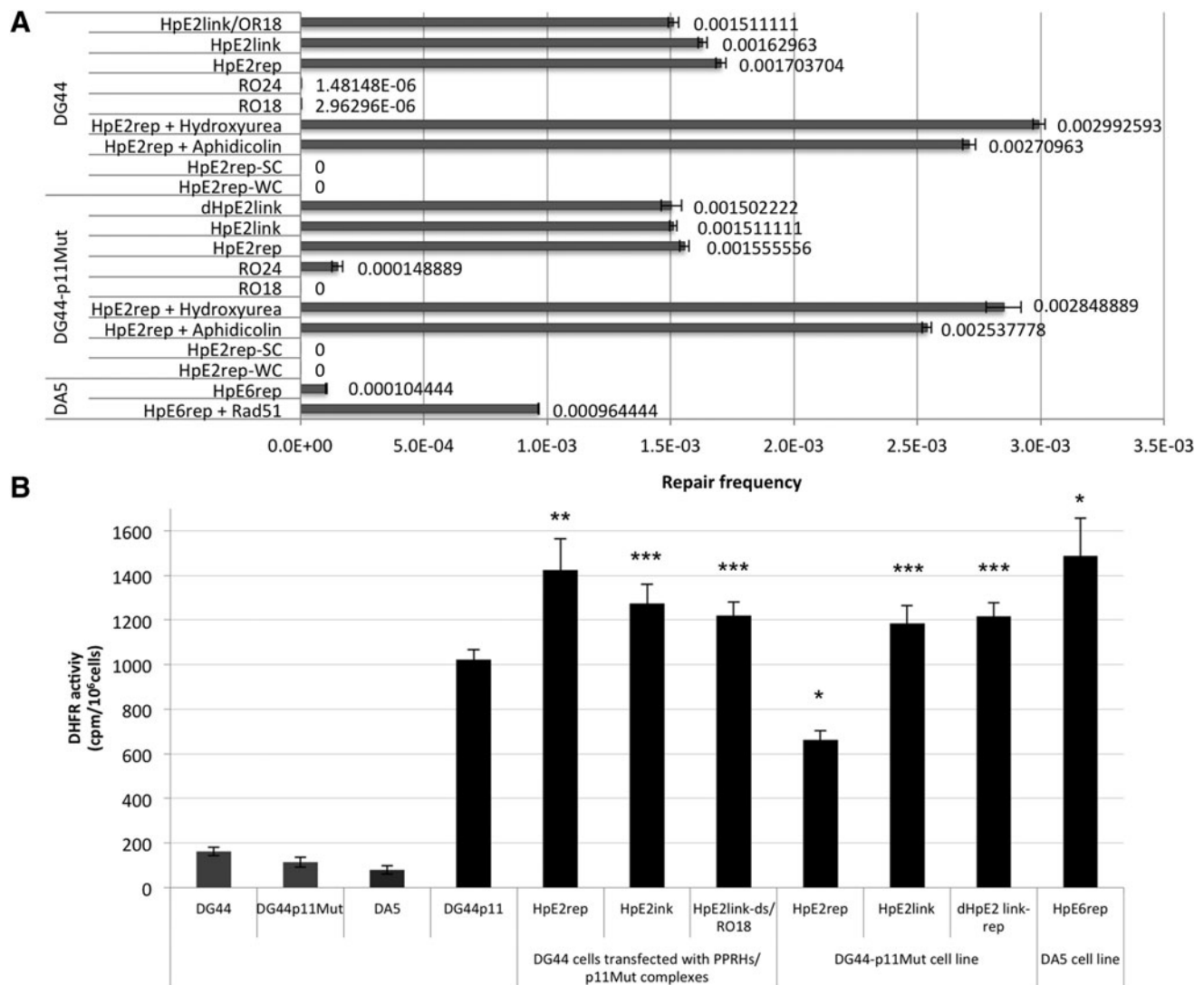


FIG. 8. Repair frequencies and DHFR activity. **(A)** Repair frequencies. Each repair-PPRH, previously incubated with the p11Mut plasmid in the DG44 cell line approach, was transfected into CHO cells. After 29–30 hr, cells were grown in selective medium to initiate the selection of repaired cells. The bars represent the frequency of cell colonies out of total cells seeded. Error bars indicate standard errors. Each assay was carried out a minimum of three times. **(B)** DHFR activity in repaired colonies from DG44, DG44p11Mut, and DA5 cells. Thirty thousand cells from each repair-PPRH approach were plated in 35 mm dishes and their DHFR activity was determined by the incorporation of 2 μ Ci of 6- 3 H] deoxyuridine to the DNA. Cells were collected and lysed with SDS after 24 hr. Radioactivity was counted in a scintillation counter. The activity was determined in repaired individual clones obtained by the transient transfection into DG44, in stably DG44-p11Mut cells and in DA5 cell line. * $p < 0.05$, ** $p < 0.01$, *** $p < 0.001$ compared with the corresponding control.

for 3 hr before transfection of the PPRHs. To carry out these experiments, we used HpE2rep/p11Mut in DG44 and HpE2rep in DG44-p11Mut. In these conditions, the frequency of repair increased by twofold (Fig. 8A). Since both aphidicolin and HU are known to increase the frequency of HR, our results are consistent with the hypothesis that repair-PPRHs promote repair of point mutations through this type of mechanism. Besides, aphidicolin is known to block the action of DNA polymerase δ and enzyme required for mismatch repair (MMR) synthesis in human cells (Papadopoulos *et al.*, 1994), and so we hypothesize that MMR mechanism could also be involved in the correction of a point mutation by repair-PPRHs.

Discussion

The main purpose of this work was to explore the possibility of repairing point mutations in mammalian cells using PPRHs. We previously described the use of PPRHs as a silencing tool in both *in vitro* and *in vivo* approaches (de Almagro *et al.*, 2009; Almagro *et al.*, 2011; Rodriguez *et al.*, 2013), by decreasing the expression of different targets. In this work we present evidence that PPRHs can also be used as a tool for gene repair. Repair-PPRHs are PPRH bearing an extended tail homologous to the point mutation region of the target, except for the nucleotide to be altered. The model we used to validate the effect of these repair-PPRHs was the

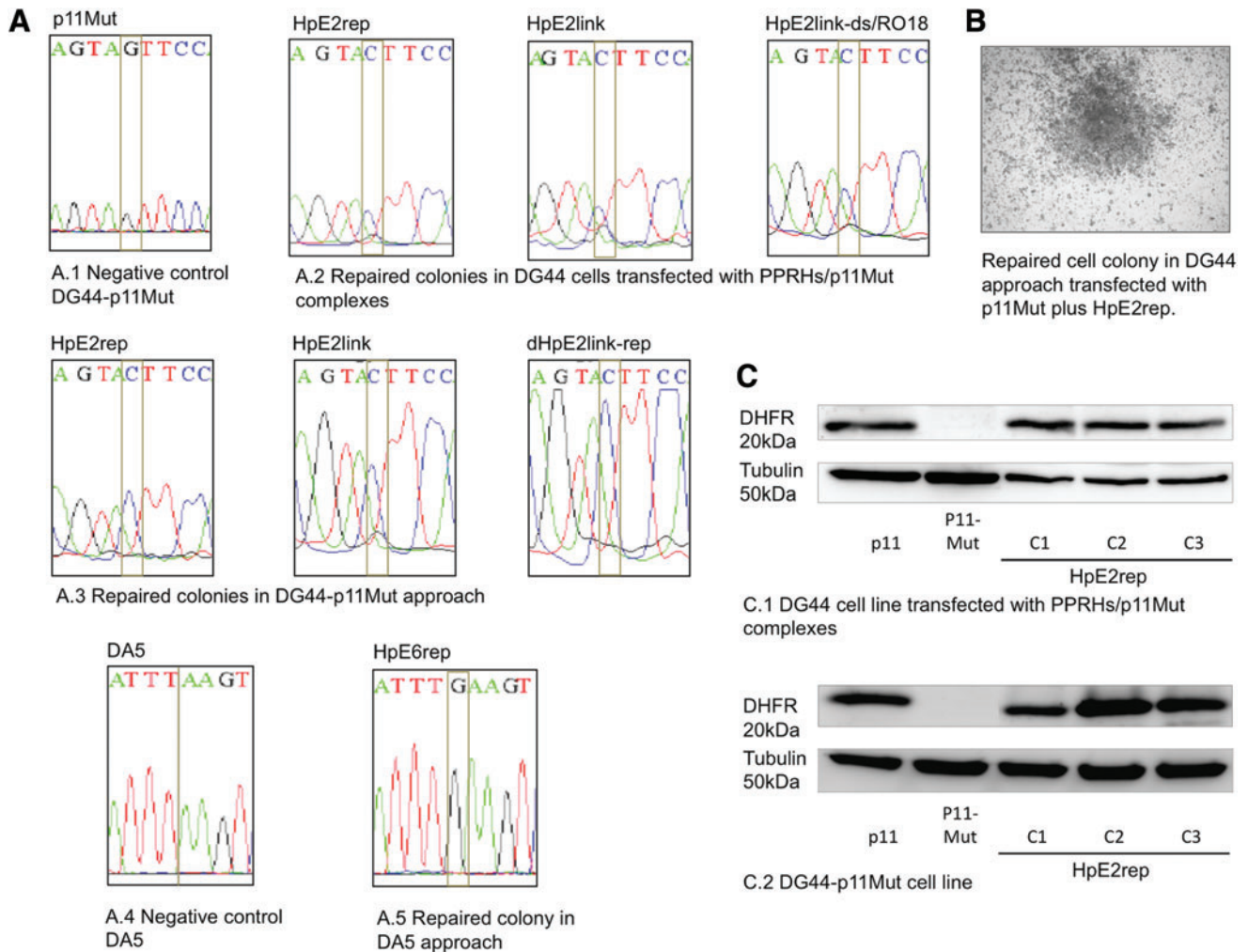


FIG. 9. DNA sequencing and DHFR protein of repaired cell colonies. (A) Sequences of the nonsense mutant of the *dhfr* minigene p11Mut, and those of repaired cells using different repair-PPRHs upon transfection in either DG44 or DG44p11Mut cell lines. (B) Repaired cell colony upon transfection of DG44 cells with the mutated version of the *dhfr* minigene (p11Mut) and HpE2rep, and selection in selective medium (w/o hypoxanthine). (C) Representative image of a Western blot showing the DHFR protein levels of DG44-p11 (positive control), DG44-p11Mut (negative control), and three repaired colonies obtained from DG44 upon transfection with p11Mut and HpE2rep, and three colonies from DG44-p11Mut transfected with HpE2rep. Color images available online at www.liebertpub.com/hgtb

repair of a nonsense mutation in exon 2 of a *dhfr* minigene (p11-Mut) in CHO cells, and a deletion point mutation in exon 6 of the genomic sequence in the *dhfr* endogenous locus (DA5 cells).

As a first step of this study, we demonstrated by binding assays the capacity of regular PPRHS to bind to dsDNA forming triplex structures, displacing the polypurine strand of the dsDNA, extending previous observations from our laboratory (Coma *et al.*, 2005). Then, we further explored the experimental conditions to maintain the dsDNA opened for the subsequent binding of a given repair oligonucleotide. Repair-PPRHs were also analyzed by binding assays before being transfected to the cells, demonstrating their ability to bind to its polypurine/polypyrimidine dsDNA target.

In cell culture experiments, correction of the nonsense mutation in p11Mut was attempted in two different settings. In the first approach, repair was accomplished by the co-incubation of the mutated target plasmid with three different

repair-PPRHs (HpE2rep, HpE2link, and HpE2link-ds/RO18) in DG44 cells. Repair-PPRHs would open the dsDNA forming a triplex and increasing HR, and at the same time they could convey the repair tail to the mutated region producing a mismatched base, thus activating DNA repair systems. It is important to note that PPRHS can inhibit transcription (de Almagro *et al.*, 2009), which in turn could trigger error-prone repair. To deepen and broaden the knowledge of repair-PPRHs, a second approach was carried out in cells stably transfected with the p11Mut plasmid (DG44-p11Mut), trying to hinder the recognition and binding of the repair-PPRH to the target sequence. The fact that HpE2link, HpE2rep, and dHpE2link-rep corrected the point mutation demonstrate the capacity of repair-PPRHs to act even when the hairpin is not preincubated with its target sequence. One of the repair oligonucleotides alone (RO24) did achieve some gene correction in DG44-p11Mut, as expected, since it is known that short oligonucleotides can

induce recombination (Campbell *et al.*, 1989; Lin *et al.*, 1990). Nevertheless, the repair frequency of this oligonucleotide (RO24) was 10 times less than the repair-PPRHs.

The hairpin core of the repair-PPRHs (HpE2) contained two adenines in front of the purine interruptions in the polypyrimidine target sequence. This fact might originate two possible problems: (1) a reduction in the binding specificity of the PPRH because of its mismatches, and (2) the possibility that those interruptions would provoke a change in the nucleotides of the target sequence. None of these two possibilities constituted a real drawback, since we demonstrated the binding of the repair-PPRHs to their target, and no mutations in the PPRH target sequence appeared when DNA sequencing of repaired colonies was carried out.

The incubation of both cell lines, DG44 and DG44-p11Mut, with the recombination inducers HU or aphidicolin (Saintigny *et al.*, 2001) before transfection increased the frequency of correction by twofold. This fact suggests that HR might play a role in the mechanism for gene correction exerted by repair-PPRHs, simultaneously with MMR, since both a single-nucleotide change and an insertion took place, and aphidicolin is an inhibitor of the DNA polymerase δ , an enzyme required for MMR (Papadopoulos *et al.*, 1994). Since aphidicolin and HU are also known to stall replication, our results are also consistent with the possibility that unwound conformation of duplex DNA during replication might be favorable to triplex formation by PPRHs. Interestingly, the only repair-PPRH that did not succeed in repairing the point mutation was HpE2ext/RO24, which is the only hairpin whose extended tail did not reach the mutated base, and the hybridized repair oligonucleotide (RO24) did not form a full double-strand molecule. This might mean that to accomplish gene repair of the point mutation, the corrected nucleotide needs to be a part of the repair-PPRH sequence. Besides, the absence of repair colonies using HpE2rep-NH that is not able to form the intramolecular Hoogsteen bonds, and HpE2rep-WC forming Watson–Crick bonds between the two domains of the hairpin core, demonstrates that the formation of the triplex structure is essential for repairing point mutations using repair-PPRHs. At the endogenous level, a deletion in the exon 6 of the *dhfr* gene was also corrected using HpE6rep, thus demonstrating the capacity of repair-PPRHs to recover a deleted nucleotide in an actual genomic environment.

In this approach we also study the importance of Rad51 protein in the methodology of repair-PPRHs. Rad51 is one of the major factors in HR (Liu *et al.*, 2002), it is required for triplex helix-induced recombination, and it can boost invasion or binding of the ssODN to its homologous target region in a structure similar to a D-loop (Symington, 2005). The results are consistent with our hypothesis that Rad51 and consequently HR are involved in correcting point mutations using repair-PPRHs, since the transfection of HpE6rep with pRad51 increased the repair frequency by 10-fold. It is worth noting that the repair at the DNA level accomplished by these repair-PPRH was verified by DNA sequencing and functionally validated at the DHFR mRNA, protein, and activity levels.

PPRHs have advantages when compared with other approaches for gene repair. They can be easily synthesized since they do not bear chemical modifications, which is an advantage in terms of toxicity (Rodríguez *et al.*, 2013) and

economy. At the same time, due to their hairpin structure, PPRHs are known to be highly resistant to endogenous nucleases (Villalobos *et al.*, 2014). Also, they do not induce mutations in the target gene of the repaired colonies, which is an important difference with TFOs (Wang *et al.*, 1996). As a matter of fact, this absence of mutations in the target sequence argues against a mechanism of repair during replication and in favor of a mechanism of HR played by the repair-PPRHs. It is also important to note that repair-PPRHs act without damaging the DNA with chemical agents, and without the requirement of DSB that is likely to result in an increase in non-HR (Vasquez *et al.*, 2001).

In summary, in this work we present an innovative technology for gene repair applying a strategy derived from PPRHs. The obtained results suggest that repair-PPRHs could provide the basis for a new therapeutic alternative to repair single-point mutation diseases that also works at the endogenous gene locus.

Acknowledgments

We acknowledge Dr. Silvia Coma for helpful suggestions.

This work was supported by “Plan Nacional de Investigación Científica” (Spain), Grant SAF2011-23582. Our group holds the Quality Mention from the “Generalitat de Catalunya” SGR2009-118. A.S. is the recipient of a fellowship (Formació d’Investigadors) from the “Generalitat de Catalunya.” X.V. is a recipient of an APIF fellowship from the University of Barcelona.

Author Disclosure Statement

The authors declare that they do not have competing financial interests.

References

- Almagro, D., Agramonte, O., Castillo, D., *et al.* (2011). Experience with a single dose of recombinant activated factor VII for the management of mild-to-moderate bleeds in haemophilia. *Haemophilia* 17, 322–323.
- Bailey, C., and Weeks, D.L. (2000). Understanding oligonucleotide-mediated inhibition of gene expression in *Xenopus laevis* oocytes. *Nucleic Acids Res.* 28, 1154–1161.
- Bentin, T., Larsen, H.J., and Nielsen, P.E. (2003). Combined triplex/duplex invasion of double-stranded DNA by “tail-clamp” peptide nucleic acid. *Biochemistry* 42, 13987–13995.
- Bibikova, M., Carroll, D., and Segal, D.J., *et al.* (2001). Stimulation of homologous recombination through targeted cleavage by chimeric nucleases. *Mol. Cell Biol.* 21, 289–297.
- Campbell, C.R., Keown, W., Lowe, L., *et al.* (1989). Homologous recombination involving small single-stranded oligonucleotides in human cells. *New Biol.* 1, 223–227.
- Chan, P.P., Lin, M., Faruqi, A.F., *et al.* (1999). Targeted correction of an episomal gene in mammalian cells by a short DNA fragment tethered to a triplex-forming oligonucleotide. *J. Biol. Chem.* 274, 11541–11548.
- Chin, J.Y., Kuan, J.Y., Lonkar, P.S., *et al.* (2008). Correction of a splice-site mutation in the beta-globin gene stimulated by triplex-forming peptide nucleic acids. *Proc. Natl. Acad. Sci. USA* 105, 13514–13519.
- Ciudad, C.J., Urlaub, G., and Chasin, L.A. (1988). Deletion analysis of the Chinese hamster dihydrofolate reductase gene promoter. *J. Biol. Chem.* 263, 16274–16282.

- Cole-Strauss, A., Gamper, H., Holloman, W.K., *et al.* (1999). Targeted gene repair directed by the chimeric RNA/DNA oligonucleotide in a mammalian cell-free extract. *Nucleic Acids Res.* 27, 1323–1330.
- Coma, S., Noe, V., Eritja, R., and Ciudad, C.J. (2005). Strand displacement of double-stranded DNA by triplex-forming antiparallel purine-hairpins. *Oligonucleotides* 15, 269–283.
- Culver, K.W., Hsieh, W.T., Huyen, Y., *et al.* (1999). Correction of chromosomal point mutations in human cells with bifunctional oligonucleotides. *Nat. Biotechnol.* 17, 989–993.
- Datta, H.J., Chan, P.P., Vasquez, K.M., *et al.* (2001). Triplex-induced recombination in human cell-free extracts. Dependence on XPA and HsRad51. *J. Biol. Chem.* 276, 18018–18023.
- De Almagro, M.C., Coma, S., Noe, V., and Ciudad, C.J. (2009). Polypurine hairpins directed against the template strand of DNA knock down the expression of mammalian genes. *J. Biol. Chem.* 284, 11579–11589.
- De Almagro, M.C., Mencia, N., Noe, V., and Ciudad, C.J. (2011). Coding polypurine hairpins cause target-induced cell death in breast cancer cells. *Hum. Gene Ther.* 22, 451–463.
- Demidov, V.V., Protozanova, E., Izvolsky, K.I., *et al.* (2002). Kinetics and mechanism of the DNA double helix invasion by pseudocomplementary peptide nucleic acids. *Proc. Natl. Acad. Sci. USA* 99, 5953–5958.
- Egholm, M., Buchardt, O., Christensen, L., *et al.* (1993). PNA hybridizes to complementary oligonucleotides obeying the Watson-Crick hydrogen-bonding rules. *Nature* 365, 566–568.
- Gupta, R.C., Bazemore, L.R., Golub, E.L., and Radding, C.M. (1997). Activities of human recombination protein Rad51. *Proc. Natl. Acad. Sci. USA* 94, 463–468.
- Hanson, K.D., and Sedivy, J.M. (1995). Analysis of biological selections for high-efficiency gene targeting. *Mol. Cell Biol.* 15, 45–51.
- Hruscha, A., Krawitz, P., Rechenberg, A., *et al.* (2013). Efficient CRISPR/Cas9 genome editing with low off-target effects in zebrafish. *Development* 140, 4982–4987.
- Joung, J.K., and Sander, J.D. (2013). TALENs: a widely applicable technology for targeted genome editing. *Nat. Rev. Mol. Cell Biol.* 14, 49–55.
- Kaihatsu, K., Shah, R.H., Zhao, X., and Corey, D.R. (2003). Extending recognition by peptide nucleic acids (PNAs): binding to duplex DNA and inhibition of transcription by tail-clamp PNA-peptide conjugates. *Biochemistry* 42, 13996–14003.
- Kayali, R., Bury, F., Ballard, M., and Bertoni, C. (2010). Site-directed gene repair of the dystrophin gene mediated by PNA-ssODNs. *Hum. Mol. Genet.* 19, 3266–3281.
- Kleinstiver, B.P., Wolfs, J.M., Kolaczyk, T., *et al.* (2012). Monomeric site-specific nucleases for genome editing. *Proc. Natl. Acad. Sci. USA* 109, 8061–8066.
- Knauert, M.P., Kalish, J.M., Hegan, D.C., and Glazer, P.M. (2006). Triplex-stimulated intermolecular recombination at a single-copy genomic target. *Mol. Ther.* 14, 392–400.
- Krejci, L., Altmannova, V., Spirek, M., and Zhao, X. (2012). Homologous recombination and its regulation. *Nucleic Acids Res.* 40, 5795–5818.
- Lin, F.L., Sperle, K., and Sternberg, N. (1990). Repair of double-stranded DNA breaks by homologous DNA fragments during transfer of DNA into mouse L cells. *Mol. Cell Biol.* 10, 113–119.
- Liu, L., Cheng, S., Van Brabant, A.J., and Kmiec, E.B. (2002). Rad51p and Rad54p, but not Rad52p, elevate gene repair in *Saccharomyces cerevisiae* directed by modified single-stranded oligonucleotide vectors. *Nucleic Acids Res.* 30, 2742–2750.
- Liu, J., Li, C., Yu, Z., *et al.* (2012). Efficient and specific modifications of the *Drosophila* genome by means of an easy TALEN strategy. *J. Genet. Genomics* 39, 209–215.
- Lohse, J., Dahl, O., and Nielsen, P.E. (1999). Double duplex invasion by peptide nucleic acid: a general principle for sequence-specific targeting of double-stranded DNA. *Proc. Natl. Acad. Sci. USA* 96, 11804–11808.
- Lonkar, P., Kim, K.H., Kuan, J.Y., *et al.* (2009). Targeted correction of a thalassemia-associated beta-globin mutation induced by pseudo-complementary peptide nucleic acids. *Nucleic Acids Res.* 37, 3635–3644.
- Maquat, L.E. (2005). Nonsense-mediated mRNA decay in mammals. *J. Cell Sci.* 118, 1773–1776.
- Moerschell, R.P., Tsunasawa, S., and Sherman, F. (1988). Transformation of yeast with synthetic oligonucleotides. *Proc. Natl. Acad. Sci. USA* 85, 524–528.
- Neu-Yilik, G., Amthor, B., Gehring, N.H., *et al.* (2011). Mechanism of escape from nonsense-mediated mRNA decay of human beta-globin transcripts with nonsense mutations in the first exon. *RNA* 17, 843–854.
- Nielsen, P.E., Egholm, M., Berg, R.H., and Buchardt, O. (1991). Sequence-selective recognition of DNA by strand displacement with a thymine-substituted polyamide. *Science* 254, 1497–1500.
- Nik-Ahd, F., and Bertoni, C. (2014). *Ex vivo* gene editing of the dystrophin gene in muscle stem cells mediated by peptide nucleic acid single stranded oligodeoxynucleotides induces stable expression of dystrophin in a mouse model for Duchenne muscular dystrophy. *Stem Cells* 32, 1817–1830.
- Noe, V., Ciudad, C.J., and Chasin, L.A. (1999). Effect of differential polyadenylation and cell growth phase on dihydrofolate reductase mRNA stability. *J. Biol. Chem.* 274, 27807–27814.
- Papadopoulos, N., Nicolaidis, N.C., Wei, Y.F., *et al.* (1994). Mutation of a mutL homolog in hereditary colon cancer. *Science* 263, 1625–1629.
- Papaioannou, I., Simons, J.P., and Owen, J.S. (2012). Oligonucleotide-directed gene-editing technology: mechanisms and future prospects. *Expert Opin. Biol. Ther.* 12, 329–342.
- Rodriguez, L., Villalobos, X., Dakhel, S., *et al.* (2013). Polypurine reverse Hoogsteen hairpins as a gene therapy tool against survivin in human prostate cancer PC3 cells *in vitro* and *in vivo*. *Biochem. Pharmacol.* 86, 1541–1554.
- Rogers, F.A., Vasquez, K.M., Egholm, M., and Glazer, P.M. (2002). Site-directed recombination via bifunctional PNA-DNA conjugates. *Proc. Natl. Acad. Sci. USA* 99, 16695–16700.
- Rouet, P., Smih, F., and Jasin, M. (1994). Introduction of double-strand breaks into the genome of mouse cells by expression of a rare-cutting endonuclease. *Mol. Cell Biol.* 14, 8096–8106.
- Saintigny, Y., Delacote, F., Vares, G., *et al.* (2001). Characterization of homologous recombination induced by replication inhibition in mammalian cells. *EMBO J.* 20, 3861–3870.
- Symington, L.S. (2005). Focus on recombinational DNA repair. *EMBO Rep.* 6, 512–517.
- Urlaub, G., Mitchell, P.J., Kas, E., *et al.* (1986). Effect of gamma rays at the dihydrofolate reductase locus: deletions and inversions. *Somat Cell Mol. Genet.* 12, 555–566.
- Urnov, F.D., Miller, J.C., Lee, Y.L., *et al.* (2005). Highly efficient endogenous human gene correction using designed zinc-finger nucleases. *Nature* 435, 646–651.

- Urnov, F.D., Rebar, E.J., Holmes, M.C., *et al.* (2010). Genome editing with engineered zinc finger nucleases. *Nat. Rev. Genet.* 11, 636–646.
- Vasquez, K.M., Marburger, K., Intody, Z., and Wilson, J.H. (2001). Manipulating the mammalian genome by homologous recombination. *Proc. Natl. Acad. Sci. USA* 98, 8403–8410.
- Villalobos, X., Rodriguez, L., Prevot, J., *et al.* (2014). Stability and immunogenicity properties of the gene-silencing polypurine reverse Hoogsteen hairpins. *Mol. Pharm.* 11, 254–264.
- Wang, Y.Y., Maher, V.M., Liskay, R.M., and McCormick, J.J. (1988). Carcinogens can induce homologous recombination between duplicated chromosomal sequences in mouse L cells. *Mol. Cell Biol.* 8, 196–202.
- Wang, G., Seidman, M.M., and Glazer, P.M. (1996). Mutagenesis in mammalian cells induced by triple helix formation and transcription-coupled repair. *Science* 271, 802–805.
- Wiedenheft, B., Sternberg, S.H., and Doudna, J.A. (2012). RNA-guided genetic silencing systems in bacteria and archaea. *Nature* 482, 331–338.
- Wigler, M., Pellicer, A., Silverstein, S., *et al.* (1979). DNA-mediated transfer of the adenine phosphoribosyltransferase locus into mammalian cells. *Proc. Natl. Acad. Sci. USA* 76, 1373–1376.
- Wood, A.J., Lo, T.W., Zeitler, B., *et al.* (2011). Targeted genome editing across species using ZFNs and TALENs. *Science* 333, 307.
- Yoon, K., Cole-Strauss, A., and Kmiec, E.B. (1996). Targeted gene correction of episomal DNA in mammalian cells mediated by a chimeric RNA:DNA oligonucleotide. *Proc. Natl. Acad. Sci. USA* 93, 2071–2076.

Address correspondence to:

Dr. Carlos J. Ciudad

Department of Biochemistry and Molecular Biology

School of Pharmacy

University of Barcelona

Av. Diagonal 643

E08028 Barcelona

Spain

E-mail: cciudad@ub.edu

Received for publication April 25, 2014;
accepted after revision September 12, 2014.

Published online: September 15, 2014.

4.1.1. Additional results to Article I

4.1.1.1. Binding assays between duplexes and hairpins at different temperatures.

The appropriate temperature to which samples must be heated before carrying out the binding reaction was studied using binding assays. A mixture of the labeled ^{32}P -polypurine/ ^{32}P -polypyrimidine dsDNA (Dup61) with hairpin-23 (Hp23) and hairpin-13 (Hp13) was subjected to a decreasing temperature gradient (from 80°C to room temperature) for 5 min. Subsequently, samples were incubated for an additional period of time of 30 min at 37°C according to the protocol used in all the previous determinations. As shown in Fig. 1, the minimum temperature at which Dup61 must be heated to observe the opening of dsDNA *in vitro* was 70°C (lane 3). This temperature is needed to observe the displacing effect of the polypurine strand of the dsDNA, and probably the PPRHs contribute to stabilize this opening of the DNA *in vitro*. However, we demonstrated that in cell culture PPRHs are operative without the need of heating. Therefore, other factors that contribute to the opening and stabilization of the opening of the DNA may take place like the action of helicases at physiological temperatures.

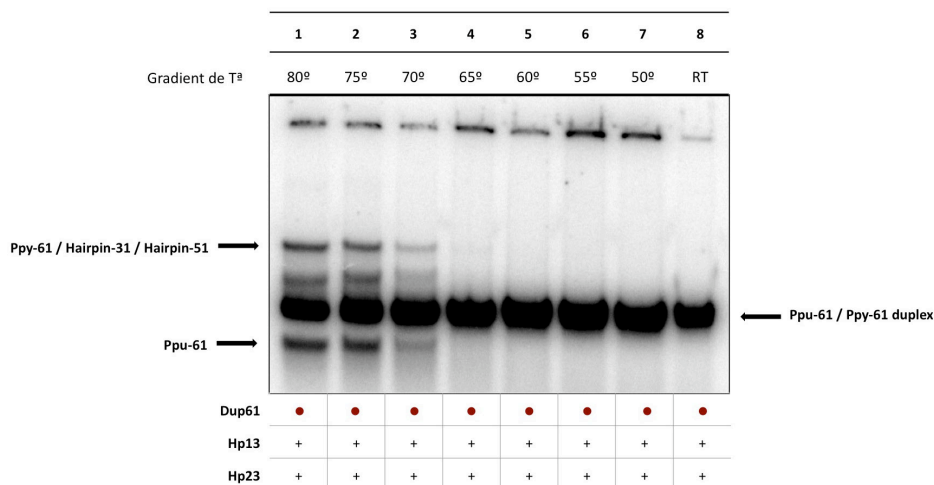


Figure 1. Temperature range was used to analyze the opening of dsDNA. Binding was performed between ^{32}P -polypurine/ ^{32}P -polypyrimidine dsDNA (Dup61) and unlabeled Hp13 and Hp23. Incubations were carried out at 37°C for 30 min after heating the mixture at the indicated temperatures for 5 min (lanes 1 to 7). In lane 8, incubation was carried out at 37°C for 30 minutes without pre-heating the sample, but leaving it at RT for 5 min before the binding reaction. Poly-dI:dC (1µg) was added to each sample. The different species of DNA (ss, ds, triplex) are indicated by arrows. Labeled oligonucleotides are indicated as (•), and unlabeled oligonucleotides are indicated as (+).

4.1.1.2. Negative and positive controls

Different controls were performed to determine the specificity of the hairpins and the oligonucleotides used. The binding between the specific oligonucleotide RO20 and its ssDNA pPu61 target was confirmed (lane 4). Negative controls were tested after incubation of radiolabeled RO20 with unlabeled polypyrimidine ssDNA of the duplex (pPy61) (lane 1), with hairpin-23 (Hp23) (lane 2), and with hairpin-13 (Hp13) (lane 3), and no binding was observed. On the other hand, the binding between labeled pPy61 and the two hairpins was also confirmed either together or separately (lane 7, 8 and 9).

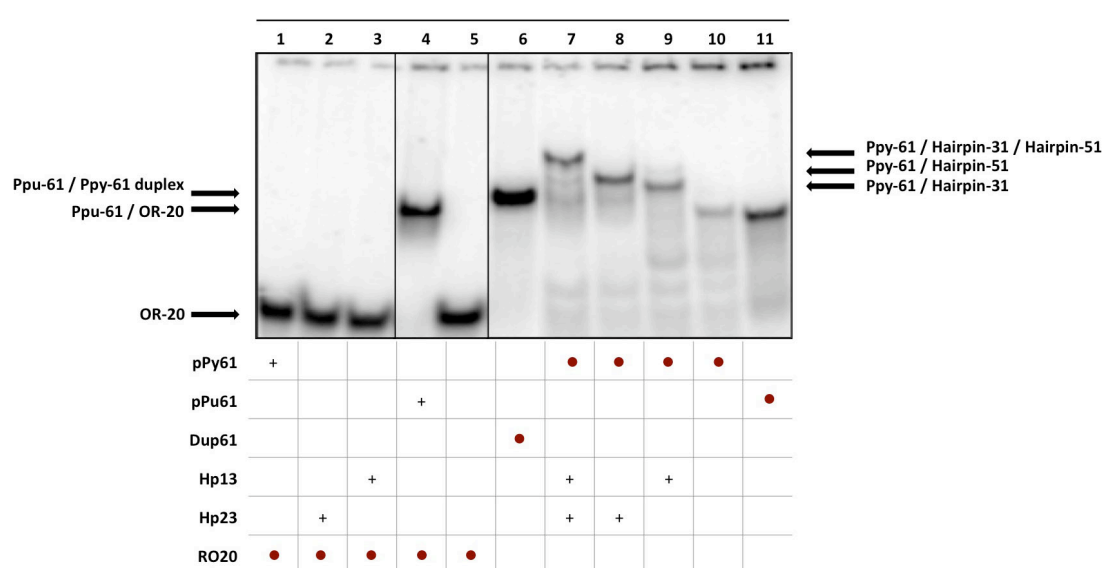


Figure 2. Controls to test the specificity of ODNs. Lane 1, labeled specific polypyrimidine ^{32}P -oligonucleotide (RO20) plus polypyrimidine ssDNA (pPy61); lane 2, ^{32}P -RO20 plus Hp23; lane 3, ^{32}P -RO20 plus unlabeled Hp13; lane 4, ^{32}P -RO20 plus polypurine ssDNA (pPu61); lane 5, ^{32}P -OR-20; lane 6, ^{32}P -polypurine/ ^{32}P -polypyrimidine duplex (Dup61); lane 7, ^{32}P -pPy61 plus unlabeled Hp13 and Hp23; lane 8, ^{32}P -pPy61 plus Hp23; lane 9, ^{32}P -pPy61 plus Hp13; lane 10, ^{32}P -pPy61; lane 11, ^{32}P -pPu61. The whole mixture of all samples was heated at 75°C before binding reaction. Incubations were performed at 37°C for 30 minutes. Poly-dI:dC ($1\mu\text{g}$) was added to each sample. The different species of DNA (ss, ds, triplex) are indicated by arrows. Labeled oligonucleotides are indicated as (•), and unlabeled oligonucleotides are indicated as (+).

4.1.1.3. Gradient of decreasing concentration of hairpins

Hairpins showed to be able to keep the dsDNA open at a concentration of 10nM; for this reason we studied lower concentrations of hairpin to determine their range of action. Hairpin-13 (Hp13) and hairpin-23 (Hp23) were incubated at concentrations of 0.3 to 10nM with the radiolabeled pPu61/pPy61 duplex (Dup61) (lane 2 – 5). The incubation resulted in the formation of three new bands, the lowest corresponding to the displaced polypurine strand, and the other two corresponding to the triplex structure formed by the polypyrimidine strand of the Dup61 and Hp13/Hp23. The binding was detectable even at 0,3nM when the two hairpins were incubated together, although the triple helical band was weak. Dup61 was also incubated with unlabeled Hp13 and Hp23 separately. The incubation with Hp13 resulted in the displacement of the polypurine strand at 3 and 10nM, but not at lower concentrations (lanes 6 – 9). With Hp23, the opening of the dsDNA was still detectable even at 0,3nM, and an upper band appeared in all cases indicating the formation of the triplex structure (lanes 10 – 13).

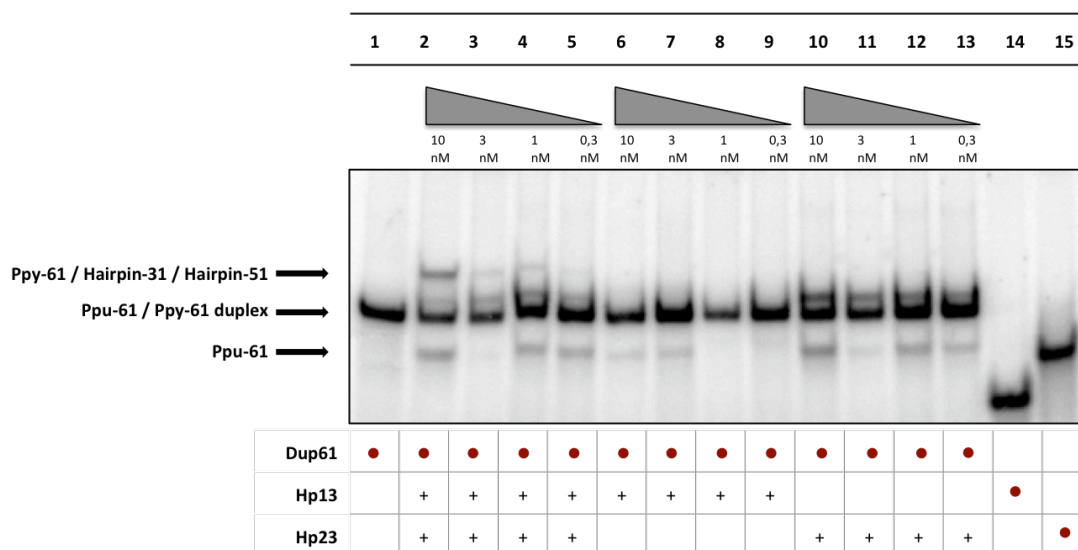


Figure 3. Decreasing concentrations of Hp13 and Hp23. Lane 1, labeled ^{32}P -polypurine/ ^{32}P -polypyrimidine dsDNA (^{32}P -Dup61); lane 2 – 5, ^{32}P -Dup61 plus unlabeled Hp13 and Hp23, both at 10nM – 0,3nM; lane 6 – 9, ^{32}P -Dup61 plus Hp13 at 10nM – 0,3nM; lane 10 – 13, ^{32}P -Dup61 plus Hp23 at 10nM – 0,3nM; lane 14, ^{32}P -Hp13; lane 15, ^{32}P -Hp23. The entire mixture of all samples was heated at 75°C before the binding reaction. Incubations were performed at 37°C for 30 minutes. Poly-dI:dC (1µg) was added to each sample. The different species of DNA (ss, ds, triplex) are indicated by arrows. Labeled oligonucleotides are indicated as (•), and unlabeled oligonucleotides are indicated as (+).

4.1.1.4. A specific oligonucleotide can bind to the displaced polypurine strand at 37°C.

We have proven that by heating the entire sample to 75°C, the hairpins were able to maintain the double-stranded DNA open (lane 3), now susceptible to be bound by a specific oligonucleotide (RO20). In addition, we also tested this fact by adding the hairpins and RO20 at different times, to verify that hairpins may act at 37°C. As shown in lane 2, the dsDNA opening was visible when the pPu61/pPy61 duplex (Dup61) was heated at 75°C for 5 minutes, then incubated at 37°C for 15 minutes, and finally added with the hairpins during 15 minutes. The condition explored in this lane confirmed that at the time of acting the hairpins, the duplex does not need to be at 75°C. Likewise, another combination was tested subsequently adding RO20. Both the duplex and the two hairpins were heated in the same mixture at 75°C for 5 minutes, and after keeping them 15 minutes at 37°C, RO20 was added for 15 minutes at 37°C. This test resulted in the appearance of a band of the same size as pPu61 plus RO20, thus confirming that a specific oligonucleotide can bind to its displaced polypurine ssDNA target at 37°C (lane 1). Moreover, we confirmed that the band belonging to the binding between pPu61 and the oligonucleotide was not formed in the absence of hairpins, although the entire mixture was heated at 75 ° C (lane 4).

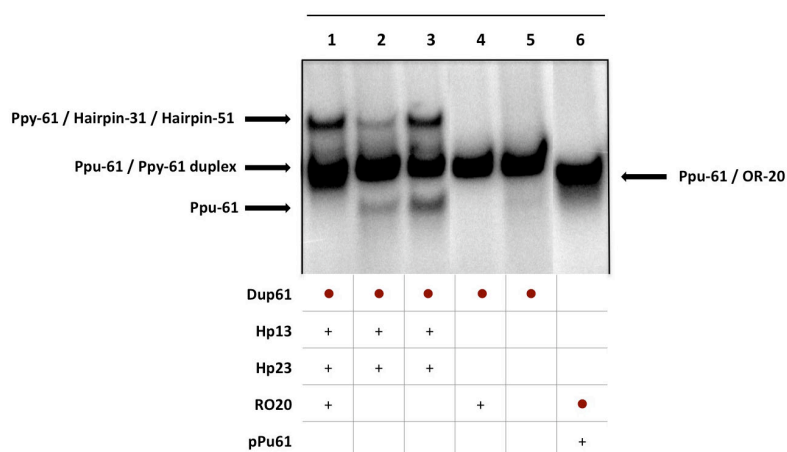


Figure 4. Binding between displaced polypurine strand of the duplex (pPu61) and a specific polypyrimidine oligonucleotide (RO20) at 37°C. Lane 1, ³²P-polypurine/³²P-polypyrimidine dsDNA (³²P-Dup61) plus Hp13 plus Hp23 plus RO20; lane 2 and 3, ³²P-Dup61 plus Hp13 plus Hp23; lane 4, ³²P-Dup61 plus RO20; lane 5, ³²P-Dup61; lane 6, ³²P-

RO20 plus polypurine ssDNA (pPu61). Poly-dI:dC (2 μ g) was added to each sample. The different species of DNA (ss, ds, triplex) are indicated by arrows. Labeled oligonucleotides are indicated as (•), and unlabeled oligonucleotides are indicated as (+).

4.1.1.5. Strand displacement using a single hairpin and posterior binding of a specific oligonucleotide.

As shown previously, each hairpin on its own was also able to maintain the dsDNA open. We evaluated whether a specific oligonucleotide (RO20) was able to bind to a displaced polypurine strand (pPu61) by the action of only one hairpin, either hairpin-13 (Hp13) or hairpin-23 (Hp23). Incubation of labeled polypurine/polypyrimidine dsDNA (Dup61) with Hp13 and RO20 (lane 3) was studied. When the mixture was incubated, the band corresponding to pPu61 (lane 2) disappeared, confirming that RO20 was able to bind to the displaced polypurine strand of the duplex. The same analysis was carried out for Hp23 (lanes 4 and 5), with the same results.

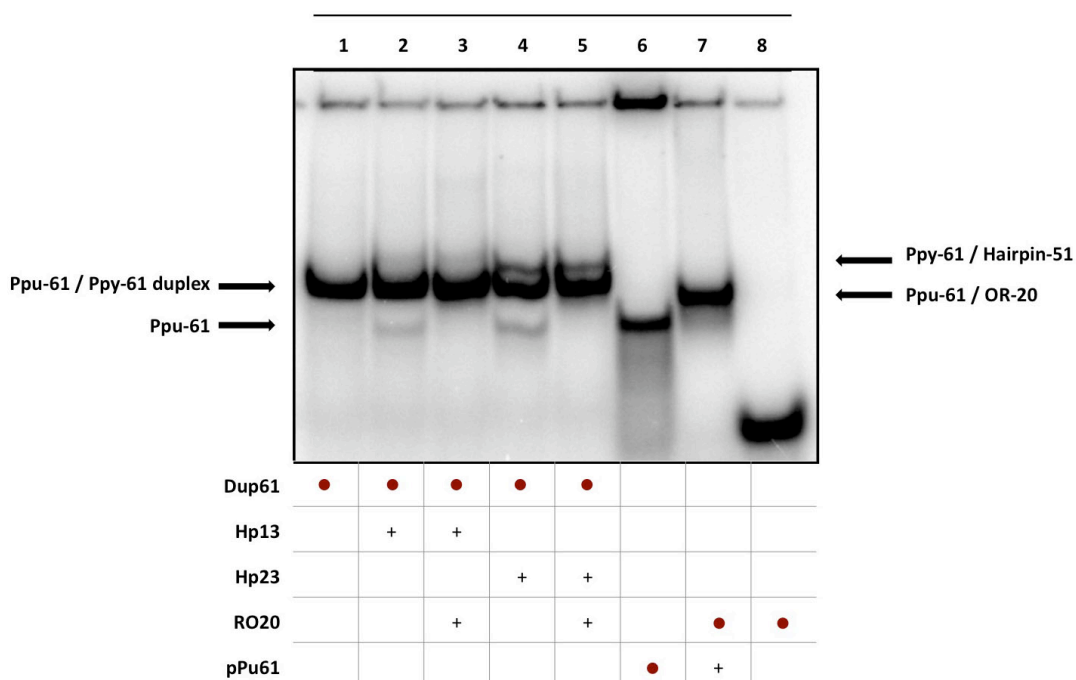


Figure 5. Binding between the displaced polypurine strand of the duplex (pPu61) and a specific polypyrimidine oligonucleotide (RO20), in the presence of only one hairpin. Lane 1, labeled 32 P-polypurine/ 32 P-polypyrimidine dsDNA (Dup61); lane 2, 32 P-

Dup61 with Hp13; lane 3, ³²P-Dup61 with Hp13 and RO20; lane 4, ³²P-Dup61 with Hp23; lane 5, ³²P-Dup61 with Hp13 and RO20; lane 6, ³²P-polypurine ssDNA (pPu61); lane 7, ³²P-RO20 plus pPu61; lane 8, ³²P-RO20. The entire mixture of all samples was heated at 75°C before the binding reaction. Incubations were performed at 37°C for 30 minutes. Poly-dI:dC (2µg) was added to each sample. The different species of DNA (ss, ds, triplex) are indicated by arrows. Labeled oligonucleotides are indicated as (●), and unlabeled oligonucleotides are indicated as (+).

4.1.1.6. G4-E2rep used as a negative control

DG44-p11Mut cell line was used to study the effect of a specific oligonucleotide bearing a G-quadruplex (G4) structure instead of a hairpin. The repair tail sequence is the same than that of the HpE2rep. However, in this design, the sequence of the PPRH core was changed by a sequence that folds into a G4 structure (Table 1).

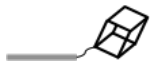
Name	Sequence (5' to 3')
G4-E2rep 	<u>GGGCGGGCGCGAGGGAGGGGTTTGAGGAGGAGGAGGTCATTCTTT</u> GGAAG G TACTTGAATTC

Table 1. Sequence of the G4-E2rep, formed by a repair tail (rep2) bearing the corrected nucleotide (in bold) linked to a G4 sequence (underlined).

After transfecting G4-E2rep into DG44-p11Mut cells using the calcium phosphate method we did not observe any surviving colony in selective -GHT medium.

This result shows that the PPRH core plays an important role in correcting the point mutation. Its function is not restricted to protect the repair oligonucleotide since this could also be accomplished by the G4 structure.

4.2 Article II

Correction of single point mutations at the endogenous *locus* of the *dihydrofolate reductase* gene in mammalian cells using Polypurine Reverse Hoogsteen hairpins

Manuscript submitted to Biochemical Pharmacology

Background: We had previously described the design and use of repair-PPRHs as a new methodology to correct a point mutation in a *dihydrofolate reductase* (*dhfr*) minigene, in Chinese Ovary Hamster (CHO) cells. Repair-PPRHs are formed by a PPRH core, following the Reverse Hoogsteen bonds rules, covalently connected to a repair tail, which is complementary to the mutated region of the dsDNA except for the nucleotide to be repaired.

Objectives: To study the ability of repair-PPRHs in correcting different types of endogenous point mutations in different CHO cell lines, using the *dhfr* gene as a model. Additionally, to further explore whether repair-PPRHs could be used even when there are not polypyrimidine domains near the point mutation region.

Results: Various point mutations in the endogenous *dhfr* gene have been successfully repaired in mammalian cells using repair-PPRHs, including a deletion, an insertion, and single and double substitutions in different regions of the gene. All repaired colonies showed high levels of DHFR protein and activity, and the corrected nucleotide was confirmed in all DNA sequences. New repair molecules were designed and tested, called short- and long-distance-repair-PPRHs (SDR-PPRH and LDR-PPRH). Since these repair-PPRHs can act from hundreds of nucleotides away from the altered region, it was no longer necessary to find polypyrimidine stretches near the mutated region.

Conclusions: Repair-PPRHs represent a new methodology for genome editing. These molecules show the ability to correct different point mutations in the endogenous *locus* of the *dhfr* gene, and could provide the basis for a new therapeutic alternative in single-point mutation genetic diseases.

Elsevier Editorial System(tm) for
Biochemical Pharmacology
Manuscript Draft

Manuscript Number:

Title: Correction of point mutations in the dihydrofolate reductase gene using Repair-PolyPurine reverse Hoogsteen hairpins in mammalian cells

Article Type: Full Length Articles

Section/Category: Antibiotics and Chemotherapeutics

Keywords: Gene correction, point mutation, PPRH, dhfr, endogenous locus

Corresponding Author: Prof. Carlos J Ciudad, PhD

Corresponding Author's Institution: University of Barcelona, School of Pharmacy

First Author: Anna Sole, MS

Order of Authors: Anna Sole, MS; Carlos J Ciudad, PhD; Lawrence A Chasin, Ph.D.; Veronique Noe, Ph.D.

Manuscript Region of Origin: Europe

Abstract: Correction of point mutations that lead to aberrant transcripts, often with pathological consequences, has been the focus of considerable research. In this work, repair-PPRHs are shown to be a new powerful tool for gene correction. Repair-PPRHs are Polypurine reverse Hoogsteen hairpins bearing an extension sequence at one end, homologous to the DNA strand to be repaired but containing the wild type nucleotide instead of the mutation.

Repair-PPRHs were designed to correct insertions, deletions, substitutions and a double substitution present in a collection of mutants at the endogenous locus of the dihydrofolate reductase (dhfr) gene, the product of which is the target of the chemotherapeutic agent methotrexate. We also describe an approach to use when the point mutation is far away from the homopyrimidine target domain. This strategy consists in designing Long-Distance- and Short-Distance-Repair-PPRHs. Surviving colonies in a DHFR selective medium were analyzed by DNA sequencing, and by mRNA, protein and enzymatic measurements, confirming that all the dhfr mutants had been corrected.

1
2 **Correction of point mutations in the dihydrofolate reductase gene using**
3
4 **Repair-PolyPurine reverse Hoogsteen hairpins in mammalian cells**
5

6
7 *Anna Solé¹, Carlos J. Ciudad^{1*}, Lawrence A. Chasin² and Véronique Noé¹*
8
9

10
11
12 ¹Department of Biochemistry and Molecular Biology, School of Pharmacy, IN2UB,
13
14 University of Barcelona, 08028, Barcelona, Spain
15

16
17 ²Department of Biological Sciences, Columbia University, NY, NY 10027
18
19
20
21
22
23
24
25
26
27
28
29
30
31
32

33
34 *Correspondence should be addressed to Carlos J. Ciudad, Department of
35
36 Biochemistry and Molecular Biology, School of Pharmacy, Av. Juan XXIII #27, E-
37
38 08028 Barcelona, Spain. Phone: +34934034455. Fax: +34934024520; e-mail:
39
40 cciudad@ub.edu
41
42
43
44
45
46
47
48
49
50
51
52
53
54
55
56
57
58
59
60
61
62
63

ABSTRACT

1
2 Correction of point mutations that lead to aberrant transcripts, often with
3
4 pathological consequences, has been the focus of considerable research. In this
5
6 work, repair-PPRHs are shown to be a new powerful tool for gene correction.
7
8 Repair-PPRHs are Polypurine reverse Hoogsteen hairpins bearing an extension
9
10 sequence at one end, homologous to the DNA strand to be repaired but containing
11
12 the wild type nucleotide instead of the mutation.
13
14 Repair-PPRHs were designed to correct insertions, deletions, substitutions and a
15
16 double substitution present in a collection of mutants at the endogenous *locus* of
17
18 the dihydrofolate reductase (*dhfr*) gene, the product of which is the target of the
19
20 chemotherapeutic agent methotrexate. We also describe an approach to use when
21
22 the point mutation is far away from the homopyrimidine target domain. This
23
24 strategy consists in designing Long-Distance- and Short-Distance-Repair-PPRHs.
25
26 Surviving colonies in a DHFR selective medium were analyzed by DNA sequencing,
27
28 and by mRNA, protein and enzymatic measurements, confirming that all the *dhfr*
29
30 mutants had been corrected.
31
32
33
34
35
36
37
38
39
40
41
42
43

44 **KEYWORDS:** Gene correction, point mutation, PPRH, *dhfr*, mammalian cells,
45
46 endogenous locus
47
48
49
50
51
52
53
54
55
56
57
58
59
60
61
62
63
64
65

1. INTRODUCTION

Mutations in somatic cells can induce pathological processes. They arise from a variety of sources, including replication errors, spontaneous lesions such as depurination and deamination, the generation of active-oxygen species or by the action of physical or chemical mutagens.

In this work, we focused on point mutations, resulting from a change in one or a few nucleotides at one location in the DNA sequence. Point mutations can be classified in: i) Substitutions, resulting in a missense or nonsense mutation, and ii) Deletions and insertions that cause frameshift mutations.

Several approaches have been sought for efficient editing of a single base pair, including ZFN, TALEN and CRISPR/Cas9 site-specific nucleases. However, there is not a definitive method yet to correct these mutations, given the difficulty in constructing and delivering exogenous enzymes, the off-target effect caused by the nucleases, and the non-homologous end joining effects stimulated after a DNA double strand break. In this work, we present an alternative method, simpler, safer and less invasive. PolyPurine Reverse Hoogsteen hairpins (PPRHs) are double stranded DNA molecules developed in our laboratory [1]. These hairpins are formed by two antiparallel homopurine domains connected by a five-thymidine loop, which fold in a hairpin structure by intramolecular Reverse Hoogsteen bonds. PPRHs bind to a third pyrimidine strand since purines can form a Watson Crick bond with a pyrimidine while they can form a Reverse Hoogsteen bond with another purine. The formation of this triplex structure displaces the fourth DNA strand *in vitro* [1]. PPRHs can be differentiated in either template- or coding-

PPRHs and were first described for gene silencing [2, 3], [4], [5], and [6].

Subsequent work established that they could also be used to correct a nonsense mutation in a *dhfr* minigene. Repair-PPRHs are Polypurine reverse Hoogsteen hairpins bearing an extension sequence at one end homologous to the DNA strand to be repaired but containing the wild type nucleotide instead of the mutation [7].

We also made a successful first attempt to correct a point mutation at the endogenous *locus* of the *dhfr* gene, the product of which is the target of the chemotherapeutic agent methotrexate. Homologous recombination was found to play an important role in the mechanism for gene correction by repair-PPRHs [7].

Here we wanted to expand the use of repair-PPRHs and improve the methodology to correct a representative collection of different types of mutations (substitutions, double substitutions, deletions and insertions) at an endogenous *locus* in a mammalian genome. To achieve this goal, we again used the *dhfr* gene as a model because it is a selectable marker that readily allows for the identification of repaired clones, and because of the availability of an extensive collection of endogenous mutants obtained by UV irradiation, and different chemicals such as N-hydroxy-aminofluorene [8-12].

2. MATERIALS AND METHODS

2.1. Cell culture

Different CHO cell lines were used for gene correction. All of them contained single or double base substitutions or insertions/deletions. Mutations in the *dhfr* gene described in Table 1. These cell lines were isolated using a variety of mutagens from UA21, a CHO cell line hemizygous for the *dhfr* gene [13], which was used here as a positive control. The following mutant cell lines were used: DA5 and DA7 [12]; DU8 [9]; DF42 [8]; DP12B and DP6B [11] and DI33A [10] and [11]. Cells were grown in Ham's F12 medium containing 7% fetal bovine serum (Invitrogen), and incubated at 37°C in a humidified 5% CO₂ atmosphere. For expansion and harvesting, cells were detached with 0.05% trypsin (Sigma).

2.2. Oligodeoxynucleotides

Unmodified PPRHs and ODNs were designed according to the rules of Hoogsteen and Watson–Crick pairing, depending on the desired interaction. Complementary bases were used at positions of interruptions in the PPRH sequence [14].

Lyophilized oligonucleotides (Sigma-Aldrich) were dissolved in sterile and RNase-free TE (1mM EDTA and 10mM Tris-HCl, pH 8.0) to attain a stock solution of 1mM, and maintained at – 20°C. The sequences of PPRHs and repair oligonucleotides are listed in Table 2.

2.3. Transfection and selection

Transfection by repair-PPRHs was carried out using the calcium phosphate method [15], which involved the addition of 250mM CaCl₂ to the DNA complex. A

1 hundred μl of DNA/ CaCl_2 solution was added drop wise to an equal volume of
2 sterile twice-concentrated HEPES-buffered saline (2X HBS; 280mM NaCl, 50mM
3 HEPES, and 1.5mM sodium phosphate, pH-adjusted to 7.1). The calcium
4 phosphate/DNA precipitate was allowed to form for 30min at room temperature
5 without agitation. The total 200 μl of the mixture was added per well to the
6 mutated cells in 1.8ml of growth medium. After 5 hr of incubation at 37°C, the
7 medium was replaced and the cells were incubated for an additional 24 hr. At that
8 time, Ham's F-12 was changed to selective Ham's F-12 medium lacking glycine,
9 hypoxanthine and thymidine (-GHT medium), the final products of DHFR activity,
10 containing 7% of dialyzed fetal bovine serum (Invitrogen), to select for repaired
11 cells. Transfection was also performed using 10 μM of the cationic liposome
12 DOTAP (Biontech) obtaining successful results. Each assay was conducted a
13 minimum of three times, and for each repair-PPRH that succeeded in repairing the
14 selected point mutation, a minimum of three colonies from each of three different
15 replicates were analyzed by DNA sequencing, and for DHFR levels of mRNA,
16 protein, and activity.

2.4. mRNA analysis

24 After selecting and growing the colonies, total RNA from repaired cells was
25 extracted using Trizol Reagent (Life Technologies, Madrid, Spain), according to the
26 manufacturer's specifications. The amount of RNA was determined by measuring
27 its absorbance (260nm) at 25°C in a Nanodrop ND-1000 spectrophotometer
28 (Thermo Scientific, Wilmington, DE). cDNA was synthesized in a 20 μl reaction
29 mixture containing 500ng of total RNA, 250ng of random hexamers (Roche,
30 Barcelona, Spain), 10mM dithiothreitol, 20 units of RNasin (Lucigen, Middleton,

1 United States), 0.5mM of each dNTP (Epicentre, Madison, United States), 4µl of
2 buffer (5X), and 200 units of Moloney murine leukemia virus reverse transcriptase
3 (RT) (Lucigen, Middleton, United States). The reaction mixture was incubated at
4 42°C for 1h. 3 µl of the cDNA mixture was used for PCR amplification by Real Time
5 PCR.
6
7
8
9
10

11 Real Time-PCR — The reaction was performed using the StepOnePlus™ Real-Time
12 PCR Systems (Applied Biosystems, Life-Technologies, S.A, Madrid, Spain) in a final
13 volume of 20µl, containing 3µl of cDNA, 2X SYBR® Select Master Mix (Applied
14 Biosystems, Life Technologies, Madrid, Spain), 0.125µM of reverse and forward
15 primers (Sigma-Aldrich, Madrid, Spain) and H₂O. Adenine
16 phosphoribosyltransferase (APRT) mRNA was used to normalize the results. The
17 primer sequences were: Dhfr2-Fw, 5'-AAGAACGGAGACCTTCCCTG-3', Dhfr2-Rv 5'-
18 CGGAACTGCCTCCAACCTATC-3'; Aprt-Fw, 5'-GCATGGCGGCAAGATCGACT-3', Aprt-
19 Rv, 5' GTTCTAAGGCGTCTTTCTGG-3'. PCR cycling conditions were 2 min at 50°C,
20 10 min denaturation at 95°C, followed by 40 cycles of 15s at 95°C and 1 min at
21 60°C, and a fourth stage of 15s at 95°C, 20s at 60°C and 15s at 95°C. The mRNA
22 amount of the target gene, normalized to APRT, was calculated by the $\Delta\Delta C_t$
23 method, where C_t is the threshold cycle indicating the fractional cycle number at
24 which the amount of amplified mRNA reached the threshold of fluorescence.
25
26
27
28
29
30
31
32
33
34
35
36
37
38
39
40
41
42
43
44
45
46
47
48

49 2.5. Western blot analyses

50 Cells were harvested by trypsinization and treated with Lysis buffer (50mM
51 HEPES, 0.5M NaCl, 1.5mM MgCl₂, 1mM EGTA, 10% glycerol, 1% Triton X-100, pH
52 7.2), supplemented with Protease Inhibitor Mixture (Sigma-Aldrich, Madrid,
53 Spain). Total extracts were maintained at 4°C for 1h with vortexing every 15 min.
54
55
56
57
58
59
60
61
62
63
64
65

1 Cell debris was removed by centrifugation (10,000 x g for 10 min). Protein
2 concentrations were determined by the Bio-Rad protein assay (based on the
3 Bradford method, using bovine serum albumin as a standard (Sigma-Aldrich,
4 Madrid, Spain)).
5
6

7
8
9 Total protein cell extracts (100µg) were electrophoresed on SDS-12%
10 polyacrylamide gels, and transferred to a polyvinylidene difluoride membrane
11 (Immobilon P, Millipore, Madrid, Spain) using a semidry electroblotter. The
12 membranes were probed with antibodies against DHFR (1:250 dilution) and
13 tubulin (1:800 dilution; CP06, Calbiochem, Merck, Darmstadt, Germany) to
14 normalize the results. Signals were detected with HRP-conjugated antibodies: anti-
15 rabbit (1:2500 dilution; P0399, Dako, Denmark) for DHFR, anti-mouse (1:2500
16 dilution; sc-2005, Santa Cruz Biotechnology, Heidelberg, Germany) for tubulin, and
17 enhanced chemiluminescence using ECL™ Prime Western Blotting Detection
18 Reagent, as recommended by the manufacturer (GE Healthcare, Barcelona, Spain).
19
20 Tubulin and total protein loading were both used to normalize the results.
21
22 Chemiluminescence was detected with ImageQuant LAS 4000 Mini (GE Healthcare,
23 Barcelona, Spain) and quantification was performed using the Image Quant 5.2
24 software.
25
26
27
28
29
30
31
32
33
34
35
36
37
38
39
40
41
42
43
44
45
46

47 2.6. DHFR activity

48
49 The method is based on the incorporation of radioactive deoxyuridine into cellular
50 DNA, which depends on the generation of tetrahydrofolate by DHFR from folate
51 supplied in the medium. Tetrahydrofolate is used in the reductive methylation of
52 deoxyuridylate to thymidylate. The latter is subsequently incorporated into DNA,
53 which is then isolated by precipitation [16].
54
55
56
57
58
59
60
61
62
63
64
65

1 Dishes (35 mm) were plated with 10×10^4 dhfr negative or repaired cells in 1ml of
2 selective medium (-GHT). After 16 hours, $2\mu\text{Ci}$ of 6- $^{[3}\text{H}]$ deoxyuridine (20
3
4
5 mCi/mmol, Moravек Biochemicals, Inc., USA) were added for 24 hours. Cells were
6
7 rinsed twice with phosphate-buffered saline and lysed in $100\mu\text{l}$ of 0.1% sodium
8
9 dodecyl sulfate. The lysate was placed onto 31ET paper (Whatman) and washed
10
11 three times with 66% cold ethanol containing 250mM NaCl, dried, and counted in a
12
13 scintillation counter.
14
15

20 2.7. DNA sequencing

21
22 Total DNA was obtained using the Wizard® Genomic DNA Purification Kit
23
24 (Promega, Madrid, Spain), according to the manufacturer's specifications. PCR was
25
26 performed to amplify the specific region containing either the point mutation or
27
28 the repaired nucleotide, using the OneTaq DNA Polymerase (New England Biolabs,
29
30 Ipswich, United States). The primer sequences were: Dhfr6-Fw
31
32 (GTCATGTGTCTTCAATGGGTG) and Dhfr6-Rv (TCTAAAGCCAACACAAGTCCC) for
33
34 the DA5 and FD42 cell lines, Dhfr-Ex3-Fw (GACAATGGTATCTTGCCTGTG) and
35
36 Dhfr-Ex3-Rv (TGTA CTGGTCTATGCTCTGGG) for the DA7 cell line, Dhfr-Int1-Fw
37
38 (GCTCTAGCTGGGAGCAAAGTC) and Dhfr-Int2-Rv (GCAAAGTTCCCAGATTCCCAC)
39
40 for the DU8 cell line, Dhfr-Int4-Fw (CAGCCACATCAGGTGGTTCA) and Dhfr-Int5-Rv
41
42 (TGTCCTTACTTGCTCCCCTTTC) for the DP12B cell line, Dhfr-Int5-Fw
43
44 (CTCACTTAGGAGTGGCTCACC) and Dhfr-Ex6.1-Rv (TCCCAGGTTCCATCTCTGGT)
45
46 for the DI33A cell line. Sequencing was carried out by Macrogen (Amsterdam, The
47
48 Netherlands).
49
50
51
52
53
54
55
56
57
58
59
60
61
62
63
64
65

3. RESULTS

To test the potential of repair-PPRHs in different types of point mutations, we used a collection of various *dhfr* mutant cells; all derived from the parental cell line UA21 [13], which carries only one copy of the *dhfr* gene. The natural stop codon is found at nucleotide 562 of the protein-coding region. All mutants used here produce termination codons either by a direct base substitution or indirectly due to frameshift by single base insertions or deletions or by exon skipping (Table 1). These mutant cells produce no functional DHFR enzyme and so are unable to grow in a DHFR selective culture medium without glycine, hypoxanthine and thymidine (-GHT).

Specific repair-PPRHs for each mutant cell line were devised by attaching to the end of one strand of the PPRH core, a sequence tail homologous to the point mutation region of the target, except for the mutated nucleotide, which was corrected (Table 2). This extended tail was added to provide the PPRHs with the ability to repair the mutation. We searched for polypyrimidine regions near to the point mutations and proceeded according to the rules of PPRH construction [2, 3]. When encountering purine interruptions in the polypyrimidine stretches, we chose the WT-PPRH strategy, which includes the base complementary to the target interruption in the PPRH core [14]. Different numbers of cells, ranging from 1,000 to 150,000 were plated and the corresponding repair-PPRHs were transfected using 2 to 5 μ g of DNA. Six random cell colonies surviving in -GHT medium from different experiments were expanded individually, and the targeted DNA region

1 was PCR-amplified and sequenced. Cells were subsequently analyzed for DHFR
2 mRNA, protein, and enzyme activity levels.
3

4 The correction of a set of mutations that include a deletion, substitutions and an
5 insertion is described below.
6
7

8 9 10 11 3.1. Correction of a deletion

12 The first cell line subjected to correction by repair-PPRHs was DA5, where the
13 deletion of a guanine in exon 6 of the *dhfr* gene results in a frameshift that
14 generates a premature opal stop codon (TGA). The repair-PPRH used (HpDE6rep)
15 contained three pyrimidine interruptions, and its hairpin core was extended with
16 25nt at the 5' end including the missing guanine. We confirmed the presence of the
17 corrected nucleotide in all repaired colonies analyzed. DHFR mRNA levels in the
18 repaired cells were higher than in the mutant DA5 cell line. The protein was
19 restored in all cases, and it showed high levels of DHFR activity (Figure 1).
20
21
22
23
24
25
26
27
28
29
30
31
32
33
34
35
36

37 3.2. Correction of a substitution that results on a premature stop codon

38 The next step was to test whether repair-PPRHs were also able to correct
39 substitutions. Thus, we chose DA7 cells that contain a substitution of a guanine by
40 a thymine in exon 3, producing an amber stop codon (TAG) *in situ*. A 20nt
41 polypyrimidine sequence in the template strand upstream of the point mutation
42 was used to design HpDE3rep. The sequence tail was extended from the 3' end of
43 the hairpin core, with the wild type guanine instead of the thymine present in the
44 mutant. After the isolation of the surviving colonies, we confirmed the corrected
45 guanine in the DNA sequence, high levels of mRNA, protein and activity compared
46 to DA7 cells (Figure 1).
47
48
49
50
51
52
53
54
55
56
57
58
59
60
61
62
63
64
65

3.3. Correction of an insertion

1
2 Insertions are another type of point mutation very detrimental due to the
3
4 disruption of the reading frame of a sequence. We chose the DI33A cell line to test
5
6 whether repair-PPRHs were able to correct an insertion of a guanine in *dhfr* exon
7
8 6. Two repair-PPRHs were designed: HpDE6-4rep using a 14nt pyrimidine
9
10 sequence found in the coding strand upstream of the mutation, and HpDE6-5rep
11
12 using a 15nt sequence in the template strand downstream of the mutation. Both
13
14 repair-PPRHs succeeded in correcting the mutation by introducing the missing
15
16 guanine in the DNA sequence, and thus restoring DHFR protein and its activity. The
17
18 amount of DHFR mRNA of repaired cells was similar than those of the mutant cells
19
20
21
22
23
24
25 (Figure 1).
26
27
28

3.4. Correction of a substitution that results in the skipping of exon 5

29
30 Substitutions can also be found in non-coding regions, without changes in the
31
32 amino acid sequence. However, an alteration in an intron may affect splicing and
33
34 lead to a frameshift in the subsequent downstream amino acid sequence. Hence,
35
36 the DP12B mutant cell line was chosen to test the capacity of repair-PPRHs to
37
38 correct a substitution of an adenine by a thymine at the penultimate position of
39
40 intron 4 that causes the skipping of exon 5 and a subsequent opal premature stop
41
42 codon in exon 6. We searched for polypyrimidine sequences in both DNA strands
43
44 near the point mutation, finding 3 different domains. HpDI4-1rep was designed
45
46 from a 16nt polypyrimidine sequence in the coding strand, two nucleotides
47
48 upstream of the mutation. HpDI4-2rep originated from a 13nt polypyrimidine
49
50 sequence in the template strand, 18nt upstream of the mutation. The third repair-
51
52
53
54
55
56
57
58
59
60
61
62
63
64
65 PPRH target was 22nt, contained one purine interruption and was found 41nt

1 upstream of the mutation. In this case, it was not feasible to design a repair tail
2 directly attached to the hairpin core, because the total repair-PPRH sequence
3 would exceed a length of 100nt in the synthesis of oligonucleotides. Therefore, we
4 attempted a different design in which the hairpin core and the repair tail were
5 connected by 5 thymidines instead of the whole intervening sequence between
6 them. This PPRH was called SDR-HpDI4-3rep, for Short-Distance-Repair hairpin,
7 since it skipped 26 nucleotides of the intron. Upon transfection, surviving colonies
8 were obtained in selective medium with HpDI4-2rep and SDR-HpDI4-3rep but not
9 with HpDI4-1rep. These colonies were isolated and analyzed, and DHFR mRNA
10 levels were comparable to the mutant cells. The DNA sequence was corrected and
11 the protein was restored showing DHFR activity (Figure 2).
12
13
14
15
16
17
18
19
20
21
22
23
24
25
26
27
28

29 3.5. Correction of a double base pair substitution

30 Our results showed that repair-PPRHs could correct different types of single
31 nucleotide mutations. The next challenge would be to repair double point mutants.
32 Thus, DU8 cells were selected to test the ability of repair-PPRHs to correct the
33 tandem mutation of two nucleotides. DU8 cells contain a substitution of 2
34 nucleotides, Gg > Aa, involving the last nucleotide of exon 2, and the first
35 nucleotide of intron 2. This change does not involve a nonsense mutation *in situ*,
36 but provokes the skipping of exon 2, which disrupts the reading frame. As a
37 consequence, an opal stop codon appears prematurely. Two different repair-
38 PPRHs were designed for this approach: HpDE2-1rep, located 7nt upstream of the
39 mutation, and HpDE2-2rep, 12nt downstream of the mutation. The structure of
40 HpDE2-1rep is that of a hairpin core of 13nt, containing two pyrimidine
41 interruptions, followed by a 24nt tail bearing the corrected nucleotides. In HpDE2-
42
43
44
45
46
47
48
49
50
51
52
53
54
55
56
57
58
59
60
61
62
63
64
65

1 2rep the hairpin core contains 10nt, with one interruption, ending in a 25nt repair
2 tail. Both repair-PPRHs succeeded in correcting the double point mutation at all
3 levels (Figure 2).
4
5
6
7
8
9

10 3.6. Correction of a substitution at long distance

11 One of the limitations of this methodology could reside in finding homopurine
12 domains relatively close to the point mutation. To solve this, we designed a Long
13 Distance Repair-PPRH (LDR-PPRH) containing a hairpin core hundreds of
14 nucleotides away from the location of the mutation, linked by 5 Ts to the repair
15 tail. This approach was tested in DF42 cells, containing a substitution of a guanine
16 by a thymine in exon 6 resulting in an ochre stop codon (TAA). We designed a
17 repair tail at the location of the point mutation, and a hairpin core targeting a
18 sequence located 662nt downstream. This repair-PPRH was called LDR-HpDE6-
19 1rep, formed by a hairpin core of 22nt in each homopurine strand containing three
20 pyrimidine interruptions, and a tail of 31nt. In parallel, we also tested HpDE6rep, a
21 regular repair-PPRH, and we obtained similar results for both approaches. The
22 levels of mRNA in the repaired cells were similar to those of the mutant. However,
23 repaired colonies recovered DHFR protein with high activity, and the nucleotide
24 was corrected in the DNA sequence (Figure 2).
25
26
27
28
29
30
31
32
33
34
35
36
37
38
39
40
41
42
43
44
45
46
47
48

49 3.7. Frequency of correction

50 The number of colonies appearing in each well after the selection process were
51 counted and divided by the number of cells initially plated. The determination was
52 performed with different number of cells and as low as 1,000 cells were used. The
53 highest frequency of correction obtained was 7.6×10^{-2} (Table 3).
54
55
56
57
58
59
60
61
62
63
64
65

3.8. Specificity of repair-PPRHs

1
2
3
4
5 Three of the repair tails were transfected alone, to test whether short repair
6
7 oligonucleotides (RO) bearing the wild type nucleotide could also correct the point
8
9 mutation without the assistance of the hairpin core. R025-HpE6rep was used in
10
11 DF42 and DA5 cells, R031-HpDI4-2rep in DP12B cells, and R028-HpDE6-4rep and
12
13 R041-HpDE6-5rep in DI33A cells, thus covering deletions, substitutions and
14
15 insertions. The transfection of these oligonucleotides without the PPRH core into
16
17 DP12B and DI33A cells did not generate any positive colony in selective medium,
18
19 whereas in DF42 cells some surviving colonies were obtained although the
20
21 frequency was very low (7×10^{-5}). In addition, a PPRH bearing a tail fully
22
23 homologous to the mutated region did not produce any repair colony.
24
25
26
27
28
29 Furthermore, the sequences corresponding to the arm of the PPRH core that binds
30
31 to the DNA plus the repair tail of all repair-PPRHs were subjected to BLAST
32
33 analyses. The length of these sequences ranged from 35 to 56 nucleotides. When
34
35 the shorter sequence (35-mer) was analyzed, the *dhfr* gene target obtained an E-
36
37 value of $3e^{-12}$, while the first unspecific target achieved an E-value of 2.3, thus
38
39 showing high specificity of the repair-PPRH and minimizing the possible off-target
40
41 effects. For the longer sequence, the E-value for the *dhfr* gene target was of $8e^{-22}$
42
43
44
45
46
47 and for the unspecific target 0.33.
48
49
50
51
52
53
54
55
56
57
58
59
60
61
62
63
64
65

4. DISCUSSION

The main conclusion of this work is that repair-PPRHs can be used to efficiently correct a variety of point mutations in mammalian cells and that they can do so across a separation of hundreds of nucleotides between the PPRH binding site and the mutational target. In previous studies, we provided evidence that repair-PPRHs were a powerful molecule to repair a point mutation using a mutated *dhfr* minigene. In this study we demonstrate that different point mutations in the endogenous *dhfr* gene of CHO cells can be precisely corrected by repair-PPRHs, allowing the expression of normal DHFR protein and survival in selective -GHT medium. Six mutant cell lines with six different types of point mutations were corrected: i) a deletion and an insertion of one nucleotide in exon 6 that cause an opal premature stop codon; ii) substitutions in exons 3 and 6 provoking *in situ* an amber and an ochre stop codon, respectively; iii) a substitution in intron 4 that causes exon skipping and a consequent stop codon; and iv) a double substitution located between exon 2 and intron 2, causing skipping of exon 2 resulting in a downstream stop codon.

An apparent limitation of repair-PPRHs could be the absence of a useful polypurine/polypyrimidine sequence near enough to the point mutation to allow hybridization of the attached repair tail. In addition, the length of the PPRH core might be relatively short depending on the occurrence of polypyrimidine stretches in the target gene, which might affect the specificity of binding of the PPRH core. Although these polypyrimidine stretches are more common than predicted by random models [2], it can be difficult to find an appropriate sequence, adjacent or close to the point mutation. We dealt with these situations by designing two new

1 repair-PPRHs called short-distance-repair-PPRH (SDR-PPRH) and long-distance-
2 repair-PPRH (LDR-PPRH) in which the short (25 to 31nt) single stranded repair
3 tail was tethered to the PPRH core by a five-thymidine spacer. Both repair-PPRHs
4 were able to efficiently correct their targeted mutation, indicating that adjacency
5 was not required for them to work. This flexibility greatly expands the number of
6 mutations that can be targeted and provides an economical alternative to the
7 synthesis of very long oligomers. Homopurine/homopyrimidine regions are
8 present on average about every kb in the human genome [17], suggesting that any
9 point mutation could be connected to an appropriate PPRH target region using
10 LDR-PPRHs.
11

12 HpDI4-1rep, tested in DP12B cells, was not successful in correcting the point
13 mutation. The main difference between this repair-PPRH and the others was the
14 position of the corrected nucleotide in the repair tail, apparently too close to the
15 hairpin core. This result indicates that a point mutation can be corrected by repair-
16 PPRHs when the corrected nucleotide is in the center of the repair tail, but not
17 when it is close to the PPRH core. Studies of mutation correction using single
18 stranded DNA oligomers alone have shown the importance of the position of the
19 corrected nucleotide, but no consistent rules have been established. A 25-mer
20 oligonucleotide with the corrected nucleotide located at the 3' end proved to be
21 the most effective to correct a point mutation in the GFP gene [18]. When a 25-mer
22 oligonucleotide was designed to correct a point mutation in the kanamycin
23 resistance gene, a decrease in the repair frequency was observed as the nucleotide
24 was moved away from the central position [19].

25 It has been suggested that single-stranded oligonucleotides designed to target the
26 coding strand are more efficient than those directed against the template strand
27

1 [20] [21] [19]. When designing the repair domain of the repair-PPRHs, we did not
2 differentiate between strands, and we concluded that no differences existed
3
4 between repair-tails homologous to either the coding or template DNA strands.
5
6 Our approach showed a higher frequency of repair compared to single-stranded
7
8 oligonucleotides used to correct a single-point mutation in the GFP gene, which
9
10 attained a maximum frequency of $2.3 \cdot 10^{-3}$ [18].
11
12

13
14 The effect of most of the mutations studied here on mRNA levels has not been
15
16 previously reported. All six mutants have mRNA levels as expected from either the
17
18 action of nonsense mediated decay (NMD) or translational read-through. Mutants
19
20 DF42, DP12B and DI33A present nonsense codons in exon 6, the terminal exon,
21
22 which should be immune to the effects of NMD [22]. Indeed all three mutants
23
24 exhibit high levels of DHFR mRNA: 83%, 66% and 61% of wild type levels,
25
26 respectively. Mutants DA7 and DA8 present nonsense codons in exon 3 and
27
28 accordingly exhibit lower levels of mRNA: 2% and 23% respectively. Mutant DA5
29
30 results in a read-through of the normal termination signal, with the next
31
32 termination signal 22nt downstream in the 3' UTR. Such read-through has been
33
34 shown to destabilize globin mRNA [23], and mutant DA5 in fact contains a
35
36 relatively low level of DHFR mRNA (17% of wild type). In addition to restoring
37
38 functional DHFR activity, in almost all cases the repaired mutant exhibited
39
40 increases in the DHFR mRNA level reduced by NMD in the mutant counterpart.
41
42 Some characteristics among all the repair-PPRHs used in this work are the
43
44 following: they are not chemically modified and have an average length of 75nt
45
46 with a minimum of 50nt and a maximum of 85nt. All contain a PPRH core with a
47
48 maximum of three pyrimidine interruptions, except for HpDE3rep that contains 5
49
50 thymines, and a covalently attached repair tail with a length between 24 and 41nt,
51
52
53
54
55
56
57
58
59
60
61
62
63
64
65

1 depending on the position of the corrected nucleotide (Figure 3A). All repair tails
2 are located at the 5' end of the PPRH core except for HpDE3rep used to correct
3 DA7 cells. Finally, SDR-PPRHs and LDR-PPRHs have the advantage of correcting
4 point mutations located far from the PPRH target sequence (Figure 3B). In
5 summary, we provide evidences that repair-PPRHs can correct different types of
6 mutations in mammalian cells. Our strategy may offer an alternative, simple and
7 powerful tool for gene therapy to correct many disorders caused by point
8 mutations.
9
10
11
12
13
14
15
16
17
18
19
20
21
22
23
24
25
26
27
28
29
30
31
32
33
34
35
36
37
38
39
40
41
42
43
44
45
46
47
48
49
50
51
52
53
54
55
56
57
58
59
60
61
62
63
64
65

Table 1. Mutant Cell lines subjected to correction using Repair-PPRHs

Cell line	Position	Alteration	Base changes	Coding change
DA5	541 (exon 6)	Deletion (-G)	GAA > -AA	Opal at 584 in exon 6 (normal termination is at 562)
DA7	235 (exon 3)	Substitution	GAG > TAG	Amber in place
DU8	136 +1 (exon2/intron2)	Double substitution	G/gt > A/at	Exon 2 skipped Opal at 139
DF42	541 (exon 6)	Substitution	GAA > TAA	Ochre in place
DP12B	370 - 2 (intron 4)	Substitution	ag > tg	Exon 5 skipped Opal at 504
DI33A	493 (exon6)	Insertion (+G)	GGG / GGGG	Opal at 505

The mutated bases are represented in the coding strand with a 5' to 3' orientation.

Position numbers are referred to the translational initiation site (ATG). For mutations that occurred in introns, the position relative to the nearest exon is given, where + indicates downstream of the exon and - means upstream of the exon.

Table 3. Frequencies of repair using repair-PPRHs

Number of cells seeded	Number of colonies	Repair frequency
150,000	15	$1 \cdot 10^{-4}$
60,000	8	$1.3 \cdot 10^{-4}$
30,000	23	$7.7 \cdot 10^{-4}$
10,000	32	$3.2 \cdot 10^{-3}$
3,000	48	$1.6 \cdot 10^{-2}$
1,000	76	$7.6 \cdot 10^{-2}$

The different number of cells indicated were seeded and transfected the day after with 3 μ g of repair-PPRHs. Upon selection in DHFR selective –GHT medium the number of surviving colonies was divided by the number of originally seeded cells.

FIGURES CAPTIONS**Fig 1 Analyses of repaired colonies from DA5, DA7 and DI33A mutants (A)**

DHFR protein levels in the repaired cells from DA5, DA7 and DI33A. Total protein extracts were obtained from surviving cell colonies upon transfection with the corresponding repair-PPRH. Western blots were performed with 100 µg of total extracts and were normalized to tubulin levels. Protein levels in the repaired colonies were referred to those of the positive control UA21. **(B)** DHFR activity in repaired colonies. One hundred thousand cells from three independent growth colonies were plated in 35mm dishes and their DHFR activity was determined by the incorporation of 2 µCi of 6-[³H] deoxyuridine to the DNA. Cells were collected and lysed with SDS after 24 hr. Radioactivity was counted in a scintillation counter **(C)** DHFR mRNA levels in repaired cells. RNA was extracted from surviving cell colonies upon transfection with the corresponding repair-PPRH. DHFR mRNA levels were determined using qRT-PCR and were normalized to APRT. DHFR mRNA levels of the repaired colonies were referred to the positive control UA21. **(D)** DNA sequences of the *dhfr* mutants, and from the corresponding repaired colonies upon transfection with repair-PPRHs. Each assay was conducted a minimum of three times, and a minimum of three colonies from three different replicates were analyzed

Fig 2 Analyses of repaired colonies from DP12B, DU8 and DF42 mutants (A)

DHFR protein levels in the repaired cells from DP12B, DU8 and DF42. Total protein extracts were obtained from surviving cell colonies upon transfection with the corresponding repair-PPRH. Western blots were performed with 100 µg of total extracts and were normalized to tubulin levels. Protein levels in the repaired

1 colonies were referred to those of the positive control UA21 (B) DHFR activity in
2 repaired colonies. One hundred thousand cells from three independent growth
3 colonies were plated in 35mm dishes and their DHFR activity was determined by
4 the incorporation of 2 μ Ci of 6-[³H] deoxyuridine to the DNA. Cells were collected
5 and lysed with SDS after 24 hr. Radioactivity was counted in a scintillation counter
6
7 (C) DHFR mRNA levels in repaired cells. RNA was extracted from surviving cell
8 colonies upon transfection with the corresponding repair-PPRH. DHFR mRNA
9 levels were determined using qRT-PCR and were normalized to APRT. DHFR
10 mRNA levels of the repaired colonies were referred to the positive control UA21.
11
12 (D) DNA sequences of the *dhfr* mutants, and from the corresponding repaired
13 colonies upon transfection with repair-PPRHs. Each assay was conducted a
14 minimum of three times, and a minimum of three colonies from three different
15 replicates were analyzed
16
17
18
19
20
21
22
23
24
25
26
27
28
29
30
31

32
33
34 **Fig 3 Scheme of the different designs of PPRHs** (A) Representation of a repair-
35 PPRH, consisting on a Hoogsteen hairpin core bearing an extension sequence at
36 one of its ends, homologous to one of the strands of the DNA except for the
37 position of the mutated nucleotide to be repaired. (B) A scheme of a short-
38 distance-repair-PPRH (SDR-PPRH) or a long-distance-repair-PPRH (LDR-PPRH),
39 containing a hairpin core, far away from the location of the point mutation, linked
40 by 5Ts to a repair tail to correct the mutation at long distance
41
42
43
44
45
46
47
48
49
50
51
52
53
54
55
56
57
58
59
60
61
62
63
64
65

ACKNOWLEDGMENTS

This work was supported by grant SAF2014-51825-R from Plan Nacional de Investigación Científica (Spain). Our group holds the Quality Mention from the Generalitat de Catalunya 2014SGR96. A.S. is the recipient of a fellowship Formació d'Investigadors (FI) from the Generalitat de Catalunya.

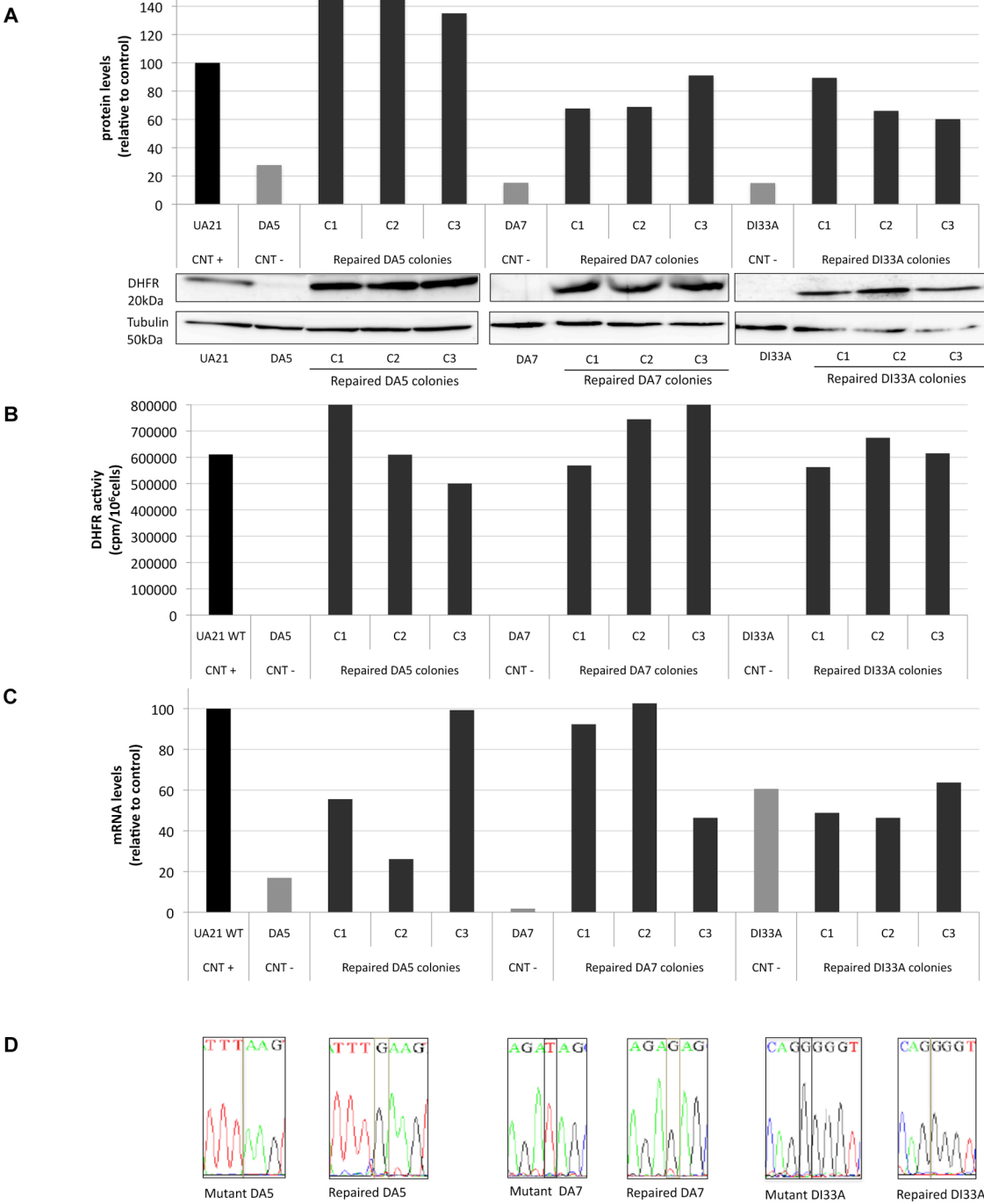
1
2
3
4
5
6
7
8
9
10
11
12
13
14
15
16
17
18
19
20
21
22
23
24
25
26
27
28
29
30
31
32
33
34
35
36
37
38
39
40
41
42
43
44
45
46
47
48
49
50
51
52
53
54
55
56
57
58
59
60
61
62
63
64
65

REFERENCES

- 1
2
3
4
5 [1] Coma S, Noe V, Eritja R, Ciudad CJ. Strand displacement of double-stranded
6 DNA by triplex-forming antiparallel purine-hairpins. *Oligonucleotides*.
7 2005;15:269-83.
- 8 [2] de Almagro MC, Coma S, Noe V, Ciudad CJ. Polypurine hairpins directed against
9 the template strand of DNA knock down the expression of mammalian genes. *The*
10 *Journal of biological chemistry*. 2009;284:11579-89.
- 11 [3] de Almagro MC, Mencia N, Noe V, Ciudad CJ. Coding polypurine hairpins cause
12 target-induced cell death in breast cancer cells. *Human gene therapy*.
13 2011;22:451-63.
- 14 [4] Rodriguez L, Villalobos X, Dakhel S, Padilla L, Hervas R, Hernandez JL, et al.
15 Polypurine reverse Hoogsteen hairpins as a gene therapy tool against survivin in
16 human prostate cancer PC3 cells in vitro and in vivo. *Biochemical pharmacology*.
17 2013;86:1541-54.
- 18 [5] Villalobos X, Rodriguez L, Prevot J, Oleaga C, Ciudad CJ, Noe V. Stability and
19 immunogenicity properties of the gene-silencing polypurine reverse Hoogsteen
20 hairpins. *Molecular pharmaceutics*. 2014;11:254-64.
- 21 [6] Villalobos X, Rodriguez L, Sole A, Lliberos C, Mencia N, Ciudad CJ, et al. Effect of
22 Polypurine Reverse Hoogsteen Hairpins on Relevant Cancer Target Genes in
23 Different Human Cell Lines. *Nucleic acid therapeutics*. 2015;25:198-208.
- 24 [7] Sole A, Villalobos X, Ciudad CJ, Noe V. Repair of single-point mutations by
25 polypurine reverse Hoogsteen hairpins. *Human gene therapy methods*.
26 2014;25:288-302.
- 27 [8] Carothers AM, Urlaub G, Steigerwalt RW, Chasin LA, Grunberger D.
28 Characterization of mutations induced by 2-(N-acetoxy-N-acetyl)aminofluorene in
29 the dihydrofolate reductase gene of cultured hamster cells. *Proceedings of the*
30 *National Academy of Sciences of the United States of America*. 1986;83:6519-23.
- 31 [9] Urlaub G, Mitchell PJ, Ciudad CJ, Chasin LA. Nonsense mutations in the
32 dihydrofolate reductase gene affect RNA processing. *Molecular and cellular*
33 *biology*. 1989;9:2868-80.
- 34 [10] Chasin LA, Urlaub G, Mitchell P, Ciudad C, Barth J, Carothers AM, et al. RNA
35 processing mutants at the dihydrofolate reductase locus in Chinese hamster ovary
36 cells. *Progress in clinical and biological research*. 1990;340A:295-304.
- 37 [11] Carothers AM, Urlaub G, Grunberger D, Chasin LA. Splicing mutants and their
38 second-site suppressors at the dihydrofolate reductase locus in Chinese hamster
39 ovary cells. *Molecular and cellular biology*. 1993;13:5085-98.
- 40 [12] Carothers AM, Urlaub G, Mucha J, Yuan W, Chasin LA, Grunberger D. A
41 mutational hot spot induced by N-hydroxy-aminofluorene in dihydrofolate
42 reductase mutants of Chinese hamster ovary cells. *Carcinogenesis*. 1993;14:2181-
43 4.
- 44 [13] Urlaub G, Kas E, Carothers AM, Chasin LA. Deletion of the diploid
45 dihydrofolate reductase locus from cultured mammalian cells. *Cell*. 1983;33:405-
46 12.
- 47 [14] Rodriguez L, Villalobos X, Sole A, Lliberos C, Ciudad CJ, Noe V. Improved
48 design of PPRHs for gene silencing. *Molecular pharmaceutics*. 2015;12:867-77.
- 49
50
51
52
53
54
55
56
57
58
59
60
61
62
63
64
65

- 1 [15] Wigler M, Pellicer A, Silverstein S, Axel R, Urlaub G, Chasin L. DNA-mediated
2 transfer of the adenine phosphoribosyltransferase locus into mammalian cells.
3 Proceedings of the National Academy of Sciences of the United States of America.
4 1979;76:1373-6.
- 5 [16] Ciudad CJ, Urlaub G, Chasin LA. Deletion analysis of the Chinese hamster
6 dihydrofolate reductase gene promoter. The Journal of biological chemistry.
7 1988;263:16274-82.
- 8 [17] Goni JR, de la Cruz X, Orozco M. Triplex-forming oligonucleotide target
9 sequences in the human genome. Nucleic acids research. 2004;32:354-60.
- 10 [18] Yin WX, Wu XS, Liu G, Li ZH, Watt RM, Huang JD, et al. Targeted correction of a
11 chromosomal point mutation by modified single-stranded oligonucleotides in a
12 GFP recovery system. Biochemical and biophysical research communications.
13 2005;334:1032-41.
- 14 [19] Agarwal S, Gamper HB, Kmiec EB. Nucleotide replacement at two sites can be
15 directed by modified single-stranded oligonucleotides in vitro and in vivo.
16 Biomolecular engineering. 2003;20:7-20.
- 17 [20] Yamamoto T, Moerschell RP, Wakem LP, Komar-Panicucci S, Sherman F.
18 Strand-specificity in the transformation of yeast with synthetic oligonucleotides.
19 Genetics. 1992;131:811-9.
- 20 [21] Liu H, Agarwal S, Kmiec E, Davis BR. Targeted beta-globin gene conversion in
21 human hematopoietic CD34(+)and Lin(-)CD38(-)cells. Gene therapy. 2002;9:118-
22 26.
- 23 [22] Maquat LE. Nonsense-mediated mRNA decay: splicing, translation and mRNP
24 dynamics. Nature reviews Molecular cell biology. 2004;5:89-99.
- 25 [23] Weiss IM, Liebhaber SA. Erythroid cell-specific determinants of alpha-globin
26 mRNA stability. Molecular and cellular biology. 1994;14:8123-32.
- 27
28
29
30
31
32
33
34
35
36
37
38
39
40
41
42
43
44
45
46
47
48
49
50
51
52
53
54
55
56
57
58
59
60
61
62
63
64
65

Figure-1



Results

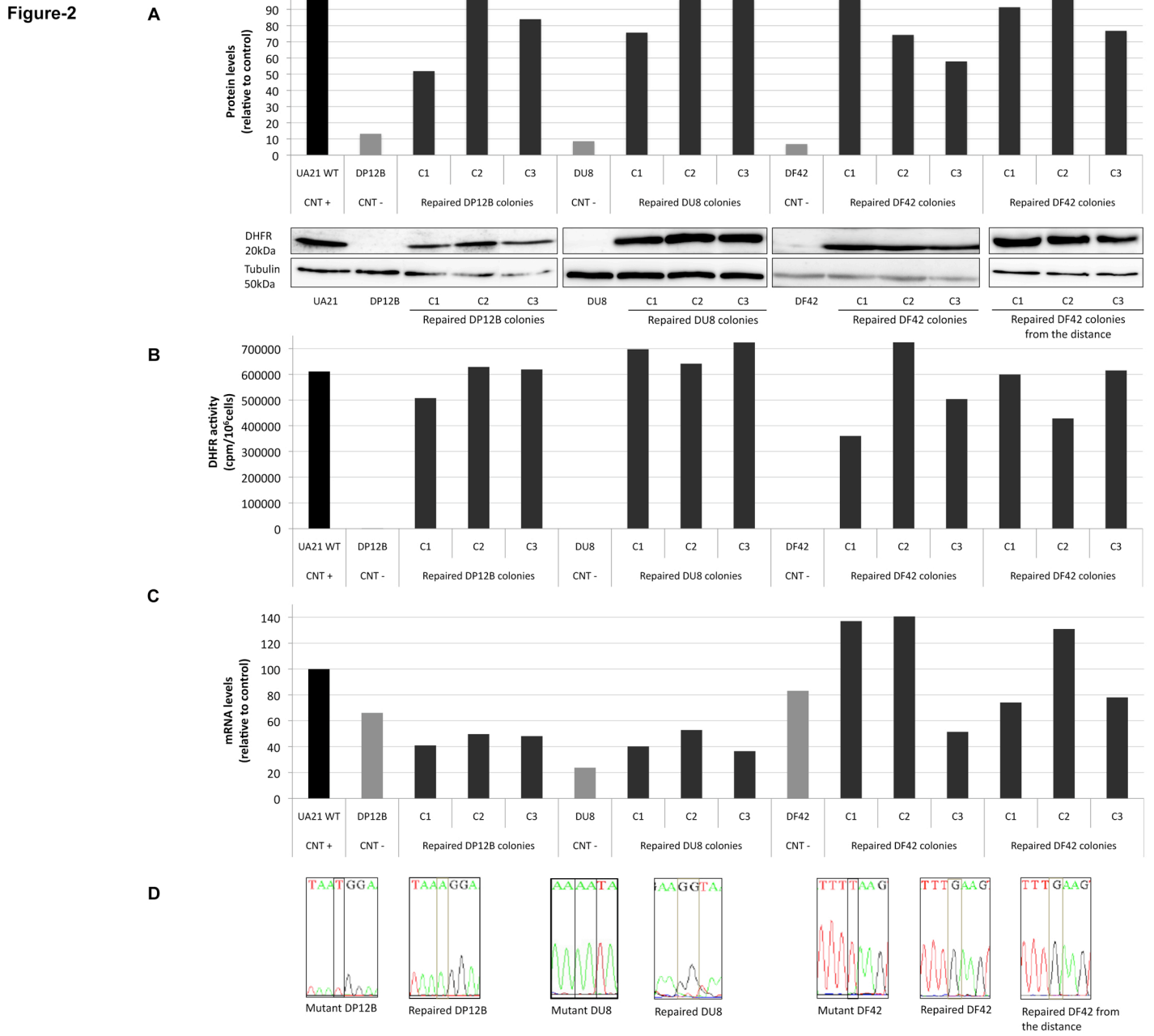
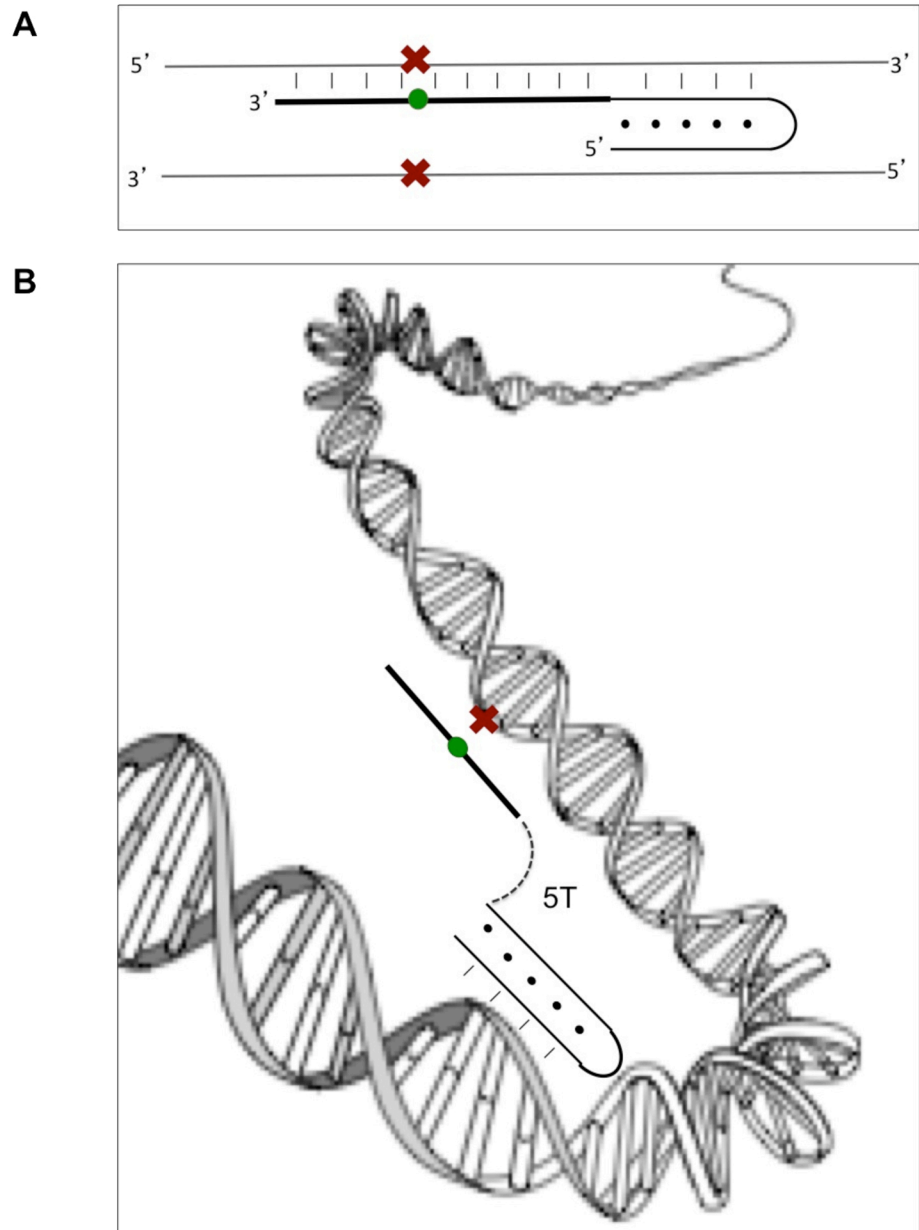
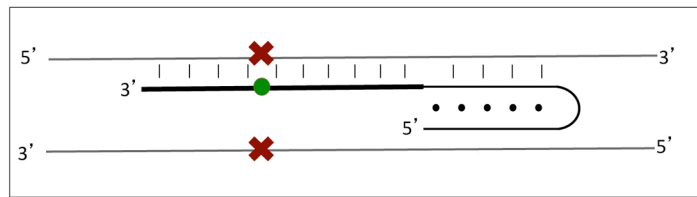


Figure-3



Results

Graphical Abstract (for review)



4.2.1. Additional results to Article II

4.2.1.1. Study of the ability of PPRHs to form a D-loop

We previously described the ability of PPRHs to form a triplex structure by binding to a polypyrimidine target sequence of the dsDNA (Coma et al. 2005), and causing a displacement of the polypurine strand leading to an open conformation of the dsDNA which it is known as displacement loop or D-loop.

An evidence of the formation of this D-loop came from experiments performed with a PPRH that containing a polypyrimidine extension on its 5'-end (wedge-PPRH). This extension was able to hybridize to the displaced polypurine strand of the target dsDNA only if the length of the extension was shorter than that of the opened displaced strand. The hybridization could not be observed when the extension was longer and thus could not fit within the displaced D-loop (Rodríguez et al. 2015). This result let us to hypothesize that PPRHs were forming a D-loop upon displacing the purine strand of the dsDNA target.

To further explore the formation of a D-loop, a similar binding assay using a specific PPRH and two different oligonucleotides was performed as follows:

As it can be observed in Figure 1, the incubation of hairpin13 (10nM strand concentration) with its radiolabeled polypurine/polypyrimidine dsDNA target resulted in the formation of a weak band with lower mobility (lane 2). When a single-stranded oligonucleotide of 15nt in length was added, the upper band increased its intensity (lane 3) compared to lane 4, in which the oligonucleotide was longer (30nt). This result showed that the PPRH maintains the dsDNA opened, since a single-stranded oligonucleotide can bind to the displaced strand, as long as this oligonucleotide is short enough to fit into the D-loop.

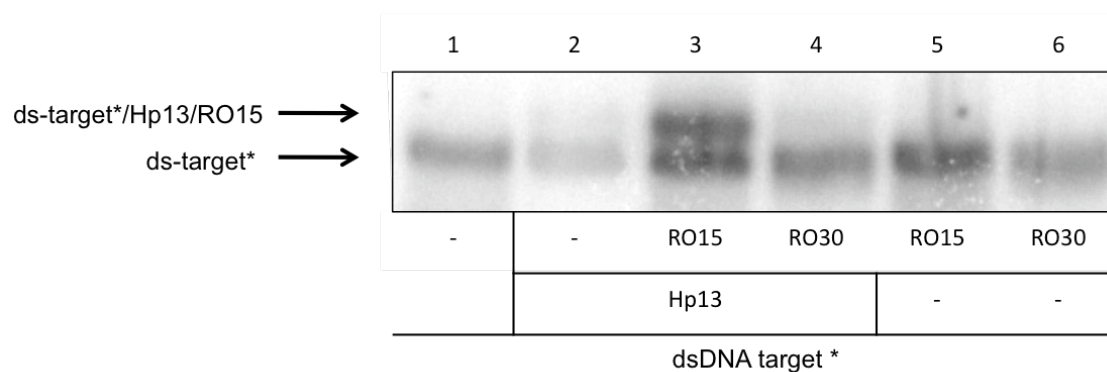


Figure 1. Comparison of the binding ability of two oligonucleotides to a purine-strand, previously displaced by a PPRH. Hairpin-13 (Hp13) was incubated with the radiolabeled ds-target sequence (20,000 cpm) (lane 2), together with an oligonucleotide of 15 (lane 3) or 30 nucleotides (lane 4). The mobility of the ds-target sequence is shown in lane 1. Negative controls are shown in lanes 5 and 6, and were performed incubating the ds-target sequence with the oligonucleotides, in the absence of Hp13. All unlabeled species were used at 10nM. The whole mixture (except for RO15 and RO30 oligonucleotides) of all samples was heated at 75°C for 5 min before the binding reaction. Incubations were performed at 37°C for 30min. An amount of 1µg of poly-dI:dC was added to each sample. ds-target and ds-target/Hp13/RO15 complex are indicated by arrows.

4.3 Article III

Polypurine reverse Hoogsteen Hairpin motifs can form triplexes with their target sequences even under conditions of folding into G-quadruplexes

Manuscript in preparation

Background: Polypurine Reverse Hoogsteen (PPRH) hairpins, originally described in our laboratory (Coma et al., 2005), are nonmodified DNA molecules formed by two antiparallel homopurine strands intramolecularly bound by reverse Hoogsteen bonds and linked by a pentathymidine loop. These molecules have the ability to bind to the dsDNA by Watson-Crick bonds with antiparallel orientation forming a triplex structure. PPRHs have been used to decrease gene expression (de Almagro et al., 2009, de Almagro et al., 2011a, Rodriguez et al., 2013, Villalobos et al., 2015) and to repair point mutations in the *dihydrofolate reductase* (*dhfr*) gene (Sole et al., 2014). Repair-PPRHs are formed by a PPRH core covalently link to a repair tail homologous to the mutated region except for the nucleotide to be corrected. HpE6rep and HpE2rep were used in mammalian CHO cells to correct a point mutation in the *dhfr* gene.

Objectives: To characterize *in vitro* the PPRH molecule alone and when bound to its pyrimidine target, and to study the effects of the high guanine content in the PPRH sequence, and as a consequence, the possible formation of secondary structures such as G-quadruplex.

Results: By performing various absorbance UV-melting and thermal difference spectra (TDS) experiments, and electrophoretic mobility assays, we compared two repair-PPRH sequences containing different amount of guanines. HpE6 and HpE6rep6, bearing no more than two guanines in a row, presented a hairpin folding in all buffer conditions, and HpE2 and HpE2rep2 showed different conformations depending on the buffer: In sodium, this molecule folded into a

reverse Hoogsteen intermolecular duplex whereas in potassium, the most stable conformation was a intramolecular G-quadruplex.

Both repair-PPRHs were then incubated with their pyrimidine targets to study the formation of the triplex structure. HpE6rep6 did not show a conclusive result by UV-melting or TDS experiments, so FRET analysis was carried out, showing a major fraction of unfolded hairpin structure when bound to the pyrimidine target, and around 10% involved in a triplex. Regarding HpE2rep2, the triplex structure was formed between the PPRH and the pyrimidine target in a KCl buffer, and it was more stable than the duplex DNA. When the pyrimidine target is added to a pre-structured HpE2rep2, the main conformation is a duplex/triplex structure, even if this PPRH motif alone folded as a G-quadruplex.

Conclusions: The high guanine content in a PPRH sequence is not necessarily a direct cause for the formation of secondary structures as G-quadruplex. Furthermore, even if PPRH alone are fold as G-quadruplex, they might also form a triplex structure when bound to their pyrimidine target.

Polypurine reverse Hoogsteen Hairpin motifs can form triplexes with their target sequences even under conditions of folding into G-quadruplexes

ABSTRACT

Polypurine reverse Hoogsteen (PPRH) oligonucleotides composed of guanine and adenine bases designed to fold, in principle, into reverse Hoogsteen hairpins. They have been conceived to bind to pyrimidine tracts of genomic DNA by forming a three-stranded structure while maintaining their hairpin structure. They have been successfully used to modulate gene expression and to repair single-point mutations. In this work, we provide a characterization (UV-spectroscopy and gel electrophoresis) of the structure and stability of two repair-PPRH oligonucleotides and of the complexes they form with their single-stranded target. We show that one of the two PPRH forms a hairpin, while the other folds, in potassium, into a stable G4. Nevertheless, surprising, the hairpin-prone oligonucleotide does not form a triplex with its target, while the G4-prone oligonucleotide forms a triplex. Our work proves that folding of a PPRH oligonucleotide into a stable G4 does not necessary impair triplex formation with its target sequence and provides an original example of swapping between different DNA non-canonical conformations.

Keywords: polypurine reverse Hoogsteen hairpin, guanine quadruplex, triplex

INTRODUCTION

Gene modification by nucleic acids has been the focus of many researches during the last years. Different nucleic acids and nucleic acid derivatives have been used *in vitro* and in cells as gene modifying tools (Lundin et al., 2015), such as antisense oligodeoxynucleotides (aODN), small-interference RNAs (siRNA), peptide nucleic acids (PNA), and, more recently, polypurine reverse Hoogsteen (PPRH) hairpins originally described in our laboratory (Coma et al., 2005).

“PPRH oligonucleotides” are non-modified oligonucleotides composed of two symmetrical purine stretches separated by five thymines. They can fold, in principle, into hairpin structures where guanines pair with guanines and adenines pair with adenines via reverse Hoogsteen bonds. They have been conceived to bind to pyrimidine sequences in genomic DNA by forming a three-stranded (or triplex) structure while maintaining their reverse Hoogsteen hairpin conformation. This kind of triplex structures are often referred to as “purine motif triplexes”; the third strand is oriented antiparallel to the Watson-Crick purine strand and their formation requires the presence of divalent cations, such as Mg^{2+} , and is relatively independent of pH (Beal and Dervan, 1991).

In previous works, we described the ability of PPRH oligonucleotides to bind to both the template and the coding strand of the double-stranded DNA target (de Almagro et al., 2009, de Almagro et al., 2011a), and to knock down the expression of the target genes with many advantages compared to other approaches (Villalobos et al., 2014, Rodriguez et al., 2015). Until now, PPRH oligonucleotides have been used for gene silencing (de Almagro et al., 2009, de Almagro et al., 2011a, Rodriguez et al., 2013, Villalobos et al., 2015) and recently in gene targeting to repair single-point mutations (Sole et al., 2014). “Repair-PPRH oligonucleotides” are formed by a PPRH motif bearing an extended DNA sequence homologous to the sequence to be repaired but containing the corrected nucleotide (figure 1).

Electrophoretic mobility shift assays (EMSA) and thermal melting experiments followed by ultraviolet light absorbance (UV-melting) have been used to study the binding of simple PPRH oligonucleotides and of repair-PPRH oligonucleotides to

single- or double-stranded DNA (Coma et al., 2005, de Almagro et al., 2009, de Almagro et al., 2011a, Sole et al., 2014). Gel shift assays allow to ascertain binding of a PPRH oligonucleotide to its pyrimidine target, but not to prove triplex formation (they do not allow determining if the third strand is bound to the Watson-Crick duplex or if it is hanging). UV-melting experiments may in some cases provide indirect evidence of triplex formation. For example, a specific PPRH oligonucleotide was found to form a complex with its single-stranded DNA target more stable than the Watson-Crick double-stranded DNA target, supporting the formation of a triplex structure (Coma et al., 2005).

Our interest is now to gain a sound knowledge into the secondary structures and stabilities of PPRH oligonucleotides and of the complexes they form with their pyrimidine target sequences. We are particularly interested in elucidating the behavior of PPRH oligonucleotides bearing runs of consecutive guanines. When designing a PPRH motif, it is important to take into consideration the possible high guanine content. The presence of runs of consecutive guanines can impair folding into a reverse Hoogsteen hairpin conformation in favor of a guanine quadruplex (G4) structure, especially under physiological conditions. G4 are four-stranded nucleic acid structures formed by the stacking of tetrads of hydrogen-bonded guanines (Burge et al., 2006). Differently from duplex or triplex structures, the stability of G4s depends on the nature of the cation present in solution; in particular they are strongly stabilized by the physiological relevant potassium ion.

In a previous work, we designed and used two repair-PPRH oligonucleotides, named HpE6*rep6* and HpE2*rep2*, to successfully correct single-point mutations in the dihydrofolate reductase (*dhfr*) gene in mammalian cell lines (in exons 6 and 2, respectively) (Sole et al., 2014). Each of the two repair-PPRH oligonucleotides HpE6*rep6* and HpE2*rep2* is composed of a PPRH motif (HpE6 and HpE2, respectively) designed to target a polypyrimidine/polypurine tract next to the *dhfr* gene sequence to be repaired, and of a 25 nucleotide single-stranded extension (*rep6* and *rep2*, respectively) homologous to the sequence to be repaired. HpE6 and HpE2 motifs have very different guanine contents. HpE6 bears only two runs of two consecutive guanines; it can in principle fold into a 23 base pair reverse Hoogsteen hairpin (as illustrated in table 1). HpE2 contains eight runs of two consecutive guanines; it can in principle fold

either into a 13 base-pair reverse Hoogsteen hairpin (as illustrated in table 1) or into a G4 structure. In this article we provide a biophysical and biochemical characterization of the structures and stabilities of HpE6 and HpE2 motifs (alone and with their *rep* extensions) and of the complexes they form with their single-stranded target sequences. Our work reveals unexpected behaviors of these two PPRH motifs. We show that HpE6 folds into a reverse Hoogsteen hairpin, while HpE2 folds, in potassium, into a stable G4; nevertheless, the hairpin-prone HpE6 motif is not able to form a triplex with its single-stranded pyrimidine target, while the G4-prone HpE2 motif forms a triplex. Besides elucidating the structure of the two repair-PPRH oligonucleotides and of the complex they form with their targets, our work provides an original example of swapping between different DNA motifs: reverse Hoogsteen hairpins, guanine quadruplexes and triplexes.

MATERIALS AND METHODS

Oligonucleotides

Oligonucleotides were purchased from Eurogentec (Belgium). Non-labeled oligonucleotides were Reverse Phase Cartridge•Gold™ purified; the double-dye labeled FAM-HpE6-Dabcyl was Reverse Phase HPLC purified. Oligonucleotides were dissolved in bi-distilled water at a concentration of 200 μM and stored at -20°C . Concentrations were determined by ultraviolet light (UV) absorption using molar extinction coefficients provided by the manufacturer. Oligonucleotide sequences are listed in Table 1.

UV absorption measurements

Oligonucleotides were dissolved in a 10 mM cacodylic acid buffer at pH 7.0 (adjusted with LiOH), containing 100 mM NaCl or 100 mM KCl, in the absence or in the presence of 10 mM MgCl_2 . Oligonucleotide strand concentrations are indicated in figure legends (error on strand concentration was estimated to be about 10%). UV absorbance as a function of temperature was recorded on a XL spectrophotometer (Secomam) according to the following protocol: samples were heated at 92°C for 2 min, cooled from 95 to 5°C at a rate of $0.2^\circ\text{C min}^{-1}$, kept at 5°C for 10 min, and heated from 5 to 95°C at a rate of $0.2^\circ\text{C min}^{-1}$; the absorbance was recorded at 260, 295 nm and 335 nm. Temperature was varied with a circulating water bath and measured with an inert glass sensor immersed into a water-filled quartz cell; evaporation at high temperatures and condensation at low temperatures were prevented by a layer of mineral oil and by a dry airflow in the sample compartment, respectively. Melting profiles were corrected for baseline drifting (the absorbance at 335 nm was subtracted from the absorbance at 260 and 295 nm). We defined “temperature of thermal transition”, T_t , the first derivative of the absorbance as a function of the temperature. Thermal difference spectra (TDS) were obtained by subtracting the absorption spectrum at low temperature (5°C) from the absorption spectrum at high temperature (95°C); absorption spectra at low temperature were recorded after annealing the samples from 95 to 5°C at $0.2^\circ\text{C min}^{-1}$. Circular dichroism (CD) spectra were recorded on a JASCO-810 spectropolarimeter.

Fluorescence measurements

Fluorescence measurements were carried on an HpE6 oligonucleotide bearing a 6-carboxyfluorescein (FAM) at its 5' extremity and a Dabcyl quencher at its 3'-extremity. For melting experiments, FAM-HpE6-Dabcyl was dissolved in a 10 mM cacodylic acid buffer at pH 7.0 (adjusted with LiOH), containing 100 mM KCl and 10 mM MgCl₂, at 0.2 μM strand concentration, in the absence or in the presence of 2 μM Y6 oligonucleotide. FAM emission as a function of temperature was recorded on a SPEX Fluorolog (HORIBA Jobin Yvon) at an excitation wavelength of 470 nm and an emission wavelength of 520 nm; temperature was raised with a circulating water bath from 5 to 80°C at 1°C min⁻¹. FAM-HpE6-Dabcyl emission as a function of temperature was normalized between the minimum and the maximum of fluorescence; we defined "temperature of half-dissociation", $T_{1/2}$, the temperature at which the normalized fluorescence was equal to 0.5.

Electrophoretic mobility shift assays (EMSA)

Single-stranded oligonucleotides (Y6rep6, Y2rep2 and Y2) were 5'-end-labeled with [γ ³²P] ATP using a T4 polynucleotide kinase (NEB) in a T4 Polynucleotide Kinase Reaction Buffer (NEB). After incubation at 37°C for 30 min, the reaction mixture was filtered on a Micro Bio-Spin column P6 (Bio-Rad).

Samples were prepared in a cacodylic acid buffer pH 7.2 (LiOH) buffer containing 100 mM NaCl or KCl and 10 mM MgCl₂ at a strand concentration of about 15 nM of radiolabeled oligonucleotides (Y6rep6, Y2rep2 and Y2) and 1.5 μM of non-radiolabeled oligonucleotides (HpE6rep6, R6rep6, HpE2rep2, R2rep2 and HpE2). Sample annealing from high to low temperature was carried out as indicated in figure legends.

12% polyacrylamide gels (acrylamide:bisacrylamide 19:1) were prepared in a TBE buffer, supplemented with 20 mM NaCl or KCl and with 10 mM MgCl₂.

Electrophoresis were run in a TBE buffer, supplemented with 20 mM NaCl or KCl and with 10 mM MgCl₂, in a cold room, at 3W/gel, for 2-2h30. The temperature of the gel during migration was about 15°C. Gels were dried and exposed to PhosphorImager screens and screens were scanned with a Typhoon 9410 Imager (Molecular Dynamics).

RESULTS AND DISCUSSION

Structure and stability of HpE6 and HpE2 motifs. Because of their sequences, the HpE6 motif can potentially fold into a 23 base-pair reverse Hoogsteen hairpin structure with three pyrimidine base-pair interruptions (as illustrated in table 1), while the HpE2 motif can potentially fold into a 13 base-pair reverse Hoogsteen hairpin structure (as illustrated in table 1) as well as into a G4 structure. In order to gain insight into the structures formed by HpE6 and HpE2 oligonucleotides and their stabilities, we carried out an UV-absorbance spectroscopic investigation under different ionic conditions (100 mM NaCl or KCl, in the absence or in the presence of 10 mM MgCl₂) and PAGE.

Consistently with the formation of a double-stranded structure, the melting profiles of HpE6 were independent of the nature of the monovalent cation, Na⁺ or K⁺, present in solution, and strongly depended on the presence of Mg²⁺: in the absence of magnesium, HpE6 did not form a stable structure (its temperature of thermal transition T_t , defined in Material and Methods section, was lower than 20°C); in the presence of magnesium, HpE6 formed a structure with a T_t of 33°C (figure S1). The independence of T_t of strand concentration (2 and 20 μM) supported folding of HpE6 into an intramolecular structure (figure S1). Overall, these data support folding of HpE6 into a reverse Hoogsteen hairpin structure.

Contrary to HpE6, the structure of HpE2 depended on the nature of the monovalent cation, as revealed by Thermal Difference Spectra (TDS). A TDS is obtained by subtracting the absorbance spectrum at low temperature (where the oligonucleotide is in its folded state) from the absorbance spectrum at high temperature (where the oligonucleotide is in its unfolded state). TDS have a specific shape for each type of nucleic acid structure, and TDS are very similar within a nucleic acid structural family (Mergny et al., 2005). In potassium, HpE2 exhibited a TDS typical of a G4 structure, with two positive maxima around 245 and 275 nm and a negative minimum around 295 nm, while in sodium it did not form a G4 (figure 2a). The G4 structure formed by HpE2 in potassium displayed a temperature of thermal transition of 78°C (figure 2b). In a non-denaturing polyacrylamide gel electrophoresis (PAGE) experiment in potassium, HpE2 migrated as a single band of fast mobility compared to the well

characterized intramolecular G4 structure formed by the 21 nucleotide long human telomeric sequence (GGGTTA)₃GGG, which supported folding into an intramolecular G4 (not shown). As shown by TDS, in sodium HpE2 did not fold into a G4; it folded into a structure whose stability increased in the presence of magnesium (T_t of 33°C in the absence of Mg²⁺, T_t of 39°C in the presence of Mg²⁺, at 2 μM strand concentration) (figure S3). Differently from HpE6, the T_t of HpE2 in sodium increased with increasing strand concentration (figure S3), which indicates the presence of intermolecular species. Non-denaturing PAGE supported that, at 2-20 μM strand concentration, the major structure of HpE2 was not the 13-base-pair hairpin but the 31-base-pair intermolecular duplex with 5 thymine base-pair interruptions (figure 2c).

We verified that the addition of *rep* extensions did not affect the stability of the HpE6 hairpin and of the HpE2 G4: normalized melting profiles of HpE6 and HpE2 were identical to normalized melting profiles of HpE6*rep6* and HpE2*rep2*, respectively (figure S4).

In conclusion, HpE6 and HpE2 behave very differently. The HpE6 motif (alone as well as with its *rep6* extension) folds into a reverse Hoogsteen hairpin. The structure of the HpE2 motif is cation-dependent: in potassium, HpE2 (alone as well as with its *rep2* extension) folds into a stable intramolecular G4 (by stable, we mean with a temperature of thermal transition far above the physiological temperature); in sodium HpE2 alone folds into a reverse Hoogsteen intermolecular duplex. Melting profiles normalized between the maximum and the minimum of absorbance, represent the oligonucleotide folded fractions.

We next investigated if HpE6 and HpE2 motifs, alone and in the *rep* context, formed triplexes with their pyrimidine target sequences under salt conditions mimicking the intracellular environment, where PPRH oligonucleotides are addressed, *i.e.* in the presence of potassium and magnesium (magnesium is also generally required to form three-stranded structures of purine motif).

Structure of the HpE6rep6 + Y6rep6 complex. To verify if the reverse Hoogsteen hairpin HpE6 motif formed a triplex structure with its single-stranded pyrimidine target, we first carried out UV-melting experiments and EMSA. Both these

approaches indicated that the complex formed by HpE6_{rep6} and Y6_{rep6} (table 1) had the same stability of the duplex formed by Y6_{rep6} and its complementary strand R6_{rep6} (figure S5); nevertheless they did not allow inferring triplex formation (they did not allow discriminating if the HpE6 motif formed a triplex structure or a duplex structure with a hanging third strand).

To ascertain triplex formation, we hence designed a fluorescent HpE6 bearing a 6-carboxyfluorescein (FAM) dye at its 5' end and a Dabcyl quencher at its 3' end, named FAM-HpE6-Dabcyl. When the oligonucleotide is folded into a hairpin, the FAM fluorescence is quenched by the Dabcyl quencher; when the oligonucleotide is in an open state, the FAM fluorescence is restored. We first recorded the fluorescence of FAM-HpE6-Dabcyl alone as a function of temperature. The melting profile followed by FAM fluorescence showed that the double-labeled oligonucleotide folded into a structure with a temperature of half-dissociation $T_{1/2}$ (defined in Material and Methods section) of 31°C, in accordance with the temperature of thermal transition determined by UV-melting for the non-labeled HpE6 (T_t of 33°C) (figure 3a). Surprisingly, when the pyrimidine target Y6 was added to the FAM-HpE6-Dabcyl solution (at a temperature where the double-labeled oligonucleotide was folded into a hairpin structure), the FAM fluorescence was completely restored (figure 3b). This revealed that HpE6 hybridized to its target and that, upon hybridization, the hairpin structure opened. Hence, despite its reverse Hoogsteen hairpin structure, HpE6 did not form a triplex with its pyrimidine target, but a duplex with a hanging third strand. Interestingly, a thermal denaturation experiment of the complex formed by the double-dye labeled HpE6 with its target Y6 revealed a small decrease in FAM emission between 10 and 30°C, suggesting that, in this range of temperatures, a small fraction of FAM-HpE6-Dabcyl (estimated to be about 10%) formed a triplex structure with its target Y6 (figure S6).

In conclusion, the hairpin-prone HpE6 motif recognizes its pyrimidine target (*i.e.* HpE6 binds to Y6); nevertheless, surprisingly, the formed complex is not a triplex: one portion of the HpE6 strand form a Watson-Crick duplex with Y6, the other portion hangs in an open state. Only a minor fraction (about 10%) of the HpE6 motif forms a triplex with its Y6 target in the 10-30°C temperature range. The three-pyrimidine base-

pair interruptions in the reverse Hoogsteen hairpin structure might be detrimental to triplex formation (Rodriguez et al., 2015).

Structure of the HpE2rep2 + Y2rep2 complex in potassium. In potassium the HpE2 motif (alone and with the *rep* extension) formed a stable intramolecular G4. EMSA experiments revealed that, despite its G4 structure, the HpE2 oligonucleotide bound to its pyrimidine target Y2 (figure S7). Nevertheless, UV-melting profiles of HpE2 + Y2 displayed no clear transitions (not shown) and did not allow gaining insight into the nature and the stability of the formed complex(es). In order to gain information about the complex(es) formed by the HpE2 motif in the *rep* context, we compared UV-melting profiles of HpE2rep2 + Y2rep2 with melting-profiles of two different duplexes: (i) the duplex formed by Y2rep2 with its complementary strand R2rep2, and (ii) the duplex formed by Y2rep2 with the shorter oligonucleotide *rep2* (table 1).

The long and the short duplexes formed by Y2rep2 with R2rep2 and *rep2* exhibited single thermal transitions at about 66°C and 60°C, respectively (figure 4a). When annealing HpE2rep2 + Y2rep2 from high to low temperature (figure 4b, blue curve), two transitions were observed: one at 67-68°C and one at 59-60°C, supporting the formation of two distinct complexes (first derivatives of absorbance with respected to temperature are shown in figure S8). The T_t of the first transition was similar to the T_t of the long duplex formed by Y2rep2 + R2rep2 (T_t 66-67°C). Hence, this transition is consistent with the formation of an extended complex where Hp2rep2 hybridizes to Y2rep2 all along its length. Nevertheless, this information does not allow inferring if, in this extended complex, the free strand of the HpE2 motif is involved in a triplex structure or it is hanging. The T_t of the second transition was similar to the T_t of the short duplex formed by Y2rep2 + *rep2* (T_t 60°C). Hence, this transition is consistent with the formation of a complex where only the *rep2* domain of HpE2rep2 hybridizes to Y2rep2, while the HpE2 motif forms a hanging G4 (as illustrated in figure 4b inset). A rough graphical analysis of the UV-melting profile of the HpE2 motif in potassium plus magnesium (figure 2) allows understanding this behavior. Above about 65°C, the HpE2 motif is in equilibrium between a G4 form and an unstructured form, hence HpE2rep2 can hybridize all along the Y2rep2 strand (and the free strand of the HpE2 motif can potentially form a triplex structure). Below about 65°C, the HpE2 motif is completely folded into a G4, hence HpE2rep2 can hybridize to Y2rep2 only along its *rep* domain.

Surprisingly, subsequent heating $\text{HpE2rep2} + \text{Y2rep2}$ from low to high temperature resulted in a single transition at 68°C (figure 4b, red curve); the heating profile was shifted of 2°C toward higher temperatures compared to the heating profile of the long duplex $\text{Y2rep2} + \text{R2rep2}$ (figure 4c and figure S8). This supports that, after annealing $\text{HpE2rep2} + \text{Y2rep2}$ from high to low temperature, a single complex is present, and that this complex is more stable than the long duplex $\text{Y2rep2} + \text{R2rep2}$. Overall, UV-melting profiles support the following folding pathway for the complex $\text{HpE2rep2} + \text{Y2rep2}$: when annealing from high to low temperature, two distinct complexes are formed: an extended complex (duplex or duplex/triplex) and a less stable duplex/G4 complex; nevertheless, during the annealing process, the duplex/G4 complexes convert into the more stable extended complex. Consistently with a structural conversion, the detection of duplex/G4 complexes depended on the temperature scan rate: at a slower temperature scan rate the 60°C transition could not be resolved (figure S9).

The presence of a single complex after annealing from high to low temperature, was confirmed by EMSA. Indeed, when HpE2rep2 and radiolabeled Y2rep2 (Y2rep2^*) were slowly annealed together from high to low temperature, a single band was observed (figure 5, lane 2). EMSA allowed also confirming that this complex was more stable than the duplex formed by Y2rep2 and its complementary R2rep2 strand (consistently with the 2°C degree difference in T_t between the complex $\text{HpE2rep2} + \text{Y2rep2}$ and the duplex $\text{Y2rep2} + \text{R2rep2}$). Indeed, when Yrep2^* was annealed with both HpE2rep2 and R2rep2 , two bands of different intensities appeared (figure 5, lane 5). The minor band migrated as the duplex formed by Y2rep2 and R2rep2 (figure 5, lane 4), while the major band had the same mobility of the band resulting from $\text{HpE2rep2} + \text{Y2rep2}$ after annealing (figure 5, lane 2). Differently, when Y2rep2^* was added to a pre-structured HpE2rep2 (separately annealed alone in the presence of potassium), two distinct complexes were formed (figure 5, lane 3). The major slow migrating complex migrated as the complex formed by HpE2rep2 and Y2rep2^* (in lane 2); the minor fast migrating complex may correspond to the duplex/G4 structure.

In conclusion, altogether UV-melting and EMSA support that, when HpE2rep2 and Y2rep2 are annealed together in potassium, they form a duplex/triplex structure

more stable than the target duplex formed by *Y2rep2* and *R2rep2*. When a pre-structured *HpE2rep2* is put in the presence of *Y2rep2*, despite the *HpE2* motif is structured in a stable G4, more than 50% of *HpE2rep2* still form a duplex/triplex structure.

CONCLUSIONS

PPRH hairpin motifs have been conceived to target pyrimidine sequences of genomic DNA via the formation of a triplex structure. PPRH oligonucleotides have been successfully used to modulate gene expression. Recently, we were able to correct single-point mutations in cell lines using two PPRH oligonucleotides, each bearing a sequence homologous to the genomic sequence to be repaired. In this work, we investigated the structure and the stability of these two repair-PPRH oligonucleotides and of the complexes they form with their single-stranded target sequences. We showed that the HpE6 motif folded into a reverse Hoogsteen hairpin, while the structure of the G-rich HpE2 motif depended on the nature of the cation present in solution: in sodium it formed a reverse Hoogsteen intermolecular duplex; in potassium it folded into a stable G4. Nevertheless, surprisingly, the HpE6 hairpin-prone motif was not able to form a triplex structure with its pyrimidine targets: upon hybridization, the hairpin structure opened, leaving a hanging third strand (figure 6). Conversely, the HpE2 G4-prone motif formed a triplex. In particular, we showed that, under ionic condition where the HpE2 motif was structured into a G4 (in potassium), a major fraction of the HpE2_{rep2} oligonucleotide hybridized to the target sequence all along its length and the HpE2 motif swapped from a G4 to a reverse Hoogsteen hairpin forming a triplex with the pyrimidine portion of the target sequence (figure 6). Our work proves that folding of a PPRH oligonucleotide into a reverse Hoogsteen hairpin does not necessarily result in triplex formation with the target sequence, while folding of a PPRH oligonucleotide into a stable G4 does not necessarily impair triplex formation; it also provides an original example of swapping between different non-canonical DNA conformations. Despite their very different structural characteristics, both repair-PPRH oligonucleotides allowed repairing single-point mutations in cell lines. We are currently further investigating which are the structural determinants, which make a PPRH oligonucleotide work in targeting genomic DNA.

FUNDING

This work was supported by “Plan Nacional de Investigación Científica” (Spain), Grant SAF2014-51825-R. Our group holds the Quality Mention from the “Generalitat de Catalunya” (2014SGR96). A.S. is the recipient of a fellowship (Formació d’Investigadors) from the “Generalitat de Catalunya.” Muséum National d’Histoire Naturelle (MNHN), Centre National de la Recherche Scientifique (CNRS), Institut National de la Santé et de la Recherche Médicale (INSERM).

ACKNOWLEDGEMENTS

We thank Pr. Tula Saison-Behmoaras for her support.

REFERENCES

- [1] Lundin KE, Gissberg O, Smith CI. Oligonucleotide Therapies: The Past and the Present. *Human gene therapy* 2015;26:475-85.
- [2] Coma S, Noe V, Eritja R, Ciudad CJ. Strand displacement of double-stranded DNA by triplex-forming antiparallel purine-hairpins. *Oligonucleotides* 2005;15:269-83.
- [3] Beal PA, Dervan PB. Second structural motif for recognition of DNA by oligonucleotide-directed triple-helix formation. *Science* 1991;251:1360-3.
- [4] de Almagro MC, Coma S, Noe V, Ciudad CJ. Polypurine hairpins directed against the template strand of DNA knock down the expression of mammalian genes. *The Journal of biological chemistry* 2009;284:11579-89.
- [5] de Almagro MC, Mencia N, Noe V, Ciudad CJ. Coding polypurine hairpins cause target-induced cell death in breast cancer cells. *Human gene therapy* 2011;22:451-63.
- [6] Villalobos X, Rodriguez L, Prevot J, Oleaga C, Ciudad CJ, Noe V. Stability and immunogenicity properties of the gene-silencing polypurine reverse Hoogsteen hairpins. *Molecular pharmaceutics* 2014;11:254-64.
- [7] Rodriguez L, Villalobos X, Sole A, Lliberos C, Ciudad CJ, Noe V. Improved design of PPRHs for gene silencing. *Molecular pharmaceutics* 2015;12:867-77.
- [8] Rodriguez L, Villalobos X, Dakhel S, Padilla L, Hervas R, Hernandez JL, et al. Polypurine reverse Hoogsteen hairpins as a gene therapy tool against survivin in human prostate cancer PC3 cells in vitro and in vivo. *Biochemical pharmacology* 2013;86:1541-54.
- [9] Villalobos X, Rodriguez L, Sole A, Lliberos C, Mencia N, Ciudad CJ, et al. Effect of Polypurine Reverse Hoogsteen Hairpins on Relevant Cancer Target Genes in Different Human Cell Lines. *Nucleic acid therapeutics* 2015;25:198-208.
- [10] Sole A, Villalobos X, Ciudad CJ, Noe V. Repair of single-point mutations by polypurine reverse Hoogsteen hairpins. *Human gene therapy methods* 2014;25:288-302.
- [11] Burge S, Parkinson GN, Hazel P, Todd AK, Neidle S. Quadruplex DNA: sequence, topology and structure. *Nucleic acids research* 2006;34:5402-15.
- [12] Mergny JL, Li J, Lacroix L, Amrane S, Chaires JB. Thermal difference spectra: a specific signature for nucleic acid structures. *Nucleic acids research* 2005;33:e138.

Table 1. Oligonucleotide sequences used in this study

<i>oligonucleotide name</i>	<i>oligonucleotide sequence</i>
HpE6	
Y6	5' -GCAAGTA- <i>TCTTTCTGTTAGCCTTTCTTCTC</i> -ATAGAC
HpE6rep6	
Y6rep6	5' - <i>TCTTTCTGTTAGCCTTTCTTCTC</i> -ATAGACTTCAAATTTATACTTGATG
R6rep6	AGAAAGACAATCGGAAAGAAGAG-TATCTGAAGTTTAAATATGAACTAC-5'
HpE2	
Y2	5' -AAGAATGA- <i>CCACCCTCCTC</i> -AGTGGAAG
HpE2rep2	
Y2rep2	5' -GAATTCAGTAGTTCCAAAAGAATGA- <i>CCACCCTCCTC</i>
R2rep2	CTTAAGTTCATGAAGGTTTCTTACT-GGAGGAGGAGGAG-5'
rep2	CTTAAGTTCATGAAGGTTTCTTACT-5'

HpE6rep6 and HpE2rep2 are composed of a PPRH motif (HpE6 and HpE2, bold font) and of a 25 nucleotide single-stranded extension (rep6 and rep2, lower case letters). Y6rep6 and Y2rep2 are the single-stranded targets of HpE6rep6 and HpE2rep2, while R6rep6 and R2rep2 are the complementary sequences of Y6rep6 and Y2rep2. In this table, HpE6 and HpE2 motifs are represented in a reverse Hoogsteen hairpin conformation; their pyrimidine target sequences are in italic font. HpE6rep6 and HpE2rep2 have a different orientation relative to their target strands: HpE6 bears its rep extension at its 5' end, while HpE2 at its 3' end. Underlined letters represents Watson-Crick base-pair mismatches.

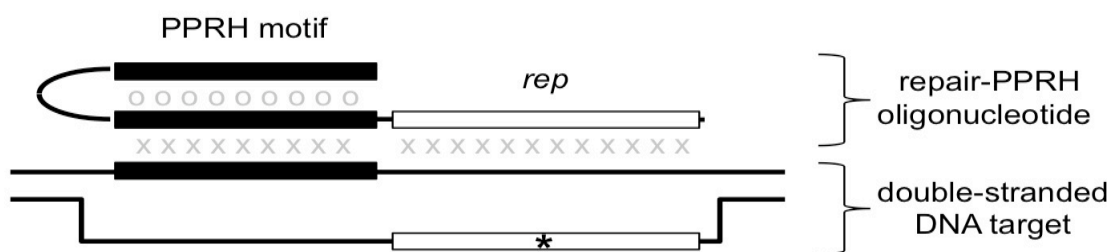


Figure 1
Schematic illustration of a PPRH-repair oligonucleotide and its genomic DNA target

Repair-PPRH oligonucleotides are composed of a PPRH motif and of a single-stranded extension (*rep*) homologous to the genomic sequence to be replaced (the asterisk symbol represents single-point mutations to be corrected). A PPRH motif is designed to fold, in principle, into reverse Hoogsteen hairpins and to form triplexes with its genomic pyrimidine target sequence (circles and crosses represent reverse Hoogsteen and Watson-Crick hydrogen bonds, respectively). When the double-stranded DNA target is in an open-state (as represented in this figure), the *rep* sequence can hybridize to the single-stranded region next to the PPRH target.

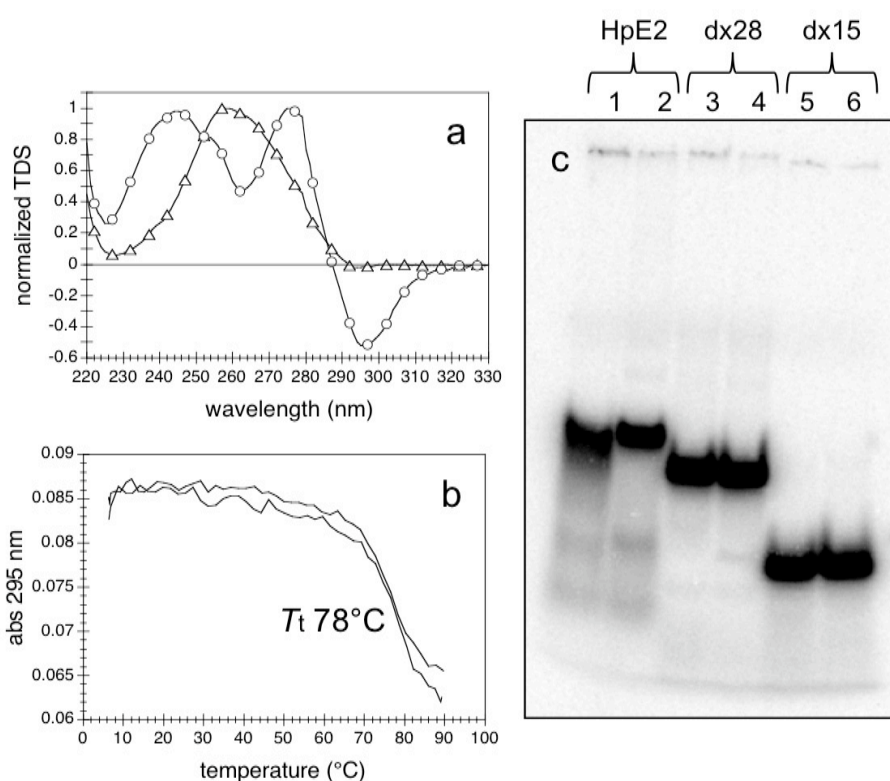


Figure 2
Structures of HpE2 in sodium and in potassium

- (a) Normalized TDS of HpE2 in 100 mM NaCl + 10 mM MgCl₂ (triangles) and in 100 mM KCl + 10 mM MgCl₂ (circles).
- (b) Absorbance at 295 nm as a function of temperature of 2 μM HpE2 in 100 mM KCl + 10 mM MgCl₂. We verified by circular dichroism that HpE2 was completely unfolded above 90°C (figure S2).
- (c) Non-denaturing PAGE of HpE2 at 2 and 20 μM strand concentration (lanes 1 and 2, respectively); dx28 and dx15 are two intermolecular duplexes of 28 and 15 base-pair length, respectively (1 μM of radiolabeled strand and 1.5 μM of non-radiolabeled complementary strand in lanes 3 and 5; 10 μM of radiolabeled strand and 15 μM of non-radiolabeled complementary strand in lanes 4 and 6). Samples were prepared in a buffer containing 100 mM NaCl + 10 mM MgCl₂, heated at 90°C for 2 min and slowly cooled at 4°C; radiolabeled strands were at nM concentrations. Both the gel and the migration buffer contained 20 mM NaCl and 10 mM MgCl₂; migration were carried out at about 15°C.

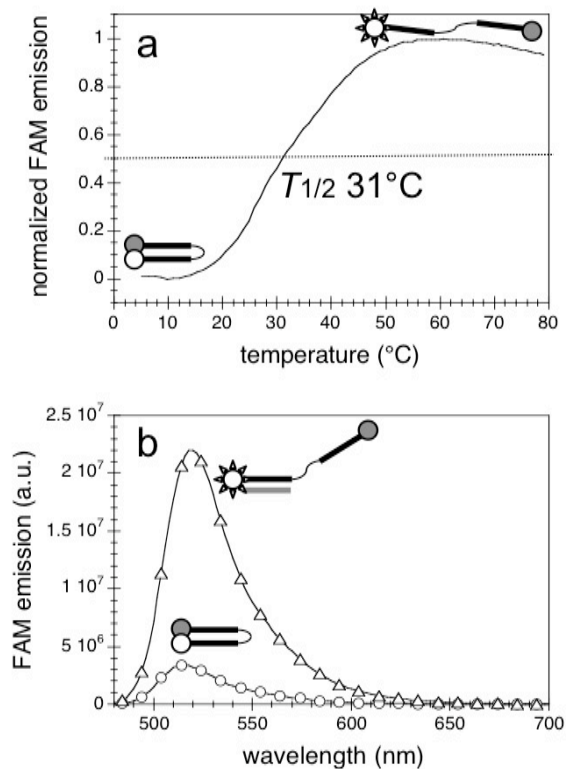


Figure 3

Structure of FAM-HpE6-Dabcyl alone and in the presence of its target Y6

- (a) Normalized FAM emission of 0.2 μM FAM-HpE6-Dabcyl; excitation wavelength 470 nm, emission wavelength 520 nm.
- (b) Emission spectra at 5°C of 0.2 μM FAM-HpE6-Dabcyl alone (circles) and upon addition of 1 μM Y6; excitation wavelength 470 nm. The intensity of FAM-HpE6-Dabcyl emission in the presence of Y6 was similar to the intensity of FAM-HpE6-Dabcyl at 80°C, where the oligonucleotide was completely unfolded.

Measurements were run in a buffer containing 100 mM KCl and 10 mM MgCl₂.

White and grey symbols in the schematic illustration of the formed structures represent FAM dye and Dabcyl quencher, respectively.

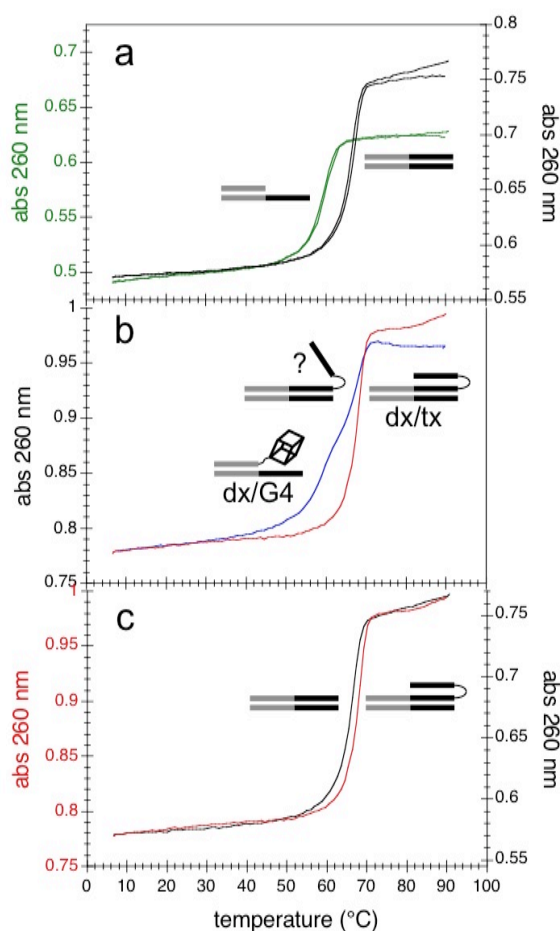


Figure 4
UV-melting profiles the complex(es) formed by HpE2rep2 and Y2rep2 in potassium

Absorbance at 260 nm as a function of temperature of

- (a) Y2rep2 + R2rep2 (black) and Y2rep2 + rep2 (green) (both cooling and heating profiles are shown)
 - (b) Y2rep2 + HpE2rep2, from 95 to 5°C (bleu) and from 5°C to 95°C (red)
 - (c) Y2rep2 + HpE2rep2 (red) and Y2rep2 + R2rep2 (black) while heating from 5°C to 95°C.
- Each oligonucleotide were at 1μM strand concentration. Measurements were run in a buffer containing 100 mM KCl and 10 mM MgCl₂, at a temperature scan rate of 0.2°C/min.

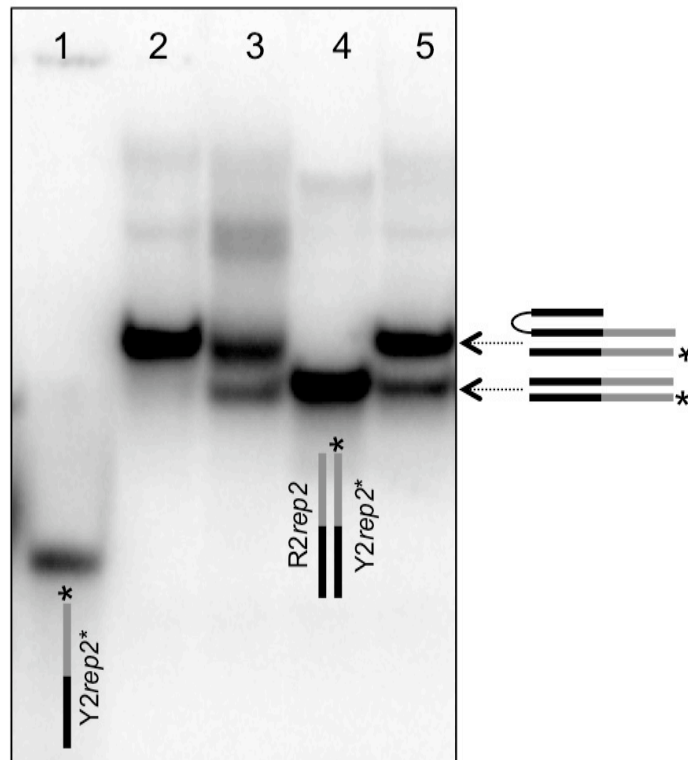


Figure 5
EMSA of the complex(es) HpE2rep2 + Y2rep2 in potassium

Electrophoretic mobility shift assay of radiolabeled Y2rep2 oligonucleotide (Y2rep2*) in KCl + MgCl₂.

Lane 1: Y2rep2*

Lane 2: HpE2rep2 + Y2rep2*; the mix was heated at 95°C and slowly cooled at 5°C.

Lane 3: HpE2rep2 was heated at 95°C and slowly cooled at 5°C, then Y2rep2* was added.

Lane 4: Y2rep2* plus its complementary strand R2rep2.

Lane 5: HpE2rep2 + Y2rep2* + R2rep2; the mix was heated at 95°C and slowly cooled at 5°C.

EMSA was carried out as describe in the Material and Methods section.

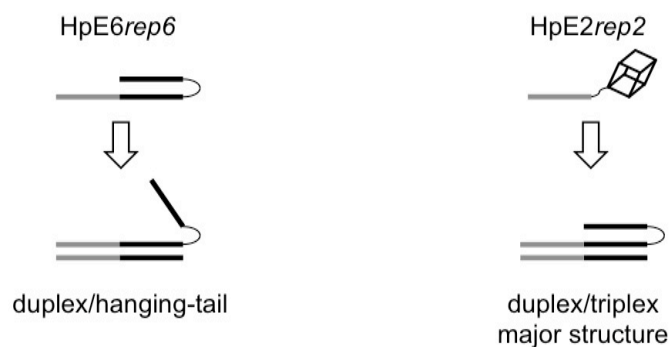


Figure 6
Schematic illustration of the structures formed by HpE6 and HpE2 motifs
alone and in the presence of their single-stranded targets.

The HpE6 motif folds into a reverse Hoogsteen hairpin; it forms a Watson-Crick duplex with its pyrimidine target sequence, nevertheless, upon hybridization, the hairpin opens. The HpE2 motif folds into a stable G4, in potassium; in the presence of its target, HpE2 forms an extended complex where the HpE2 motif is in a triplex conformation with its pyrimidine target sequence.

Supplementary Information

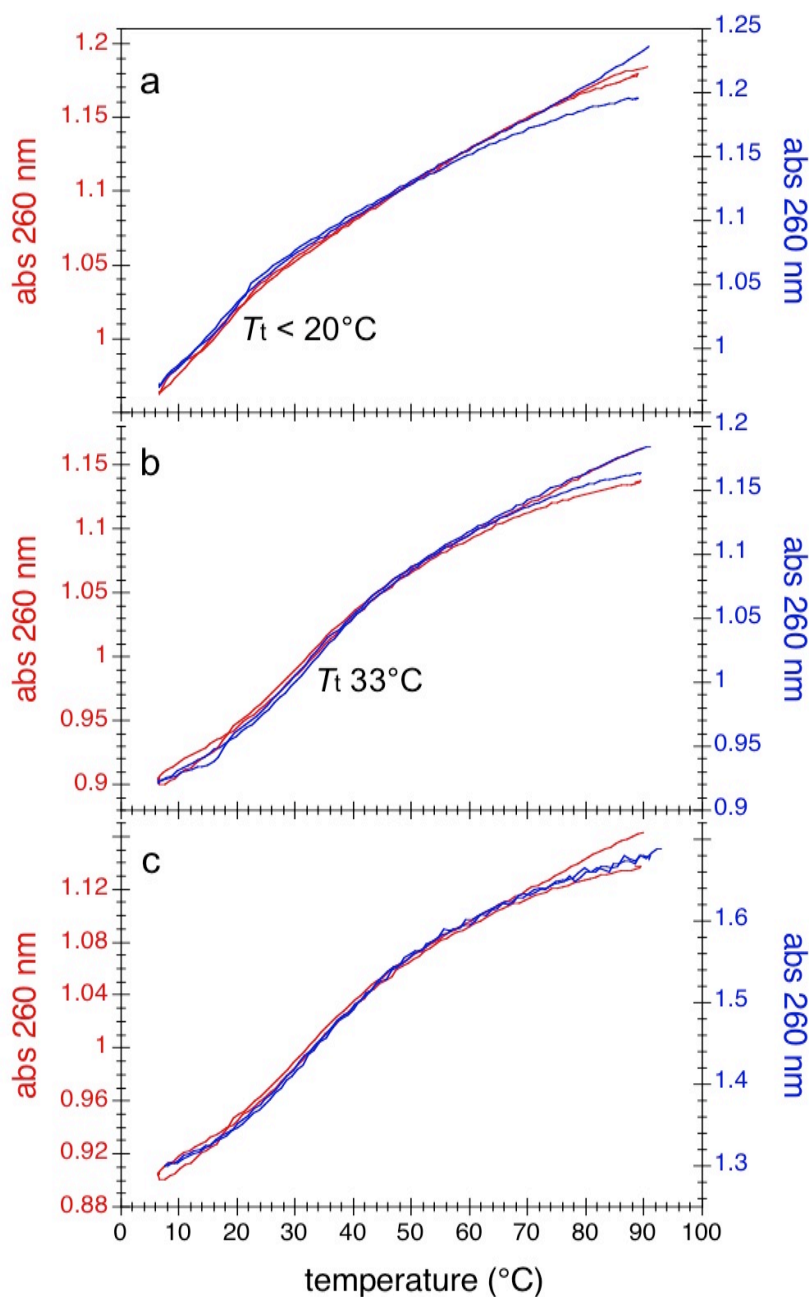


Figure S1
UV-melting profiles of HpE6 oligonucleotide

Absorbance at 260 nm as a function of temperature of
 (a) 2 μM HpE6 in 100 mM NaCl (red) and in 100 mM KCl (blue),
 (b) 2 μM HpE6 in 100 mM NaCl + 10 mM MgCl₂ (red) and in 100 mM KCl + 10 mM MgCl₂ (blue).
 (c) 2 μM (red) and 20 μM (blue) HpE6 2 in 100 mM NaCl + 10 mM MgCl₂.

The optical path length was 10 mm for 2 μM HpE2 and 1 mm for 20 μM HpE2.

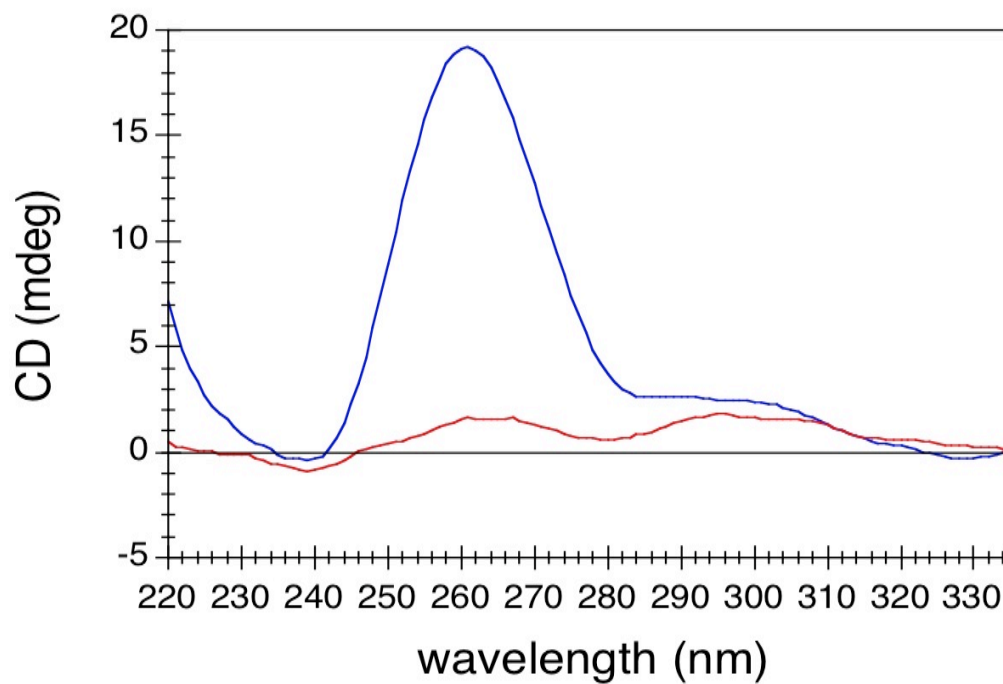


Figure S2
CD spectra of HpE2 oligonucleotide in potassium

Circular dichroism spectra of 2 μ M HpE6 in 100 mM KCl + 10 mM MgCl₂, at 5°C (blue) and 90°C (red).

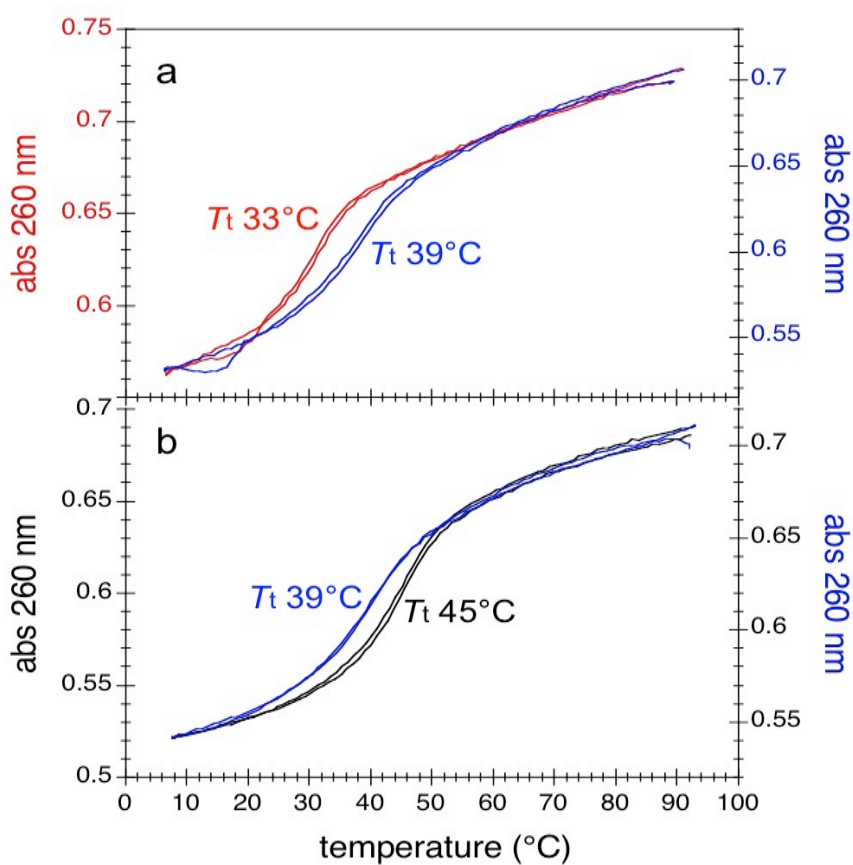


Figure S3
UV-melting profiles of HpE2 oligonucleotide in sodium

- (a) Absorbance at 260 nm as a function of temperature of 2 μ M HpE2 in 100 mM NaCl (red) and in 100 mM NaCl + 10 mM MgCl₂ (bleu).
- (b) Absorbance at 260 nm as a function of temperature of HpE2 in 100 mM NaCl + 10 mM MgCl₂, at 2 μ M (blue) and 20 μ M (black) strand concentration.

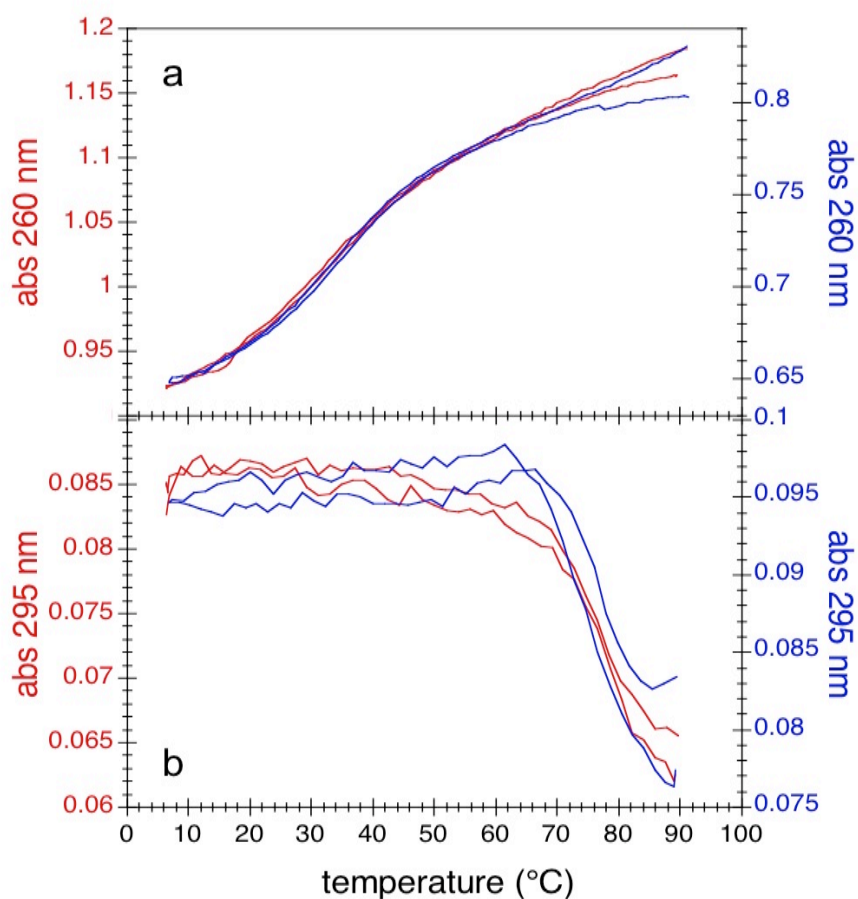


Figure S4
UV-melting profiles of HpE6(*rep6*) and Hp2(*rep2*) oligonucleotides

(a) Absorbance at 260 nm as a function of temperature of HpE6 (red) and HpE6*rep6* (bleu).
(b) Absorbance at 295 nm as a function of temperature of HpE2 (red) and HpE2*rep2* (bleu).
Measurements were carried out at 2 μ M strand concentration for HpE6 and HpE2 and at 1.5 μ M strand concentration for HpE6*rep6* and HpE2*rep2*, in a buffer containing 100 mM KCl and 10 mM MgCl₂.

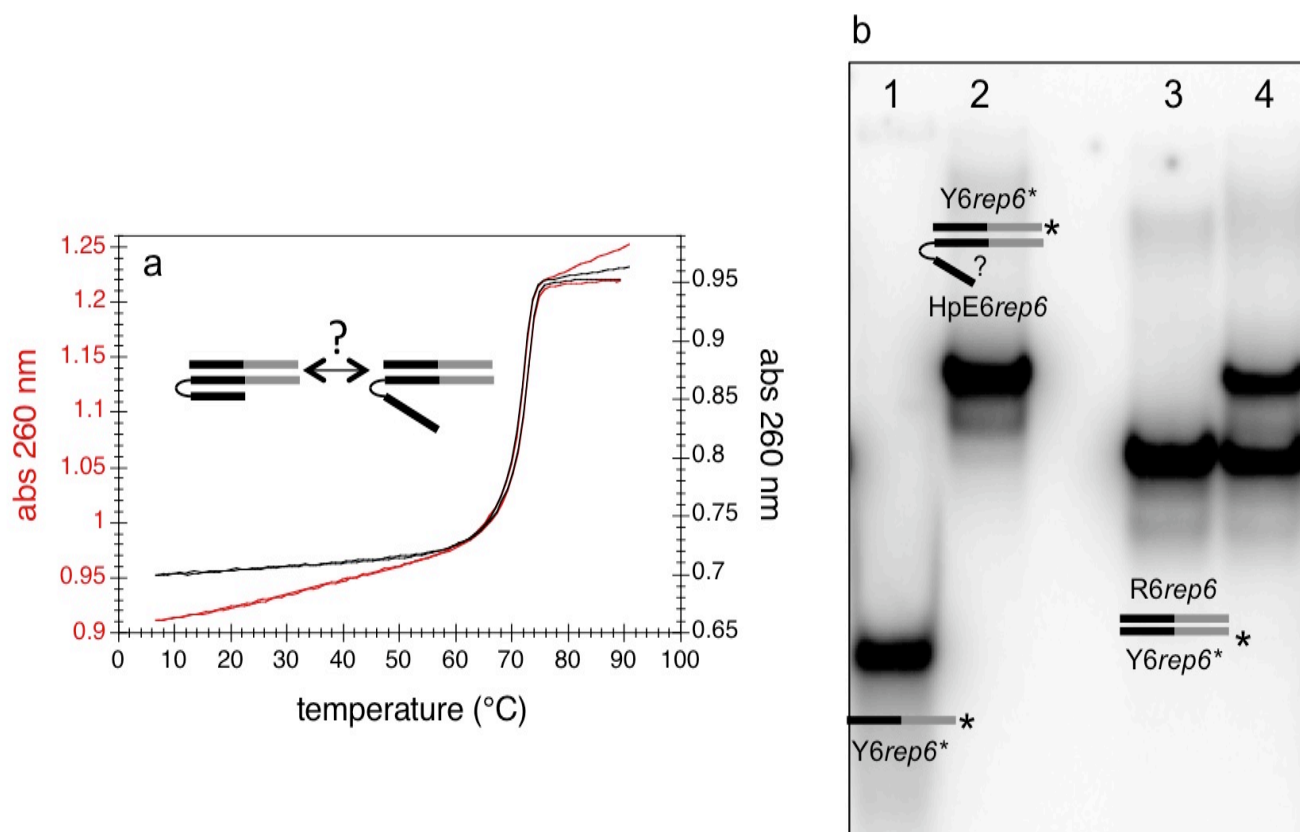


Figure S5
UV-melting profiles and EMSA of the complex HpE6rep6 + Y6rep6

- (a) Absorbance at 260 nm as a function of temperature of 1 μM Y6rep6 + 1 μM HpE6rep6 (black) and of 1 μM Y6rep6 + 1 μM R6rep6 (red), in 100 mM NaCl + 10 mM MgCl₂.
 (b) Electrophoretic mobility shift assay of radiolabeled Y6rep6 oligonucleotide (Y6rep6*) in NaCl + MgCl₂.

Lane 1: Y6rep6*;

lane 2: HpE6rep6 + Y6rep6*;

lane 3: Y6rep6* plus its complementary strand R6rep6;

lane 4: HpE6rep6 + Y6rep6* + R6rep6.

All samples were heated at 95°C and slowly cooled at 5°C.

EMSA was carried out as describe in the Material and Methods section.

The UV-melting profile of Y6rep6 + HpE6rep6 is similar to the one of the duplex formed by Y6rep6 and its complementary strand R6rep6; both exhibit a single melting transition at 73°C. This demonstrates that the HpE6rep6 forms a duplex with Y6rep6, but does not allow inferring triplex formation by the HpE6 motif.

In EMSA, annealing of Y6rep6* in the presence of both HpE6rep6 and Rrep6 results in the formation of two bands of similar intensities (lane 4), one corresponding to the duplex formed by Y6rep6* + R6rep6 (in lane 3), the other migrating as the complex formed by Y6rep6* + HpE6rep6 (in lane 2). The fact that the two bands have similar intensities indicates that the structure formed by HpE6rep6 with its target Y6rep6 is as stable as the duplex formed by Y6rep6 with its complementary strand R6rep6.

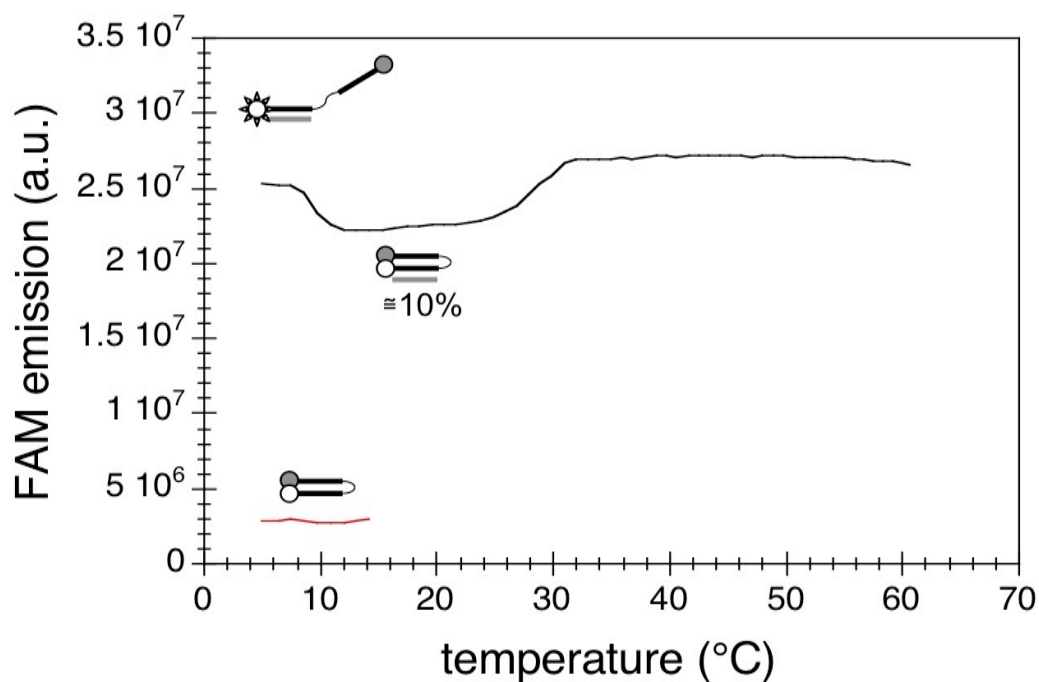


Figure S6
Melting profile, followed by FAM fluorescence, of the complex formed by
FAM-HpE6-Dabcyl and its target Y6

FAM emission as a function of temperature of 0.2 μM FAM-HpE6-Dabcyl in the presence of 1 μM Y6, in a buffer containing 100 mM KCl and 10 mM MgCl₂; excitation wavelength 470 nm, emission wavelength 520 nm. The red line is the FAM emission intensity of 0.2 μM FAM-HpE6-Dabcyl alone (folded state).

The decrease in FAM emission in the 10-30°C temperature range corresponds to about 10% of the maximal FAM emission; this allow estimating that, in this range of temperature, about 10% of the complex FAM-HpE6-Dabcyl + Y6 is in the triplex state.

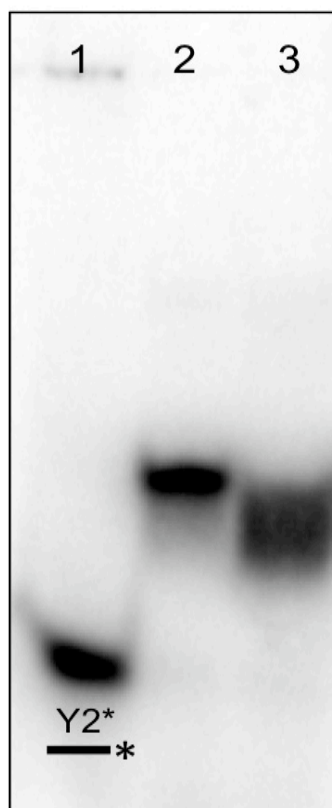


Figure S7
EMSA of the complex HpE2 + Y2 in potassium

Electrophoretic mobility shift assay of the HpE6 system in KCl + MgCl₂.

Lane 1: radiolabeled Y2 strand (Y2*);

lane 2: Y2* + HpE2; the mix was heated at 95°C and slowly annealed at 5°C;

lane 3: HpE2 was heated at 95°C and slowly annealed at 5°C, then Y2* was added.

EMSA was carried out as describe in the Material and Methods section.

Annealing of HpE2 with Y2* from high to low temperature resulted in a single thin band (lane1), supporting the formation of a single complex (a Watson-Crick duplex with a hanging third strand or a triplex?); while incubation of Y2* with a structured HpE2 (separately annealed alone in the presence of potassium) resulted in a smear, supporting the formation of multiple or unstable complexes.

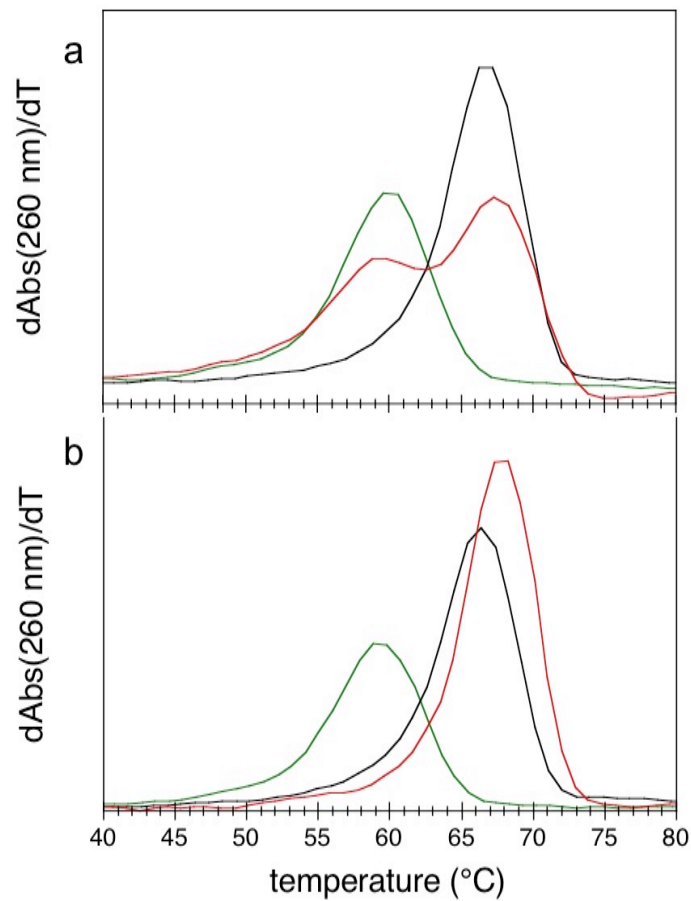


Figure S8
dAbs/dT of UV-melting profiles shown in figure 4

First derivatives of absorbance at 260 nm with respect to temperature of the complex(es) *Y2rep2* + *HpE2rep2* (red), of the long duplex *Y2rep2* + *R2rep2* (black) and of the short duplex *Y2rep2* + *rep2* (green), upon cooling (a) and upon heating (b), in 100 mM KCl + 10 mM MgCl₂.

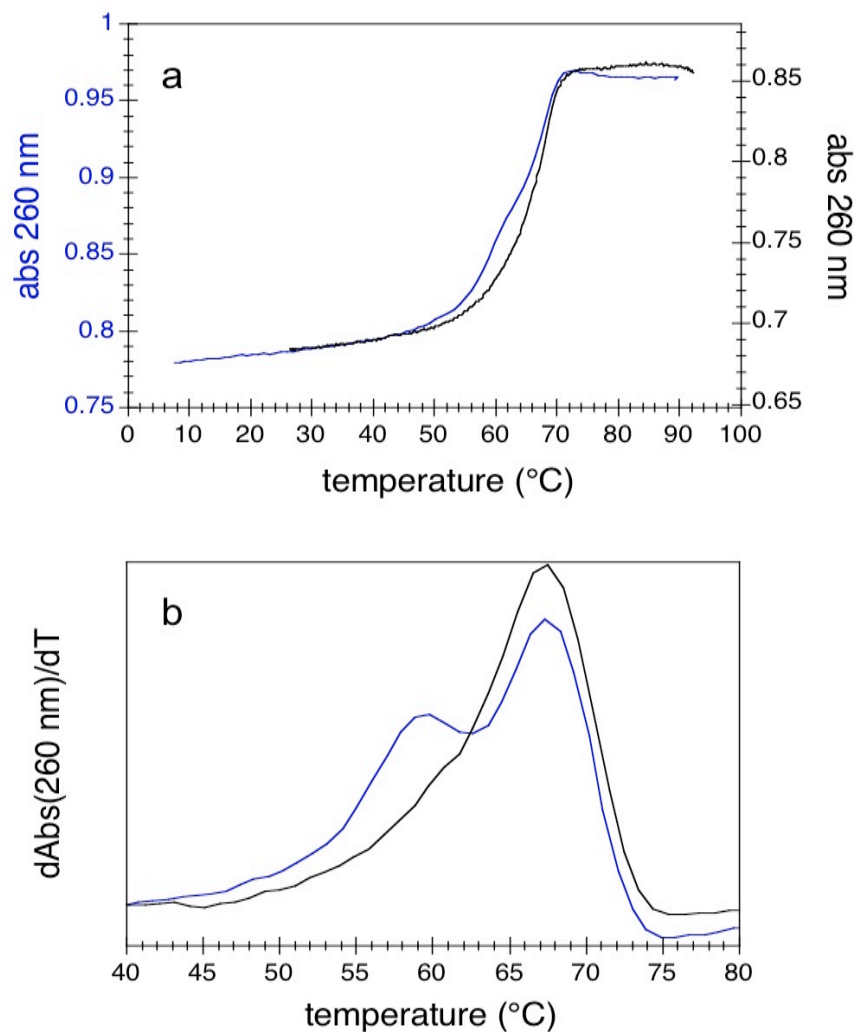


Figure S9
UV-annealing profiles of the complex(es) formed by
HpE2rep2 and Y2rep2 in potassium at different temperature scanning rates

- (a) Absorbance at 260 nm as a function of temperature from 95°C to 5°C of Y2rep2 + HpE2rep2 at a scanning rate of 0.2°C/min (blue) and of 0.05°C/min (black).
 (b) First derivative of absorbance as a function of temperature of the annealing profiles shown in (a). Each oligonucleotide were at 1µM strand concentration. Measurements were run in a buffer containing 100 mM KCl and 10 mM MgCl₂.

4.4 Article IV

Validation of miRNA-mRNA interactions by electrophoretic mobility shift assays

Anna Solé, Núria Mencia, Xenia Villalobos, Véronique Noé and Carlos J. Ciudad

BMC Res Notes. 2013 Nov 12;6:454. doi: 10.1186/1756-0500-6-454.

Background: MicroRNAs regulate gene expression by recognizing and binding to sequences of the 3'-UTR region of the mRNA of target genes. This binding leads to a decrease in protein levels of genes via mRNA degradation or through the inhibition of translation. Identification of target genes for a specific miRNA is performed by bioinformatics algorithms, which require experimental validation. The interaction of a miRNA with its target gene is usually studied by co-transfection of the miRNA with a reporter vector containing the 3'-UTR region of the gene. Although this method suggests a physical and functional interaction, it does not prove directly the interaction with its target miRNA gene (Iorio and Croce, 2012). In a previous work, binding assays or electrophoretic mobility shift assays (EMSA) were proved to be a useful tool to validate a direct interaction between a miRNA and the mRNA of its target gene (Mencia et al., 2011).

Objectives: To evaluate binding assays as a methodology to validate the interaction between miRNA-mRNA, by using miR-224 and its target SLC4A4 as a model.

Results: Using representative radiolabeled molecules of the mature form of miR-224 and the 3'-UTR region of SLC4A4 mRNA, we proved that miR224 was able to bind to the mRNA of the SLC4A4 gene directly and specifically.

Additionally, after confirming the binding between the inhibitor molecule anti-miR-224 and miR-224, we proved that anti-miR-224 could prevent the interaction between miR-224 and the 3'-UTR region of the *SLC4A4* gene, when the binding reaction was carried out in the presence of the three molecules together. Simultaneously, when competition assays were performed with SLC4A4 3'UTR:

miR224 binding and an unlabeled excess of SLC4A4 3'UTR, we could observed a progressive decrease in the band corresponding to the SLC4A4 3'UTR:miR-224 interaction, depending on the concentration of the unlabeled oligonucleotide.

Conclusions: Binding assays or EMSA provide a simple and useful tool to validate the direct and specific interaction between a miRNA and its target genes.

TECHNICAL NOTE

Open Access

Validation of miRNA-mRNA interactions by electrophoretic mobility shift assays

Anna Solé[†], Núria Mencia[†], Xenia Villalobos, Véronique Noé and Carlos J Ciudad^{*}

Abstract

Background: MicroRNAs are small non-coding RNAs involved in gene expression regulation by targeting specific regions in the 3'-UTR of the mRNA of their target genes. This binding leads to a decrease in the protein levels of such genes either by mRNA degradation or mRNA destabilization and translation inhibition. The interaction between a miRNA and its target mRNAs is usually studied by co-transfection of a reporter expression vector containing the 3'-UTR region of the mRNA and an inhibitory or precursor molecule for the miRNA. This approach, however, does not measure the direct and physical interaction between a miRNA and a specific mRNA.

Findings: RNA molecules corresponding to miR-224 and to the 3'-UTR of SLC4A4 were incubated together and their interaction studied under different binding conditions using electrophoretic mobility shift assays. A direct and specific interaction between miR-224 and SLC4A4 mRNA was observed. This interaction was abolished in the presence of competitors.

Conclusions: In this study, we explored a new application for the electrophoretic mobility shift assay and we demonstrated that it is a useful alternative method to assess, in a direct and specific manner, whether a miRNA binds to a specific predicted target mRNA.

Keywords: 3'-UTR, Binding assay, miRNA, Target validation, EMSA

Introduction

MiRNAs are a new class of small, non protein-encoding RNAs [1,2] responsible for gene expression regulation at a post-transcriptional level. MiRNAs recognize and bind to the 3'-UTR of the mRNA of their target genes. Only 6-7nt of the miRNA (miRNA seed) are complementary to the target mRNA. Imperfect base pairing between miRNAs and their target mRNAs leads to repression of translation and/or deadenylation, followed by destabilization of the target [3]. Many cellular pathways are regulated by miRNAs such as development, proliferation, differentiation, cell fate determination, apoptosis, signal transduction, organ development, host-viral interactions and tumorigenesis [4]. MiRNAs play key roles in the pathogenesis of cancer and many miRNAs have been shown to function as either oncomirs or tumor suppressors [5-11] (for review see [12]). Furthermore, miRNAs have an important role in the development of chemosensitivity

or chemoresistance in different types of cancer (summarized in [13]). The prediction of target genes for a given miRNA is carried out using bioinformatic algorithms that require experimental validation. The interaction of the miRNA target gene with a specific miRNA is usually studied by co-transfection of an inhibitory molecule (anti-miR) or miRNA precursor molecule together with a reporter vector containing the 3'-UTR region of the gene. Although this method suggests a physical and functional interaction, it does not prove a direct interaction of the target gene with the miRNA [14]. More complex methods based on immunoprecipitation of the complex miRNA/mRNA have been used to address this issue [15,16].

In a previous study, we studied the role of miR-224 in methotrexate resistance in HT-29 colon cancer cells. The underexpression of miR-224 resulted in a decrease in MTX sensitivity and an increase in the mRNA levels of three genes (*CDS2*, *HSPC159* and *SLC4A4*) whose role in MTX resistance was also functionally validated. After confirming within the cell that miR-224 was functionally regulating these three genes,

* Correspondence: cciudad@ub.edu

[†]Equal contributors

Department of Biochemistry and Molecular Biology, School of Pharmacy, University of Barcelona, Avenue Diagonal 643, Barcelona E-08028, Spain

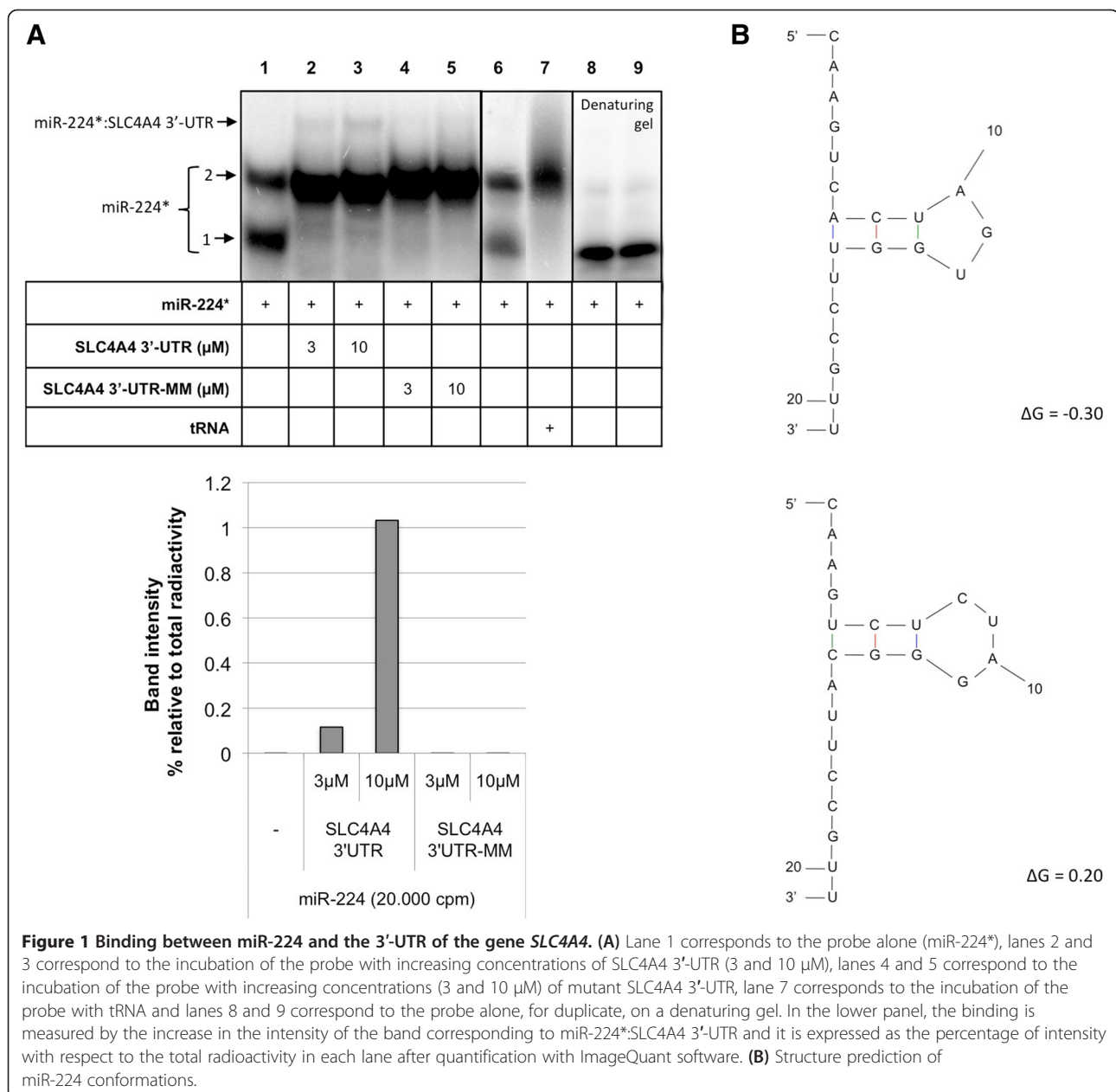
Table 1 Sequences of all the molecules used for the binding assays

Molecule	Sequence
miR-224	3' UUGCCUUGGUGAUCACUGAAC 5'
SLC4A4 3'-UTR	5' AAGCUUUCUAUUGUGACUUU 3'
anti-miR-224	5' A*A*C*GGAAC*C*AC*T*AGT*GAC*T*T*G 3'
anti-miR-13MIS	5' T*T*G*CCT AC*CAC*T*ACAC*T*G*A*A*G 3'
SLC4A4 3'-UTR-MM	5' AAGCUUUCUAUUCACUGAAU 3'

Sequences of the RNA and DNA molecules used in this study. For antisense oligodeoxynucleotides, phosphorothioate-modified bonds were designed according to the minimal modification criteria [21] and are indicated as *. Mismatch bases are indicated in italics.

we validated the direct and physical interaction between miR-224 and *CDS2*, *HSPC159* or *SLC4A4* using binding assays [17].

EMSA or electrophoretic mobility shift assays are widely used to confirm the binding of a nucleic acid to a protein or another nucleic acid [18-20]. However, there have been no reports regarding the use of EMSA to study the interaction of a miRNA with its target. Therefore, we propose EMSA as an alternative method to validate in a direct and specific fashion whether or not a miRNA binds to its target genes. This study describes the experiments carried out to develop this methodology.



Materials and methods

Materials

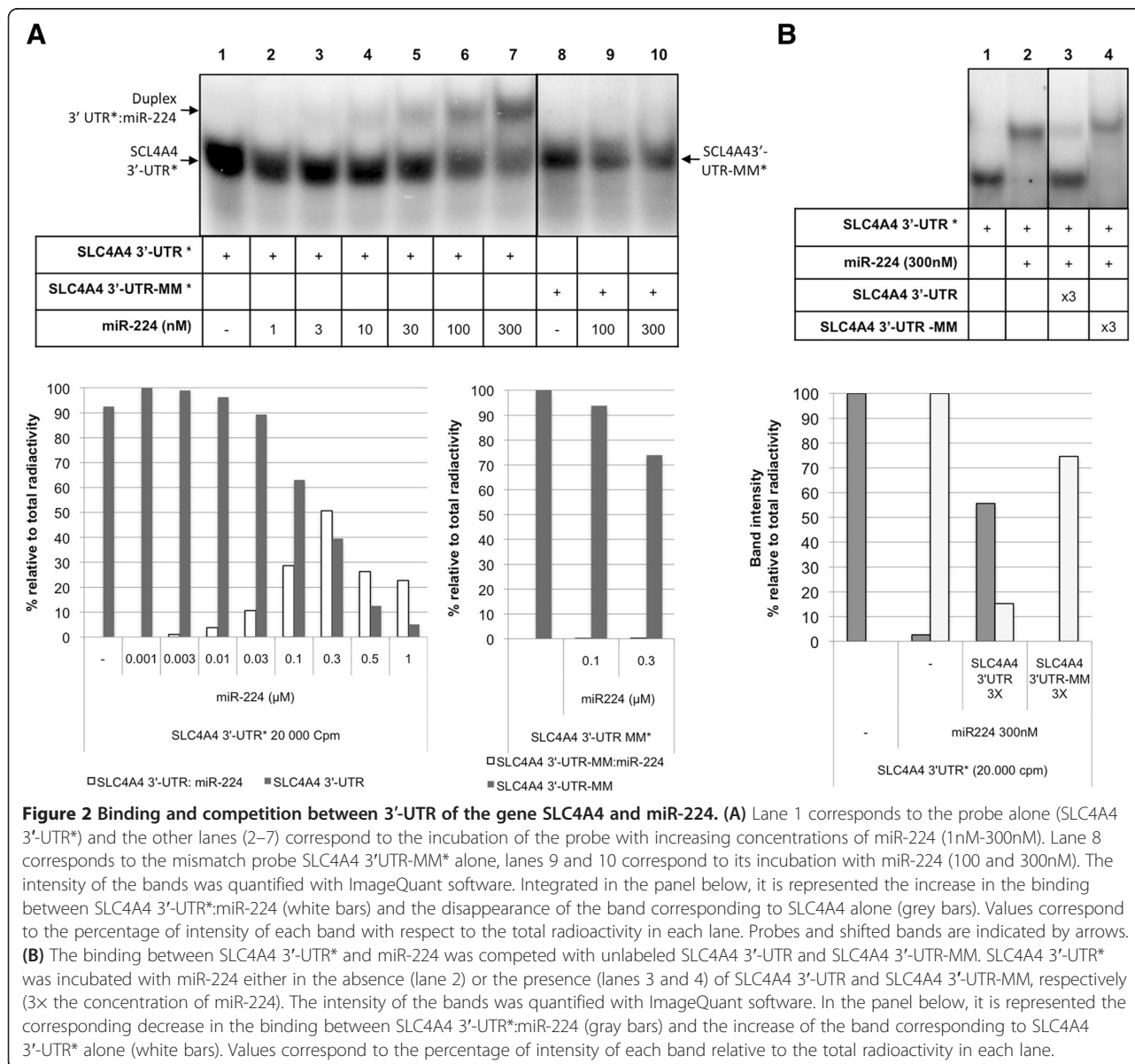
For binding assays, the following molecules were used: *miR-224*, RNA sequence corresponding to the mature form of miRNA-224; *SLC4A4 3'-UTR*, a 20-mer RNA sequence for the 3'-UTR corresponding to SLC4A4 bearing the target site for miR-224; *SLC4A4 3'UTR-MM*, a negative control 3'UTR sequence for the SLC4A4 RNA, bearing 6 mismatches in the target site for miR-224, *anti-miR-224*, a modified antisense oligodeoxynucleotide complementary to the sequence of the mature form of miR-224; and *anti-miR-13MIS*, antisense oligodeoxynucleotides containing 13 mismatches, compared to anti-miR-224.

The sequence corresponding to the 3'-UTR of the gene was 20 nucleotides long to allow better visualization of the shifted band, to be more specific and to avoid secondary structures that longer sequences might acquire, and that most likely would interfere with the analysis.

All RNA and DNA oligonucleotides were purchased from Sigma-Aldrich (Madrid, Spain) and their specific sequences are listed in Table 1.

Binding assays

Radiolabelled probes (20 000 cpm, [³²P]) were incubated for 30 minutes at 37°C with the corresponding RNA or DNA molecules in the presence of 10 mM MgCl₂, 100 mM NaCl, 50 mM HEPES pH 7.2 (AppliChem,



Ecogen, Barcelona, Spain) and 5% Glycerol (Sigma-Aldrich, Madrid, Spain). Binding reactions were run in a 12% polyacrylamide gel (10 mM MgCl₂, 5% Glycerol, 50 mM HEPES, pH 7.2) for 4 h at 190 V (4°C). Samples for denaturing gels were heated at 95°C for 5 min in loading buffer containing 95% formamide before electrophoresis in 5% polyacrylamide gels (1xTBE plus 8 M urea).

Gels were dried for 90 minutes at 80°C, exposed overnight to Europium plates and scanned in a Storm 840 scanner (Molecular Dynamics, GE Healthcare, Barcelona, Spain).

MiRNA secondary structure prediction

The miR-224 secondary structures were predicted using the mfold program, v2.3, (<http://mfold.rna.albany.edu/?q=mfold>) [22]. This program determines the optimal and suboptimal secondary structures of RNA calculated for a 1 M NaCl solution at 37°C. The prediction was performed with the suboptimality parameter set at 5% so that it shows all the structures that have a free energy of formation of up to 5% higher than the optimal.

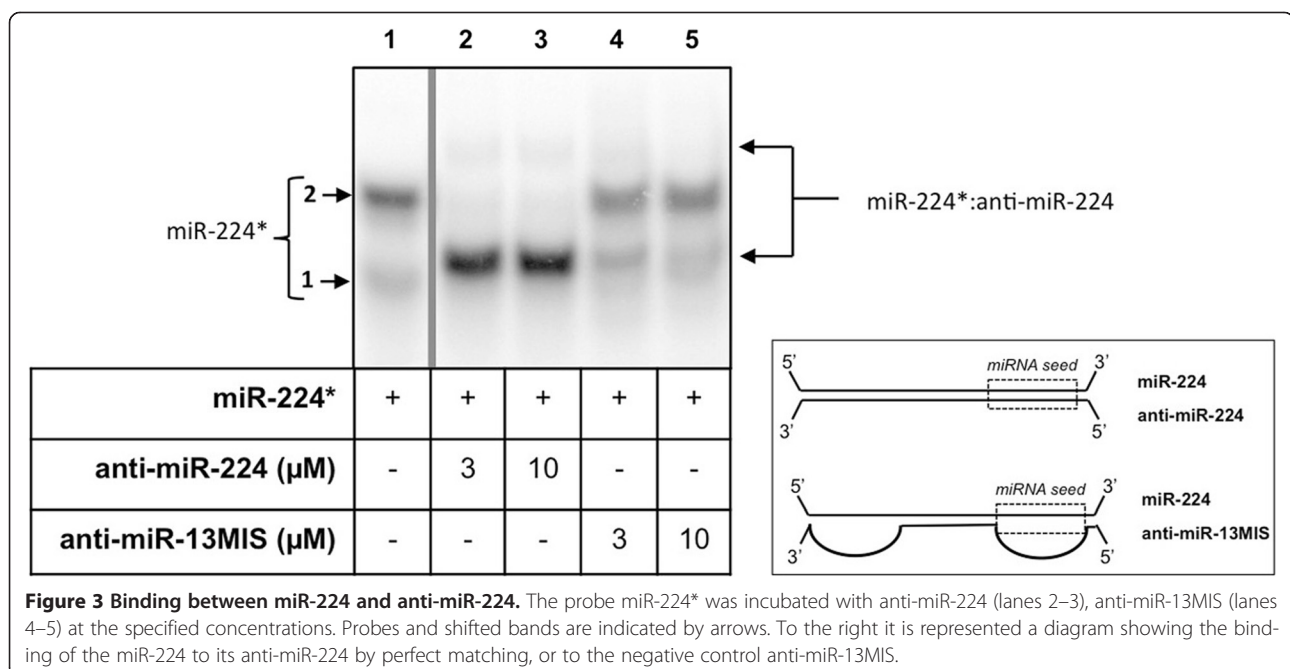
Findings and discussion

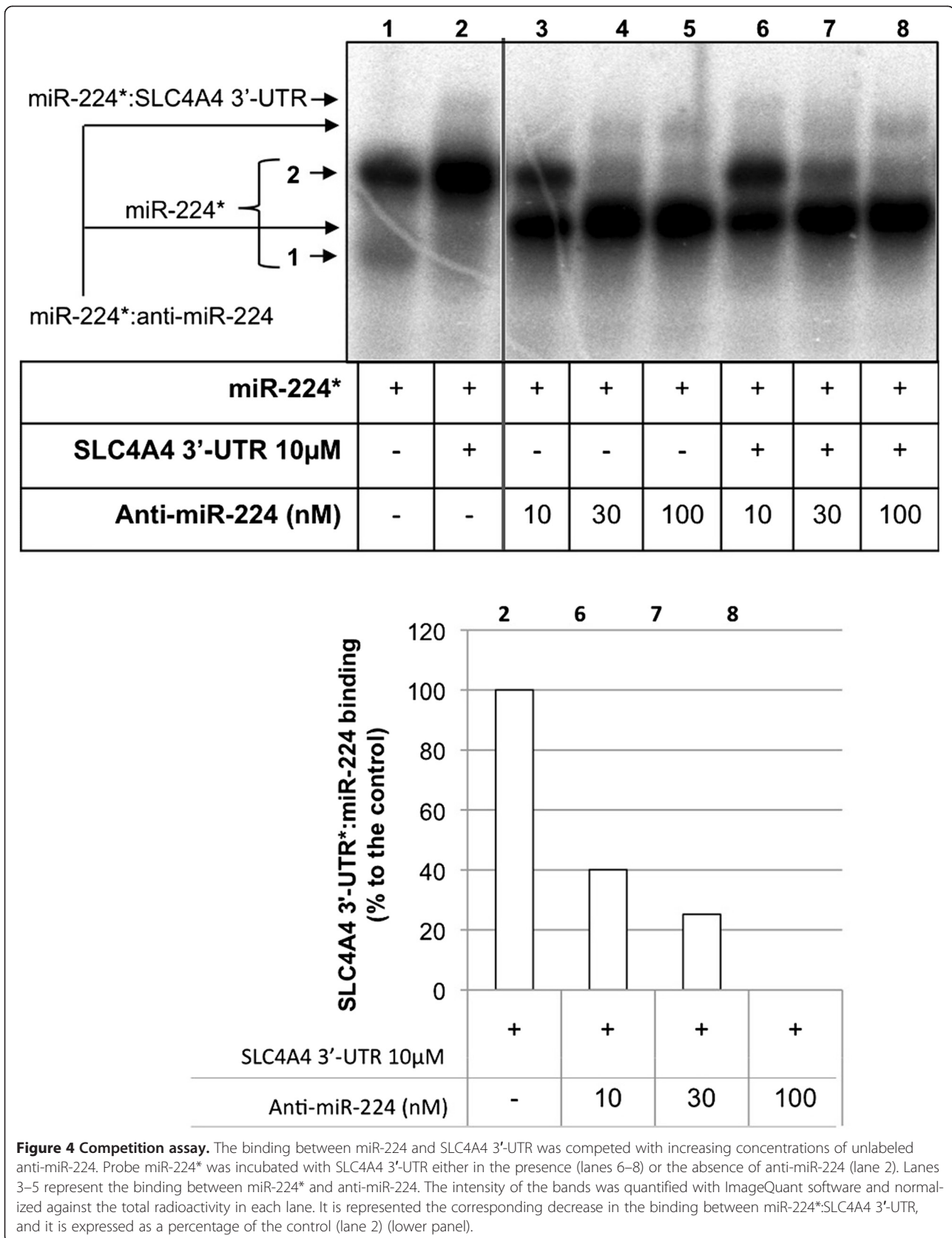
The first set of binding assays was performed using the radiolabeled miRNA-224 sequence (miR-224*) as the probe. MiR-224* displays two bands (Figure 1A, lane 1), one with higher mobility (band 1) and another band with lower mobility (band 2). When miR-224* was incubated with increasing concentrations of the 3'-UTR region of the gene *SLC4A4* (3 and 10 μM) we could observe the formation of a third band with lower

electrophoretic mobility. This third band corresponds to the specific binding of the two molecules miR-224*: *SLC4A4* 3'-UTR (Figure 1A, lanes 2 and 3) since it is not formed with *SCL4A4* 3'-UTR-MM (lanes 4 and 5). Band number 1 switched to band number 2 in the presence of *SLC4A4* 3'-UTR, either the wild type or the mutant sequence. The conformation with faster electrophoretic mobility also disappeared in the presence of tRNA (lane 7). These results indicate that the upper band (lanes 2 and 3) represents the specific binding between miR-224 and *SLC4A4* 3'-UTR, rather than a multicomplex. MiR224 alone was also run on a denaturing gel to test whether or not the two bands present in native gels were two conformations of the same miRNA. As shown in Figure 1A (lanes 8 and 9), only one band was observed.

Thus, *in vitro*, miR-224 alone takes at least two conformations with different mobility. Structure prediction using the mfold software [22] showed different conformations with free energies of $\Delta G = -0.30$ and $\Delta G = 0.20$ (Figure 1B), indicating plasticity in the molecule. Therefore, the secondary structure of miRNA may alternate between conformations.

The binding of miR-224 to its target gene was also confirmed using as radiolabeled probe the sequence corresponding to the 3'-UTR of *SLC4A4* (Figure 2A, lanes 1–7). When using *SCL4A4* 3'-UTR-MM sequence, the binding with miR-224 was not observed (Figure 2A, lanes 9 and 10). These results proved that miR-224 binds specifically to the 3'-UTR sequence of its target *SLC4A4*. Indeed, the experiments involving labeled 3'UTRs gave an easier read-out to understand (Figures 2A and 2B), where the bands appeared more defined and the proportion of





binding was higher, which strongly supports a physical interaction of miR-224 with SLC4A 3'-UTR *in vitro*.

To complete the usefulness of the assay we performed competition experiments of the interaction between miR-224 and SLC4A4 3'-UTR*. As shown in Figure 2B, this interaction was competed by wild type SLC4A4 3'-UTR but not by a mutated version of the sequence (mismatch).

When miR-224 was used as the probe, the necessary concentration of the corresponding unlabeled SLC4A4 3'-UTR sequence for the formation of the binding was 3 μ M (Figure 1A, lane 2). However, when using SLC4A4 3'-UTR as the probe the necessary concentrations for the formation of such duplexes ranged from 10 to 300 nM of cold miR-224 (Figure 2A), therefore suggesting that the binding of miR-224 to a radiolabeled SLC4A4 3'-UTR is stronger and more specific than using miR-224 as probe.

Next, miR-224 was incubated with anti-miR-224, the molecule used to successfully inhibit miR-224 function, and with the corresponding negative control used in functional assays, anti-miR-13MIS. This anti-miR contains 7 mismatches located in the miR-224 seed region and 6 additional mismatches in its 3' region. As can be observed in Figure 3, miR-224 was bound by anti-miR-224 forming the corresponding miR-224*:anti-miR-224 duplex (lanes 2–3). A major band appeared between bands 1 and 2 of miR-224 alone (lane 1) and a more retarded band that might correspond to a different conformation of the duplex miR-224*:anti-miR-224. It is interesting to note that anti-miR-224 was also able to bind to the band number 2 of the probe alone corresponding to folded miR-224, at variance of SLC4A4 3'-UTR. This difference can be explained by the fact that anti-miR-224 is completely complementary to miR-224, in contrast to SLC4A4 3'-UTR, which has only 7nt complementary to the miRNA (miRNA seed). Therefore, anti-miR-224 can unfold miR-224* and form the observed duplex.

The effect of incubating miR-224 with anti-miR-13MIS can be observed in lanes 4 and 5 (Figure 3), showing that it is not able to bind miR-224, since it presents 13 mismatches with respect to miR-224, confirming its validity as a negative control.

Figure 4 shows the binding of miR-224* to SLC4A4 3'-UTR (lane 2) and the formation of the duplex miR-224*:anti-miR-224 after incubation with increasing concentrations of anti-miR-224 (lanes 3–5). In this case, the band pattern observed was the same as the one in Figure 3 (lanes 2 and 3). When competition experiments were performed in the presence of miR-224*, 3'-UTR SLC4A4 and anti-miR-224, it was observed that increasing concentrations of anti-miR-224 were able to displace the binding of miR-224* to the 3'-UTR of the gene *SLC4A4*. This was

evidenced by the disappearance of the upper band corresponding to the binding of miR-224*:SLC4A4 3'-UTR (Figure 4, lanes 6–8 compared to lane 2). The competition between anti-miR-224 and SLC4A4 3'-UTR for the binding to miR-224* was also evidenced by the fact that higher concentrations of anti-miR-224 were needed to completely bind to miR-224 (lanes 6–7 compared to lanes 3–4).

Conclusions

The results presented in this study show that EMSA is an easy, useful tool to validate in a direct and specific manner the interaction between a given miRNA and a determined cellular target mRNA, specially when using as probe the target 3'-UTR sequence rather than the miRNA. Using two synthetic RNA molecules corresponding to the mature form of a miRNA and to a fragment of the 3'-UTR region of a predicted target mRNA, this assay provides a view of the direct physical interaction between these two molecules.

Abbreviations

3'-UTR: 3'-untranslated region; miR and miRNA: microRNA; SLC4A: Na/bicarbonate cotransporter 1; CDS2: CDP-diaclylglycerol synthase (phosphatidatcytidyltransferase) 2; HSPC159: Galectin-related protein; EMSA: Electrophoretic mobility shift assay.

Competing interests

The authors declare that they have no competing interests.

Authors' contributions

AS, NM and XV performed the experimental work. VN and CJC helped with data interpretation and supervised the experimental work. All authors wrote and approved the final manuscript.

Acknowledgements

This work was supported by grants SAF2008-00043 and SAF2011-23582 from "Plan Nacional de Investigación Científica", and ISCIII-RTICC RD06/0020/0046. Our research group holds the "quality distinction" from the "Generalitat de Catalunya" SGR2009-118. A.S. is a recipient of a fellowship (FI) from Generalitat of Catalunya. N.M. was a recipient of a fellowship (APIF) from the University of Barcelona (UB).

Received: 20 June 2013 Accepted: 8 November 2013

Published: 12 November 2013

References

- Bartel DP: MicroRNAs: genomics, biogenesis, mechanism, and function. *Cell* 2004, **116**(2):281–297.
- Carrington JC, Ambros V: Role of microRNAs in plant and animal development. *Science* 2003, **301**(5631):336–338.
- Pillai RS, Bhattacharyya SN, Filipowicz W: Repression of protein synthesis by miRNAs: how many mechanisms? *Trends Cell Biol* 2007, **17**(3):118–126.
- Huang Y, Shen XJ, Zou Q, Wang SP, Tang SM, Zhang GZ: Biological functions of microRNAs: a review. *J Physiol Biochem* 2010, **67**(1):129–139.
- Calin GA, Dumitru CD, Shimizu M, Bichi R, Zupo S, Noch E, Aldler H, Rattan S, Keating M, Rai K, et al: Frequent deletions and down-regulation of micro-RNA genes miR15 and miR16 at 13q14 in chronic lymphocytic leukemia. *Proc Natl Acad Sci U S A* 2002, **99**(24):15524–15529.
- Cimmino A, Calin GA, Fabbri M, Iorio MV, Ferracin M, Shimizu M, Wojcik SE, Aqeilan RI, Zupo S, Dono M, et al: miR-15 and miR-16 induce apoptosis by targeting BCL2. *Proc Natl Acad Sci U S A* 2005, **102**(39):13944–13949.
- Hayashita Y, Osada H, Tatematsu Y, Yamada H, Yanagisawa K, Tomida S, Yatabe Y, Kawahara K, Sekido Y, Takahashi T: A polycistronic microRNA

- cluster, miR-17-92, is overexpressed in human lung cancers and enhances cell proliferation. *Cancer Res* 2005, **65**(21):9628–9632.
8. Iorio MV, Ferracin M, Liu CG, Veronese A, Spizzo R, Sabbioni S, Magri E, Pedriali M, Fabbri M, Campiglio M, et al: **MicroRNA gene expression deregulation in human breast cancer.** *Cancer Res* 2005, **65**(16):7065–7070.
 9. Metzler M, Wilda M, Busch K, Viehmann S, Borkhardt A: **High expression of precursor microRNA-155/BIC RNA in children with burkitt lymphoma.** *Genes Chromosomes Cancer* 2004, **39**(2):167–169.
 10. Murakami Y, Yasuda T, Saigo K, Urashima T, Toyoda H, Okanoue T, Shimotohno K: **Comprehensive analysis of microRNA expression patterns in hepatocellular carcinoma and non-tumorous tissues.** *Oncogene* 2006, **25**(17):2537–2545.
 11. Voorhoeve PM, Le Sage C, Schrier M, Gillis AJ, Stoop H, Nagel R, Liu YP, Van Duijse J, Drost J, Griekspoor A, et al: **A genetic screen implicates miRNA-372 and miRNA-373 as oncogenes in testicular germ cell tumors.** *Cell* 2006, **124**(6):1169–1181.
 12. Garofalo M, Croce CM: **microRNAs: Master regulators as potential therapeutics in cancer.** *Annu Rev Pharmacol Toxicol* 2011, **51**:25–43.
 13. Ma J, Dong C, Ji C: **MicroRNA and drug resistance.** *Cancer Gene Ther* 2010, **17**(8):523–531.
 14. Iorio MV, Croce CM: **MicroRNA involvement in human cancer.** *Carcinogenesis* 2012, **33**(6):1126–1133.
 15. Chi SW, Zang JB, Mele A, Darnell RB: **Argonaute HITS-CLIP decodes microRNA-mRNA interaction maps.** *Nature* 2009, **460**(7254):479–486.
 16. Hsu PW, Huang HD, Hsu SD, Lin LZ, Tsou AP, Tseng CP, Stadler PF, Washietl S, Hofacker IL: **MIRNAP: genomic maps of microRNA genes and their target genes in mammalian genomes.** *Nucleic Acids Res* 2006, **34**(Database issue):D135–D139.
 17. Mencia N, Selga E, Noe V, Ciudad CJ: **Underexpression of miR-224 in methotrexate resistant human colon cancer cells.** *Biochem Pharmacol* 2011, **82**(11):1572–1582.
 18. Coma S, Noe V, Eritja R, Ciudad CJ: **Strand displacement of double-stranded DNA by triplex-forming antiparallel purine-hairpins.** *Oligonucleotides* 2005, **15**(4):269–283.
 19. Hellman LM, Fried MG: **Electrophoretic mobility shift assay (EMSA) for detecting protein-nucleic acid interactions.** *Nat Protoc* 2007, **2**(8):1849–1861.
 20. Morita T, Maki K, Aiba H: **Detection of sRNA-mRNA interactions by electrophoretic mobility shift assay.** *Methods Mol Biol* 2012, **905**:235–244.
 21. Peyman A, Uhlmann E: **Minimally modified oligonucleotides - combination of end-capping and pyrimidine-protection.** *Biol Chem Hoppe Seyler* 1996, **377**(1):67–70.
 22. Zuker M: **Mfold web server for nucleic acid folding and hybridization prediction.** *Nucleic Acids Res* 2003, **31**(13):3406–3415.

doi:10.1186/1756-0500-6-454

Cite this article as: Solé et al.: Validation of miRNA-mRNA interactions by electrophoretic mobility shift assays. *BMC Research Notes* 2013 **6**:454.

Submit your next manuscript to BioMed Central and take full advantage of:

- Convenient online submission
- Thorough peer review
- No space constraints or color figure charges
- Immediate publication on acceptance
- Inclusion in PubMed, CAS, Scopus and Google Scholar
- Research which is freely available for redistribution

Submit your manuscript at
www.biomedcentral.com/submit



5. DISCUSSION

5.1. Repair-PPRHs

In addition to gene silencing, oligonucleotides can also be used in other fields of gene therapy, such as gene editing. Therefore, the main purpose of this work was to explore the capacity of PPRHs to repair point mutations present in the *dhfr* gene. Thus we established the bases to design oligonucleotides able to repair point mutations in genes responsible for monogenic diseases such as cystic fibrosis or sickle cell anemia. As a model, we used the *dhfr* hamster gene because of the availability of a collection of mutants that result in the loss of function of this gene. In addition, we also have available a selection method based on the culture medium, which allows us to discriminate between the repaired cells (DHFR +) and the mutants (DHFR -).

Repair-PPRHs are formed by a PPRH core linked to a repair tail. The repair tail is complementary to the DNA receptor except for the position to be corrected. The PPRH core design follows the same rules as the PPRHs used for gene silencing, and in addition to conduct the repair tail to the region of the genome where the mutation is located, it is believed that it could be inducing homologous recombination between the mutated sequence and the repair tail (Broitman et al., 1999, Faruqi et al., 1996, Vasquez et al., 2000, Vasquez et al., 1999, Wang and Glazer, 1995).

As a first step of this work, we studied the ability of regular PPRHs to bind to the pyrimidine strand of the dsDNA by binding assays. PPRHs are shown to be able to maintain the displacement of the polypurine strand, extending previous observations from Coma et al (Coma et al., 2005). We then further explored the capability of a putative repair single-stranded oligonucleotide (ssO) to bind to the displaced polypurine strand.

Taking into account the results observed in the binding assays, we designed five different repair-PPRHs, adapted to cellular experiments. All of them contained the same PPRH core linked to different repair tails to correct a nonsense mutation in exon 2 of the *dhfr* minigene (p11-Mut) in CHO cells. All repair-PPRHs were first analyzed by binding assays to confirm their ability to bind to its dsDNA target, before being transfected to the cells.

Two approaches were carried out as a first attempt to correct a point mutation in mammalian cells. In the first approach, we validated the effect of three different repair-PPRHs (HpE2rep, HpE2link, HpE2link-ds/ R018) to correct the nonsense mutation when repair-PPRH were pre-incubated with the mutated target plasmid, and then transfected all together in the minus-*dhfr* DG44 cell line. In the second approach, the correction of the nonsense mutation was accomplished by HpE2rep, HpE2link and dHpE2link-rep, when the mutated plasmid was previously and stably transfected in DG44 (DG44-p11Mut), and repair-PPRHs were transfected alone. This approach would resemble more closely to the goal of repairing a point mutation of a gene in its endogenous *locus*, since even though the number of *dhfr* copies are higher than in a regular genome, the recognition and binding of the repair-PPRH to the target would be similar. A first attempt of correcting a point mutation in the endogenous *locus* of a gene was also accomplished in DA5 cells, containing a deletion in the exon six of the *dhfr* gene, using HpE6rep. Therefore, the capacity of repair-PPRHs to restore a deleted nucleotide was also demonstrated in an actual genomic environment. In all cases, the correction of the mutation was verified by DNA sequencing, and functionally validated at the DHFR mRNA, protein and activity levels. As far as we know, it is worth noting that the genotypic and phenotypic changes observed in the repaired cells are permanent.

When repair oligonucleotides were transfected alone, some surviving colonies were obtained with R018 and R024. However, the frequency of correction was ten times less than the frequency obtained with repair-PPRHs. This result was not surprising since ssOs have been described as a tool to correct point mutations (Campbell et al., 1989, Lin et al., 1990) in different approaches, such as in yeast (Moerschell et al., 1988), mammalian cells (Igoucheva et al., 2001, Yin et al., 2005) and mice (Fan and Yoon, 2003). However, frequencies of ssOs are low and very variable when used for gene repair (Aarts et al., 2006, Hu et al., 2005). In fact, our results present a higher frequency of correction compared to other works using ssOs to repair point mutations, such as in the GFP gene in HeLa cells, which obtained a maximum frequency of $2.3 \cdot 10^{-3}$ (Yin et al., 2005).

When we searched for pyrimidine sequences near to the nonsense mutation to design the PPRH core (HpE2), the most appropriate sequence contained two

purine interruptions, which were substituted by adenines in the PPRH core sequence. Binding assays demonstrated that this fact did not affect the binding specificity of the PPRH, and any alteration in the target sequence was observed when DNA of surviving colonies was analyzed.

The mechanism expected for the repair-PPRHs to correct a point mutation would be the formation of a triplex by the PPRH core, thus inducing or increasing the homologous recombination, at the same time that it conveys the repair tail to the mutated region. At this step, the repair tail, homologous to the dsDNA except for the altered nucleotide would be used as a template to correct the mutation, probably through the homologous directed repair mechanism.

To support this hypothesis, various experiments were carried out. DG44 and DG44-p11Mut were incubated with hydroxyurea or aphidicolin, which are known to be recombination inducers (Saintigny et al., 2001). That resulted in an increase of the frequency of correction by two-fold, thus providing evidences of the important role of homologous recombination in the mechanism exercised by repair-PPRHs.

On the other hand, the role of mismatch repair (MMR) system has been extensively studied in genome editing, but it is not clearly understood. Some studies showed that MMR activity was required for successful correct a mutation (Bertoni et al., 2009, Igoucheva et al., 2008, Kow et al., 2007), while in other studies MMR has been described to hamper the correction (Dekker et al., 2003, Dekker et al., 2006, Hu et al., 2005). Interestingly, one study found that MMR was a key pathway for genome editing in yeast, whereas it appears to be a barrier in mammalian cells (Maguire and Kmiec, 2007). In this direction we could observe that MMR could be an impediment in repairing a point mutation by repair-PPRHs, since cells pre-incubated with aphidicolin, which is an inhibitor of the DNA polymerase δ , (enzyme required for MMR) (Papadopoulos et al., 1994), showed higher degree of repair frequency.

Another condition to take into account is the role that hydroxyurea and aphidicolin exert in replication, and the consequence that it might cause in the repair-PPRHs mechanism. Both compounds are involved in the cell cycle process by stalling replication. In this way, cells would be arrested at S phase until transfection. When

these drugs were removed at the time of transfection, the replication rate would increase, thus considering the possibility that unwound conformation of the dsDNA would give advantage to PPRH core to form the triplex structure.

To deepen the knowledge of the repair-PPRHs mechanism, the role of Rad51 was also studied. Rad51 has been described as one of the major proteins involved in HR (Liu et al., 2002b, McLachlan et al., 2009). It plays an important role in the recombination process induced by the triplex structure, and it can stimulate the formation of a structure resembling of a D-loop (Symington, 2005, Petukhova et al., 1998, Van Komen et al., 2000), thus increasing the probability of invasion and/or binding of the ssODN to its target region. When cells were co-incubated with repair-PPRHs plus pRad51, the results showed an increase of ten-fold in the repair frequency, supporting the hypothesis that HR is involved in the mechanism of repair-PPRHs to correct point mutations.

Furthermore, we did not observed any surviving colony after transfection of the negative controls HpE2rep-NH, which is not able to fold as a hairpin structure, and HpE2rep-WC that cannot bind to the target sequence. In addition, a repair tail sequence linked to a G-quadruplex structure instead of a hairpin was also tested and no colonies were observed in selective medium. Thus we could conclude that the formation of the triplex structure is essential for the activity of repair-PPRHs.

Other observations have been taken into account after the results obtained in cellular experiments; Out of a total of five repair-PPRHs tested, only HpE2ext/RO24 did not accomplish to correct the point mutation in any of the approaches. Interestingly, this repair-PPRH does not contain the repair tail (RO24) covalently linked to the PPRH core, but it is hybridized to an extension domain of the PPRH core that does not reach the mutated base. Hence, we can conclude that to be effective, repair-PPRHs require the corrected nucleotide, and therefore the repair tail, to be part of the same molecule as the PPRH core.

5.1.1. Repair-PPRHs in an endogenous locus

To broaden the use of repair-PPRHs, they have been tested in a widely collection of endogenous *dhfr* mutants derived from the UA21 mammalian cell line, when the

PPRH core of the repair-PPRH was targeted near the point mutation, and when a separation of hundreds of nucleotides existed between the mutated nucleotide and the PPRH core binding site. Therefore, after the evidences that repair-PPRHs could be a new tool for genome editing using a mutated plasmid, we further demonstrated that results could be extended to an endogenous *locus*, by correcting different types of mutations in the *dhfr* gene of CHO cells.

Six cell lines, all containing different types of mutations in *dhfr* gene were repaired: DA7 and DF42; containing a substitution of a single nucleotide in exon 3 or exon 6 respectively, both provoking a stop codon in place, DU8 and DP12B; which contain a single or double substitution in an intron, and cause downstream premature stop codons, DI33A and DA5; bearing an extra nucleotide or a deletion, respectively, and thus causing opal stop codons.

One of the basic requirements to design a PPRH core is to localize a pyrimidine region in the dsDNA. When PPRHs are used to inhibit gene expression, this prerequisite is not a real issue, since it should not be laborious to find a suitable target throughout a whole gene. However, for genome editing, the PPRH core needed to be directed against a region near enough to the altered nucleotide to allow the repair tail to hybridize to the mutated region. Therefore, even though pyrimidine regions are more frequent in the genome than predicted by models (Goni et al., 2004) it could be a limitation to find an appropriate sequence, long enough to not affect the specificity of binding of the PPRH core, and with no more than 3-purine interruptions.

In this work, we show that this limitation can be overcome by new designs called short- or long-distance-repair-PPRH (SDR-PPRH or LDR-PPRH). These molecules are formed by a PPRH core and a short (25 to 31nt) single-stranded repair tail, directed against separate sequences in the genome, but linked by a five-thymidine spacer to the PPRH sequence. SDR-HpDI4-3rep, used in DP12B was designed with a PPRH core 41nt upstream the mutated nucleotide, and the PPRH core of LDR-HpDE6-1rep, tested in DF42 cells, was located 662bp downstream the mutation. The fact that these repair-PPRHs were able to correct the targeted point mutation expands the potential use of these molecules in the genome-editing field. Almost any location of the genome affected by point mutations could be corrected by an

appropriate LDR-repair-PPRH considering that homopyrimidine regions are detected in the human genome on average about every kb (Goni et al., 2004).

It is worth mentioning that one repair-PPRH that did not accomplish to correct the DNA alteration was HpDI4-1rep, used in DP12B cell line. This repair-PPRH presents a major difference in the structure compared to the other designs, the position of the corrected nucleotide in the repair tail. We usually placed the wild type base in the center of the tail sequence, but in this case it was located closer to the PPRH core. The fact that no surviving colonies were obtained suggests that it is an important factor to take into consideration when designing repair-PPRHs. Several studies have been carried out regarding the most favorable position for the corrected nucleotide in ssOs. Chih-Chuan Liang's laboratory established that the most effective location for the nucleotide to correct a mutation in the GFP gene was at the 3' end of a 25-mer oligonucleotide (Yin et al., 2005). However, others showed that the frequency of repair decreased as nucleotide moved from the central position toward the ends of the repair ssO (Agarwal et al., 2003). Therefore, there is no definitive conclusion with regard to the position of the corrected nucleotide.

Some groups have proved that the coding strand is more convenient to be targeted by repair ssOs than the template strand, since the frequency of correction is higher in those cases (Agarwal et al., 2003, Liu et al., 2002a, Yamamoto et al., 1992). In our work, however, no differences were observed when comparing the results obtained from repair-PPRHs bearing a repair tail directed against the coding or the template strand of the DNA.

It is important to point out the analyses of the mRNA levels of the repaired colonies and the mutant cells, since the effect of most of these point mutations have not been previously reported. If nonsense mediated decay (NMD) mechanism and translational read-through are considered, all mutant cells studied display the expected mRNA levels. DF42, DP12B and DI33A cell lines exhibit all high levels of DHFR mRNA (83%, 66% and 61%, respectively). This result is consistent with the fact that they all contain mutations producing nonsense codons at the terminal exon of the *dhfr*, and therefore, the NMD mechanism should not affect them (Maquat, 2004). On the other hand, the lower mRNA levels showed by DA7 and

DU8 cells (2% and 23%, respectively), agreed with the location of the premature stop codons, in exon 3. DA5 also presented low levels of DHFR mRNA: 17%. In this case, the nonsense codon provoked by the deletion is located 22nt downstream in the 3'UTR, thus resulting in a read-through of the normal termination signal, which has been shown to destabilize mRNA (Weiss and Liebhaber, 1994). Remarkably, in almost all cases that DHFR mRNA levels were reduced in the mutant cells, they increased in repaired colonies. Besides, the functional DHFR activity was recovered in all cases.

Advantages of repair-PPRHs include its economy and the significant facility of design and synthesis, since they are not chemically modified. Additionally, they never exceed 100 nucleotides in length (average length of 75nt). This aspect could also be an advantage in terms of toxicity (Rodriguez et al., 2013). With a PPRH core with a maximum of 3 pyrimidine interruptions and a repair tail with a length between 24 and 41nt, these molecules present a high specificity when bound to their target. The specificity of repair-PPRHs was confirmed by BLAST analyses in all cases. Besides, PPRHs have shown a high resistance to endogenous nucleases (Villalobos et al., 2014) due to the hairpin folding. Since it was described that the 3' end of a single-stranded oligonucleotide is more susceptible to the effect of nucleases, in almost all cases the repair tails are designed at the 5' end of the PPRH core.

In the past decade, a new approach has emerged as a new genome editing technology, which is based on artificial endonucleases composed by a DNA-binding domain linked to a non-specific cleavage module. These nucleases, including ZFN, TALENs and the most recent CRISPR/Cas9, are designed to cause a DSB in a specific site of the DNA, which has showed to activate proteins involved in recombinational repair (Ferrara and Kmiec, 2004, Storici et al., 2006), and DNA repair mechanisms including error-prone NHEJ and HDR (Wyman and Kanaar, 2006). In the absence of a homologous DNA template, the DSB is basically repaired by NHEJ causing insertions or deletions (indels), and efficiencies can be up to 50% (Ding et al., 2014). However, the low efficiency of HDR in the presence of a synthetic DNA template (Xie et al., 2014, Yang et al., 2013) might limit these

molecules to therapies directed to gene disruption. Furthermore, these procedures lead to a high number of off-target effects (Pattanayak et al., 2013, Fu et al., 2013, Kim and Kim, 2014), caused by unwanted DSB or due to unintended re-ligation between cuts after the DSB, where HDR competes with mutagenic NHEJ. On the other hand, the design and engineering that these molecules require can be challenging and time-consuming, in addition to the size of the DNA-binding domain plus the nuclease domain construction, which could hamper the delivery and use of these techniques.

Altogether, we can conclude that the use and mechanism of repair-PPRHs still show some unknowns, and must be more extensively studied, but they have provided evidences to be a simple and powerful alternative for genome editing, to correct disorders caused by point mutations.

5.1.2. *G-quadruplex*

The use of repair-PPRHs could present an inconvenience due to their structure, since the high amount of guanines in their sequence might cause the formation of secondary intra- and intermolecular structures such as G-quadruplex (Cheng et al., 1998). In this direction, we carried out an *in vitro* study on the PPRH structure and thermal stability; either alone or when bound to their pyrimidine target, by means of UV absorption and fluorescence measurements, and electrophoretic mobility shift assays (EMSA).

The ability of PPRHs to bind to dsDNA was already shown by binding assays (Coma et al., 2005, de Almagro et al., 2009, de Almagro et al., 2011a, Rodriguez et al., 2015, Sole et al., 2014, Villalobos et al., 2014), and the hairpin structure is physically possible due to the ability of purines to form a Watson-Crick bond with a pyrimidine, and at the same time to form a Reverse Hoogsteen bond with another purine. However, evidences were needed to prove the secondary formation of a hairpin and the triplex structure.

In this regard, two repair-PPRH sequences containing different amount of guanines were compared to study the possible formation of G-quadruplex

structures, an effect caused by the high guanine content in the sequence, and their ability to form triplexes.

When the PPRH cores of these molecules were studied alone, without the repair tails, we concluded that the most stable conformation of HpE6 was the hairpin folding in all buffer conditions. The T_m was independent of the cation and increased in the presence of $MgCl_2$, arguing in favor of the hairpin formation. In addition, the TDS spectrum of HpE6 would resemble the spectrum of a “GA” DNA duplex (Mergny et al., 2005). This result was consistent with the absence of many guanines in the sequence. Regarding HpE2, results showed different conformations depending on the buffer conditions. As expected by the high guanine content in the sequence, the T_m and the TDS suggested a G-quadruplex structure in KCl buffer. Surprisingly, in the presence of NaCl, the spectrum recalled a hairpin conformation, and the T_t of HpE2 increased with the increasing strand concentration, which indicates the folding into a reverse Hoogsteen intermolecular hairpin. The addition of the repair tails in the sequence did not affect the folding structure or the thermal stability of HpE6 and HpE2.

The incubation of both PPRHs with their pyrimidine targets led us to different conclusions depending on the PPRH and the buffer conditions. When HpE6rep plus its target was analyzed, no evidences of the formation of a triplex structure were obtained, either by UV-melting, CD or non-denaturing gels. FRET experiments further demonstrated that most of the hairpin structure unfolded when bound to the pyrimidine target. Interestingly, about 10% of the molecule is involved in the triplex structure, which is consistent with the two bands obtained by the binding assays when HpE6rep was incubated with its pyrimidine target (Figure S5 of Article III). On the other hand, the analyses of HpE2rep with its target showed that in potassium, where the HpE2 motif was structured into a G4, the major fraction (>50%) of HpE2 swapped from the G4 conformation to a triplex structure when bound to its target with a higher stability than the dsDNA duplex.

In summary, the results of this work showed that the quantity of guanines in the PPRH sequence is not necessarily significant to the secondary conformation that the molecule will adopt, and even a G-quadruplex structure can adopt a triplex conformation when bound to the target. It is worth mentioning that this is an *in*

vitro study, and it has been carried out in specific buffer and temperature conditions. Therefore, the behavior of repair-PPRHs in cells does not need to strictly correlate with these results.

5.2. miRNAs:

The involvement of miRNAs in the development of resistance to MTX was previously demonstrated in our laboratory, as well as the identification of their targets by which the response to MTX is regulated (Mencia et al., 2011). miR-224 was one of the most differentially expressed miRNAs, and the only underexpressed in resistant HT29 cells. By confronting the possible targets of miR-224 with the overexpressed genes in resistant cells, a list of 7 genes was obtained, including CDS2, HSPC159 and SLC4A4. Viability assays showed that the reduction of miR-224 levels together with an increase of its target genes CDS2, HSPC159 and SLC4A4 led to desensitization towards MTX.

In this work we evaluated the effectiveness and utility of binding assays as a tool to determine the direct physical interaction between a miRNA and one of its target genes. The incubation of a RNA molecule corresponding to the 3'-UTR region of the SLC4A4 gene containing a miR-224 binding site, with an RNA molecule corresponding to the mature miR-224, generates a band with lower electrophoretic mobility than those observed in the lanes corresponding to miR-224 or the SLC4A4 3'-UTR alone. This shifted band corresponds to the binding of the two molecules miR-224:SLC4A4 3'-UTR, and it is not formed after the incubation of miR-224 with a mutated SCL4A4 3'-UTR, which bears 6 mismatches in the target site for miR-224 (Figure 1 of Article IV).

Furthermore, we demonstrated that anti-miR-224 is able to bind with high affinity to miR-224, while the corresponding negative control anti-miR-13MIS, containing 7 mismatches located in the miR-224 seed region and 6 additional mismatches in its 3' region is not. This observation is in agreement with the results of the functional experiments in which anti-miR-13MIS (and also anti-miR-7MIS) were not able to reproduce the effects observed with the anti-miR-224 (Mencia et al., 2011).

Additionally, competition assays show that the presence of anti-miR-224 prevents the binding of miR-224 to SLC4A4 3'-UTR. This fact could impede the regulatory activity of miR-224 on its target genes.

Thus, binding assays, along with the corresponding functional validation, are a useful technique for studying the regulation of an mRNA by a miRNA.

Some studies have shown the relation between miRNAs, MTX and DHFR. Bertino's group showed that the presence of a SNP near the target site for miR-24 interferes with the inhibitory effect of miR-24 in the 3'-UTR of DHFR mRNA. This leads to overexpression of the protein and allows the cell to overcome the cytotoxic effect induced by MTX, a fact that would lead to resistance to MTX (Mishra et al., 2007, Mishra et al., 2008, Mishra et al., 2009). It has also been described the correlation between the overexpression of miR-140 (Song et al., 2009) or miR-125 (Song et al., 2010) with the resistance to MTX. In both cases, the effect on the sensitivity to MTX was not due to specific changes in the MTX pathway, but rather to a regulatory effect on the cell cycle. Overexpression of miR-215 and miR-140 led to a stop in the cell cycle, and a decrease in the proliferation rate.

One of the most important drawbacks of MTX therapy is that, after various administrations, cells can develop resistance to this drug, mainly due to *dhfr* gene amplification. In addition, in a previous study (Selga et al., 2009), the expression patterns associated with resistance to MTX were determined and compared in seven cell lines representing five types of cancer (colon, breast, pancreas, leukemia and osteosarcoma), and *dhfr* was the only differentially expressed gene common to all the cell lines studied. Therefore, the study of *dhfr* gene has been the focus of our laboratory during many years, and different strategies have been developed to overcome the disadvantage of drug resistance, including methods based on gene therapy to decrease *dhfr* gene expression.

Although in this work we focus the use of PPRHs to correct point mutations, PPRHs have been widely used in our laboratory to modulate gene expression. These molecules can specifically bind to the target DNA and/or mRNA and cause gene

silencing through different mechanisms (de Almagro et al., 2009, de Almagro et al., 2011a, Rodriguez et al., 2013). The use of PPRHs as a silencing tool has been described *in vitro* and *in vivo* approaches (de Almagro et al., 2009, de Almagro et al., 2011a, Rodriguez et al., 2013), by decreasing the expression of different target genes, including *dhfr*.

6. CONCLUSIONS

1. PPRHs have the ability to maintain the dsDNA in an open conformation for the subsequent binding of a putative repair single-stranded oligonucleotide.
2. Repair-PPRHs can specifically correct a point mutation in a *dihydrofolate reductase (dhfr)* minigene (p11Mut) either when the repair-PPRH/p11Mut complex is previously incubated, or when the plasmid is stably transfected to the cells.
3. Pre-incubation of cells with the recombination inhibitors aphidicolin and hydroxyurea results in an increase of the repair frequency.
4. Rad51 and therefore, homologous recombination, plays an important role in the mechanism of repair-PPRHs to correct a point mutation.
5. Different types of point mutation in the endogenous *dhfr* gene of mammalian cells, such as deletions, insertions and single and double substitutions can be repaired by repair-PPRHs. The corrected nucleotide needs to be located in the middle of the repair tail, and not too close to the PPRH core.
6. Short- and Long-Distance-Repair-PPRHs (SDR- and LDR-PPRHs) can be successfully used in the absence of a proper polypyrimidine sequence near to the point mutation.
7. A high guanine content in a PPRH sequence does not impede the formation of the triplex structure with its target, even if the PPRH folds as a G-quadruplex when it is analyzed alone.
8. Binding assays are an effective and innovative approach to determine the direct binding of a miRNA to the 3'-UTR region of its target genes.

Conclusions

9. MiR-224 binds to the 3'-UTR region of the *SLC4A4* gene. This union is not observed when the sequence corresponding to the 3'-UTR region of this gene bears mismatched bases.

10. Anti-miR-224 can prevent the interaction between miR-224 and the 3'-UTR region of the *SLC4A4* gene.

BIBLIOGRAPHY

A

- AARTS, M., DEKKER, M., DE VRIES, S., VAN DER WAL, A. & TE RIELE, H. 2006. Generation of a mouse mutant by oligonucleotide-mediated gene modification in ES cells. *Nucleic Acids Res*, 34, e147.
- AGARWAL, S., GAMPER, H. B. & KMIEC, E. B. 2003. Nucleotide replacement at two sites can be directed by modified single-stranded oligonucleotides in vitro and in vivo. *Biomol Eng*, 20, 7-20.
- ALEXEEV, V., IGOUCHEVA, O., DOMASHENKO, A., COTSARELIS, G. & YOON, K. 2000. Localized in vivo genotypic and phenotypic correction of the albino mutation in skin by RNA-DNA oligonucleotide. *Nat Biotechnol*, 18, 43-7.
- ALEXEEV, V., IGOUCHEVA, O. & YOON, K. 2002. Simultaneous targeted alteration of the tyrosinase and c-kit genes by single-stranded oligonucleotides. *Gene Ther*, 9, 1667-75.
- ALEXEEV, V. & YOON, K. 1998. Stable and inheritable changes in genotype and phenotype of albino melanocytes induced by an RNA-DNA oligonucleotide. *Nat Biotechnol*, 16, 1343-6.
- ALLEGRA, C. J., CHABNER, B. A., DRAKE, J. C., LUTZ, R., RODBARD, D. & JOLIVET, J. 1985. Enhanced inhibition of thymidylate synthase by methotrexate polyglutamates. *J Biol Chem*, 260, 9720-6.
- ALLEGRA, C. J., HOANG, K., YEH, G. C., DRAKE, J. C. & BARAM, J. 1987. Evidence for direct inhibition of de novo purine synthesis in human MCF-7 breast cells as a principal mode of metabolic inhibition by methotrexate. *J Biol Chem*, 262, 13520-6.
- ALT, F. W., KELLEMS, R. E., BERTINO, J. R. & SCHIMKE, R. T. 1978. Selective multiplication of dihydrofolate reductase genes in methotrexate-resistant variants of cultured murine cells. *J Biol Chem*, 253, 1357-70.
- ANDRIEU-SOLER, C., CASAS, M., FAUSSAT, A. M., GANDOLPHE, C., DOAT, M., TEMPE, D., GIOVANNANGELI, C., BEHAR-COHEN, F. & CONCORDET, J. P. 2005. Stable transmission of targeted gene modification using single-stranded oligonucleotides with flanking LNAs. *Nucleic Acids Res*, 33, 3733-42.
- ANDRIEU-SOLER, C., HALHAL, M., BOATRIGHT, J. H., PADOVE, S. A., NICKERSON, J. M., STODULKOVA, E., STEWART, R. E., CIAVATTA, V. T., DOAT, M., JEANNY, J. C., DE BIZEMONT, T., SENNLAUB, F., COURTOIS, Y. & BEHAR-COHEN, F. 2007. Single-stranded oligonucleotide-mediated in vivo gene repair in the rd1 retina. *Mol Vis*, 13, 692-706.
- ASSARAF, Y. G. 2007. Molecular basis of antifolate resistance. *Cancer Metastasis Rev*, 26, 153-81.

B

- BAGGOTT, J. E., VAUGHN, W. H. & HUDSON, B. B. 1986. Inhibition of 5-aminoimidazole-4-carboxamide ribotide transformylase, adenosine deaminase and 5'-adenylate deaminase by polyglutamates of methotrexate and oxidized folates and by 5-aminoimidazole-4-carboxamide riboside and ribotide. *Biochem J*, 236, 193-200.

- BANDYOPADHYAY, P., MA, X., LINEHAN-STIEERS, C., KREN, B. T. & STEER, C. J. 1999. Nucleotide exchange in genomic DNA of rat hepatocytes using RNA/DNA oligonucleotides. Targeted delivery of liposomes and polyethyleneimine to the asialoglycoprotein receptor. *J Biol Chem*, 274, 10163-72.
- BANIN, S., MOYAL, L., SHIEH, S., TAYA, Y., ANDERSON, C. W., CHESSA, L., SMORODINSKY, N. I., PRIVES, C., REISS, Y., SHILOH, Y. & ZIV, Y. 1998. Enhanced phosphorylation of p53 by ATM in response to DNA damage. *Science*, 281, 1674-7.
- BARNES, D. E. 2001. Non-homologous end joining as a mechanism of DNA repair. *Curr Biol*, 11, R455-7.
- BARTEL, D. P. 2004. MicroRNAs: genomics, biogenesis, mechanism, and function. *Cell*, 116, 281-97.
- BARTLETT, R. J., STOCKINGER, S., DENIS, M. M., BARTLETT, W. T., INVERARDI, L., LE, T. T., THI MAN, N., MORRIS, G. E., BOGAN, D. J., METCALF-BOGAN, J. & KORNEGAY, J. N. 2000. In vivo targeted repair of a point mutation in the canine dystrophin gene by a chimeric RNA/DNA oligonucleotide. *Nat Biotechnol*, 18, 615-22.
- BAUMANN, P. & WEST, S. C. 1998. Role of the human RAD51 protein in homologous recombination and double-stranded-break repair. *Trends Biochem Sci*, 23, 247-51.
- BEAL, P. A. & DERVAN, P. B. 1991. Second structural motif for recognition of DNA by oligonucleotide-directed triple-helix formation. *Science*, 251, 1360-3.
- BELOUSOV, E. S., AFONINA, I. A., PODYMINOGIN, M. A., GAMPER, H. B., REED, M. W., WYDRO, R. M. & MEYER, R. B. 1997. Sequence-specific targeting and covalent modification of human genomic DNA. *Nucleic Acids Res*, 25, 3440-4.
- BENDER, M. & DOUTHITT SEIBE, G. 2003. *Sickle Cell Disease*, GeneReviews.
- BENTIN, T., LARSEN, H. J. & NIELSEN, P. E. 2003. Combined triplex/duplex invasion of double-stranded DNA by "tail-clamp" peptide nucleic acid. *Biochemistry*, 42, 13987-95.
- BERGINK, S., TOUSSAINT, W., LUIJSTERBURG, M. S., DINANT, C., ALEKSEEV, S., HOEIJMAKERS, J. H., DANTUMA, N. P., HOUTSMULLER, A. B. & VERMEULEN, W. 2012. Recognition of DNA damage by XPC coincides with disruption of the XPC-RAD23 complex. *J Cell Biol*, 196, 681-8.
- BERNSTEIN, C., PRASAD, A. R., NFONSAM, V. & BERNSTEIN, H. 2013. *DNA Damage, DNA Repair and Cancer*, InTech.
- BERTONI, C., MORRIS, G. E. & RANDO, T. A. 2005. Strand bias in oligonucleotide-mediated dystrophin gene editing. *Hum Mol Genet*, 14, 221-33.
- BERTONI, C. & RANDO, T. A. 2002. Dystrophin gene repair in mdx muscle precursor cells in vitro and in vivo mediated by RNA-DNA chimeric oligonucleotides. *Hum Gene Ther*, 13, 707-18.
- BERTONI, C., RUSTAGI, A. & RANDO, T. A. 2009. Enhanced gene repair mediated by methyl-CpG-modified single-stranded oligonucleotides. *Nucleic Acids Res*, 37, 7468-82.
- BHAYANI, M. K., CALIN, G. A. & LAI, S. Y. 2012. Functional relevance of miRNA sequences in human disease. *Mutat Res*, 731, 14-9.
- BOCH, J. & BONAS, U. 2010. Xanthomonas AvrBs3 family-type III effectors: discovery and function. *Annu Rev Phytopathol*, 48, 419-36.

- BOCH, J., SCHOLZE, H., SCHORNACK, S., LANDGRAF, A., HAHN, S., KAY, S., LAHAYE, T., NICKSTADT, A. & BONAS, U. 2009. Breaking the code of DNA binding specificity of TAL-type III effectors. *Science*, 326, 1509-12.
- BROITMAN, S., AMOSOVA, O., DOLINNAYA, N. G. & FRESCO, J. R. 1999. Repairing the sickle cell mutation. I. Specific covalent binding of a photoreactive third strand to the mutated base pair. *J Biol Chem*, 274, 21763-8.
- BURGE, S., PARKINSON, G. N., HAZEL, P., TODD, A. K. & NEIDLE, S. 2006. Quadruplex DNA: sequence, topology and structure. *Nucleic Acids Res*, 34, 5402-15.

C

- CAI, X., HAGEDORN, C. H. & CULLEN, B. R. 2004. Human microRNAs are processed from capped, polyadenylated transcripts that can also function as mRNAs. *RNA*, 10, 1957-66.
- CAMPBELL, C. R., KEOWN, W., LOWE, L., KIRSCHLING, D. & KUCHERLAPATI, R. 1989. Homologous recombination involving small single-stranded oligonucleotides in human cells. *New Biol*, 1, 223-7.
- CANMAN, C. E., LIM, D. S., CIMPRICH, K. A., TAYA, Y., TAMAI, K., SAKAGUCHI, K., APPELLA, E., KASTAN, M. B. & SILICIANO, J. D. 1998. Activation of the ATM kinase by ionizing radiation and phosphorylation of p53. *Science*, 281, 1677-9.
- CARLSON, D. F., TAN, W., LILICO, S. G., STVERAKOVA, D., PROUDFOOT, C., CHRISTIAN, M., VOYTAS, D. F., LONG, C. R., WHITELAW, C. B. & FAHRENKRUG, S. C. 2012. Efficient TALEN-mediated gene knockout in livestock. *Proc Natl Acad Sci U S A*, 109, 17382-7.
- CARMAN, M. D., SCHORNAGEL, J. H., RIVEST, R. S., SRIMATKANDADA, S., PORTLOCK, C. S., DUFFY, T. & BERTINO, J. R. 1984. Resistance to methotrexate due to gene amplification in a patient with acute leukemia. *J Clin Oncol*, 2, 16-20.
- CAROTHERS, A. M., URLAUB, G., GRUNBERGER, D. & CHASIN, L. A. 1993a. Splicing mutants and their second-site suppressors at the dihydrofolate reductase locus in Chinese hamster ovary cells. *Mol Cell Biol*, 13, 5085-98.
- CAROTHERS, A. M., URLAUB, G., MUCHA, J., YUAN, W., CHASIN, L. A. & GRUNBERGER, D. 1993b. A mutational hot spot induced by N-hydroxyaminofluorene in dihydrofolate reductase mutants of Chinese hamster ovary cells. *Carcinogenesis*, 14, 2181-4.
- CAROTHERS, A. M., URLAUB, G., STEIGERWALT, R. W., CHASIN, L. A. & GRUNBERGER, D. 1986. Characterization of mutations induced by 2-(N-acetoxy-N-acetyl)aminofluorene in the dihydrofolate reductase gene of cultured hamster cells. *Proc Natl Acad Sci U S A*, 83, 6519-23.
- CARRINGTON, J. C. & AMBROS, V. 2003. Role of microRNAs in plant and animal development. *Science*, 301, 336-8.
- CARROLL, D. 2014. Genome engineering with targetable nucleases. *Annu Rev Biochem*, 83, 409-39.
- CHAN, P. P., LIN, M., FARUQI, A. F., POWELL, J., SEIDMAN, M. M. & GLAZER, P. M. 1999. Targeted correction of an episomal gene in mammalian cells by a

- short DNA fragment tethered to a triplex-forming oligonucleotide. *J Biol Chem*, 274, 11541-8.
- CHASIN, L. A., URLAUB, G., MITCHELL, P., CIUDAD, C., BARTH, J., CAROTHERS, A. M., STEIGERWALT, R. & GRUNBERGER, D. 1990. RNA processing mutants at the dihydrofolate reductase locus in Chinese hamster ovary cells. *Prog Clin Biol Res*, 340A, 295-304.
- CHEN, F., PRUETT-MILLER, S. M., HUANG, Y., GJOKA, M., DUDA, K., TAUNTON, J., COLLINGWOOD, T. N., FRODIN, M. & DAVIS, G. D. 2011. High-frequency genome editing using ssDNA oligonucleotides with zinc-finger nucleases. *Nat Methods*, 8, 753-5.
- CHEN, Z. S., LEE, K., WALTHER, S., RAFTOGIANIS, R. B., KUWANO, M., ZENG, H. & KRUIH, G. D. 2002. Analysis of methotrexate and folate transport by multidrug resistance protein 4 (ABCC4): MRP4 is a component of the methotrexate efflux system. *Cancer Res*, 62, 3144-50.
- CHENG, A. J., WANG, J. C. & VAN DYKE, M. W. 1998. Self-association of G-rich oligodeoxyribonucleotides under conditions promoting purine-motif triplex formation. *Antisense Nucleic Acid Drug Dev*, 8, 215-25.
- CHIN, J. Y., KUAN, J. Y., LONKAR, P. S., KRAUSE, D. S., SEIDMAN, M. M., PETERSON, K. R., NIELSEN, P. E., KOLE, R. & GLAZER, P. M. 2008. Correction of a splice-site mutation in the beta-globin gene stimulated by triplex-forming peptide nucleic acids. *Proc Natl Acad Sci U S A*, 105, 13514-9.
- CHRISTMANN, M., TOMICIC, M. T., ROOS, W. P. & KAINA, B. 2003. Mechanisms of human DNA repair: an update. *Toxicology*, 193, 3-34.
- CHU, E., GREM, J. L., JOHNSTON, P. G. & ALLEGRA, C. J. 1996. New concepts for the development and use of antifolates. *Stem Cells*, 14, 41-6.
- CIUDAD, C. J., URLAUB, G. & CHASIN, L. A. 1988. Deletion analysis of the Chinese hamster dihydrofolate reductase gene promoter. *J Biol Chem*, 263, 16274-82.
- COLE-STRAUSS, A., YOON, K., XIANG, Y., BYRNE, B. C., RICE, M. C., GRYN, J., HOLLOMAN, W. K. & KMIEC, E. B. 1996. Correction of the mutation responsible for sickle cell anemia by an RNA-DNA oligonucleotide. *Science*, 273, 1386-9.
- COMA, S., NOE, V., ERITJA, R. & CIUDAD, C. J. 2005. Strand displacement of double-stranded DNA by triplex-forming antiparallel purine-hairpins. *Oligonucleotides*, 15, 269-83.
- CULVER, K. W., HSIEH, W. T., HUYEN, Y., CHEN, V., LIU, J., KHRIPINE, Y. & KHORLIN, A. 1999. Correction of chromosomal point mutations in human cells with bifunctional oligonucleotides. *Nat Biotechnol*, 17, 989-93.
- CURT, G. A., COWAN, K. H. & CHABNER, B. A. 1984. Gene amplification in drug resistance: of mice and men. *J Clin Oncol*, 2, 62-4.

D

- DATTA, H. J., CHAN, P. P., VASQUEZ, K. M., GUPTA, R. C. & GLAZER, P. M. 2001. Triplex-induced recombination in human cell-free extracts. Dependence on XPA and HsRad51. *J Biol Chem*, 276, 18018-23.

- DE ALMAGRO, M. C., COMA, S., NOE, V. & CIUDAD, C. J. 2009. Polypurine hairpins directed against the template strand of DNA knock down the expression of mammalian genes. *J Biol Chem*, 284, 11579-89.
- DE ALMAGRO, M. C., MENCIA, N., NOE, V. & CIUDAD, C. J. 2011a. Coding polypurine hairpins cause target-induced cell death in breast cancer cells. *Hum Gene Ther*, 22, 451-63.
- DE ALMAGRO, M. C., SELGA, E., THIBAUT, R., PORTE, C., NOE, V. & CIUDAD, C. J. 2011b. UDP-glucuronosyltransferase 1A6 overexpression in breast cancer cells resistant to methotrexate. *Biochem Pharmacol*, 81, 60-70.
- DE SEMIR, D., NADAL, M., GONZALEZ, J. R., LARRIBA, S., AVINYO, A., NUNES, V., CASALS, T., ESTIVILL, X. & ARAN, J. M. 2003. Suitability of oligonucleotide-mediated cystic fibrosis gene repair in airway epithelial cells. *J Gene Med*, 5, 625-39.
- DEKKER, M., BROUWERS, C., AARTS, M., VAN DER TORRE, J., DE VRIES, S., VAN DE VRUGT, H. & TE RIELE, H. 2006. Effective oligonucleotide-mediated gene disruption in ES cells lacking the mismatch repair protein MSH3. *Gene Ther*, 13, 686-94.
- DEKKER, M., BROUWERS, C. & TE RIELE, H. 2003. Targeted gene modification in mismatch-repair-deficient embryonic stem cells by single-stranded DNA oligonucleotides. *Nucleic Acids Res*, 31, e27.
- DEMIDOV, V., FRANK-KAMENETSKII, M. D., EGHOLM, M., BUCHARDT, O. & NIELSEN, P. E. 1993. Sequence selective double strand DNA cleavage by peptide nucleic acid (PNA) targeting using nuclease S1. *Nucleic Acids Res*, 21, 2103-7.
- DENG, D., YAN, C., PAN, X., MAHFOUZ, M., WANG, J., ZHU, J. K., SHI, Y. & YAN, N. 2012. Structural basis for sequence-specific recognition of DNA by TAL effectors. *Science*, 335, 720-3.
- DIAZ-FONT, A., CORMAND, B., CHABAS, A., VILAGELIU, L. & GRINBERG, D. 2003. Unsuccessful chimeroplast strategy for the correction of a mutation causing Gaucher disease. *Blood Cells Mol Dis*, 31, 183-6.
- DICKER, A. P., VOLKENANDT, M., SCHWEITZER, B. I., BANERJEE, D. & BERTINO, J. R. 1990. Identification and characterization of a mutation in the dihydrofolate reductase gene from the methotrexate-resistant Chinese hamster ovary cell line Pro-3 MtxRIII. *J Biol Chem*, 265, 8317-21.
- DING, Q., LEE, Y. K., SCHAEFER, E. A., PETERS, D. T., VERES, A., KIM, K., KUPERWASSER, N., MOTOLA, D. L., MEISSNER, T. B., HENDRIKS, W. T., TREVISAN, M., GUPTA, R. M., MOISAN, A., BANKS, E., FRIESEN, M., SCHINZEL, R. T., XIA, F., TANG, A., XIA, Y., FIGUEROA, E., WANN, A., AHFELDT, T., DAHERON, L., ZHANG, F., RUBIN, L. L., PENG, L. F., CHUNG, R. T., MUSUNURU, K. & COWAN, C. A. 2013. A TALEN genome-editing system for generating human stem cell-based disease models. *Cell Stem Cell*, 12, 238-51.
- DING, Q., STRONG, A., PATEL, K. M., NG, S. L., GOSIS, B. S., REGAN, S. N., COWAN, C. A., RADER, D. J. & MUSUNURU, K. 2014. Permanent alteration of PCSK9 with in vivo CRISPR-Cas9 genome editing. *Circ Res*, 115, 488-92.
- DIXON, K. H., LANPHER, B. C., CHIU, J., KELLEY, K. & COWAN, K. H. 1994. A novel cDNA restores reduced folate carrier activity and methotrexate sensitivity to transport deficient cells. *J Biol Chem*, 269, 17-20.

DOUDNA, J. A. & CHARPENTIER, E. 2014. Genome editing. The new frontier of genome engineering with CRISPR-Cas9. *Science*, 346, 1258096.

E

EGHOLM, M., BUCHARDT, O., CHRISTENSEN, L., BEHRENS, C., FREIER, S. M., DRIVER, D. A., BERG, R. H., KIM, S. K., NORDEN, B. & NIELSEN, P. E. 1993. PNA hybridizes to complementary oligonucleotides obeying the Watson-Crick hydrogen-bonding rules. *Nature*, 365, 566-8.

EICHHORN, S. W., GUO, H., MCGEARY, S. E., RODRIGUEZ-MIAS, R. A., SHIN, C., BAEK, D., HSU, S. H., GHOSHAL, K., VILLEN, J. & BARTEL, D. P. 2014. mRNA destabilization is the dominant effect of mammalian microRNAs by the time substantial repression ensues. *Mol Cell*, 56, 104-15.

F

FAN, W. & YOON, K. 2003. In vivo alteration of the keratin 17 gene in hair follicles by oligonucleotide-directed gene targeting. *Exp Dermatol*, 12, 832-42.

FARBER, S., PINKEL, D., SEARS, E. M. & TOCH, R. 1956. Advances in chemotherapy of cancer in man. *Adv Cancer Res*, 4, 1-71.

FARUQI, A. F., SEIDMAN, M. M., SEGAL, D. J., CARROLL, D. & GLAZER, P. M. 1996. Recombination induced by triple-helix-targeted DNA damage in mammalian cells. *Mol Cell Biol*, 16, 6820-8.

FERRARA, L. & KMIEC, E. B. 2004. Camptothecin enhances the frequency of oligonucleotide-directed gene repair in mammalian cells by inducing DNA damage and activating homologous recombination. *Nucleic Acids Res*, 32, 5239-48.

FERRERI, A. J., DELL'ORO, S., CAPELLO, D., PONZONI, M., IUZZOLINO, P., ROSSI, D., PASINI, F., AMBROSETTI, A., ORVIETO, E., FERRARESE, F., ARRIGONI, G., FOPPOLI, M., RENI, M. & GAIDANO, G. 2004. Aberrant methylation in the promoter region of the reduced folate carrier gene is a potential mechanism of resistance to methotrexate in primary central nervous system lymphomas. *Br J Haematol*, 126, 657-64.

FILIPOWICZ, W., JASKIEWICZ, L., KOLB, F. A. & PILLAI, R. S. 2005. Post-transcriptional gene silencing by siRNAs and miRNAs. *Curr Opin Struct Biol*, 15, 331-41.

FOX, J. T. & STOVER, P. J. 2008. Folate-mediated one-carbon metabolism. *Vitam Horm*, 79, 1-44.

FU, Y., FODEN, J. A., KHAYTER, C., MAEDER, M. L., REYON, D., JOUNG, J. K. & SANDER, J. D. 2013. High-frequency off-target mutagenesis induced by CRISPR-Cas nucleases in human cells. *Nat Biotechnol*, 31, 822-6.

G

- GAMPER, H. B., JR., COLE-STRAUSS, A., METZ, R., PAREKH, H., KUMAR, R. & KMIEC, E. B. 2000. A plausible mechanism for gene correction by chimeric oligonucleotides. *Biochemistry*, 39, 5808-16.
- GARLAND, W., FRENZEL, B., KARG, T., WIPKE, T. & KONOPELSKI, J. 2009. Methotrexate adjuvants to reduce toxicity and methods for using the same. Google Patents.
- GIANNELLI, F., GREEN, P. M., HIGH, K. A., LOZIER, J. N., LILLICRAP, D. P., LUDWIG, M., OLEK, K., REITSMA, P. H., GOOSSENS, M., YOSHIOKA, A. & ET AL. 1990. Haemophilia B: database of point mutations and short additions and deletions. *Nucleic Acids Res*, 18, 4053-9.
- GONEN, N. & ASSARAF, Y. G. 2012. Antifolates in cancer therapy: structure, activity and mechanisms of drug resistance. *Drug Resist Updat*, 15, 183-210.
- GONI, J. R., DE LA CRUZ, X. & OROZCO, M. 2004. Triplex-forming oligonucleotide target sequences in the human genome. *Nucleic Acids Res*, 32, 354-60.
- GRISHOK, A., PASQUINELLI, A. E., CONTE, D., LI, N., PARRISH, S., HA, I., BAILLIE, D. L., FIRE, A., RUVKUN, G. & MELLO, C. C. 2001. Genes and mechanisms related to RNA interference regulate expression of the small temporal RNAs that control *C. elegans* developmental timing. *Cell*, 106, 23-34.

H

- HARUTA, M., TOMITA, Y., YUNO, A., MATSUMURA, K., IKEDA, T., TAKAMATSU, K., HAGA, E., KOBA, C., NISHIMURA, Y. & SENJU, S. 2013. TAP-deficient human iPS cell-derived myeloid cell lines as unlimited cell source for dendritic cell-like antigen-presenting cells. *Gene Ther*, 20, 504-13.
- HAVRE, P. A., GUNTHER, E. J., GASPARRO, F. P. & GLAZER, P. M. 1993. Targeted mutagenesis of DNA using triple helix-forming oligonucleotides linked to psoralen. *Proc Natl Acad Sci U S A*, 90, 7879-83.
- HESS, M. T., SCHWITTER, U., PETRETTA, M., GIESE, B. & NAEGELI, H. 1997. Bipartite substrate discrimination by human nucleotide excision repair. *Proc Natl Acad Sci U S A*, 94, 6664-9.
- HOCKEMEYER, D., WANG, H., KIANI, S., LAI, C. S., GAO, Q., CASSADY, J. P., COST, G. J., ZHANG, L., SANTIAGO, Y., MILLER, J. C., ZEITLER, B., CHERONE, J. M., MENG, X., HINKLEY, S. J., REBAR, E. J., GREGORY, P. D., URNOV, F. D. & JAENISCH, R. 2011. Genetic engineering of human pluripotent cells using TALE nucleases. *Nat Biotechnol*, 29, 731-4.
- HOOIJBERG, J. H., PETERS, G. J., ASSARAF, Y. G., KATHMANN, I., PRIEST, D. G., BUNNI, M. A., VEERMAN, A. J., SCHEFFER, G. L., KASPERS, G. J. & JANSEN, G. 2003. The role of multidrug resistance proteins MRP1, MRP2 and MRP3 in cellular folate homeostasis. *Biochem Pharmacol*, 65, 765-71.
- HOUTGRAAF, J. H., VERSMISSEN, J. & VAN DER GIESSEN, W. J. 2006. A concise review of DNA damage checkpoints and repair in mammalian cells. *Cardiovasc Revasc Med*, 7, 165-72.
- HRYNIUK, W. M. & BERTINO, J. R. 1969. Treatment of leukemia with large doses of methotrexate and folinic acid: clinical-biochemical correlates. *J Clin Invest*, 48, 2140-55.

- HU, Y., PAREKH-OLMEDO, H., DRURY, M., SKOGEN, M. & KMIEC, E. B. 2005. Reaction parameters of targeted gene repair in mammalian cells. *Mol Biotechnol*, 29, 197-210.
- HUANG, Y., SHEN, X. J., ZOU, Q., WANG, S. P., TANG, S. M. & ZHANG, G. Z. 2011. Biological functions of microRNAs: a review. *J Physiol Biochem*, 67, 129-39.
- HUMPHREYS, D. T., WESTMAN, B. J., MARTIN, D. I. & PREISS, T. 2005. MicroRNAs control translation initiation by inhibiting eukaryotic initiation factor 4E/cap and poly(A) tail function. *Proc Natl Acad Sci U S A*, 102, 16961-6.
- HUTVAGNER, G., MCLACHLAN, J., PASQUINELLI, A. E., BALINT, E., TUSCHL, T. & ZAMORE, P. D. 2001. A cellular function for the RNA-interference enzyme Dicer in the maturation of the let-7 small temporal RNA. *Science*, 293, 834-8.

I

- IFERGAN, I., MELLER, I., ISSAKOV, J. & ASSARAF, Y. G. 2003. Reduced folate carrier protein expression in osteosarcoma: implications for the prediction of tumor chemosensitivity. *Cancer*, 98, 1958-66.
- IGOUCHEVA, O., ALEXEEV, V., ANNI, H. & RUBIN, E. 2008. Oligonucleotide-mediated gene targeting in human hepatocytes: implications of mismatch repair. *Oligonucleotides*, 18, 111-22.
- IGOUCHEVA, O., ALEXEEV, V. & YOON, K. 2001. Targeted gene correction by small single-stranded oligonucleotides in mammalian cells. *Gene Ther*, 8, 391-9.
- IORIO, M. V. & CROCE, C. M. 2012. microRNA involvement in human cancer. *Carcinogenesis*, 33, 1126-33.

J

- JACKSON, S. P. & BARTEK, J. 2009. The DNA-damage response in human biology and disease. *Nature*, 461, 1071-8.
- JANSEN, G., MAURITZ, R., DRORI, S., SPRECHER, H., KATHMANN, I., BUNNI, M., PRIEST, D. G., NOORDHUIS, P., SCHORNAGEL, J. H., PINEDO, H. M., PETERS, G. J. & ASSARAF, Y. G. 1998. A structurally altered human reduced folate carrier with increased folic acid transport mediates a novel mechanism of antifolate resistance. *J Biol Chem*, 273, 30189-98.
- JINEK, M., CHYLINSKI, K., FONFARA, I., HAUER, M., DOUDNA, J. A. & CHARPENTIER, E. 2012. A programmable dual-RNA-guided DNA endonuclease in adaptive bacterial immunity. *Science*, 337, 816-21.
- JOLIVET, J., COWAN, K. H., CURT, G. A., CLENDENINN, N. J. & CHABNER, B. A. 1983. The pharmacology and clinical use of methotrexate. *N Engl J Med*, 309, 1094-104.

K

- KABACK, M. M. & DESNICK, R. J. 2011. Hexosaminidase A Deficiency. *In*: PAGON, R. A., ADAM, M. P., ARDINGER, H. H., WALLACE, S. E., AMEMIYA, A., BEAN, L. J. H., BIRD, T. D., FONG, C. T., MEFFORD, H. C., SMITH, R. J. H. & STEPHENS, K. (eds.) *GeneReviews(R)*. Seattle (WA).
- KAIHATSU, K., SHAH, R. H., ZHAO, X. & COREY, D. R. 2003. Extending recognition by peptide nucleic acids (PNAs): binding to duplex DNA and inhibition of transcription by tail-clamp PNA-peptide conjugates. *Biochemistry*, 42, 13996-4003.
- KASTRUP, I. B., WORM, J., RALFKIAER, E., HOKLAND, P., GULDBERG, P. & GRONBAEK, K. 2008. Genetic and epigenetic alterations of the reduced folate carrier in untreated diffuse large B-cell lymphoma. *Eur J Haematol*, 80, 61-6.
- KAYALI, R., BURY, F., BALLARD, M. & BERTONI, C. 2010. Site-directed gene repair of the dystrophin gene mediated by PNA-ssODNs. *Hum Mol Genet*, 19, 3266-81.
- KENNER, O., KNEISEL, A., KLINGLER, J., BARTELT, B., SPEIT, G., VOGEL, W. & KAUFMANN, D. 2002. Targeted gene correction of hpert mutations by 45 base single-stranded oligonucleotides. *Biochem Biophys Res Commun*, 299, 787-92.
- KEREM, B., ROMMENS, J. M., BUCHANAN, J. A., MARKIEWICZ, D., COX, T. K., CHAKRAVARTI, A., BUCHWALD, M. & TSUI, L. C. 1989. Identification of the cystic fibrosis gene: genetic analysis. *Science*, 245, 1073-80.
- KIM, H. & KIM, J. S. 2014. A guide to genome engineering with programmable nucleases. *Nat Rev Genet*, 15, 321-34.
- KIM, Y. G., CHA, J. & CHANDRASEGARAN, S. 1996. Hybrid restriction enzymes: zinc finger fusions to Fok I cleavage domain. *Proc Natl Acad Sci U S A*, 93, 1156-60.
- KLINGLER, K. R., ZECH, D. & WIELCKENS, K. 2000. Haemochromatosis: automated detection of the two point mutations in the HFE gene: Cys282Tyr and His63Asp. *Clin Chem Lab Med*, 38, 1225-30.
- KLOOSTERMAN, W. P., WIENHOLDS, E., KETTING, R. F. & PLASTERK, R. H. 2004. Substrate requirements for let-7 function in the developing zebrafish embryo. *Nucleic Acids Res*, 32, 6284-91.
- KOTANI, H. & KMIEC, E. B. 1994. A role for RNA synthesis in homologous pairing events. *Mol Cell Biol*, 14, 6097-106.
- KOW, Y. W., BAO, G., REEVES, J. W., JINKS-ROBERTSON, S. & CROUSE, G. F. 2007. Oligonucleotide transformation of yeast reveals mismatch repair complexes to be differentially active on DNA replication strands. *Proc Natl Acad Sci U S A*, 104, 11352-7.
- KREN, B. T., BANDYOPADHYAY, P. & STEER, C. J. 1998. In vivo site-directed mutagenesis of the factor IX gene by chimeric RNA/DNA oligonucleotides. *Nat Med*, 4, 285-90.
- KREN, B. T., COLE-STRAUSS, A., KMIEC, E. B. & STEER, C. J. 1997. Targeted nucleotide exchange in the alkaline phosphatase gene of HuH-7 cells mediated by a chimeric RNA/DNA oligonucleotide. *Hepatology*, 25, 1462-8.
- KREN, B. T., PARASHAR, B., BANDYOPADHYAY, P., CHOWDHURY, N. R., CHOWDHURY, J. R. & STEER, C. J. 1999. Correction of the UDP-

glucuronosyltransferase gene defect in the gunn rat model of crigler-najjar syndrome type I with a chimeric oligonucleotide. *Proc Natl Acad Sci U S A*, 96, 10349-54.

KREN, B. T., WONG, P. Y. & STEER, C. J. 2003. Short, single-stranded oligonucleotides mediate targeted nucleotide conversion using extracts from isolated liver mitochondria. *DNA Repair (Amst)*, 2, 531-46.

KUNKEL, T. A. 2004. DNA replication fidelity. *J Biol Chem*, 279, 16895-8.

L

LEE, T., WANG, N., HOUEL, S., COUTS, K., OLD, W. & AHN, N. 2015. Dosage and temporal thresholds in microRNA proteomics. *Mol Cell Proteomics*, 14, 289-302.

LEE, Y., AHN, C., HAN, J., CHOI, H., KIM, J., YIM, J., LEE, J., PROVOST, P., RADMARK, O., KIM, S. & KIM, V. N. 2003. The nuclear RNase III Drosha initiates microRNA processing. *Nature*, 425, 415-9.

LEE, Y., KIM, M., HAN, J., YEOM, K. H., LEE, S., BAEK, S. H. & KIM, V. N. 2004. MicroRNA genes are transcribed by RNA polymerase II. *EMBO J*, 23, 4051-60.

LEE, Y. J., CHEN, H. Y., WONG, M. L. & HSU, W. L. 2010. Molecular detection of autosomal-dominant feline polycystic kidney disease by multiplex amplification refractory mutation system polymerase chain reaction. *J Vet Diagn Invest*, 22, 424-8.

LI, H. L., FUJIMOTO, N., SASAKAWA, N., SHIRAI, S., OHKAME, T., SAKUMA, T., TANAKA, M., AMANO, N., WATANABE, A., SAKURAI, H., YAMAMOTO, T., YAMANAKA, S. & HOTTA, A. 2015. Precise correction of the dystrophin gene in duchenne muscular dystrophy patient induced pluripotent stem cells by TALEN and CRISPR-Cas9. *Stem Cell Reports*, 4, 143-54.

LI, T., LIU, B., SPALDING, M. H., WEEKS, D. P. & YANG, B. 2012. High-efficiency TALEN-based gene editing produces disease-resistant rice. *Nat Biotechnol*, 30, 390-2.

LI, Y., JENKINS, C. W., NICHOLS, M. A. & XIONG, Y. 1994. Cell cycle expression and p53 regulation of the cyclin-dependent kinase inhibitor p21. *Oncogene*, 9, 2261-8.

LIANG, P., XU, Y., ZHANG, X., DING, C., HUANG, R., ZHANG, Z., LV, J., XIE, X., CHEN, Y., LI, Y., SUN, Y., BAI, Y., SONGYANG, Z., MA, W., ZHOU, C. & HUANG, J. 2015. CRISPR/Cas9-mediated gene editing in human tripronuclear zygotes. *Protein Cell*, 6, 363-72.

LIANI, E., ROTHEM, L., BUNNI, M. A., SMITH, C. A., JANSEN, G. & ASSARAF, Y. G. 2003. Loss of folylpoly-gamma-glutamate synthetase activity is a dominant mechanism of resistance to polyglutamylation-dependent novel antifolates in multiple human leukemia sublines. *Int J Cancer*, 103, 587-99.

LIAO, H. K., GU, Y., DIAZ, A., MARLETT, J., TAKAHASHI, Y., LI, M., SUZUKI, K., XU, R., HISHIDA, T., CHANG, C. J., ESTEBAN, C. R., YOUNG, J. & IZPISUA BELMONTE, J. C. 2015. Use of the CRISPR/Cas9 system as an intracellular defense against HIV-1 infection in human cells. *Nat Commun*, 6, 6413.

- LIN, F. L., SPERLE, K. & STERNBERG, N. 1990. Repair of double-stranded DNA breaks by homologous DNA fragments during transfer of DNA into mouse L cells. *Mol Cell Biol*, 10, 113-9.
- LIN, S. R., YANG, H. C., KUO, Y. T., LIU, C. J., YANG, T. Y., SUNG, K. C., LIN, Y. Y., WANG, H. Y., WANG, C. C., SHEN, Y. C., WU, F. Y., KAO, J. H., CHEN, D. S. & CHEN, P. J. 2014. The CRISPR/Cas9 System Facilitates Clearance of the Intrahepatic HBV Templates In Vivo. *Mol Ther Nucleic Acids*, 3, e186.
- LIPS, J. & KAINA, B. 2001. DNA double-strand breaks trigger apoptosis in p53-deficient fibroblasts. *Carcinogenesis*, 22, 579-85.
- LIU, H., AGARWAL, S., KMIIEC, E. & DAVIS, B. R. 2002a. Targeted beta-globin gene conversion in human hematopoietic CD34(+) and Lin(-)CD38(-) cells. *Gene Ther*, 9, 118-26.
- LIU, L., CHENG, S., VAN BRABANT, A. J. & KMIIEC, E. B. 2002b. Rad51p and Rad54p, but not Rad52p, elevate gene repair in *Saccharomyces cerevisiae* directed by modified single-stranded oligonucleotide vectors. *Nucleic Acids Res*, 30, 2742-50.
- LODISH, H., BERK, A., MATSUDAIRA, P., KAISER, C., KRIEGER, M. A., SCOTT, M., ZIPURSKY, S. & DARNELL, J. 2004. *Molecular Biology of the Cell*.
- LOHSE, J., DAHL, O. & NIELSEN, P. E. 1999. Double duplex invasion by peptide nucleic acid: a general principle for sequence-specific targeting of double-stranded DNA. *Proc Natl Acad Sci U S A*, 96, 11804-8.
- LONG, C., MCANALLY, J. R., SHELTON, J. M., MIREAULT, A. A., BASSEL-DUBY, R. & OLSON, E. N. 2014. Prevention of muscular dystrophy in mice by CRISPR/Cas9-mediated editing of germline DNA. *Science*, 345, 1184-8.
- LONKAR, P., KIM, K. H., KUAN, J. Y., CHIN, J. Y., ROGERS, F. A., KNAUERT, M. P., KOLE, R., NIELSEN, P. E. & GLAZER, P. M. 2009. Targeted correction of a thalassemia-associated beta-globin mutation induced by pseudo-complementary peptide nucleic acids. *Nucleic Acids Res*, 37, 3635-44.
- LU, I. L., LIN, C. Y., LIN, S. B., CHEN, S. T., YEH, L. Y., YANG, F. Y. & AU, L. C. 2003a. Correction/mutation of acid alpha-D-glucosidase gene by modified single-stranded oligonucleotides: in vitro and in vivo studies. *Gene Ther*, 10, 1910-6.
- LU, Q. L., MANN, C. J., LOU, F., BOU-GHARIOS, G., MORRIS, G. E., XUE, S. A., FLETCHER, S., PARTRIDGE, T. A. & WILTON, S. D. 2003b. Functional amounts of dystrophin produced by skipping the mutated exon in the mdx dystrophic mouse. *Nat Med*, 9, 1009-14.
- LUBAMBA, B., DHOOGHE, B., NOEL, S. & LEAL, T. 2012. Cystic fibrosis: insight into CFTR pathophysiology and pharmacotherapy. *Clin Biochem*, 45, 1132-44.
- LUCH, A. 2005. Nature and nurture - lessons from chemical carcinogenesis. *Nat Rev Cancer*, 5, 113-25.
- LUNDIN, K. E., GISSBERG, O. & SMITH, C. I. 2015. Oligonucleotide Therapies: The Past and the Present. *Hum Gene Ther*, 26, 475-85.
- LYTLE, J. R., YARIO, T. A. & STEITZ, J. A. 2007. Target mRNAs are repressed as efficiently by microRNA-binding sites in the 5' UTR as in the 3' UTR. *Proc Natl Acad Sci U S A*, 104, 9667-72.

M

- MA, J., DONG, C. & JI, C. 2010. MicroRNA and drug resistance. *Cancer Gene Ther*, 17, 523-31.
- MAGUIRE, K. K. & KMIEC, E. B. 2007. Multiple roles for MSH2 in the repair of a deletion mutation directed by modified single-stranded oligonucleotides. *Gene*, 386, 107-14.
- MAJUMDAR, A., KHORLIN, A., DYATKINA, N., LIN, F. L., POWELL, J., LIU, J., FEI, Z., KHRIPINE, Y., WATANABE, K. A., GEORGE, J., GLAZER, P. M. & SEIDMAN, M. M. 1998. Targeted gene knockout mediated by triple helix forming oligonucleotides. *Nat Genet*, 20, 212-4.
- MAK, A. N., BRADLEY, P., CERNADAS, R. A., BOGDANOVA, A. J. & STODDARD, B. L. 2012. The crystal structure of TAL effector PthXo1 bound to its DNA target. *Science*, 335, 716-9.
- MALI, P., YANG, L., ESVELT, K. M., AACH, J., GUELL, M., DICARLO, J. E., NORVILLE, J. E. & CHURCH, G. M. 2013. RNA-guided human genome engineering via Cas9. *Science*, 339, 823-6.
- MANDAL, P. K., FERREIRA, L. M., COLLINS, R., MEISSNER, T. B., BOUTWELL, C. L., FRIESEN, M., VRBANAC, V., GARRISON, B. S., STORTCHEVOI, A., BRYDER, D., MUSUNURU, K., BRAND, H., TAGER, A. M., ALLEN, T. M., TALKOWSKI, M. E., ROSSI, D. J. & COWAN, C. A. 2014. Efficient ablation of genes in human hematopoietic stem and effector cells using CRISPR/Cas9. *Cell Stem Cell*, 15, 643-52.
- MANZANO, A., MOHRI, Z., SPERBER, G., OGRIS, M., GRAHAM, I., DICKSON, G. & OWEN, J. S. 2003. Failure to generate atheroprotective apolipoprotein AI phenotypes using synthetic RNA/DNA oligonucleotides (chimeraplasts). *J Gene Med*, 5, 795-802.
- MAQUAT, L. E. 2004. Nonsense-mediated mRNA decay: splicing, translation and mRNP dynamics. *Nat Rev Mol Cell Biol*, 5, 89-99.
- MARGISON, G. P. & SANTIBANEZ-KOREF, M. F. 2002. O6-alkylguanine-DNA alkyltransferase: role in carcinogenesis and chemotherapy. *Bioessays*, 24, 255-66.
- MARTINHO, R. G., LINDSAY, H. D., FLAGGS, G., DEMAGGIO, A. J., HOEKSTRA, M. F., CARR, A. M. & BENTLEY, N. J. 1998. Analysis of Rad3 and Chk1 protein kinases defines different checkpoint responses. *EMBO J*, 17, 7239-49.
- MATHONNET, G., FABIAN, M. R., SVITKIN, Y. V., PARSYAN, A., HUCK, L., MURATA, T., BIFFO, S., MERRICK, W. C., DARZYNKIEWICZ, E., PILLAI, R. S., FILIPOWICZ, W., DUCHAINE, T. F. & SONENBERG, N. 2007. MicroRNA inhibition of translation initiation in vitro by targeting the cap-binding complex eIF4F. *Science*, 317, 1764-7.
- MCLACHLAN, J., FERNANDEZ, S., HELLEDAY, T. & BRYANT, H. E. 2009. Specific targeted gene repair using single-stranded DNA oligonucleotides at an endogenous locus in mammalian cells uses homologous recombination. *DNA Repair (Amst)*, 8, 1424-33.
- MEMISOGLU, A. & SAMSON, L. 2000. Base excision repair in yeast and mammals. *Mutat Res*, 451, 39-51.
- MENCIA, N., SELGA, E., NOE, V. & CIUDAD, C. J. 2011. Underexpression of miR-224 in methotrexate resistant human colon cancer cells. *Biochem Pharmacol*, 82, 1572-82.

- MENCIA, N., SELGA, E., RICO, I., DE ALMAGRO, M. C., VILLALOBOS, X., RAMIREZ, S., ADAN, J., HERNANDEZ, J. L., NOE, V. & CIUDAD, C. J. 2010. Overexpression of S100A4 in human cancer cell lines resistant to methotrexate. *BMC Cancer*, 10, 250.
- MERGNY, J. L., LI, J., LACROIX, L., AMRANE, S. & CHAIRES, J. B. 2005. Thermal difference spectra: a specific signature for nucleic acid structures. *Nucleic Acids Res*, 33, e138.
- MIGLIORE, C. & GIORDANO, S. 2013. Resistance to targeted therapies: a role for microRNAs? *Trends Mol Med*, 19, 633-42.
- MILLER, J. C., HOLMES, M. C., WANG, J., GUSCHIN, D. Y., LEE, Y. L., RUPNIEWSKI, I., BEAUSEJOUR, C. M., WAITE, A. J., WANG, N. S., KIM, K. A., GREGORY, P. D., PABO, C. O. & REBAR, E. J. 2007. An improved zinc-finger nuclease architecture for highly specific genome editing. *Nat Biotechnol*, 25, 778-85.
- MISHRA, P. J., HUMENIUK, R., MISHRA, P. J., LONGO-SORBELLO, G. S., BANERJEE, D. & BERTINO, J. R. 2007. A miR-24 microRNA binding-site polymorphism in dihydrofolate reductase gene leads to methotrexate resistance. *Proc Natl Acad Sci U S A*, 104, 13513-8.
- MISHRA, P. J., MISHRA, P. J., BANERJEE, D. & BERTINO, J. R. 2008. MiRSNPs or MiR-polymorphisms, new players in microRNA mediated regulation of the cell: Introducing microRNA pharmacogenomics. *Cell Cycle*, 7, 853-8.
- MISHRA, P. J., SONG, B., MISHRA, P. J., WANG, Y., HUMENIUK, R., BANERJEE, D., MERLINO, G., JU, J. & BERTINO, J. R. 2009. MiR-24 tumor suppressor activity is regulated independent of p53 and through a target site polymorphism. *PLoS One*, 4, e8445.
- MIYAOKA, Y., CHAN, A. H., JUDGE, L. M., YOO, J., HUANG, M., NGUYEN, T. D., LIZARRAGA, P. P., SO, P. L. & CONKLIN, B. R. 2014. Isolation of single-base genome-edited human iPS cells without antibiotic selection. *Nat Methods*, 11, 291-3.
- MIYASHITA, T. & REED, J. C. 1995. Tumor suppressor p53 is a direct transcriptional activator of the human bax gene. *Cell*, 80, 293-9.
- MOERSCHHELL, R. P., TSUNASAWA, S. & SHERMAN, F. 1988. Transformation of yeast with synthetic oligonucleotides. *Proc Natl Acad Sci U S A*, 85, 524-8.
- MOSCOU, M. J. & BOGDANOVA, A. J. 2009. A simple cipher governs DNA recognition by TAL effectors. *Science*, 326, 1501.
- MOSKOWITZ, S. M., CHMIEL, J. F., STERNEN, D. L., CHENG, E. & CUTTING, G. R. 2008. CFTR-Related Disorders. In: PAGON, R. A., ADAM, M. P., ARDINGER, H. H., WALLACE, S. E., AMEMIYA, A., BEAN, L. J. H., BIRD, T. D., FONG, C. T., MEFFORD, H. C., SMITH, R. J. H. & STEPHENS, K. (eds.) *GeneReviews(R)*. Seattle (WA).
- MUSSOLINO, C., MORBITZER, R., LUTGE, F., DANNEMANN, N., LAHAYE, T. & CATHOMEN, T. 2011. A novel TALE nuclease scaffold enables high genome editing activity in combination with low toxicity. *Nucleic Acids Res*, 39, 9283-93.

N

- NESHER, G., MOORE, T. L. & DORNER, R. W. 1991. In vitro effects of methotrexate on peripheral blood monocytes: modulation by folinic acid and S-adenosylmethionine. *Ann Rheum Dis*, 50, 637-41.
- NESHER, G., OSBORN, T. G. & MOORE, T. L. 1996. In vitro effects of methotrexate on polyamine levels in lymphocytes from rheumatoid arthritis patients. *Clin Exp Rheumatol*, 14, 395-9.
- NICKERSON, H. D. & COLLEDGE, W. H. 2003. A comparison of gene repair strategies in cell culture using a lacZ reporter system. *Gene Ther*, 10, 1584-91.
- NIELSEN, P. E. 2004. PNA Technology. *Mol Biotechnol*, 26, 233-48.
- NIELSEN, P. E., EGHOLM, M., BERG, R. H. & BUCHARDT, O. 1991. Sequence-selective recognition of DNA by strand displacement with a thymine-substituted polyamide. *Science*, 254, 1497-500.
- NIK-AHD, F. & BERTONI, C. 2014. Ex vivo gene editing of the dystrophin gene in muscle stem cells mediated by peptide nucleic acid single stranded oligodeoxynucleotides induces stable expression of dystrophin in a mouse model for Duchenne muscular dystrophy. *Stem Cells*, 32, 1817-30.
- NOE, V., ALEMANY, C., CHASIN, L. A. & CIUDAD, C. J. 1998. Retinoblastoma protein associates with SP1 and activates the hamster dihydrofolate reductase promoter. *Oncogene*, 16, 1931-8.
- NOE, V. & CIUDAD, C. J. 1995. Protein kinase C inhibitors reduce phorbol ester-induced resistance to methotrexate in Chinese hamster ovary cells. *Biochem Pharmacol*, 50, 337-46.
- NOE, V., CIUDAD, C. J. & CHASIN, L. A. 1999. Effect of differential polyadenylation and cell growth phase on dihydrofolate reductase mRNA stability. *J Biol Chem*, 274, 27807-14.
- NOE, V., MACKENZIE, S. & CIUDAD, C. J. 2003. An intron is required for dihydrofolate reductase protein stability. *J Biol Chem*, 278, 38292-300.
- NOTTROT, S., SIMARD, M. J. & RICHTER, J. D. 2006. Human let-7a miRNA blocks protein production on actively translating polyribosomes. *Nat Struct Mol Biol*, 13, 1108-14.

O

- OCHIAI, H. 2015. Single-Base Pair Genome Editing in Human Cells by Using Site-Specific Endonucleases. *Int J Mol Sci*, 16, 21128-37.
- OCHIAI, H., MIYAMOTO, T., KANAI, A., HOSOBABA, K., SAKUMA, T., KUDO, Y., ASAMI, K., OGAWA, A., WATANABE, A., KAJII, T., YAMAMOTO, T. & MATSUURA, S. 2014. TALEN-mediated single-base-pair editing identification of an intergenic mutation upstream of BUB1B as causative of PCS (MVA) syndrome. *Proc Natl Acad Sci U S A*, 111, 1461-6.
- OLSEN, E. A. 1991. The pharmacology of methotrexate. *J Am Acad Dermatol*, 25, 306-18.
- OLSEN, P. A., RANDOL, M. & KRAUSS, S. 2005. Implications of cell cycle progression on functional sequence correction by short single-stranded DNA oligonucleotides. *Gene Ther*, 12, 546-51.

OUSTEROUT, D. G., KABADI, A. M., THAKORE, P. I., MAJOROS, W. H., REDDY, T. E. & GERSBACH, C. A. 2015. Multiplex CRISPR/Cas9-based genome editing for correction of dystrophin mutations that cause Duchenne muscular dystrophy. *Nat Commun*, 6, 6244.

P

- PAPADOPOULOS, N., NICOLAIDES, N. C., WEI, Y. F., RUBEN, S. M., CARTER, K. C., ROSEN, C. A., HASELTINE, W. A., FLEISCHMANN, R. D., FRASER, C. M., ADAMS, M. D. & ET AL. 1994. Mutation of a mutL homolog in hereditary colon cancer. *Science*, 263, 1625-9.
- PATTANAYAK, V., LIN, S., GUILINGER, J. P., MA, E., DOUDNA, J. A. & LIU, D. R. 2013. High-throughput profiling of off-target DNA cleavage reveals RNA-programmed Cas9 nuclease specificity. *Nat Biotechnol*, 31, 839-43.
- PENUELAS, S., NOE, V. & CIUDAD, C. J. 2005a. Modulation of IMPDH2, survivin, topoisomerase I and vimentin increases sensitivity to methotrexate in HT29 human colon cancer cells. *FEBS J*, 272, 696-710.
- PENUELAS, S., NOE, V., MORALES, R. & CIUDAD, C. J. 2005b. Sensitization of human erythroleukemia K562 cells resistant to methotrexate by inhibiting IMPDH. *Med Sci Monit*, 11, BR6-12.
- PEREZ, E. E., WANG, J., MILLER, J. C., JOUVENOT, Y., KIM, K. A., LIU, O., WANG, N., LEE, G., BARTSEVICH, V. V., LEE, Y. L., GUSCHIN, D. Y., RUPNIEWSKI, I., WAITE, A. J., CARPENITO, C., CARROLL, R. G., ORANGE, J. S., URNOV, F. D., REBAR, E. J., ANDO, D., GREGORY, P. D., RILEY, J. L., HOLMES, M. C. & JUNE, C. H. 2008. Establishment of HIV-1 resistance in CD4+ T cells by genome editing using zinc-finger nucleases. *Nat Biotechnol*, 26, 808-16.
- PETUKHOVA, G., STRATTON, S. & SUNG, P. 1998. Catalysis of homologous DNA pairing by yeast Rad51 and Rad54 proteins. *Nature*, 393, 91-4.
- PIERCE, E. A., LIU, Q., IGOUCHEVA, O., OMARRUDIN, R., MA, H., DIAMOND, S. L. & YOON, K. 2003. Oligonucleotide-directed single-base DNA alterations in mouse embryonic stem cells. *Gene Ther*, 10, 24-33.
- PILLAI, R. S., BHATTACHARYYA, S. N., ARTUS, C. G., ZOLLER, T., COUGOT, N., BASYUK, E., BERTRAND, E. & FILIPOWICZ, W. 2005. Inhibition of translational initiation by Let-7 MicroRNA in human cells. *Science*, 309, 1573-6.
- PORTEUS, M. H. & CARROLL, D. 2005. Gene targeting using zinc finger nucleases. *Nat Biotechnol*, 23, 967-73.

Q

QUINTON, P. M. 1990. Cystic fibrosis: a disease in electrolyte transport. *FASEB J*, 4, 2709-17.

R

- RAHMAN, N. & STRATTON, M. R. 1998. The genetics of breast cancer susceptibility. *Annu Rev Genet*, 32, 95-121.
- RANDO, T. A., DISATNIK, M. H. & ZHOU, L. Z. 2000. Rescue of dystrophin expression in mdx mouse muscle by RNA/DNA oligonucleotides. *Proc Natl Acad Sci U S A*, 97, 5363-8.
- RHEE, M. S., WANG, Y., NAIR, M. G. & GALIVAN, J. 1993. Acquisition of resistance to antifolates caused by enhanced gamma-glutamyl hydrolase activity. *Cancer Res*, 53, 2227-30.
- RODRIGUEZ, L., VILLALOBOS, X., DAKHEL, S., PADILLA, L., HERVAS, R., HERNANDEZ, J. L., CIUDAD, C. J. & NOE, V. 2013. Polypurine reverse Hoogsteen hairpins as a gene therapy tool against survivin in human prostate cancer PC3 cells in vitro and in vivo. *Biochem Pharmacol*, 86, 1541-54.
- RODRIGUEZ, L., VILLALOBOS, X., SOLE, A., LLIBEROS, C., CIUDAD, C. J. & NOE, V. 2015. Improved design of PPRHs for gene silencing. *Mol Pharm*, 12, 867-77.
- ROGERS, F. A., VASQUEZ, K. M., EGHOLM, M. & GLAZER, P. M. 2002. Site-directed recombination via bifunctional PNA-DNA conjugates. *Proc Natl Acad Sci U S A*, 99, 16695-700.
- ROTHERM, L., STARK, M. & ASSARAF, Y. G. 2004. Impaired CREB-1 phosphorylation in antifolate-resistant cell lines with down-regulation of the reduced folate carrier gene. *Mol Pharmacol*, 66, 1536-43.
- ROTHKAMM, K., KRUGER, I., THOMPSON, L. H. & LOBRICH, M. 2003. Pathways of DNA double-strand break repair during the mammalian cell cycle. *Mol Cell Biol*, 23, 5706-15.
- ROTS, M. G., WILLEY, J. C., JANSEN, G., VAN ZANTWIJK, C. H., NOORDHUIS, P., DEMUTH, J. P., KUIPER, E., VEERMAN, A. J., PIETERS, R. & PETERS, G. J. 2000. mRNA expression levels of methotrexate resistance-related proteins in childhood leukemia as determined by a standardized competitive template-based RT-PCR method. *Leukemia*, 14, 2166-75.
- ROY, K., EGAN, M. G., SIRLIN, S. & SIROTNAK, F. M. 1997. Posttranscriptionally mediated decreases in folylpolyglutamate synthetase gene expression in some folate analogue-resistant variants of the L1210 cell. Evidence for an altered cognate mRNA in the variants affecting the rate of de novo synthesis of the enzyme. *J Biol Chem*, 272, 6903-8.
- ROY, K., TOLNER, B., CHIAO, J. H. & SIROTNAK, F. M. 1998. A single amino acid difference within the folate transporter encoded by the murine RFC-1 gene selectively alters its interaction with folate analogues. Implications for intrinsic antifolate resistance and directional orientation of the transporter within the plasma membrane of tumor cells. *J Biol Chem*, 273, 2526-31.

S

- SAINTIGNY, Y., DELACOTE, F., VARES, G., PETITOT, F., LAMBERT, S., AVERBECK, D. & LOPEZ, B. S. 2001. Characterization of homologous recombination induced by replication inhibition in mammalian cells. *EMBO J*, 20, 3861-70.

- SAKURABA, H., OSHIMA, A., FUKUHARA, Y., SHIMMOTO, M., NAGAO, Y., BISHOP, D. F., DESNICK, R. J. & SUZUKI, Y. 1990. Identification of point mutations in the alpha-galactosidase A gene in classical and atypical hemizygotes with Fabry disease. *Am J Hum Genet*, 47, 784-9.
- SCOTT, S. A., EDELMANN, L., LIU, L., LUO, M., DESNICK, R. J. & KORNREICH, R. 2010. Experience with carrier screening and prenatal diagnosis for 16 Ashkenazi Jewish genetic diseases. *Hum Mutat*, 31, 1240-50.
- SEBASTIANO, V., MAEDER, M. L., ANGSTMAN, J. F., HADDAD, B., KHAYTER, C., YEO, D. T., GOODWIN, M. J., HAWKINS, J. S., RAMIREZ, C. L., BATISTA, L. F., ARTANDI, S. E., WERNIG, M. & JOUNG, J. K. 2011. In situ genetic correction of the sickle cell anemia mutation in human induced pluripotent stem cells using engineered zinc finger nucleases. *Stem Cells*, 29, 1717-26.
- SELGA, E., MORALES, C., NOE, V., PEINADO, M. A. & CIUDAD, C. J. 2008a. Role of caveolin 1, E-cadherin, Enolase 2 and PKCalpha on resistance to methotrexate in human HT29 colon cancer cells. *BMC Med Genomics*, 1, 35.
- SELGA, E., NOE, V. & CIUDAD, C. J. 2008b. Transcriptional regulation of aldo-keto reductase 1C1 in HT29 human colon cancer cells resistant to methotrexate: role in the cell cycle and apoptosis. *Biochem Pharmacol*, 75, 414-26.
- SELGA, E., OLEAGA, C., RAMIREZ, S., DE ALMAGRO, M. C., NOE, V. & CIUDAD, C. J. 2009. Networking of differentially expressed genes in human cancer cells resistant to methotrexate. *Genome Med*, 1, 83.
- SOLDNER, F., LAGANIERE, J., CHENG, A. W., HOCKEMEYER, D., GAO, Q., ALAGAPPAN, R., KHURANA, V., GOLBE, L. I., MYERS, R. H., LINDQUIST, S., ZHANG, L., GUSCHIN, D., FONG, L. K., VU, B. J., MENG, X., URNOV, F. D., REBAR, E. J., GREGORY, P. D., ZHANG, H. S. & JAENISCH, R. 2011. Generation of isogenic pluripotent stem cells differing exclusively at two early onset Parkinson point mutations. *Cell*, 146, 318-31.
- SOLE, A., VILLALOBOS, X., CIUDAD, C. J. & NOE, V. 2014. Repair of single-point mutations by polypurine reverse Hoogsteen hairpins. *Hum Gene Ther Methods*, 25, 288-302.
- SONG, B., WANG, Y., TITMUS, M. A., BOTCHKINA, G., FORMENTINI, A., KORNMANN, M. & JU, J. 2010. Molecular mechanism of chemoresistance by miR-215 in osteosarcoma and colon cancer cells. *Mol Cancer*, 9, 96.
- SONG, B., WANG, Y., XI, Y., KUDO, K., BRUHEIM, S., BOTCHKINA, G. I., GAVIN, E., WAN, Y., FORMENTINI, A., KORNMANN, M., FODSTAD, O. & JU, J. 2009. Mechanism of chemoresistance mediated by miR-140 in human osteosarcoma and colon cancer cells. *Oncogene*, 28, 4065-74.
- SONODA, E., TAKATA, M., YAMASHITA, Y. M., MORRISON, C. & TAKEDA, S. 2001. Homologous DNA recombination in vertebrate cells. *Proc Natl Acad Sci U S A*, 98, 8388-94.
- SONTHEIMER, E. J. 2005. Assembly and function of RNA silencing complexes. *Nat Rev Mol Cell Biol*, 6, 127-38.
- SRIMATKANDADA, S., SCHWEITZER, B. I., MOROSON, B. A., DUBE, S. & BERTINO, J. R. 1989. Amplification of a polymorphic dihydrofolate reductase gene expressing an enzyme with decreased binding to methotrexate in a human colon carcinoma cell line, HCT-8R4, resistant to this drug. *J Biol Chem*, 264, 3524-8.

- STARK, M. & ASSARAF, Y. G. 2006. Loss of Sp1 function via inhibitory phosphorylation in antifolate-resistant human leukemia cells with down-regulation of the reduced folate carrier. *Blood*, 107, 708-15.
- STORICI, F., SNIPE, J. R., CHAN, G. K., GORDENIN, D. A. & RESNICK, M. A. 2006. Conservative repair of a chromosomal double-strand break by single-strand DNA through two steps of annealing. *Mol Cell Biol*, 26, 7645-57.
- SUN, J., HE, Z. G., CHENG, G., WANG, S. J., HAO, X. H. & ZOU, M. J. 2004. Multidrug resistance P-glycoprotein: crucial significance in drug disposition and interaction. *Med Sci Monit*, 10, RA5-14.
- SUN, N. & ZHAO, H. 2014. Seamless correction of the sickle cell disease mutation of the HBB gene in human induced pluripotent stem cells using TALENs. *Biotechnol Bioeng*, 111, 1048-53.
- SYMINGTON, L. S. 2005. Focus on recombinational DNA repair. *EMBO Rep*, 6, 512-7.
- SZCZEPEK, M., BRONDANI, V., BUCHEL, J., SERRANO, L., SEGAL, D. J. & CATHOMEN, T. 2007. Structure-based redesign of the dimerization interface reduces the toxicity of zinc-finger nucleases. *Nat Biotechnol*, 25, 786-93.

T

- TAGALAKIS, A. D., GRAHAM, I. R., RIDDELL, D. R., DICKSON, J. G. & OWEN, J. S. 2001. Gene correction of the apolipoprotein (Apo) E2 phenotype to wild-type ApoE3 by in situ chimeraplasty. *J Biol Chem*, 276, 13226-30.
- TAGALAKIS, V., KAHN, S. R., LIBMAN, M. & BLOSTEIN, M. 2002. The epidemiology of peripheral vein infusion thrombophlebitis: a critical review. *Am J Med*, 113, 146-51.
- TAUBES, G. 2002. Gene therapy. The strange case of chimeraplasty. *Science*, 298, 2116-20.
- TIBBETTS, R. S., BRUMBAUGH, K. M., WILLIAMS, J. M., SARKARIA, J. N., CLIBY, W. A., SHIEH, S. Y., TAYA, Y., PRIVES, C. & ABRAHAM, R. T. 1999. A role for ATR in the DNA damage-induced phosphorylation of p53. *Genes Dev*, 13, 152-7.

U

- URLAUB, G., KAS, E., CAROTHERS, A. M. & CHASIN, L. A. 1983. Deletion of the diploid dihydrofolate reductase locus from cultured mammalian cells. *Cell*, 33, 405-12.
- URLAUB, G., MITCHELL, P. J., CIUDAD, C. J. & CHASIN, L. A. 1989. Nonsense mutations in the dihydrofolate reductase gene affect RNA processing. *Mol Cell Biol*, 9, 2868-80.
- URLAUB, G., MITCHELL, P. J., KAS, E., CHASIN, L. A., FUNANAGE, V. L., MYODA, T. T. & HAMLIN, J. 1986. Effect of gamma rays at the dihydrofolate reductase locus: deletions and inversions. *Somat Cell Mol Genet*, 12, 555-66.
- URNOV, F. D., MILLER, J. C., LEE, Y. L., BEAUSEJOUR, C. M., ROCK, J. M., AUGUSTUS, S., JAMIESON, A. C., PORTEUS, M. H., GREGORY, P. D. & HOLMES, M. C. 2005. Highly efficient endogenous human gene correction using designed zinc-finger nucleases. *Nature*, 435, 646-51.

V

- VAN KOMEN, S., PETUKHOVA, G., SIGURDSSON, S., STRATTON, S. & SUNG, P. 2000. Superhelicity-driven homologous DNA pairing by yeast recombination factors Rad51 and Rad54. *Mol Cell*, 6, 563-72.
- VASQUEZ, K. M., NARAYANAN, L. & GLAZER, P. M. 2000. Specific mutations induced by triplex-forming oligonucleotides in mice. *Science*, 290, 530-3.
- VASQUEZ, K. M., WANG, G., HAVRE, P. A. & GLAZER, P. M. 1999. Chromosomal mutations induced by triplex-forming oligonucleotides in mammalian cells. *Nucleic Acids Res*, 27, 1176-81.
- VASUDEVAN, S., TONG, Y. & STEITZ, J. A. 2007. Switching from repression to activation: microRNAs can up-regulate translation. *Science*, 318, 1931-4.
- VERKADE, H. M., BUGG, S. J., LINDSAY, H. D., CARR, A. M. & O'CONNELL, M. J. 1999. Rad18 is required for DNA repair and checkpoint responses in fission yeast. *Mol Biol Cell*, 10, 2905-18.
- VILLALOBOS, X., RODRIGUEZ, L., PREVOT, J., OLEAGA, C., CIUDAD, C. J. & NOE, V. 2014. Stability and immunogenicity properties of the gene-silencing polypurine reverse Hoogsteen hairpins. *Mol Pharm*, 11, 254-64.
- VILLALOBOS, X., RODRIGUEZ, L., SOLE, A., LLIBEROS, C., MENCIA, N., CIUDAD, C. J. & NOE, V. 2015. Effect of Polypurine Reverse Hoogsteen Hairpins on Relevant Cancer Target Genes in Different Human Cell Lines. *Nucleic Acid Ther*, 25, 198-208.
- VOIT, R. A., MCMAHON, M. A., SAWYER, S. L. & PORTEUS, M. H. 2013. Generation of an HIV resistant T-cell line by targeted "stacking" of restriction factors. *Mol Ther*, 21, 786-95.

W

- WANG, G. & GLAZER, P. M. 1995. Altered repair of targeted psoralen photoadducts in the context of an oligonucleotide-mediated triple helix. *J Biol Chem*, 270, 22595-601.
- WANG, G., SEIDMAN, M. M. & GLAZER, P. M. 1996. Mutagenesis in mammalian cells induced by triple helix formation and transcription-coupled repair. *Science*, 271, 802-5.
- WANG, Y., ZHANG, W. Y., HU, S., LAN, F., LEE, A. S., HUBER, B., LISOWSKI, L., LIANG, P., HUANG, M., DE ALMEIDA, P. E., WON, J. H., SUN, N., ROBBINS, R. C., KAY, M. A., URNOV, F. D. & WU, J. C. 2012. Genome editing of human embryonic stem cells and induced pluripotent stem cells with zinc finger nucleases for cellular imaging. *Circ Res*, 111, 1494-503.
- WEISS, I. M. & LIEBHABER, S. A. 1994. Erythroid cell-specific determinants of alpha-globin mRNA stability. *Mol Cell Biol*, 14, 8123-32.
- WEITZ, C. J., MIYAKE, Y., SHINZATO, K., MONTAG, E., ZRENNER, E., WENT, L. N. & NATHANS, J. 1992. Human tritanopia associated with two amino acid substitutions in the blue-sensitive opsin. *Am J Hum Genet*, 50, 498-507.
- WETTERGREN, Y., ODIN, E., NILSSON, S., WILLEN, R., CARLSSON, G. & GUSTAVSSON, B. 2005. Low expression of reduced folate carrier-1 and folylpolyglutamate synthase correlates with lack of a deleted in colorectal

- carcinoma mRNA splice variant in normal-appearing mucosa of colorectal carcinoma patients. *Cancer Detect Prev*, 29, 348-55.
- WIEDENHEFT, B., STERNBERG, S. H. & DOUDNA, J. A. 2012. RNA-guided genetic silencing systems in bacteria and archaea. *Nature*, 482, 331-8.
- WIGLER, M., PELLICER, A., SILVERSTEIN, S., AXEL, R., URLAUB, G. & CHASIN, L. 1979. DNA-mediated transfer of the adenine phosphoribosyltransferase locus into mammalian cells. *Proc Natl Acad Sci U S A*, 76, 1373-6.
- WINTER, J., JUNG, S., KELLER, S., GREGORY, R. I. & DIEDERICHS, S. 2009. Many roads to maturity: microRNA biogenesis pathways and their regulation. *Nat Cell Biol*, 11, 228-34.
- WOOD, A. J., LO, T. W., ZEITLER, B., PICKLE, C. S., RALSTON, E. J., LEE, A. H., AMORA, R., MILLER, J. C., LEUNG, E., MENG, X., ZHANG, L., REBAR, E. J., GREGORY, P. D., URNOV, F. D. & MEYER, B. J. 2011. Targeted genome editing across species using ZFNs and TALENs. *Science*, 333, 307.
- WORM, J., KIRKIN, A. F., DZHANDZHUGAZYAN, K. N. & GULDBERG, P. 2001. Methylation-dependent silencing of the reduced folate carrier gene in inherently methotrexate-resistant human breast cancer cells. *J Biol Chem*, 276, 39990-40000.
- WU, Y., LIANG, D., WANG, Y., BAI, M., TANG, W., BAO, S., YAN, Z., LI, D. & LI, J. 2013. Correction of a genetic disease in mouse via use of CRISPR-Cas9. *Cell Stem Cell*, 13, 659-62.
- WYMAN, C. & KANAAR, R. 2006. DNA double-strand break repair: all's well that ends well. *Annu Rev Genet*, 40, 363-83.

X

- XIANG, Y., COLE-STRAUSS, A., YOON, K., GRYN, J. & KMIEC, E. B. 1997. Targeted gene conversion in a mammalian CD34⁺-enriched cell population using a chimeric RNA/DNA oligonucleotide. *J Mol Med (Berl)*, 75, 829-35.
- XIE, F., YE, L., CHANG, J. C., BEYER, A. I., WANG, J., MUENCH, M. O. & KAN, Y. W. 2014. Seamless gene correction of beta-thalassemia mutations in patient-specific iPSCs using CRISPR/Cas9 and piggyBac. *Genome Res*, 24, 1526-33.

Y

- YAMAMOTO, T., MOERSCHELL, R. P., WAKEM, L. P., KOMAR-PANICUCCI, S. & SHERMAN, F. 1992. Strand-specificity in the transformation of yeast with synthetic oligonucleotides. *Genetics*, 131, 811-9.
- YANG, L., GUELL, M., BYRNE, S., YANG, J. L., DE LOS ANGELES, A., MALI, P., AACH, J., KIM-KISELAK, C., BRIGGS, A. W., RIOS, X., HUANG, P. Y., DALEY, G. & CHURCH, G. 2013. Optimization of scarless human stem cell genome editing. *Nucleic Acids Res*, 41, 9049-61.
- YI, R., QIN, Y., MACARA, I. G. & CULLEN, B. R. 2003. Exportin-5 mediates the nuclear export of pre-microRNAs and short hairpin RNAs. *Genes Dev*, 17, 3011-6.
- YIN, H., KANASTY, R. L., ELTOUKHY, A. A., VEGAS, A. J., DORKIN, J. R. & ANDERSON, D. G. 2014a. Non-viral vectors for gene-based therapy. *Nat Rev Genet*, 15, 541-55.

- YIN, H., XUE, W., CHEN, S., BOGORAD, R. L., BENEDETTI, E., GROMPE, M., KOTELIANSKY, V., SHARP, P. A., JACKS, T. & ANDERSON, D. G. 2014b. Genome editing with Cas9 in adult mice corrects a disease mutation and phenotype. *Nat Biotechnol*, 32, 551-3.
- YIN, W. X., WU, X. S., LIU, G., LI, Z. H., WATT, R. M., HUANG, J. D., LIU, D. P. & LIANG, C. C. 2005. Targeted correction of a chromosomal point mutation by modified single-stranded oligonucleotides in a GFP recovery system. *Biochem Biophys Res Commun*, 334, 1032-41.
- YOON, K., COLE-STRAUSS, A. & KMIEC, E. B. 1996. Targeted gene correction of episomal DNA in mammalian cells mediated by a chimeric RNA.DNA oligonucleotide. *Proc Natl Acad Sci U S A*, 93, 2071-6.
- YU, M. & MELERA, P. W. 1993. Allelic variation in the dihydrofolate reductase gene at amino acid position 95 contributes to antifolate resistance in Chinese hamster cells. *Cancer Res*, 53, 6031-5.
- YUSA, K., RASHID, S. T., STRICK-MARCHAND, H., VARELA, I., LIU, P. Q., PASCHON, D. E., MIRANDA, E., ORDONEZ, A., HANNAN, N. R., ROUHANI, F. J., DARCHE, S., ALEXANDER, G., MARCINIAK, S. J., FUSAKI, N., HASEGAWA, M., HOLMES, M. C., DI SANTO, J. P., LOMAS, D. A., BRADLEY, A. & VALLIER, L. 2011a. Targeted gene correction of alpha1-antitrypsin deficiency in induced pluripotent stem cells. *Nature*, 478, 391-4.
- YUSA, K., ZHOU, L., LI, M. A., BRADLEY, A. & CRAIG, N. L. 2011b. A hyperactive piggyBac transposase for mammalian applications. *Proc Natl Acad Sci U S A*, 108, 1531-6.

Z

- ZHAO, R. & GOLDMAN, I. D. 2003. Resistance to antifolates. *Oncogene*, 22, 7431-57.
- ZHAO, R., SHARINA, I. G. & GOLDMAN, I. D. 1999. Pattern of mutations that results in loss of reduced folate carrier function under antifolate selective pressure augmented by chemical mutagenesis. *Mol Pharmacol*, 56, 68-76.
- ZU, Y., TONG, X., WANG, Z., LIU, D., PAN, R., LI, Z., HU, Y., LUO, Z., HUANG, P., WU, Q., ZHU, Z., ZHANG, B. & LIN, S. 2013. TALEN-mediated precise genome modification by homologous recombination in zebrafish. *Nat Methods*, 10, 329-31.

APPENDIXES

In these appendixes, two works carried out by the PhD student as co-author in the research group in which the thesis has been conducted are included.

These works do not form an intrinsic part of the body of the thesis, but are related to different aspects of the PPRH molecule, including its application as gene silencing tool and the improvement of its design.

These publications, which are detailed below illustrate the collaboration of the different members of the research team.

IMPROVED DESIGN OF PPRHS FOR GENE SILENCING

Laura Rodríguez, Xenia Villalobos, Anna Solé, Carolina Lliberós, Carlos J. Ciudad and Véronique Noé

Molecular Pharmaceutics, 2015 Mar 2;12(3):867-877

EFFECT OF POLYPURINE REVERSE HOOGSTEEN HAIRPINS ON RELEVANT CANCER TARGET GENES IN DIFFERENT HUMAN CELL LINES

Xenia Villalobos, Laura Rodríguez, Anna Solé, Carolina Lliberós, Núria Mencia, Carlos J. Ciudad and Verónique Noé

Nucleic Acid Therapeutics. 2015 Aug;25(4):198-208.

ARTICLE V

IMPROVED DESIGN OF PPRHS FOR GENE SILENCING

Laura Rodríguez, Xenia Villalobos, Anna Solé, Carolina Lliberós, Carlos J. Ciudad
and Véronique Noé

Molecular Pharmaceutics, 2015 Mar 2;12(3):867-877

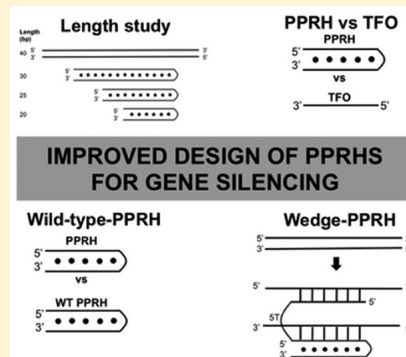
Improved Design of PPRHs for Gene Silencing

Laura Rodríguez, Xenia Villalobos, Anna Solé, Carolina Lliberós, Carlos J. Ciudad, and Véronique Noé*

Department of Biochemistry and Molecular Biology, School of Pharmacy, University of Barcelona, 08028 Barcelona, Spain

ABSTRACT: Nowadays, the modulation of gene expression by nucleic acids has become a routine tool in biomedical research for target validation and it is also used to develop new therapeutic approaches. Recently, we developed the so-called polypurine reverse Hoogsteen hairpins (PPRHs) that show high stability and a low immunogenic profile and we demonstrated their efficacy both in vitro and in vivo. In this work, we explored different characteristics of PPRHs to improve their usage as a tool for gene silencing. We studied the role of PPRH length in the range from 20 to 30 nucleotides. We also proved their higher affinity of binding and efficacy on cell viability compared to nonmodified TFOs. To overcome possible off-target effects, we tested wild-type PPRHs, which proved to be capable of binding to their target sequence with more affinity, displaying a higher stability of binding and a higher effect in terms of cell viability. Moreover, we developed a brand new molecule called Wedge-PPRH with the ability to lock the ds-DNA into the displaced structure and proved its efficacy in prostate and breast cancer cell lines.

KEYWORDS: gene silencing, PPRH, wild-type, Wedge-PPRH, nucleic acid



INTRODUCTION

In 1957, Felsenfeld described the existence of triple-stranded nucleic acids¹ and K. Hoogsteen justified triplex formation with the finding of Hoogsteen bonds.² These discoveries prompted the development of a gene-silencing tool called triplex forming oligonucleotides (TFOs), capable of binding to the purine strand in the major groove of the double helix by hydrogen bonds. The study of their mechanism of action concluded that TFOs interfered with the transcription process.^{3–5} Purine TFOs have several advantages over pyrimidine TFOs because they bind to their target sequence in a pH-independent manner, with higher affinity and faster kinetics.⁶ Kool and colleagues found out that purine sequences in a hairpin or a circular structure could form triplexes with their single-stranded pyrimidine target sequence with a higher binding affinity.⁷

All these studies led us to develop the polypurine reverse Hoogsteen hairpins (PPRHs), which are composed of two antiparallel polypurine domains, which form intramolecular reverse-Hoogsteen bonds linked by a five-thymidine loop, therefore forming a hairpin structure. PPRHs are capable of binding to polypyrimidine stretches in the DNA, causing strand displacement.⁸ Template-PPRHs are directed against the template strand and cause inhibition of transcription.⁹ Coding PPRHs are directed against the coding strand and can also bind to the mRNA. Depending on the location of the target sequence, either in introns or promoters, PPRHs act through different mechanisms. A coding-PPRH against an intronic sequence in the *dhfr* gene caused a splicing alteration by preventing the binding of the splicing factor U2AF65 to its target sequence.¹⁰ PPRHs against promoter sequences, both a template-PPRH (HpsPr-T) and a coding-PPRH (HpsPr-C) directed against two different regions of the *survivin* promoter, prevented the binding of transcription factors specific for the corresponding target

sequences -Sp1, Sp3 and GATA-3-, causing a decrease in *survivin* expression.¹¹

The main limitation for the design of either TFOs or PPRHs would be the presence of polypurine/polypyrimidine stretches. However, their rate of occurrence in the genome has been proved to be higher than predicted by random models,^{12,13} which opens the possibility to design sequence-specific molecules against genes that play important roles in cancer, such as *survivin* or *TERT*.

We have previously studied the role of *survivin* in cancer using siRNAs and ODNs,¹⁴ and more recently, we used PPRHs against *survivin* to validate this new technology both in vitro and in vivo. This approach allowed us to confirm their efficacy in terms of decrease in mRNA and protein levels, resulting in a decrease in cell viability and increase in apoptosis in vitro. Using a xenografted model of prostate cancer we proved that the administration of a PPRH against a promoter sequence in the *survivin* gene caused a reduction in tumor growth, through the decrease in survivin levels and in blood vessel formation, thus establishing the proof of principle for PPRHs usage in vivo.¹¹

We have also studied important properties of PPRHs and concluded that they are less immunogenic and much more stable than siRNAs.¹⁵ Even though these advantages make PPRHs an attractive tool for gene silencing, there is room for improvement.

The aim of this work was to further improve PPRHs in terms of affinity and specificity and to compare them with nonmodified TFOs. To do so, we studied the influence of length and

Received: October 17, 2014

Revised: December 16, 2014

Accepted: January 15, 2015

Published: January 15, 2015

pyrimidine interruptions within the PPRHs and developed the Wedge-PPRH, a brand new molecule based on PPRHs.

MATERIALS AND METHODS

Design and Usage of PPRHs. PPRHs of different length against an intronic sequence of the *telomerase* gene (Table 1) and

Table 1. DNA Oligonucleotides Sequences and PPRHs of Different Lengths against the *Telomerase* Gene

Name*	Sequence (5'-3')
TERT target sequence	5' CAGGCAGGACAAGGAAGCGGAGGAAGGCAGGAGCTCTT 3' 3' GTCCGTCCTGTTCTTTCGCCCTCCTCCGTCCTCCGAGAA 5'
Hpt110-T	5' AGGAAAAGGAAGAGGGAGGAAGGAAGGAGG 3' 3' AGGAAAAGGAAGAGGGAGGAAGGAAGGAGG 5'
Hpt110-T2	5' AAGGAAGAGGGAGGAAGGAAGGAGG 3' 3' AAGGAAGAGGGAGGAAGGAAGGAGG 5'
Hpt110-T3	5' GAAGAGGGAGGAAGGAAGGA 3' 3' GAAGAGGGAGGAAGGAAGGA 5'

PPRH hairpins against the template strand of intron 10 of the *telomerase* gene (TERT target): Hpt110-T, 30 nt carrying three A-substitutions in place of the pyrimidine interruptions in each domain. Hpt110-T2, 25 nt carrying two A-substitutions and Hpt110-T3, 20 nt carrying two A-substitutions. Interruptions are marked in bold. Bullets represent reverse-Hoogsteen bonds and lines Watson–Crick bonds.

PPRHs and nonmodified TFOs against promoter sequences of the *survivin* gene (Table 2) were used in these experiments. The Triplex-Forming Oligonucleotide Target Sequence Search software (M.D. Anderson Cancer Center, Houston, TX) (www.spi.mdanderson.org/tfo/) was used to find polypurine sequences and BLAST software was carried out to confirm the specificity of the designed molecules. The nomenclature used in this study was: Hp for PPRH hairpin; s for survivin; t for TERT; Pr for promoter; I10 for intron 10; T for template-PPRH; C for coding-PPRH; and WT for wild type. Wedge-PPRHs were designed by extending the 5' end of HpsPr-T WT, with a pyrimidine sequence complementary to the upper strand that is displaced by the PPRH (Table 3). PPRHs were synthesized as nonmodified oligodeoxynucleotides by Sigma-Aldrich (Madrid, Spain) (0.05 μ mol scale; DESALT-unmodified and desalted). Lyophilized PPRHs were resuspended in sterile Tris-EDTA buffer (1 mM EDTA and 10 mM Tris, pH 8.0) and stored at -20°C .

Preparation of Polypurine/Polypyrimidine Duplexes.

The duplexes to be targeted by the hairpins corresponded to the intronic sequence within the *TERT* gene (Table 1) and two promoter sequences of the *survivin* gene (Table 2). The single-stranded molecules were purchased from Sigma and resuspended in Tris-EDTA buffer. To make the duplexes, 25 μ g of each single-stranded (ss) polypurine and polypyrimidine oligodeoxynucleotides were incubated with 150 mM NaCl at 90°C for 5 min as described by de Almagro et al.⁹

Oligodeoxynucleotide Labeling. One hundred nanograms of PPRHs or double stranded (ds) oligodeoxynucleotides were 5'-end-labeled with T4 polynucleotide kinase (New England Biolabs, Beverly, MA) and [γ - ^{32}P]ATP as described by de Almagro et al.⁹

Table 2. DNA Oligonucleotides Sequences, PPRHs, and TFOs Directed against the *Survivin* Gene

Name*	Sequence (5'-3')
Template-PPRHs and Coding-TFO against the <i>survivin</i> promoter sequence at -1009	
Target sequence	5' ATTAAGAATGGGGCGGGGTGGGAGGGGTGG 3' 3' TAATTCCTACCCCGCCGCCACCTCCGCCACC 5'
HpsPr-T	5T (AAAGAAAAGGGGAGGGGAGGGGAGGGG 3' AAAGAAAAGGGGAGGGGAGGGGAGGGG 5')
HpsPr-T WT	5T (AAAGAATGGGGCGGGGTGGGAGGGG 3' AAAGAATGGGGCGGGGTGGGAGGGG 5')
TFO-sPr-C	5' GGGGAGGGAGGGGAGGGGAAAAGAAA 3'
Coding-PPRHs and Template-TFO against the <i>survivin</i> promoter sequence at -525	
Target sequence	5' CTGCTGCACTCCATCCCTCCCTGTT 3' 3' GACGACGTGAGGTAGGGAGGGGACAA 5'
HpsPr-C	5T (GAAGAGAGAAAGGGAGGGGA 3' GAAGAGAGAAAGGGAGGGGA 5')
HpsPr-C WT	5T (GACGTGAGGTAGGGAGGGGA 3' GACGTGAGGTAGGGAGGGGA 5')
TFO-sPr-T	5' GAAGAGAGAAAGGGAGGGGA 3'
Negative controls	
Hps-WC	5' CCCTCCCTCCCTCCCTCCCTTTCTTT 3' 3' GGGGAGGGAGGGGAGGGGAAAAGAAA 5'
Hps-Sc	5' AAGAGAAAAGAGAAAAGAGAGAGGG 3' 3' AAGAGAAAAGAGAAAAGAGAGAGGG 5'
TFO-Sc	5' GGAAAAAGGAGGA 3'

* PPRH hairpins and TFO against the *survivin* promoter at -1009 : HpsPr-T, 26 nt carrying three A-substitutions in place of the pyrimidine interruptions in each domain; HpsPr-T WT 26 nt carrying the corresponding three pyrimidine interruptions in each domain; TFO-sPr-C carrying three A-substitutions in place of the pyrimidine interruptions. PPRH hairpins and TFO against the *survivin* promoter at -525 : HpsPr-C, 20 nt carrying three A-substitutions in place of the pyrimidine interruptions in each domain; HpsPr-T WT 20 nt carrying the corresponding three pyrimidine interruptions in each domain; TFO-sPr-T carrying three A-substitutions in place of the pyrimidine interruptions. Negative controls: Hps-WC is a hairpin with intramolecular Watson–Crick bonds; Hps-Sc is a hairpin with intramolecular reverse-Hoogsteen bond and no target in the genome; TFO-Sc is a polypurine sequence and no target in the human genome. Interruptions are marked in bold. Bullets represent reverse-Hoogsteen bonds and lines Watson–Crick bonds.

PPRH and TFO DNA Binding Analyses. Binding studies for PPRHs and TFOs were performed using radiolabeled ds-target sequences (20 000 cpm). The radiolabeled sequences were incubated with increasing concentrations (0.1 μM , 1 μM , and 10 μM) of each PPRH or TFO in a buffer containing 10 mM MgCl_2 , 100 mM NaCl, and 50 mM HEPES, pH 7.2 and 0.5 μg of poly dI-dC (Sigma-Aldrich) as a nonspecific competitor. Binding reactions (20 μL) were preincubated for 5 min at 65°C , followed by 30 min at 37°C and then, loaded in nondenaturing 12% polyacrylamide gels (PAGE) containing 10 mM MgCl_2 , 5% glycerol and 50 mM HEPES, pH 7.2. Electrophoresis was carried

Table 3. Sequence of Wedge-PPRHs against the *Survivin* Gene*

Name	Sequence (5'-3')
Target sequence	<pre> 5' ATTAAAGAAATGGGGGCGGGGTGGGAGGGGTGG 3' 3' TAATTTCTTACCCCGCCCGCCACCTCCACC 5' </pre>
Wedge-PPRH-23	<pre> 5T(TTTCTTACCCCGCCCGCCACCTC 5' AAAGAATGGGGGCGGGGTGGGAGGGG)5T 3' AAAGAATGGGGGCGGGGTGGGAGGGG </pre>
Wedge-PPRH-17	<pre> 5T(TTTCTTACCCCGCCCGCC 5' AAAGAATGGGGGCGGGGTGGGAGGGG)5T 3' AAAGAATGGGGGCGGGGTGGGAGGGG </pre>
Wedge-PPRH WC	<pre> 5T(TTTCTTACCCCGCCCGCC 5' AAAGAATGGGGGCGGGGTGGGAGGGG)5T 3' TTTCTTACCCCGCCCGCCACCTCCACC </pre>

*Wedge-PPRH-23 is constituted of HpsPr-T WT with a 23-nt 5' extension corresponding to the polypyrimidine sequence complementary to the coding strand of the target sequence. Wedge-PPRH-17 is constituted of HpsPr-T WT with a shorter 5' extension of 17-nt. Wedge-PPRH WC is constituted of Hps-WC with the same 17-nt 5' extension as Wedge-PPRH-17. Interruptions are marked in bold. Bullets represent reverse-Hoogsteen bonds and lines Watson-Crick bonds.

out for approximately 4 h at 10 V/cm at 4 °C. After drying the gel, it was exposed to Europium plates OVN and analyzed using a Storm 840 Phosphorimager (Molecular Dynamics, Sunnyvale, CA).

UV Absorption Studies. Previous to the analyses, the PPRHs in combination with their single-stranded target sequence (0.5 μM of each strand) were incubated in a buffer containing 100 mM NaCl and 50 mM HEPES, pH 7.2, heated to 90 °C during 5 min, cooled slowly to room temperature, and stored at 4 °C.

Melting experiments were performed using a V-650 Spectrophotometer (Jasco, Madrid, Spain) connected to a temperature controller that increased temperature at a rate of 1 °C/min from 10 to 90 °C. Absorbance of the samples was measured in a 1 cm path length quartz cells.

The MeltWin 3.5 software was used to perform a thermodynamic analysis to calculate melting temperatures (T_m) and free energy values (ΔG) as the mean of two independent melting experiments.

Cell Culture. PC3 prostate adenocarcinoma cells (ECACC), SKBR3 breast adenocarcinoma cells (ATCC) and MiaPaCa-2 pancreas carcinoma cells (ATCC) were cultivated in Ham's F-12 medium supplemented with 7% fetal bovine serum (GIBCO, Invitrogen, Barcelona, Spain) and incubated at 37 °C in a humidified 5% CO₂ atmosphere.

Transfection. The transfection procedure consisted in mixing the appropriate amount of either PPRH or TFO and the transfection reagent DOTAP (Roche, Mannheim, Germany or Biontex, Germany) for 20 min in a volume of 200 μL of medium at room temperature, followed by the addition of the mixture to the cells plated in 35 mm-diameter dishes in a total volume of 1 mL.

MTT Assay. MiaPaCa 2 (5000), PC3 (10 000), or SKBR3 (10 000) cells were plated in 35 mm-diameter dishes in F12 medium and treated with the appropriate concentration of each molecule. After 6 days, MTT assay was performed as described by Rodríguez et al.¹¹

mRNA Analyses. A total of 60 000 PC3 or MiaPaCa 2 cells were plated in 35 mm-diameter dishes in F12 medium and total RNA was extracted 48 or 72 h after transfection, using Ultraspec (Biontex) or Trizol (Life Technologies, Madrid, Spain), following the manufacturer's specifications. Quantification of RNA was performed measuring its absorbance (260 nm) at 25 °C using a Nanodrop ND-1000 spectrophotometer.

Reverse Transcription. cDNA was synthesized using 1 μg of total RNA, as described by Rodríguez et al.¹¹ for *TERT* mRNA levels determination.

For *survivin* mRNA levels, 500 ng were used in a total volume of 20 μL of reaction containing 2 μL of Buffer 10x (500 mM Tris-HCl pH 8.3, 750 mM KCl, 30 mM MgCl₂, 100 mM DTT) (Lucigen, Middleton, Wisconsin), 12.5 ng of random hexamers (Roche), 0.5 mM each dNTP (AppliChem, Barcelona, Spain), 20 units of NxGen RNase inhibitor (Lucigen) and 200 units of NxGen M-MuLV reverse transcriptase (Lucigen). The reaction was incubated at 37 °C for 1 h and 3 μL of the cDNA per sample were used for qRT-PCR.

Real Time-PCR. The StepOnePlus Real-Time PCR Systems (Applied Biosystems, Barcelona, Spain) was used to perform these experiments.

SYBR was used to determine *TERT* mRNA levels. Primer sequences were: *TERT*-Fw, 5'-GCGGAAGACAGTGGT-GAACT-3'; *TERT*-Rv, 5'-AGCTGGAGTAGTCGCTCTGC-3'; and the endogenous control, *APRT*-Fw, 5'-AAGGCT-GAGCTGGAGATTCA-3'; *APRT*-Rv, 5'-GGTACAGGTGC-CAGCTTCTC-3'.

The final volume of the reaction was 20 μL, containing 10 μL of Biotools Mastermix (2X) (Biotools, Madrid, Spain), 1 μL of SYBR (dilution 1/1000, Life technologies), 0.25 μM of each primer, 3 μL of cDNA and H₂O mQ. PCR cycling conditions were 2 min at 50 °C, 10 min denaturation at 95 °C, followed by 35 cycles of 15 s at 95 °C and 1 min at 60 °C.

To determine *survivin* mRNA levels, the following TaqMan probes were used: *Survivin* (BIRC5) (HS04194392_S1), and adenine phosphoribosyl-transferase (*APRT*) (HS00975725_M1) and 18S rRNA (HS99999901_S1), as endogenous controls. The reaction contained 1x TaqMan Universal PCR Mastermix (Applied Biosystems), 1x TaqMan probe (Applied Biosystems), 3 μL of cDNA and H₂O mQ to a final volume of 20 μL. PCR cycling conditions were 10 min denaturation at 95 °C, followed by 40 cycles of 15 s at 95 °C and 1 min at 60 °C.

The mRNA quantification was calculated using the $\Delta\Delta C_T$ method, where C_T is the threshold cycle that corresponds to the cycle where the amount of amplified mRNA reaches the threshold of fluorescence.

RESULTS

Design of PPRHs. Different PPRHs were designed to assess the effect of length, their efficacy compared with TFOs, and how to cope with the presence of purine interruptions in the polypyrimidine target sequence. Furthermore, we tested new designs for improving the effectiveness of the PPRHs. The specific design in each case is described below. To test for specificity, we performed BLAST analyses with all PPRHs using as a database the reference genomic sequence of *Homo sapiens*. In

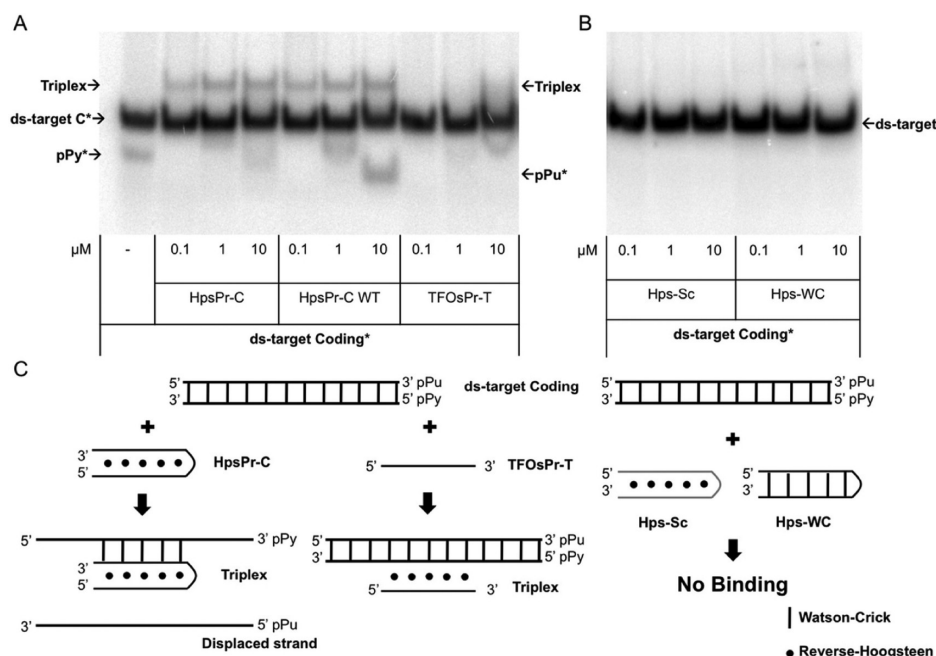


Figure 3. Binding of coding-PPRHs and TFO to their target sequence. (A) Binding of the coding-PPRH either with adenines in the pyrimidine interruptions (HpsPr-C) or the wild-type version (HpsPr-C WT) and the TFOsPr-T after incubation with increasing concentrations of their radiolabeled ds-target sequence (20 000 cpm). Shifted bands are indicated by arrows. (B) Binding of the negative controls, either Hps-Sc or Hps-WC to the radiolabeled ds-target sequence (20 000 cpm) for the specific PPRHs. (C) Schematic representation of the binding of the different molecules used in this study, including HpsPr-C, HpsPr-C WT, TFOsPr-T, Hps-Sc, Hps-WC.

all experiments, we used as negative controls either a PPRH with a scrambled sequence (Hps-Sc) or a PPRH with intramolecular Watson–Crick bonds instead of Hoogsteen bonds (Hps-WC), which is not able to form triplexes with the DNA. We also used as negative control a TFO with a scrambled sequence without target in the human genome (TFO-Sc).

Effect of PPRHs Length on Binding to the Target, Cell Viability and mRNA. To compare the effects of PPRHs with different lengths, we needed to start with a gene containing a polypurine/polypyrimidine stretch long enough to allow the design of PPRHs with different number of nucleotides. We found a 30 nucleotides polypyrimidine sequence within intron 10 of the *TERT* gene that opened the possibility to test PPRHs lengthening 20, 25, or 30 nucleotides against the same target sequence (Table 1, Figure 1A). HptI10-T had 3 pyrimidine interruptions, whereas HptI10-T2 and HptI10-T3 had two interruptions. For these experiments, we used PPRHs where the pyrimidine interruptions were substituted by adenines in both strands of the PPRH. As shown in Figure 1B the three PPRHs tested were capable of binding to their target sequence at a concentration as low as 1 μM . However, in terms of cell viability, we observed that the longer the sequence, the higher the effect. Specifically, the 20-, 25-, and 30-nucleotide PPRHs decreased cell viability by 15%, 30%, and 60%, respectively (Figure 1C). In the case of TERT inhibitors, reaching 60% decrease in cell viability can be considered a notable effect because a long time is needed for the cell to shorten the telomeres enough to enter senescence. For that reason, inhibitors of TERT are commonly used in combination with other drugs.¹⁶ We also determined the mRNA levels of TERT using the longest PPRH that caused a dose-dependent decrease, reaching 60% at 300 nM (Figure 1D).

Comparison between PPRHs and Nonmodified TFOs. Binding to Target Sequences. For the comparative analyses, we used PPRHs against the promoter sequence of *survivin*, which

have been previously validated in terms of efficacy in prostate cancer cells and in a xenografted tumor model.¹¹ Those PPRHs were designed against two different sequences within the promoter, one against a distal region, at-1009, in the template strand of the DNA (Template-PPRH), and another against a more proximal region, at -525, in the coding strand (Coding-PPRH). Thus, the corresponding TFOs that would bind to the same sequence as PPRHs were designed. PPRHs are double-stranded molecules formed by two polypurine strands that bind to the pyrimidine target in the DNA sequence by Watson–Crick bonds, whereas TFOs are single-stranded polypurine molecules that will bind to the purine strand in the DNA by reverse-Hoogsteen bonds forming a triplex structure. Therefore, the TFO that binds to the same region as the template-PPRH will bind to the coding strand, and the TFO that binds to the same region as the coding-PPRH will bind to the template strand. PPRHs and TFOs sequences are listed in Table 2.

The binding was analyzed using the corresponding radiolabeled ds-target sequence for each PPRH either template or coding, shown in Figures 2 and 3.

We observed that both the Template-PPRH (HpsPr-T) and the corresponding TFO (TFOsPr-C) were specific for their target sequence, as indicated by the shifted bands (Figure 2A), whereas the two negative controls, Hps-Sc and Hps-WC, did not bind to the target sequences (Figure 2B). The template-PPRH against the promoter sequence (HpsPr-T) was bound to the target sequence forming a triplex structure-binding of the PPRH to the pyrimidine target sequence- and quadruplex structure-binding of the PPRH to the duplex, whereas the TFO formed a single triplex structure-binding of the TFO to the duplex (Figure 2A and 2C).

Regarding the coding-PPRH, we also observed specificity of both HpsPr-C and TFOsPr-T, as indicated by the shifted band (Figure 3), in contrast to the two negative controls, Hps-Sc and

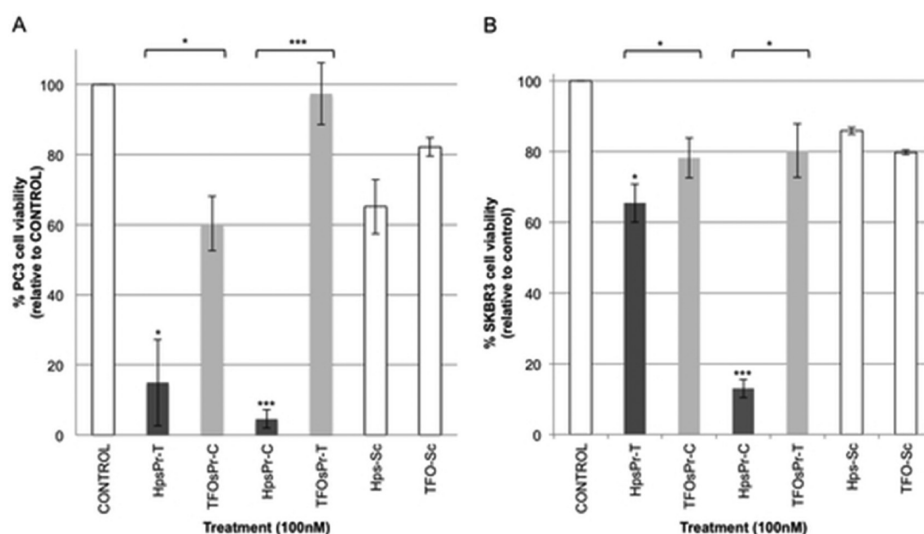


Figure 4. Effect of PPRHs and TFOs against *survivin* on cell viability. (A) Cell viability in PC3 cells upon incubation with 100 nM of the two PPRHs (dark gray) or the two TFOs (light gray) against the *survivin* gene. Negative controls -Hps-Sc and TFO-Sc (blank bars)- were tested at the same conditions. CONTROL cells are untreated PC3 cells. (B) Cell viability in SKBR3 cells upon incubation with 100 nM of the two PPRHs (dark gray) or the two TFOs (light gray) against the *survivin* gene. Negative controls -Hps-Sc and TFO-Sc (blank bars)- were tested at the same conditions. CONTROL cells are untreated SKBR3 cells. MTT assays to determine cell survival were performed 6 days after transfection. DOTAP was used at 10 μ M. Data are mean \pm SEM values of at least three experiments. * $p < 0.05$, ** $p < 0.01$, *** $p < 0.005$.

Hps-WC, which did not bind to the target sequence (Figure 3B). HpsPr-C was capable of binding to its target sequence from 100 nM to 10 μ M, causing strand displacement at 10 μ M. On the other hand, the TFO against the same sequence only showed some binding at 10 μ M (Figure 3A), proving that it had less affinity to the target sequence than the coding-PPRH. In Figure 3C there is a representation of the different structures observed in the binding assays. In this case, we only observed the triplex structure because the PPRH was capable of displacing the purine strand completely. The different length of their target sequences might cause the difference of binding between the template- and coding-PPRH. In the case of the coding-PPRH, the target sequence is shorter, and in consequence, easier to displace.

Cell Viability. We compared the effect of PPRHs and TFOs in two cell lines, PC3 from prostate cancer and SKBR3 from breast cancer, upon incubation with 100 nM of the DNA molecules (PPRH or TFO) plus 10 μ M of the liposomal reagent DOTAP (Roche). In both cell lines, there was a significant difference between the use of PPRHs vs TFOs; both template- and coding-PPRHs exerted a higher decrease in cell viability than the corresponding TFOs at 100 nM, as shown in Figure 4. Negative controls for each type of molecule -Hps-Sc and TFO-Sc- were used at the same conditions and a rather small effect was observed upon incubation in both cell lines, probably due to the transfection reagent.

It was also observed that PPRHs and TFOs caused a higher decrease in viability in PC3 than in SKBR3 cells. This could be caused by the different transfection efficiency of DOTAP in each cell line. PC3 cells internalize almost four times more PPRH than SKBR3 using the same conditions of transfection, as determined in uptake experiments using flow cytometry and fluorescently labeled PPRHs. Using this methodology, we also compared the uptake of fluorescently labeled PPRH and TFO, observing that 24 h after transfection, more than 90% of PC3 cells showed a similar mean intensity of fluorescence with either molecule (data not shown). This result indicated that the difference in effect of

PPRHs and TFOs was due to a different intrinsic efficacy rather than a different uptake.

Comparison between PPRHs Carrying Adenines and Wild-Type Sequences. Binding to Their Target Sequence.

Once we had compared PPRHs and nonmodified TFOs, we wanted to improve our PPRHs in terms of efficacy and specificity. To do so, we decided to explore the usage of wild-type PPRHs including pyrimidine interruptions in their sequences instead of substituting the interruptions by adenines. We had previously stated that the best base—in terms of binding and cytotoxicity—to substitute a single interruption was adenine;⁹ however, it is usual to find polypurine stretches with several interruptions that could compromise the specificity of the molecule. We studied HpsPr-T and HpsPr-C against *survivin*, both of which contained three interruptions substituted by adenines, and their counterparts, HpsPr-T WT and HpsPr-C WT, in which the wild-type sequence was used. PPRHs sequences are listed in Table 2, including a scheme of the molecules. It is important to mention the difference between the two approaches: The A-substitution involved using two adenines in each interruption, one in the Watson–Crick strand (that will bind to the pyrimidine target sequence) and one in the reverse-Hoogsteen strand (that forms the hairpin structure). In the wild-type version, the same pyrimidine (C or T) of the interruption was used in both strands of the PPRH.

When performing BLAST analyses using the wild-type sequences, the first match with the lowest e-value and maximum identity was always the target sequence within the *survivin* gene. However, when using the sequences where the pyrimidines were substituted by adenines, several sequences were found with the same identity but higher e-value, indicating possible off-target effects.

In the binding assays with the *survivin* promoter shown in Figure 2 and 3, there was the general tendency that the wild-type PPRHs were capable of binding to the polypyrimidine target sequences with more affinity and at lower concentrations than the PPRHs with adenines in front of the purine interruptions. In

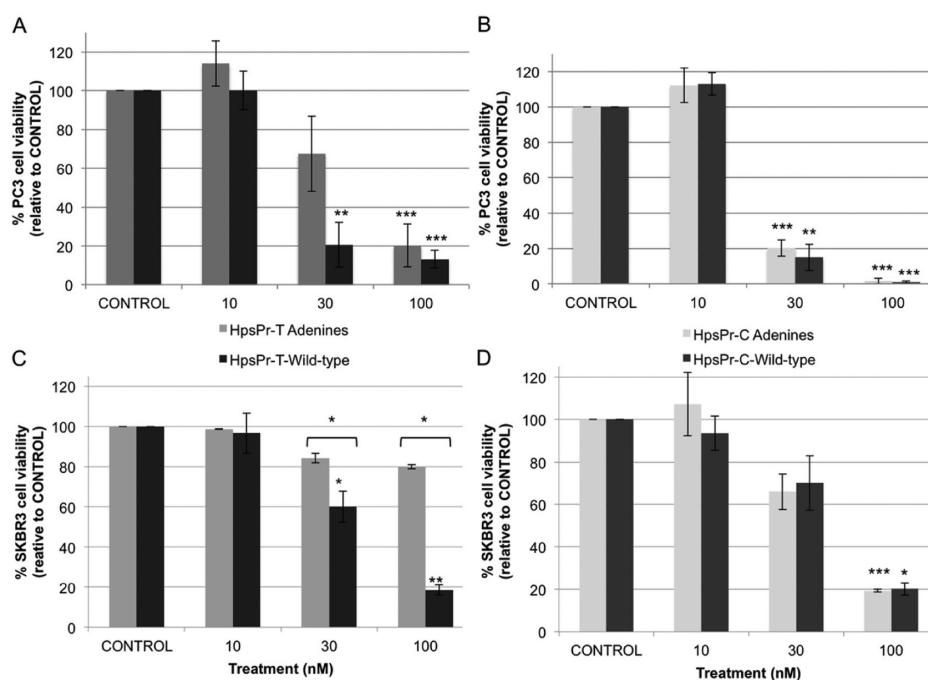


Figure 5. Effect of PPRHs against *survivin* on cell viability. (A) Dose response of template-PPRHs against *survivin* in PC3 cells. (B) Dose response of coding-PPRHs against *survivin* in PC3 cells. (C) Dose response of template-PPRHs against *survivin* in SKBR3 cells. (D) Dose response of coding-PPRHs against *survivin* in SKBR3 cells. DOTAP was used at 5 μM to transfect 10 nM and 30 nM and at 10 μM to transfect 100 nM PPRH. CONTROL cells are untreated cells. MTT assays to determine cell survival were performed 6 days after transfection. Data are mean \pm SEM values of at least three experiments. * $p < 0.05$, ** $p < 0.01$, *** $p < 0.005$. Light gray corresponds to the adenine version and dark gray to the wild-type version.

the case of the template-PPRH, there was a clear difference in the binding affinity between HpsPr-T and HpsPr-T WT, only the wild-type version bound to its target at concentrations as low as at 1 μM , whereas the other PPRH did not generate a shifted band up until 10 μM (Figure 2A). In the case of the coding-PPRH, both PPRHs originated a band corresponding to the triplex at all concentrations tested (from 0.1 to 10 μM), but the wild-type showed five times more strand displacement upon binding (Figure 3A).

Cell Viability Assays. To compare the effect of PPRHs with or without pyrimidine interruptions, dose response studies in PC3 and SKBR3 were performed and the IC_{50} for each molecule was calculated. The resulting cell viabilities are shown in Figure 5 and the IC_{50} 's in Table 4. Template and coding-PPRHs decreased cell viability in a dose-dependent manner in both cell lines, and in all cases, the wild-type counterpart presented a lower IC_{50} .

Melting Experiments. Melting temperatures and $-\Delta G$ were obtained using the MeltWin 3.5 software¹⁷ and are displayed in Table 5. We measured the changes in absorbance at 260 nm when increasing temperature from 10 to 90 $^{\circ}\text{C}$; in all cases, sigmoidal curves with a single transition corresponding to the

Table 4. IC_{50} Calculated for PPRHs and Wedge-PPRH in PC3 and SKBR3

PPRH*	PC3	SKBR3
	IC_{50} (nM)	IC_{50} (nM)
HpsPr-T A	46.21	346.57
HpsPr-T WT	30.14	40.77
HpsPr-C A	16.50	43.32
HpsPr-C WT	14.44	43.32
Wedge-PPRH-17	21.62	41.17

*A indicates adenines and WT wild-type.

Table 5. Melting Transition Temperatures, T_m , and Free Energies, ΔG , at pH 7.2

complex*	$T_m \pm \text{std error}$ ($^{\circ}\text{C}$)	$\Delta G \pm \text{std error}$ (kcal/mol, at 37 $^{\circ}\text{C}$)
HpsPr-T A + Ppy	54.05 \pm 0.23	-12.60 \pm 0.13
HpsPr-T WT + Ppy	73.47 \pm 0.30	-19.81 \pm 0.70
HpsPr-C A + Ppy	37.24 \pm 2.42	-9.29 \pm 0.53
HpsPr-C WT + Ppy	66.45 \pm 0.07	-25.96 \pm 2.29

*A indicates adenines and WT wild-type.

switch from bound complex to random coil were observed, which corresponds to a bimolecular melting curve, previously described in ref 18. Comparison between the PPRH containing interruptions substituted by adenines and the wild-type counterpart showed a clear difference of around 20 $^{\circ}\text{C}$, the wild-type presenting the higher temperature and the lower ΔG , meaning these PPRHs had a higher affinity for the target sequence. It was also clear that the longer the PPRH, the higher the melting temperature; therefore, the template-PPRH, which is 26 nucleotides long, had a higher temperature than the coding-PPRH that was 20 nucleotides long.

Survivin mRNA Levels. Treatment for 48 h of wild-type PPRHs against *survivin* caused a decrease in its expression. Specifically, HpsPr-T WT caused a 2.4-fold decrease and HpsPr-C WT caused a 3-fold decrease in mRNA levels, whereas no effect was observed with the negative control HpsPr-WC (Figure 6).

Wedge-PPRH. *Design.* Concurrently to the study of wild-type PPRHs, we decided to further improve PPRHs by designing a structure that would lock the strand displacement, which may stabilize the PPRH-DNA complex and cause a higher effect. The design consisted in extending the 5' with the sequence of polypyrimidines complementary to the polypurine strand. The

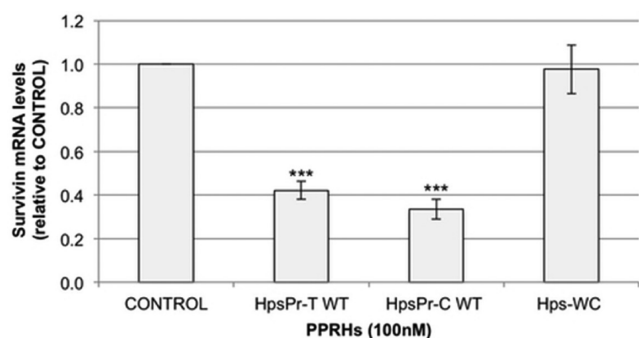


Figure 6. Effect of wild-type PPRHs on *survivin* mRNA levels. RNA was extracted from PC3 cells treated with 100 nM of HpsPr-T WT, HpsPr-C WT and the negative control Hps-WC for 48 h. mRNA levels were determined using qRT-PCR and referred to the levels of *APRT* as an endogenous control. DOTAP was used at 8 μ M. Data are mean \pm SEM values of at least three experiments. * $p < 0.05$, ** $p < 0.01$, *** $p < 0.005$.

rationale was that such PPRH could open the double strand and the extension could bind to the coding strand, as detailed in Figure 7B.

The Template-PPRH was selected to perform this study. We designed two Wedge-PPRHs; one had a 5' extension of 23 bases complementary to the purine sequence, linked by a 5T loop to give flexibility for the turn, and another with a shorter extension of 17 nucleotides. As a negative control we used Wedge-PPRH WC, which presented the 17-nucleotide complementary sequence followed by a hairpin that formed Watson–Crick bonds instead of reverse-Hoogsteen bonds, a useful control to determine the importance of the PPRH in this structure. All the sequences are listed in Table 3.

Binding to the Target Sequence. We performed binding analyses for the three wedge structures. We observed a similar pattern of binding between the Wedge-PPRH-23 and the HpsPr-T WT (Figure 7A compared to Figure 2A), indicating that the presence of the 5' extension did not prevent the binding of the PPRH to its target sequence. Wedge-PPRH-23 formed two bands corresponding to a triplex and a quadruplex structure (Figure 7B). We expected to observe an additional band (quintuplex) if the 5' extension could bind to the displaced polypurine strand which was not seen with the Wedge-PPRH-23. Therefore, we tested a shorter version of the Wedge-PPRH with an extension of only 17 nucleotides, so it could hybridize to the polypurine displaced strand. Using Wedge-PPRH-17 we observed an additional shifted band corresponding to the quintuplex structure (Figure 7B). Moreover, Wedge-PPRH-17 bound to the target sequence at a lower concentration (100 nM) than when using PPRHs and Wedge-PPRH-23. It is important to note that binding with the Wedge-PPRH WC showed a low intensity band that might correspond to the binding of the 17-nucleotide extension to its complementary sequence, no additional bands were observed because of the lack of PPRH structure, indicating the importance of this structure for the opening of the dsDNA.

To really demonstrate the identity of the quintuplex, we performed binding experiments with both the Wedge-PPRH-17 and the duplex and competing with either the coding strand (pPu) (Figure 8A and B), the pyrimidine strand (pPy), or the duplex (dsT) (Figure 8B). In Figure 8A, we observed the competition between the polypurine sequence (at 20 \times , lanes 3 and 6; or 50 \times , lanes 4 and 7) and the radiolabeled duplex (20 000 cpm) at different concentrations of Wedge-PPRH-17 (100 nM, lanes 2–4; and 1 μ M, lanes 5–7). The disappearance of the

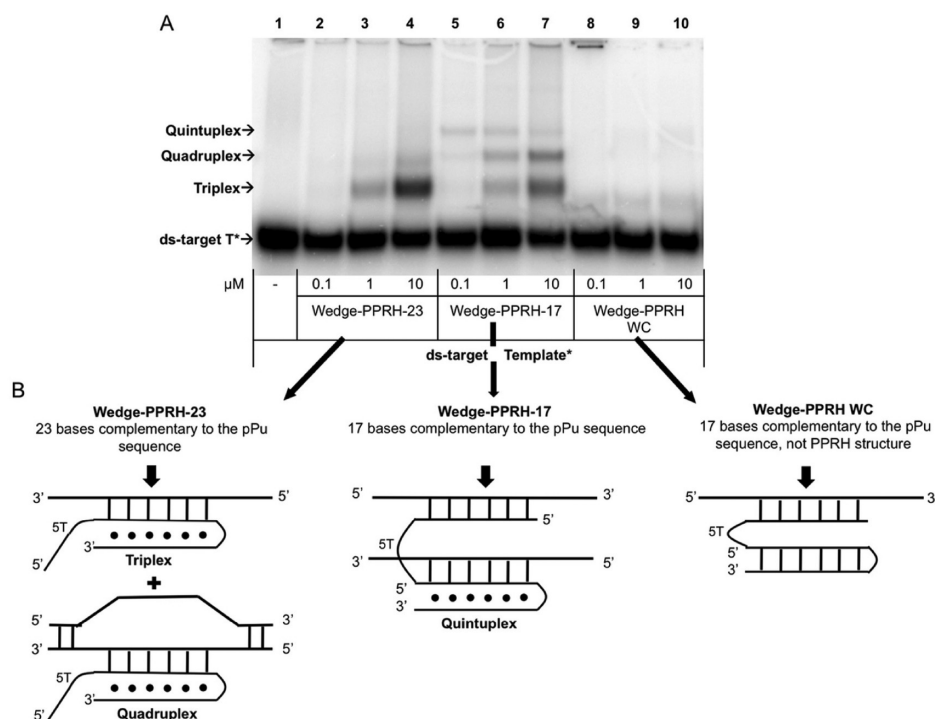


Figure 7. Binding of Wedge-PPRH to its target sequence. (A) Binding of Wedge-PPRH to its radiolabeled ds-target sequence (20 000 cpm). The mobility of the ds-target sequence is shown in lane 1. Binding of Wedge-PPRH-23 is shown in lane 2, 3, and 4. Binding of Wedge-PPRH-17 is shown in lane 5, 6, and 7. The negative control, Wedge-PPRH WC is shown in lane 8, 9, and 10. Shifted bands are indicated by arrows. (B) Schematic representation of the structures corresponding to the different bands observed in the electrophoresis.

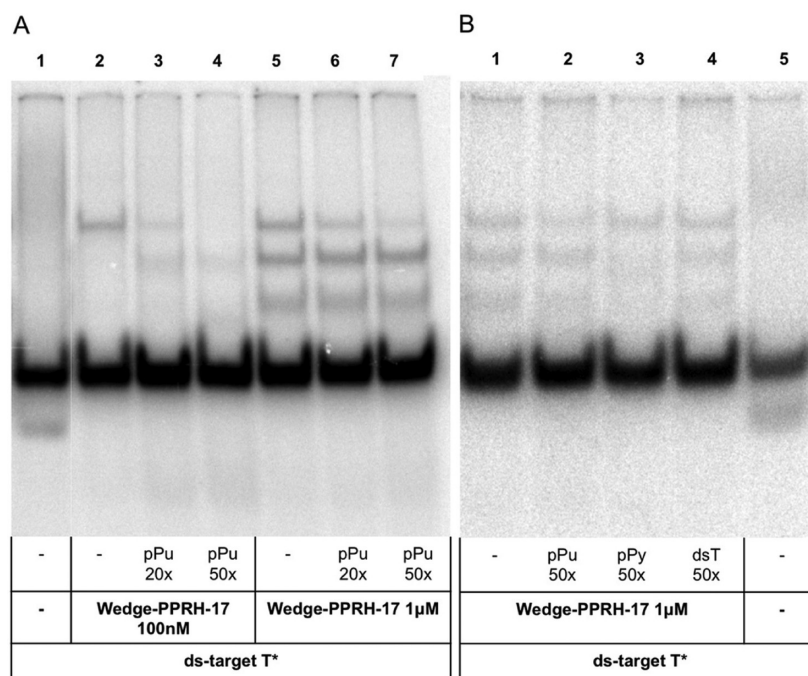


Figure 8. Identification of the shifted bands in the binding assays with Wedge-PPRH-17. (A) Binding of Wedge-PPRH-17 to its radiolabeled ds-target sequence (20 000 cpm). The mobility of the ds-target sequence is shown in lane 1. The binding pattern of the Wedge-PPRH-17 is shown at two different concentrations of Wedge-PPRH: 100 nM (lane 2–4) and 1 μ M (lane 5–7); competition assays were performed using 20-fold (lane 3 and 6) and 50-fold (lane 4 and 7) excess of the coding strand of the target sequence. (B) Binding of Wedge-PPRH-17 at 1 μ M to its radiolabeled ds-target sequence (20 000 cpm). The mobility of the ds-target sequence is shown in lane 5. The binding pattern of the Wedge-PPRH is shown in lane 1 and competition assays were performed using 50-fold excess of either the coding (lane 2) or the template strand (lane 3) or the ds-target sequence (lane 4).

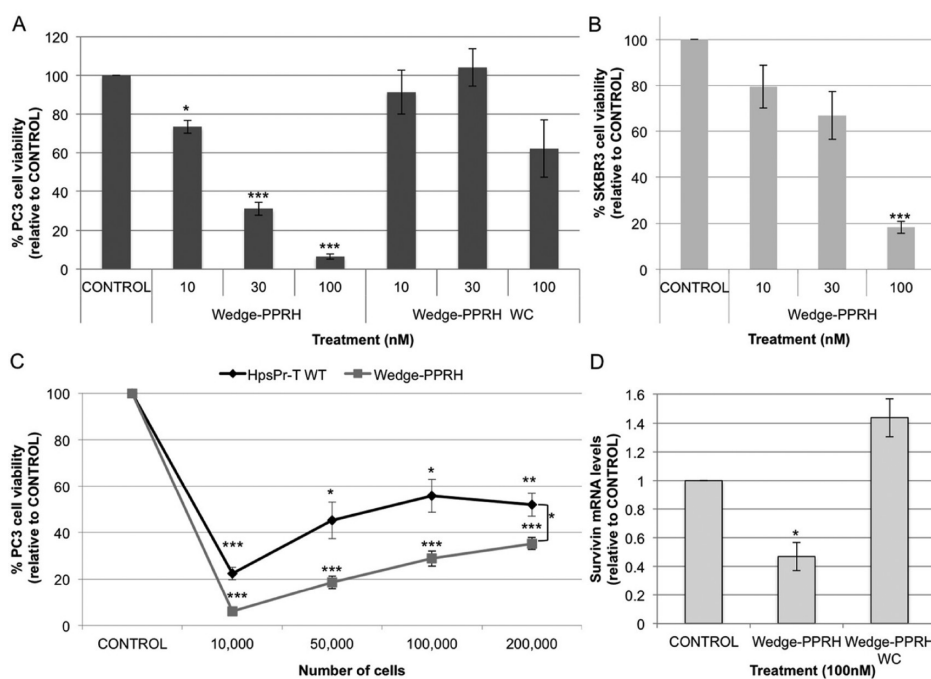


Figure 9. Effect of Wedge-PPRH-17 on cell viability and *survivin* mRNA levels. (A) Effect in PC3 cells. (B) Effect in SKBR3 cells. In both cases, DOTAP was used at 5 μ M to transfect 10 nM and 30 nM, and at 10 μ M to transfect 100 nM of Wedge-PPRH. CONTROL cells are untreated cells. MTT assays to determine cell survival were performed 6 days after transfection. Data are mean \pm SEM values of at least three experiments. * p < 0.05, ** p < 0.01, *** p < 0.005. (C) Effect of HpsPr-T WT and Wedge-PPRH-17 on cell viability when scaling-up the number of PC3 cells. (D) RNA was extracted from PC3 cells treated with 100 nM of Wedge-PPRH-17 or Wedge-PPRH WC for 48 h. DOTAP was used at 8 μ M. mRNA levels were determined using qRT-PCR and referred to the levels of the endogenous control *18S*. Data are mean \pm SEM values of at least three experiments. * p < 0.05.

upper band, corresponding to the quintuplex, indicates its high affinity to the polypurine sequence and that the 5' pyrimidine

extension was binding to the displaced polypurine sequence. In fact, when using the lowest concentration of Wedge-PPRH-17

(100 nM), the competition by pPu (20× or 50×) produced the disappearance of the quintuplex while the quadruplex appeared. When the Wedge-PPRH-17 was increased at 1 μ M, the competition with pPu also decreased the intensity of the band corresponding to the quintuplex.

In Figure 8B, aside from competing the duplex with pPu (lane 2), we competed with pPy (lane 3) and the duplex (lane 4). Competition with pPy caused a decrease in the intensity of the bands corresponding to the triplex and quadruplex structures, but not the quintuplex, reaffirming the quintuplex was the band most difficult to displace because it had the highest affinity. In lane 4, we observed the decrease of the three shifted bands because the competition was performed with the duplex.

Cell Viability Assays and Survivin mRNA Levels. We decided to further explore the effect of the Wedge-PPRH with the extension of 17-nucleotides in terms of cell viability and mRNA levels because we had shown that it was capable of forming the locked structure.

In PC3 cells, we observed a similar effect on cell viability of the Wedge-PPRH-17 compared to the original or wild-type-PPRHs (Figure 9A compared to Figure 5A). However, when analyzing the data, the Wedge-PPRH-17 presented a lower IC_{50} than HpsPr-T WT (Table 4), indicating that the Wedge-PPRH-17 had a higher efficacy. Wedge-PPRH WC was innocuous at 10 and 30 nM and caused only a slight decrease at 100 nM (Figure 9A). In SKBR3, Wedge-PPRH-17 had a dose-dependent effect (Figure 9B) similar to HpsPr-T WT (Figure 5D) and, as a result, a similar IC_{50} was obtained (Table 4).

We performed a scale-up experiment to figure out the effect of PPRHs when increasing the number of cells. Keeping the concentration of either the PPRH or the Wedge-PPRH (100 nM) unchanged, we observed that there was a slight loss of effect when increasing the number of cells, but both molecules maintained its efficacy up to 200 000 cells. As shown in Figure 9C, Wedge-PPRH-17 maintained its efficacy significantly in a more stable way.

Regarding mRNA levels, Wedge-PPRH-17 caused a 2-fold decrease at 100 nM, whereas Wedge-PPRH WC did not cause a decrease in *survivin* mRNA level. (Figure 9D).

DISCUSSION

The purpose of this study was to improve the suitability of the polypurine reverse Hoogsteen hairpins as gene targeting tools by exploring several characteristics. Specifically, we focused on the following properties of PPRHs: (i) nucleotide length to define the optimal range in their design, (ii) affinity and effect compared with nonmodified TFOs, (iii) specificity toward the target sequence by using wild-type-PPRHs, and (iv) development of a new structure termed Wedge-PPRH.

PPRH Nucleotide Length. The possibility to design PPRHs depends on the presence of polypurine/polypyrimidine sequences in the target genes. Goñi et al.¹³ reported that triplex target sequences were overrepresented in the human genome, finding them commonly in regulatory regions. This abundance allows the design of PPRHs against almost any gene although each one will present different options of length for targeting. From our study, we can conclude that whenever possible, the longer the PPRH, the greater the effect, starting with a minimum of 20 nucleotides. In the case of the *TERT* gene used in this study, we observed binding of the PPRHs to their target from 20 to 30 nucleotides but the higher effect was obtained with the longest one.

Comparison between PPRHs and Nonmodified TFOs.

One difference between PPRHs and TFOs is that PPRHs are double-stranded DNA molecules whereas TFOs are single-stranded. Because of this, their binding differs: PPRHs form intramolecular reverse Hoogsteen bonds and bind by Watson–Crick bonds to their polypyrimidine target sequence, TFOs form Hoogsteen bonds with the purine strand in the double helix. Using the same binding conditions of pH and salt composition, and taking into account that the PPRH and the corresponding TFO have the same sequence, we observed that PPRHs bind at lower concentrations than TFOs to the target sequence, indicating a higher affinity. Moreover, in terms of cell viability, both PPRHs exerted a higher effect in PC3 and SKBR3 cells than TFOs, indicating that PPRHs were more effective.

Kool and colleagues¹⁸ had previously shown that hairpin structures formed by two purine domains could bind to the pyrimidine target sequence in a cooperative fashion and with higher affinity than the two separate strands. Thus, the existence of the hairpin structure represents a clear advantage over single-stranded molecules and proves that the strand that does not interact directly with the DNA contributes to the binding. In our work, we corroborated that the strand that allows the formation of the intramolecular Hoogsteen bonds within the PPRH favors its binding to the target sequence with higher affinity than TFOs. In addition, we prove that the increase in affinity displayed by PPRHs is reflected in a stronger effect in terms of cell viability.

Specificity of PPRHs. In the mismatches study, T_m experiments showed that the presence of mismatches caused a decrease in T_m , indicating less affinity for the target sequence, in accordance with previous results from Kool.¹⁸ In the case of HpsPr-T, 3 mismatches caused a decrease of around 17 °C in the T_m relative to the wild-type, whereas HpsPr-C, which also contained three mismatches, had a melting temperature of 25 °C below its wild-type counterpart. Therefore, T_m is affected not only by the length of the oligonucleotide but also by the presence of mismatches, proving the wild-type version is a better choice. Wang et al.⁷ also reported that the presence of a hairpin structure stabilized the binding, then allowing for the presence of mismatches, even though with a lower T_m .

Currently, one of the main problems of gene-silencing technologies is the off-target effects caused by lack of specificity. siRNAs are known to activate TLRs, leading to inflammation and other off-target effects.¹⁹ In this regard, PPRHs avoid off-target effects caused by activation of the immune system as opposed to siRNAs.¹⁵

Another problem intrinsic to the siRNA pathway is that siRNAs could bind to nontarget genes by acting as miRNAs.¹⁹ Other authors have reported that as few as 11 nucleotides are sufficient to silence nontargeted genes, so although degradation of siRNA is occurring, they can cause off-target effects.²⁰ Degradation of siRNAs is meant to occur earlier than in the case of PPRHs because their half-life is much shorter.¹⁵

In this work, we prove that wild-type PPRHs have a higher affinity to their target sequence, and therefore, they are meant to have less off-target effects caused by their binding to nontargeted sequences. That is, the more interruptions substituted by adenines, the lower the T_m and affinity, increasing the possible off-target effects. However, up to 3 mismatches in a sequence of 20 nucleotides has proved to be effective both in vitro and in vivo without known off-target effects.¹¹ Avoidance of off-target effects using the wild-type version and prevention of activation of the immune response are appreciable advantages of PPRHs over siRNAs.

Wedge-PPRH. As previously stated, PPRHs are highly stable and resistant without the need of chemical modifications, which is another advantage over aODNs, TFOs, or siRNAs. However, there is room for improvement in terms of binding or effect. For this reason, we developed a new molecule called Wedge-PPRH, which binds simultaneously to both strands of the target sequence. Other authors have tested similar strategies based on triplexes capable of binding to adjacent polypyrimidine and polypurine sequences in both strands, using what they called alternate-strand triplex formation.^{21,22} A Wedge-PPRH of the adequate length had a slightly better effect than PPRHs in decreasing cell viability and its effect was more constant as the number of incubated cells increases. Considering that the only difference between the Wedge-PPRH and the HpsPr-T WT is the 5' extension, we can conclude that the formation of the quintuplex structure, which locks the displaced strand of the dsDNA, contributes to the higher effect observed with the Wedge-PPRH.

As a summary, in this work, we investigated characteristics to improve the performance of PPRHs as a gene silencing tool and suggest a number of criteria to take into account when designing these molecules.

AUTHOR INFORMATION

Corresponding Author

*E-mail: vnove@ub.edu. Phone: +34 93 403 4455. Fax: +34 93 402 4520. Address: Department of Biochemistry and Molecular Biology, School of Pharmacy, Av. Diagonal 643, E-08028 Barcelona, Spain.

Notes

The authors declare no competing financial interest.

ACKNOWLEDGMENTS

The work was supported by Grant SAF2014-51825-R from “Plan Nacional de Investigación Científica” (Spain). Our group holds the Quality Mention from the “Generalitat de Catalunya” 2014-SGR96. L.R. and A.S. are recipients of FI fellowships from the “Generalitat de Catalunya”. X.V. is recipient of APIF fellowship from University of Barcelona. We thank Maria Tintoré and Sonia Pérez from CSIC for their help with T_m experiments and the use of MeltWin 3.5 software.

ABBREVIATIONS:

PPRH, polypurine reverse Hoogsteen hairpin; TFO, triplex-forming oligonucleotide; WT, wild-type; DOTAP, *N*-[1-(2,3-dioleoyloxy)propyl]-*N,N,N*-trimethylammonium methylsulfate; MTT, (3-(4,5-dimethylthiazol-2-yl)-2,5-diphenyltetrazolium bromide

REFERENCES

- (1) Felsenfeld, G.; Rich, A. Studies on the formation of two- and three-stranded polyribonucleotides. *Biochim. Biophys. Acta* **1957**, *26* (3), 457–68.
- (2) Hoogsteen, K. The crystal and molecular structure of a hydrogen-bonded complex between 1-methylthymine and 9-methyladenine. *Acta Crystallogr.* **1963**, *16*, 907–916.
- (3) Hewett, P. W.; Daft, E. L.; Laughton, C. A.; Ahmad, S.; Ahmed, A.; Murray, J. C. Selective inhibition of the human tie-1 promoter with triplex-forming oligonucleotides targeted to Ets binding sites. *Mol. Med.* **2006**, *12* (1–3), 8–16.
- (4) Postel, E. H.; Flint, S. J.; Kessler, D. J.; Hogan, M. E. Evidence that a triplex-forming oligodeoxyribonucleotide binds to the c-myc promoter

in HeLa cells, thereby reducing c-myc mRNA levels. *Proc. Natl. Acad. Sci. U.S.A.* **1991**, *88* (18), 8227–31.

(5) Praseuth, D.; Guieysse, A. L.; Helene, C. Triple helix formation and the antigene strategy for sequence-specific control of gene expression. *Biochim. Biophys. Acta* **1999**, *1489* (1), 181–206.

(6) Faucon, B.; Mergny, J. L.; Helene, C. Effect of third strand composition on the triple helix formation: purine versus pyrimidine oligodeoxynucleotides. *Nucleic Acids Res.* **1996**, *24* (16), 3181–8.

(7) Wang, S.; Kool, E. T. Recognition of Single-Stranded Nucleic Acids by Triplex Formation: The Binding of Pyrimidine-Rich Sequences. *J. Am. Chem. Soc.* **1994**, *116* (19), 8857–8858.

(8) Coma, S.; Noe, V.; Eritja, R.; Ciudad, C. J. Strand displacement of double-stranded DNA by triplex-forming antiparallel purine-hairpins. *Oligonucleotides* **2005**, *15* (4), 269–83.

(9) de Almagro, M. C.; Coma, S.; Noe, V.; Ciudad, C. J. Polypurine hairpins directed against the template strand of DNA knock down the expression of mammalian genes. *J. Biol. Chem.* **2009**, *284* (17), 11579–89.

(10) de Almagro, M. C.; Mencia, N.; Noe, V.; Ciudad, C. J. Coding polypurine hairpins cause target-induced cell death in breast cancer cells. *Human Gene Therapy* **2011**, *22* (4), 451–63.

(11) Rodriguez, L.; Villalobos, X.; Dakhel, S.; Padilla, L.; Hervas, R.; Hernandez, J. L.; Ciudad, C. J.; Noe, V. Polypurine reverse Hoogsteen hairpins as a gene therapy tool against survivin in human prostate cancer PC3 cells in vitro and in vivo. *Biochem. Pharmacol.* **2013**, *86* (11), 1541–54.

(12) Goni, J. R.; de la Cruz, X.; Orozco, M. Triplex-forming oligonucleotide target sequences in the human genome. *Nucleic Acids Res.* **2004**, *32* (1), 354–60.

(13) Goni, J. R.; Vaquerizas, J. M.; Dopazo, J.; Orozco, M. Exploring the reasons for the large density of triplex-forming oligonucleotide target sequences in the human regulatory regions. *BMC Genomics* **2006**, *7*, 63.

(14) Coma, S.; Noe, V.; Lavarino, C.; Adan, J.; Rivas, M.; Lopez-Matas, M.; Pagan, R.; Mitjans, F.; Vilaro, S.; Piulats, J.; Ciudad, C. J. Use of siRNAs and antisense oligonucleotides against survivin RNA to inhibit steps leading to tumor angiogenesis. *Oligonucleotides* **2004**, *14* (2), 100–13.

(15) Villalobos, X.; Rodriguez, L.; Prevot, J.; Oleaga, C.; Ciudad, C. J.; Noe, V. Stability and immunogenicity properties of the gene-silencing polypurine reverse Hoogsteen hairpins. *Mol. Pharmaceutics* **2014**, *11* (1), 254–64.

(16) Philippi, C.; Loretz, B.; Schaefer, U. F.; Lehr, C. M. Telomerase as an emerging target to fight cancer-opportunities and challenges for nanomedicine. *J. Controlled Release* **2010**, *146* (2), 228–40.

(17) McDowell, J. A.; Turner, D. H. Investigation of the structural basis for thermodynamic stabilities of tandem GU mismatches: solution structure of (rGAGGUCUC)₂ by two-dimensional NMR and simulated annealing. *Biochemistry* **1996**, *35* (45), 14077–89.

(18) Vo, T.; Wang, S.; Kool, E. T. Targeting pyrimidine single strands by triplex formation: structural optimization of binding. *Nucleic Acids Res.* **1995**, *23* (15), 2937–44.

(19) Burnett, J. C.; Rossi, J. J.; Tiemann, K. Current progress of siRNA/shRNA therapeutics in clinical trials. *Biotechnol. J.* **2011**, *6* (9), 1130–46.

(20) Jackson, A. L.; Bartz, S. R.; Schelter, J.; Kobayashi, S. V.; Burchard, J.; Mao, M.; Li, B.; Cavet, G.; Linsley, P. S. Expression profiling reveals off-target gene regulation by RNAi. *Natu. Biotechnol.* **2003**, *21* (6), 635–7.

(21) Balatskaya, S. V.; Belotserkovskii, B. P.; Johnston, B. H. Alternate-strand triplex formation: modulation of binding to matched and mismatched duplexes by sequence choice in the Pu-Pu-Py block. *Biochemistry* **1996**, *35* (41), 13328–37.

(22) Jayasena, S. D.; Johnston, B. H. Oligonucleotide-directed triple helix formation at adjacent oligopurine and oligopyrimidine DNA tracts by alternate strand recognition. *Nucleic Acids Res.* **1992**, *20* (20), 5279–88.

ARTICLE VI

**EFFECT OF POLYPURINE REVERSE HOOGSTEEN HAIRPINS ON RELEVANT
CANCER TARGET GENES IN DIFFERENT HUMAN CELL LINES**

Xenia Villalobos, Laura Rodríguez, Anna Solé, Carolina Lliberós, Núria Mencia,
Carlos J. Ciudad and Véronique Noé

Nucleic Acid Therapeutics. 2015 Aug;25(4):198-208.

Effect of Polypurine Reverse Hoogsteen Hairpins on Relevant Cancer Target Genes in Different Human Cell Lines

Xenia Villalobos, Laura Rodríguez, Anna Solé, Carolina Lliberós,
Núria Mencia, Carlos J. Ciudad, and Véronique Noé

We studied the ability of polypurine reverse Hoogsteen hairpins (PPRHs) to silence a variety of relevant cancer-related genes in several human cell lines. PPRHs are hairpins formed by two antiparallel polypurine strands bound by intramolecular Hoogsteen bonds linked by a pentathymidine loop. These hairpins are able to bind to their target DNA sequence through Watson–Crick bonds producing specific silencing of gene expression. We designed PPRHs against the following genes: *BCL2*, *TOP1*, *mTOR*, *MDM2*, and *MYC* and tested them for mRNA levels, cytotoxicity, and apoptosis in prostate, pancreas, colon, and breast cancer cell lines. Even though all PPRHs were effective, the most remarkable results were obtained with those against *BCL2* and mammalian target of rapamycin (*mTOR*) in decreasing cell survival and mRNA levels and increasing apoptosis in prostate, colon, and pancreatic cancer cells. In the case of *TOP1*, *MDM2*, and *MYC*, their corresponding PPRHs produced a strong effect in decreasing cell viability and mRNA levels and increasing apoptosis in breast cancer cells. Thus, we confirm that the PPRH technology is broadly useful to silence the expression of cancer-related genes as demonstrated using target genes involved in metabolism (*DHFR*), proliferation (*mTOR*), DNA topology (*TOP1*), lifespan and senescence (*telomerase*), apoptosis (*survivin*, *BCL2*), transcription factors (*MYC*), and proto-oncogenes (*MDM2*).

Introduction

GENE SILENCING HAS BECOME an essential technique for molecular biology validation and therapeutics. Up until now, RNA-targeting approaches such as antisense oligodeoxynucleotides (aODNs) and small interfering RNAs (siRNAs) have been used, and recently, protein-based approaches [zinc-finger nucleases (ZFN), TALENs, and CRISPR/Cas9] have emerged [1,2,3–5]. As an additional tool, we developed a new type of silencing molecules called polypurine reverse Hoogsteen hairpins (PPRHs). These molecules have the advantages of increased stability and low immunogenicity compared to siRNAs [6].

PPRHs are nonmodified DNA molecules formed by two antiparallel polypurine strands linked by a pentathymidine loop that allows the formation of intramolecular reverse-Hoogsteen bonds between both strands, acquiring a hairpin structure. The hairpins bind by Watson–Crick bonds to polypyrimidine stretches in the DNA, which can be located in the promoter, exonic, and intronic regions. We described the ability of PPRHs to bind both the template [7] and coding [8] strands of the dsDNA, forming a triplex structure that knocks down the expression of the target genes. Template-PPRHs bind to the template strand of the DNA, whereas coding-PPRHs bind to the coding sequence of the DNA and can also

bind to transcribed RNA. The mechanism of action of PPRHs depends on the location of their target; we demonstrated that a coding-PPRH directed against a polypyrimidine region in intron 3 of *DHFR* pre-mRNA produced a splicing alteration by preventing the binding of the splicing factor U2AF65. On the other hand, two PPRHs directed against the template or coding strand of the *survivin* promoter sequence decreased the binding of transcription factors Sp1 and GATA-3, respectively. The *in vivo* administration of the coding-PPRH against the promoter region of the *survivin* gene was able to delay tumor growth in a prostate xenograft mouse model [9].

Several genes have been described as relevant for cancer. These include the antiapoptotic protein *BCL2*, the proto-oncogene *MDM2*, the transcription factor *MYC*, the enzyme Topoisomerase-1 (*TOP1*), which is a clinically validated target, and the protein kinase *mTOR*. These targets are usually overexpressed either by gene amplification or by overactivation in tumors [10–16].

The aim of this study was to demonstrate the general applicability of PPRHs as silencing tools in cancer therapy. Therefore, we tested several PPRHs directed against an array of relevant genes in different cancer cell lines, including pancreatic cancer MIA PaCa-2 cells, colon cancer HCT 116 cells, prostate cancer PC-3 cells, and breast cancer cell lines

MCF7, MDA-MB-468, and SKBR3. The ability of the designed PPRHs to decrease cell survival of the different cell lines by causing apoptosis and their effect on the mRNA levels of the targets were evaluated.

Materials and Methods

Oligonucleotides

PPRHs and primers were synthesized as nonmodified oligodeoxynucleotides by Sigma-Aldrich. They were dissolved at 1 mM (stock solution) in a sterile RNase-free Tris-EDTA buffer (1 mM EDTA and 10 mM Tris, pH 8.0) and stored at -20°C until use. PPRHs were designed using the Triplex-Forming Oligonucleotide Target Sequence Search tool available at <http://spi.mdanderson.org/tfo/> to find the polypurine tracks present in a gene and, thus, the polypyrimidine targets. If purine interruptions (up to three) were present in the pyrimidine target sequence, when designing the PPRHs those positions were substituted by either an adenine or the complementary pyrimidine. The specificity of the chosen polypurine tracks was evaluated by BLAST analyses.

Two types of negative controls were used for every targeted gene: (1) sequences that form intramolecular Watson-Crick bonds (Hp-WC), instead of reverse Hoogsteen bonds, thus preventing the formation of an additional W:C bond to the target DNA, and consequently triplex formation [7,8] and (2) scrambled sequences that do not bind to the target (Hp-Sc). For the initial screening of the study, we used several PPRHs for either BCL2 or mTOR. Then, we used the same scrambled PPRH to corroborate that an oligonucleotide with a hairpin conformation did not affect cellular viability. For the rest of the genes, Topoisomerase, MDM2, and Myc, we decided to use specific scrambled PPRHs for each gene containing a similar G/A polypurine content. Therefore, globally we used a collection of different negative controls. Table 1 describes all oligonucleotide names and sequences used in this work.

Cell culture

Pancreatic cancer MIA PaCa-2, prostate cancer PC-3, colon cancer HCT 116, and breast cancer SKBR3, MCF7, and MDA-MB-468 cell lines were used throughout the study. Cell lines were routinely grown in Ham's F-12 medium supplemented with 7% fetal calf serum (both from Gibco) at 37°C in a 5% CO_2 -controlled humidified atmosphere.

Transfection of PPRHs

Cells were plated the day before transfection, which consisted in mixing the appropriate amount of PPRH and N-[1-(2,3-dioleoyloxy)propyl]-N,N,N-trimethylammonium methylsulfate (DOTAP; Roche or Biontex) for 20 min in a volume of 200 μL of medium at room temperature, followed by the addition of the mixture to the cells in a total volume of 1 mL. When transfecting the PPRHs at 100 nM (final concentration), DOTAP was used at 10 μM ; for lower concentrations of PPRH, DOTAP was used at 5 μM .

Cellular uptake of PPRHs

One hundred fifty thousand cells were plated in 50-mm dishes with 2 mL complete F-12 medium and transfected with

100 nM of a fluorescent-labeled PPRH and DOTAP (10 μM). Twenty-four hours after transfection, cells were collected, centrifuged at 800g at 4°C for 5 min, and washed once in phosphate-buffered saline (PBS). The pellet was resuspended in 500 μL PBS plus propidium iodide (PI, final concentration 5 $\mu\text{g}/\text{mL}$; Sigma-Aldrich). Cells were kept on ice for no longer than 30 min before flow cytometry analysis was performed in a Coulter XL cytometer (Beckman Coulter, Inc.).

RNA extraction

At the end of the experiments, total RNA was extracted from cells using either Ultraspec (Biotecx) or TRIzol (Life Technologies) following the manufacturer's specifications. Quantification of RNA was conducted measuring its absorbance at 260 nm using a NanoDrop ND-1000 spectrophotometer (Thermo Scientific).

RNA determination

cDNA was synthesized by reverse transcription in a 20 μL reaction mixture containing 1 μg of total RNA, 125 ng of random hexamers (Roche), 10 mM dithiothreitol, 20 U of RNasin (Promega), 0.5 mM of each dNTP (AppliChem), 4 μL of buffer (5 \times), and 200 U of Moloney murine leukemia virus reverse transcriptase (Invitrogen). The reaction was incubated at 37°C for 1 h. Three microliters of the cDNA mixture was used for real-time PCR amplification using StepOnePlus™ Real-Time PCR Systems (Applied Biosystems, Life-Technologies) with specific primers for each gene to be determined.

In the case of BCL2 and mammalian target of rapamycin (mTOR), RNA levels were determined using the assays-on-demand (HS00608023_M1) and (HS00234508_M1), respectively, and HS00975725_M1 for adenine phosphoribosyltransferase (APRT) as the endogenous control (all from Applied Biosystems). The reaction was performed following the manufacturer's recommendations. For MDM2, MYC, and TOP1, mRNA levels were determined by SYBR-Green reverse transcription quantitative-PCR and the pair of primers listed in Table 2, using APRT as an endogenous control. Fold changes in gene expression were calculated using the standard $\Delta\Delta\text{Ct}$ method.

Cell survival experiments (MTT)

Cells were plated in six-well dishes in the Ham's F-12 medium. Six days after PPRH transfection, 0.63 mM of 3-(4,5-dimethylthiazol-2-yl)-2,5-diphenyltetrazolium bromide and 100 μM of sodium succinate (both from Sigma-Aldrich) were added to the culture medium and allowed to react for 3 h at 37°C before the addition of the solubilization reagent (0.57% acetic acid and 10% SDS in DMSO). Cell viability was measured at 570 nm in a WPA S2100 Diode Array Spectrophotometer. The results were expressed as the percentage of cell survival relative to the control (untreated cells).

Apoptosis

Apoptosis was determined by measuring the activity of caspase-3 and caspase-7 with the Caspase-Glo® 3/7 Assay (Promega). Cells (5,000) were plated in 96-well plates in the F12 medium. After 24 h, 100 nM of each PPRH was

TABLE 1. POLYPURINE REVERSE HOOGSTEEN HAIRPINS USED IN THIS STUDY

Name	Sequence (5' → 3')	Location	Type
HpBcl2Pr-C	GGAGAGGGGAGGGGAGAAGGAGGTTTTTGGAGGAAGAGGGGAGGGGA GAGG	Promoter - 378	+
HpBcl2E1-C	GAGGGGAGAGGGGAGAAAAATTTTTAAAAAAGAGGGAGAGGGGAG	Exon 1 +65	+
HpBcl2I2-T	GAAGGGGAAGAAGAGAGAGAAGAGAGAGATTTTTAGAGAGAGAAGA GAGAGAAGAAGGGGGAAG	Intron 2 + 32279	+
HpBcl2I2-C	GGGGAGGAGGAAAAGAAGGAAGGAAGAGGTTTTTGGAGAAGGAAG GAAGAAAAGGAGGAGGGG	Intron 2 + 112542	+
HpBcl2E1-WC	CTCCCCTCTCCCTCTTTTTTTTTTTAAAAAAGAGGGAGAGGGGAG	-	-
HpTorPr-C	GGGAGCGAGGGAAGGAGGGTTTTTGGGAGGAAGGGAGCGAGGG	Promoter - 3137	+
HpTorE5-C	GGAAGAAGAAGGAAGGGAAGTTTTTGAAGGAAGGAAGAAGAAGG	Exon 5 149614	+
HpTor-T	GATGGTGGAGAAAGGAAGAGAGGGTTTTTGGGAGAGAAGGAAA GAGGTGGTAG	Intron 15 126405	+
HpTorI17-C	GGGAAAGGGGAGGGAAAAAAGATTTTTAGAAAAAAGGGAGGG GAAAGGG	Intron 17 124527	+
HpTorPr-WC	CCCTCCTTCCCTCGCTCCCTTTTTTGGGAGGAAGGGAGCGAGGG	Promoter - 3137	-
Hp-Sc1	AAGAGAAAAAGAGAAAGAAGAGAGGGTTTTTGGGAGAGAAGAAAGA GAAAAAGAGAA	-	-
HpTopI2-T	GGAGAGGAGGAGGGGAGAAAAATTTTTAAAAGAGGGAGGAGGAGAGG	Intron 2 + 2363	+
HpTopI2-WC	CCTCACCTCCTCCCTCTTTTTTTTTTAAAAGAGGGAGGAGGAGAGG	Intron 2 + 2363	-
Hp-Sc2	AGAGGAGAGAAGGAAGGAGGTTTTTGGAGGAAGGAAGAGAGGAGA	-	-
HpMdmI7-T	GGGAAGGAAAGAAGAAGGGAGTTTTT GAGGGAAGAAGAAAGGAAGGG	Intron 7 + 17644	+
HpMdmI7-WC	CCCTTCCTGTCTTCTGCCCGCTTTTT GAGGGAAGAAGAAAGGAAGGG	Intron 7 + 17644	-
Hp-Sc3	GAGAAGAGGAAGAGAGGAAGGTTTTTGGAAAGGAGAGAAGGAGAAGAG	-	-
HpMycI1-T	GGGAAAAAGGGAGAAAGGAAGAGGAGGGAAAGAATTTTTAAGAAGG GAGAGGAGAAGGAAGAGGGAAAAAGGG	Intron 1 + 745	+
HpMycI1-WC	CCTTTTTCCCTTTCCTTCTCCTTCCCTTTTTTTAAGAAGGGAGAG GAGAAGGAAGAGGGAAAAAGGG	Intron 1 + 745	-
Hp-Sc4	AGAGAAGAGGAAGAGAGGAAAGAGAGGAAGAGGATTTTTAGGAGAAG GAGAGAAAGGAGAGAAGGAGAAGAGA	-	-

Name, sequence, gene location, and type: specific (+) or negative control (-) of the PPRHs used in this study. Letters in *bold* indicate the bases placed opposite the purine interruptions present in the pyrimidine target, either adenine substitutions or the complementary pyrimidine.

transfected using 10 μ M of DOTAP (final concentration) in a volume of 50 μ L, and 24 h after transfection, 50 μ L of the Caspase-Glo 3/7 reagent was added. Luminescence was measured after 1 h using a ModulusTM Microplate luminometer (Turner Biosystems; Promega). The F12 medium was considered the blank control and untreated cells the background. In the case of SKBR3, MCF7, and MDA-MB-

468 cells, apoptosis was also determined by the rhodamine method: cells (120,000) were plated in 50-mm dishes with 2 mL of complete F-12 medium and transfected with 100 nM of each PPRH. Twenty-four hours after treatment, rhodamine (final concentration 5 μ g/mL) (Sigma-Aldrich) was added for 30 min, the cells were collected, centrifuged at 800g at 4°C for 5 min, and washed once in PBS. The pellet

TABLE 2. PRIMERS USED FOR REVERSE TRANSCRIPTION QUANTITATIVE-PCR

	FWD primer (5'-3')	REV primers (5'-3')	Amplicon (bp)
MDM2	CAGCTTCGGAACAAGAGACC	GTCCGATGATTCCTGCTGAT	293
MYC	TTCGGGTAGTGGAACCAG	CCTCCTCGTCGCAGTAGAAA	120
TOP1	GAGAAGGACCGGGAAAAGTC	TATTTTTGCATCCCCAGAGG	186
APRT	GCAGCTGGTTGAGCAGCGGAT	AGAGTGGGGCCTGGCAGCTTC	272

Sequence of the primers used for determining MDM2, MYC, and TOP1 RNA levels and amplicon length.

TABLE 3. TRANSFECTION EFFICIENCY OF THE DIFFERENT CELL LINES

Cell line	% Positive cells	Mean fluorescence
MIA PaCa2	85.05 ± 6.3	57 ± 24.8
PC3	90.2 ± 2.9	555.3 ± 166.7
HCT 116	90.8 ± 8.2	241 ± 81
SKBR3	89.8 ± 4.5	434.5 ± 49.5
MCF7	81.95 ± 16.1	762.5 ± 117
MDA-MB-468	95.8 ± 3.6	498.4 ± 103.5

Percentage of fluorescent cells and the raw mean fluorescence 24 h after transfection. Cells were incubated with 100 nM fluorescent PPRHs for 24 h. Fluorescence was determined by flow cytometry.

was resuspended in 500 µL of PBS with PI (final concentration 5 µg/mL; (Sigma-Aldrich). Flow cytometry analyses were performed in a Coulter XL cytometer, and data were analyzed using the software Summit v4.3. The percentage of Rho-negative and IP-negative cells corresponded to the apoptotic population.

Statistical methods

Values are expressed as the mean ± SE. Data were evaluated by unpaired Student's *t*-test when analyzing the difference between two conditions, control and treated. The analyses were performed using the software IBM SPSS Statistics v20. Differences with *P* values < 0.05 were taken as statistically significant.

Results and Discussion

The goal of this work was to evaluate whether PPRHs could be used as silencing agents against different targets in cell lines corresponding to several cancer types to expand the usage of PPRHs in cancer therapy and prove their general applicability. For this purpose, we chose an array of therapeutically interesting genes to act as reporter genes for the silencing activity of the PPRHs. The chosen target genes encompass a variety of biological functions: antiapoptotic genes, topoisomerases, protein kinases, and transcription factors. We were able to design PPRHs directed against polypyrimidine stretches of every gene to be targeted; three of these stretches were located in introns (*MYC*, *MDM2*, *TOP1*), one in a promoter region (*mTOR*), and one in an

exonic sequence (*BCL2*), which were tested in a variety of cell lines (HCT 116, PC-3, MIA PaCa-2, SKBR3, MCF7, and MDA-MB-468).

The transfection efficiency was determined through uptake experiments performed by transfecting 100 nM of fluorescent PPRHs with 10 µM DOTAP in the different cell lines. In Table 3 it can be seen that the percentage of fluorescent cells in all cell lines was very high, although the mean intensity varied among them.

The results obtained for each PPRH are presented and discussed below.

BCL2 protein

BCL2 is an antiapoptotic protein, the overexpression of which in multiple cell lines contributes to cancer progression and it is also related to resistance to chemotherapy [17]. Regarding solid tumors, *BCL2* is overexpressed in 30%–60% of prostate cancers at diagnosis and in nearly 100% of castration-resistant prostate cancer [12] and its content has been related to increased resistance to gemcitabine [18]. Antisense oligonucleotides (oblimersen), antibodies, peptides, and small molecules against *BCL2* are under development. Even though partially successful, none of these approaches has been proven to be useful in the clinic because they present problems of specificity, side effects, short half-life, and delivery [17].

We performed an initial screening of four PPRHs against different target sequences within the *BCL2* gene (Fig. 1); the screening consisted in determining the cell survival of three different cell lines (MIA PaCa-2, PC-3, and HCT 116) after transfecting the PPRHs at different concentrations (30 and 100 nM). In Fig. 2, it can be observed that not all PPRHs were equally effective and, in this case, the most effective PPRH was HpBcl2E1-C, directed against the coding strand of exon 1, which was able to decrease survival by 90%–95% in all cell lines at a concentration of 100 nM. As negative controls, HpBcl2E1-WC and Hp-Sc1 were used; these did not cause a significant decrease of survival in any cell line.

We explored whether a combination of two different PPRHs was able to increase their efficiency. As seen in Fig. 3a, when cotransfecting HpBcl2E1-C and HpBcl2Pr-C at low concentrations (12.5 nM each, 25 nM in total), their effect was greater than when transfecting 25 nM of each PPRH separately. For higher concentrations, we did not observe any improvement since the PPRHs by themselves, especially

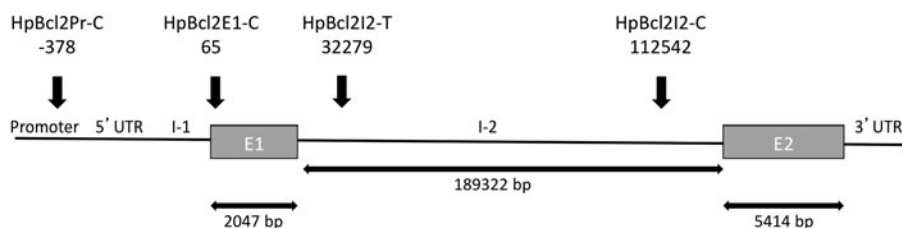


FIG. 1. Scheme representing the target sequences of the polypurine reverse Hoogsteen hairpins (PPRHs) against the *BCL2* gene. Four PPRHs were designed for the *BCL2* gene directed against the promoter (HpBcl2Pr-C), exon 1 within the 5'UTR (HpBcl2E1-C) and two other PPRHs against intron 2, one template (HpBcl2I2-T) and one coding (HpBcl2I2-C). The nomenclature used was Hp (Hairpin), Bcl2 (*BCL2*), Pr (promoter), I (intron), and E (exon). The numbering below the PPRHs corresponds to the target sequence start referred to the transcriptional start site of the gene. The arrows indicate the length of each gene element.

FIG. 2. Initial screening of PPRHs against *BCL2*. Ten thousand MIA PaCa-2 (■, black bars), PC-3 (▒, gray), and HCT 116 (□, white) cells were plated and transfected the following day with either 30 or 100 nM of the different PPRHs. MTT assays to determine cell survival were performed 6 days after transfection. Data are the mean ± SE values of at least three experiments. As negative controls HpBcl2-WC and Hp-Sc1 at 100 nM were used.

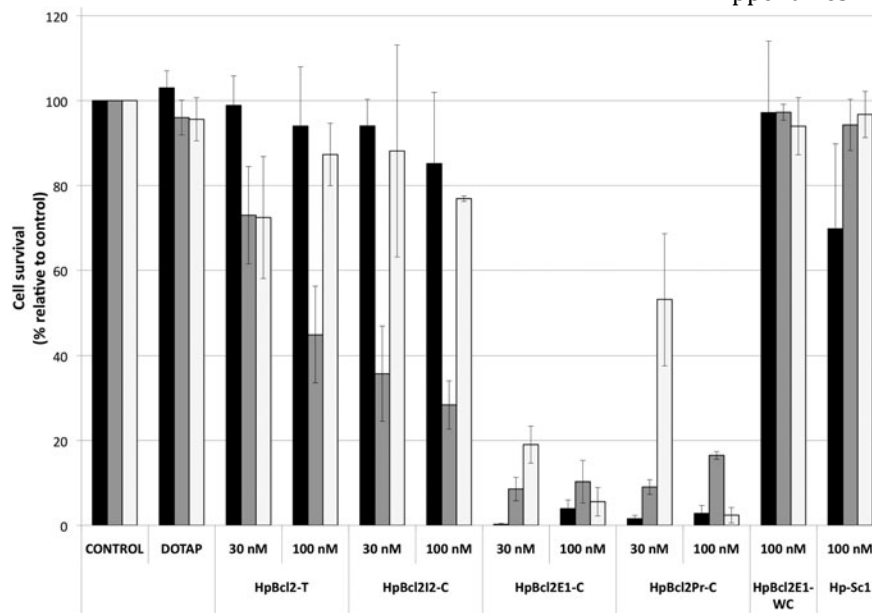
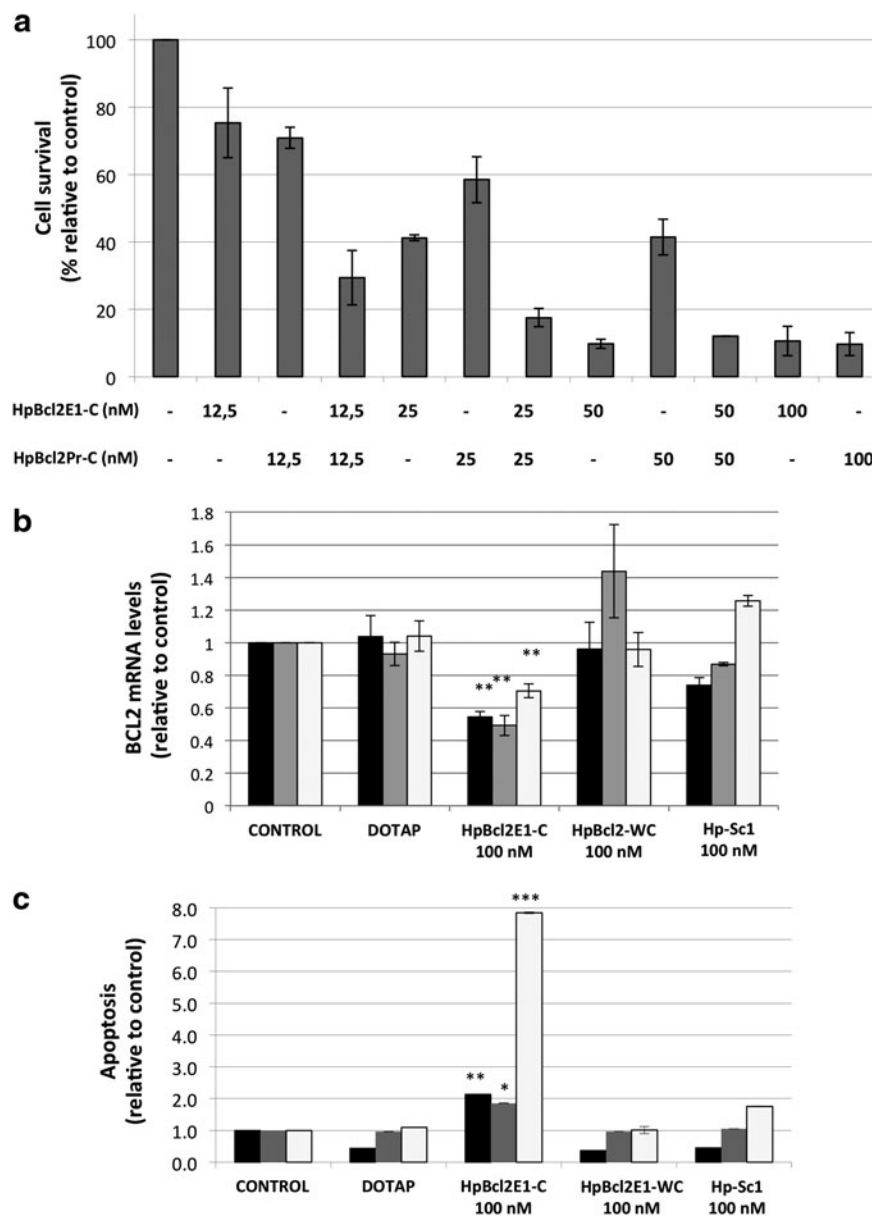


FIG. 3. Effect of HpBcl2E1-C on cell viability, *BCL2* mRNA levels, and apoptosis. (a) MTT assays to determine survival of PC-3 (▒, gray) cells were performed 6 days after transfecting different concentrations of HpBcl2E1-C and HpBcl2Pr-C. (b) Total RNA was extracted from MIA PaCa-2 (■, black bars), PC-3, and HCT 116 (□, white) cells (60,000) 24 h after the transfection with the different PPRHs at a concentration of 100 nM. (c) MIA PaCa-2, PC-3, and HCT 116 cells were transfected with 100 nM of either HpBcl2E1-C or the negative controls HpBcl2-WC and Hp-Sc1. Apoptosis was determined by the activity of caspase-3 and caspase-7 after 24 h of transfection. All results are expressed as change in relative light units (RLU) relative to control. Data are the mean ± SE values of at least three experiments. * $P < 0.05$, ** $P < 0.01$, *** $P < 0.005$ compared with control.



HpBcl2E1-C, are very efficient. The subsequent mRNA determinations were performed for HpBcl2E1-C. This reduction in cell survival was accompanied by a twofold decrease in BCL2 mRNA levels in MIA PaCa-2 and PC3 cells and by a 1.4-fold decrease in HCT 116 cells (Fig. 3b) when HpBcl2E1-C was transfected, but not when the negative controls were used. It has been reported [19] that a twofold decrease in BCL2 caused a decrease in tumor growth. Since BCL2 acts as an antiapoptotic protein, we studied whether the decrease in cell survival was due to an increase in apoptosis. We transfected HpBcl2E1-C into the different cell lines, and after a 24-h incubation, we determined the activity of caspase-3 and caspase-7 with the Caspase-Glo 3/7 Assay. Apoptosis was increased 2.2-, 2-, and 7.8-fold in MIA PaCa-2, PC-3, and HCT 116 cells, respectively (Fig. 3c).

Topoisomerase-1

Topoisomerase-1 is a clinically validated target; TOP1 inhibitors, such as camptothecin (CPT) and its derivatives (irinotecan and topotecan), have been used as anticancer therapy since the late 90s. The cytotoxicity of these drugs is dependent on the expression of topoisomerase I, which is overexpressed in tumors, relative to the corresponding normal tissue [20] and during DNA replication [21,22]. We examined if silencing the expression of this gene using a

specific PPRH led to decreased survival as well. The target sequence for the PPRH against *TOP1* (HpTopI2-T) is located in the template strand of intron 2. Our results showed that inhibition of TOP1 produced a decrease in cell survival of 95%, 60%, and 85% in SKBR3, MCF7, and MDA-MB-468 cell lines, respectively (Fig. 4a). The negative controls HpTopI2-WC and Hp-Sc2 produced a slight decrease in cell survival, between 20% and 40% depending on the cell line, but this decrease did not reach significance. The decrease in cell survival when the specific PPRH was transfected was paralleled by a decrease in TOP1 mRNA levels of 1.8-, 2-, and 1.4-fold in SKBR3, MCF7, and MDA-MB-468 cells, respectively (Fig. 4b). HpTopI2-T at 100 nM caused a 4.2-fold increase in apoptosis measured by the caspase 3/7 method in MDA-MB-468 cells, while in SKBR3 cells, apoptosis was not detected (Fig. 4c). Since MCF7 cells do not express caspase-3, the apoptosis produced by HpTopI2-T was measured by the rhodamine method in the three cell lines, observing an increase of apoptotic cells in all these cell lines (Fig. 4d).

Mammalian target of rapamycin

mTOR is a 289 kDa serine/threonine protein kinase. mTOR is a central modulator of cell growth and plays a critical role in transducing proliferative signals mediated by the PI3K/AKT/

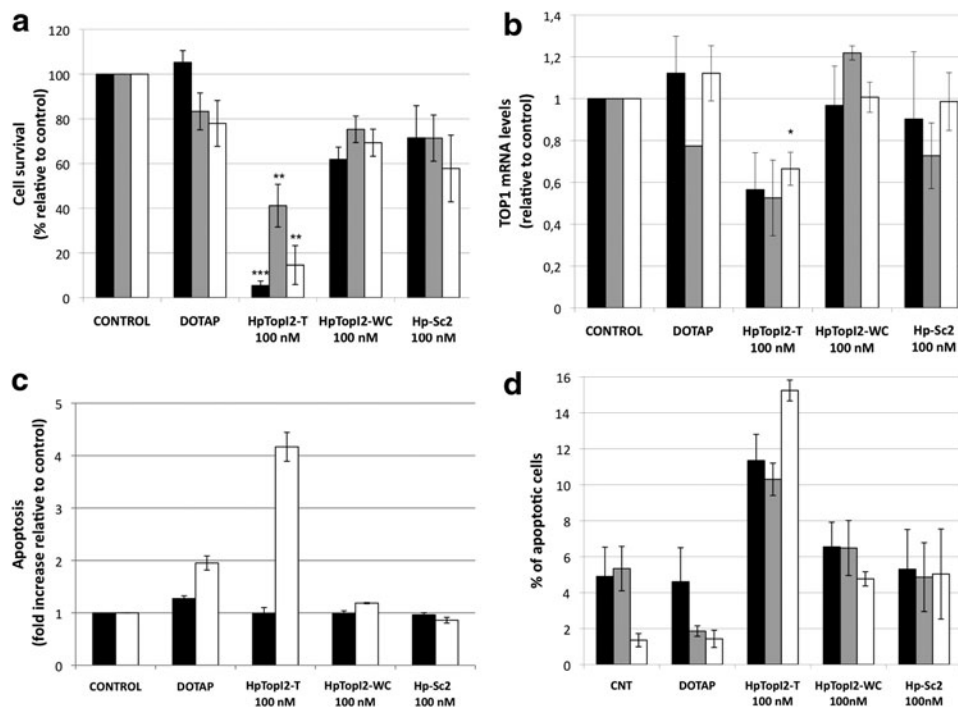


FIG. 4. Effect of HpTopI2-T on cell viability, TOP1 mRNA levels, and apoptosis. **(a)** SKBR3 (■, black bars), MCF7 (■, gray), and MDA-MB-468 (□, white) cells (30,000) were plated in six-well dishes and transfected with HpTopI2-T and the negative controls HpTopI2-WC and Hp-Sc2 at 100 nM. MTT assays to determine the cell survival were performed 6 days after transfection. **(b)** RNA was extracted from SKBR3, MCF7, and MDA-MB-468 cells (30,000) 48 h after the transfection with HpTopI2-T, HpTopI2-WC, and Hp-Sc2 at 100 nM. **(c)** Apoptosis in SKBR3 and MDA-MB-468 cells was measured with the Caspase-Glo[®] 3/7 Assay. All results are expressed as change in RLU relative to the control. **(d)** Apoptosis in SKBR3, MCF7, and MDA-MB-468 cells (120,000) determined by the rhodamine method. Rho123-negative and IP-negative cells were considered as apoptotic cells. Data are the mean ± SE values of at least three experiments. **P* < 0.05, ***P* < 0.01, ****P* < 0.005, compared with control.

mTOR signaling pathway in response to nutrient availability and growth factor stimuli [23,24]. The PI3K/AKT/mTOR pathway is a prosurvival pathway that is constitutively activated in many types of cancer. It plays an important role in cancer development, progression, and therapeutic resistance.

We designed four PPRHs against the *mTOR* gene, one against a polypyrimidine stretch in the template strand of intron 15 and three against different regions of the coding strand: promoter, exon 5, and intron 17. After the initial screening in HCT 116 cells (Fig. 5a), we determined that the PPRH against the promoter region (HpTorPr-C) was the most effective, causing a decrease on cell survival higher than 90%. We incubated cells for different periods of time before renewing the culture medium to determine the time dependency, observing that short incubations already had a strong effect on cell survival. Figure 5b shows that incubations as short as 24 h with 100 nM of HpTorPr-C produced a 70% decrease in cell survival; cell survival further decreased as the incubation time with the PPRH increased. We corroborated the effect of HpTorPr-C by determining mTOR mRNA levels, which decreased 1.6-fold (Fig. 5c) 48 h after transfecting the specific PPRH. The negative controls, HpTorPr-WC and Hp-Sc1, did not produce a sig-

nificant decrease in cell survival or in mRNA levels. Apoptosis measured by the caspase 3/7 method increased fourfold after 24 h of treatment with HpTorPr-C (Fig. 5d) compared with the slight effect observed by the transfection agent DOTAP or the negative controls. These results confirm the efficacy of HpTorPr-C in disrupting the PI3K/AKT/mTOR pathway in HCT 116 cells.

MDM2 regulator

MDM2 is a negative regulator of the tumor suppressor protein p53, which is the most frequently mutated gene in human cancer [25]. Releasing p53 from MDM2 has been suggested as a mechanism for cancer therapy [26], especially in cancer types with wild-type p53 and overexpressed MDM2. In 2004, Nutlins, MDM2 inhibitors, were identified and studies with these compounds have strengthened the idea that p53 activation might represent an alternative to chemotherapy [27]. A way of mimicking the activation of p53 through inhibition of MDM2 is by silencing the expression of MDM2. We designed a template-PPRH that targets intron 7 of the *MDM2* gene. Transfection of this PPRH led to a decrease in cell survival of 50%, 60%, and 85% in SKBR3,

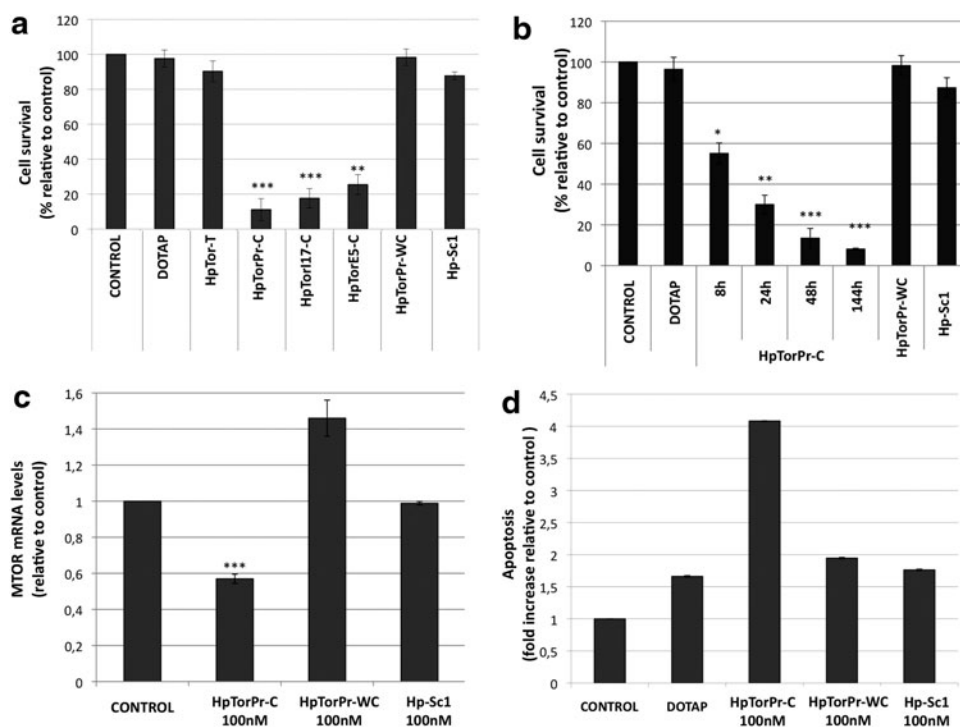


FIG. 5. Screening of PPRHs against mammalian target of rapamycin (mTOR), time course, and effect of HpTorPr-C on mTOR mRNA levels, and apoptosis. (a) HCT 116 cells (5,000) were plated in six-well dishes and transfected with 100 nM of four different PPRHs (HpTor-B, HpTorPr-C, HpTor17-C, HpTorE5-C). MTT assays to determine cell survival were performed 6 days after transfection. (b) Time course of HpTorPr-C on cell viability was performed by renewing the medium after 8, 24, 48, or 144 h of the transfection. The negative controls HpTorPr-WC and Hp-Sc1 were transfected at 100 nM for 144 h. MTT assays of all time points were performed 6 days after the initial transfection. (c) Total RNA was extracted from HCT 116 cells (60,000) 48 h after the transfection with either HpTorPr-C or the negative controls HpTorPr-WC and Hp-Sc1 at a concentration of 100 nM. (d) HCT 116 cells (5,000) were plated in 96-well dishes and transfected with 100 nM of either HpTorPr-C or the negative controls HpTorPr-WC and Hp-Sc1. Apoptosis was measured by the activity of caspase-3 and -7 after 24 h of transfection. All results are expressed as change in RLU relative to control. Data are the mean \pm SE values of at least three experiments. * $P < 0.05$, ** $P < 0.01$, *** $P < 0.005$, compared with control.

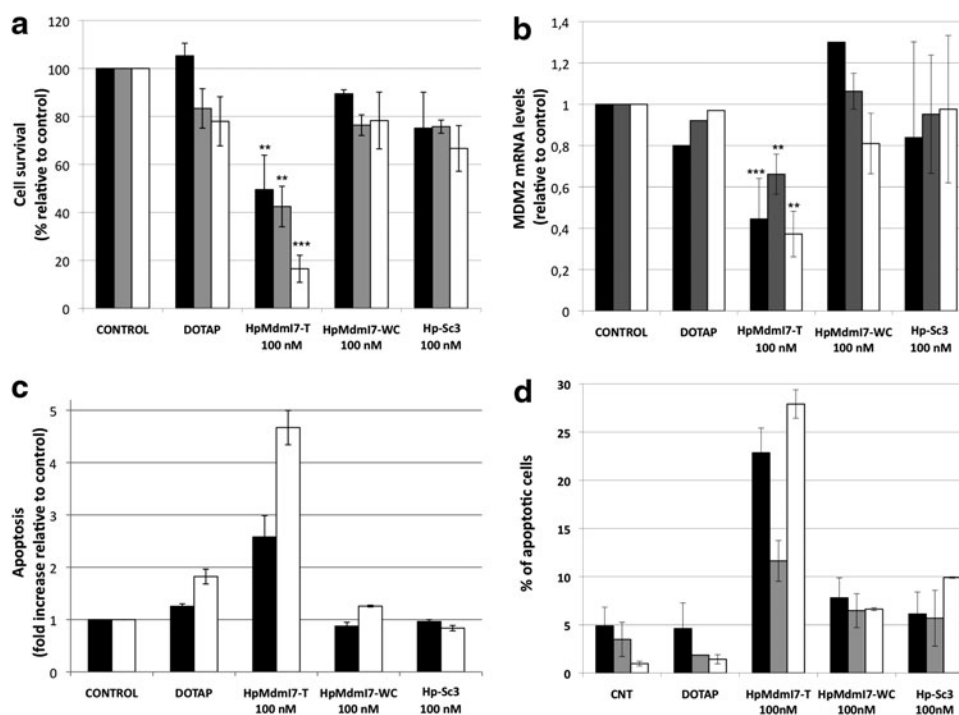


FIG. 6. Effect of HpMdmI7-T on cell viability, MDM2 mRNA levels, and apoptosis. (a) SKBR3 (■, black bars), MCF7 (■, gray), and MDA-MB-468 (□, white) cells (30,000) were plated in six-well dishes and transfected with HpMdmI7-T and the negative controls HpMdmI7-WC and Hp-Sc3 at 100 nM. MTT assays to determine the cell survival were performed 6 days after transfection. (b) Total RNA was extracted from SKBR3, MCF7, and MDA-MB-468 cells (30,000) 48 h after the transfection with either HpMdmI7-T or the negative controls HpMdmI7-WC and Hp-Sc3 100 nM. (c) Apoptosis in SKBR3 and MDA-MB-468 cells was measured with the Caspase-Glo 3/7 Assay. All results are expressed as change in RLU relative to the control. (d) Apoptosis in SKBR3, MCF7, and MDA-MB-468 cells (120,000) determined by the rhodamine method. Rho123-negative and IP-negative cells were considered as apoptotic cells. Data are the mean ± SE values of at least three experiments. ** $P < 0.01$, *** $P < 0.005$, compared with control.

MCF7, and MDA-MB-468 cells, respectively (Fig. 6a); the negative controls HpMdmI7-WC and Hp-Sc3 did not cause any relevant effect on cell survival. A decrease in MDM2 mRNA levels was also evident achieving a 2.3-, 1.5-, and 2.7-fold decrease depending on the cell line (Fig. 6b). Regarding apoptosis, it increased 2.6-fold in SKBR3 cells and 4.7-fold in MDA-MB-468 cells (Fig. 6c) as measured by the caspase 3/7 method, whereas the negative controls did not have any significant effect. Rhodamine determination showed that the percentage of apoptotic cells greatly increased in the three cell lines (Fig. 6d).

Interestingly, our results show that releasing p53 from MDM2 significantly reduces survival of the three cell lines, regardless of their p53 status; SKBR3 cells and MDA-MB-468 cells contain a mutated version of p53, while MCF7 cells contain wild-type p53. In this sense, our results are in agreement with Wang and collaborators [28] who described that silencing of MDM2, using antisense oligonucleotides, in MCF7 and MDA-MB-468 cell lines had significant antitumor activity, both *in vitro* and *in vivo*. It is possible that silencing MDM2 using the PPRH technology is an alternative way to cause cell death through p53-dependent and p53-independent mechanisms.

MYC transcription factor

MYC is a transcription factor involved in many biological processes, including cell growth, cell cycle progression, me-

tabolism, and survival. It has been established that MYC overexpression is essential for tumor initiation and maintenance [29] and its overactivation frequently results in the dependence of tumor survival on high levels of MYC, also called MYC addiction. The direct inhibition of MYC through small molecules has not been accomplished; as a transcription factor, MYC represents a challenging target since it functions through protein-protein interactions and lacks enzymatic activity. Therefore, MYC is considered the prototype of an undruggable target. The template-PPRH HpMycI1-T targets intron 1 of the MYC gene.

Our results showed that silencing of MYC using HpMycI1-T produced a decrease in cell viability in all the breast cancer cell lines used: 85% in SKBR3 cells, 80% in MCF7 cells, and 95% in MDA-MB-468 cells (Fig. 7a). The negative control HpMycI1-WC had a slight effect on cell survival that can be due to the binding of the negative control to the target, because it shares the target-binding sequence with the specific PPRH (HpMycI1-T). The decrease in cell viability was accompanied by a decrease in the levels of mRNA of 2.5-, 2.1-, and 1.4-fold in SKBR3, MCF7, and MDA-MB-468 cells, respectively (Fig. 7b). Apoptosis by the caspase 3/7 method was increased after transfection with HpMycI1-T in MDA-MB-468 cells (6.2-fold) and in SKBR3 cells (2-fold) (Fig. 7c). Rhodamine determination showed that the percentage of apoptotic cells greatly increased in the three cell lines. The negative controls did not produce an important

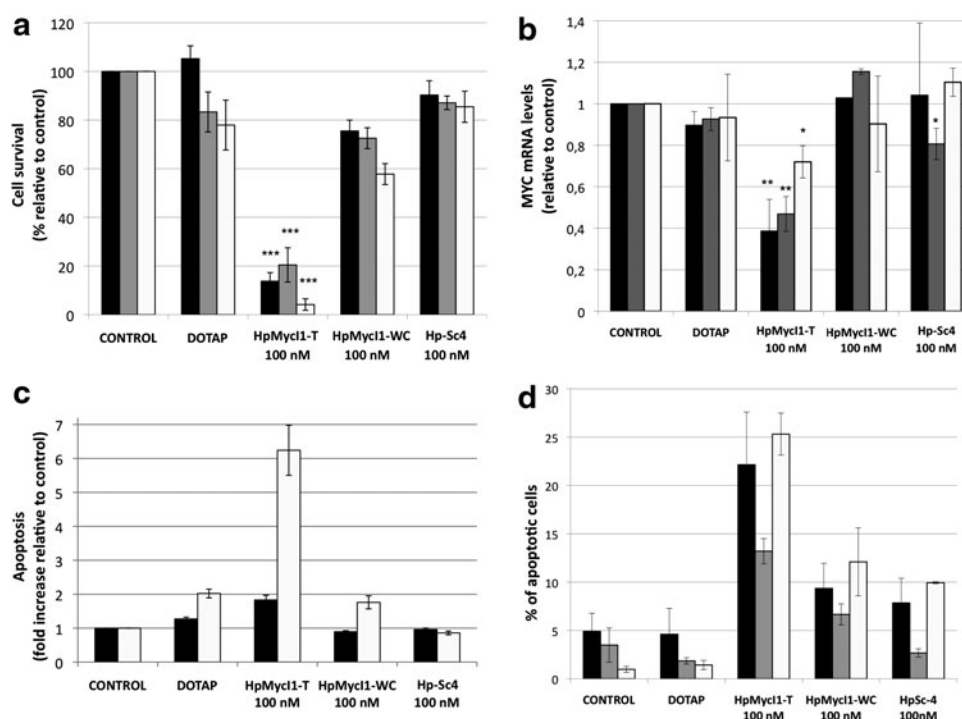


FIG. 7. Effect of HpMycI1-T on cell viability, MYC mRNA levels, and apoptosis. **(a)** SKBR3 (■, black bars), MCF7 (■, gray), and MDA-MB-468 (□, white) cells (30,000) were plated in six-well dishes and transfected with HpMycI1-T or the negative controls HpMycI1-WC and Hp-Sc4 at 100 nM. MTT assays to determine the cell survival were performed 6 days after transfection. **(b)** Total RNA was extracted from SKBR3, MCF7, and MDA-MB-468 cells (30,000) 48 h after the transfection with 100 nM of either HpMycI1-T or the negative controls HpMycI1-WC and Hp-Sc4. **(c)** Apoptosis in SKBR3 and MDA-MB-468 cells was measured with the Caspase-Glo 3/7 Assay. All results are expressed as change in RLU relative to the control. **(d)** Apoptosis in SKBR3, MCF7, and MDA-MB-468 cells (120,000) determined by the rhodamine method. Rho123-negative and IP-negative cells were considered as apoptotic cells. Data are the mean \pm SE values of at least three experiments. * $P < 0.05$, ** $P < 0.01$, *** $P < 0.005$, compared with control.

increase in apoptosis. It is interesting to note that the triple-negative cell line MDA-MB-468 was affected in greater measure by the inhibition of MYC, despite maintaining relatively high MYC mRNA levels, compared to the other cell lines. On the other hand, HER2⁺ cells (SKBR3) showed a substantial decrease in cell survival, in line with the observed decrease on mRNA levels and increase in apoptosis. These results are in agreement with Kang and collaborators [30], who found that HER2⁺ cell proliferation is dependent on MYC function. Finally, MCF7 cells also showed decreased survival and decreased MYC mRNA levels. It is possible that for each cell line, there is a specific threshold level of MYC required to maintain cell proliferation [29,31]. These results show that PPRHs could represent a valid alternative for nondruggable targets.

Taking these results into account, PPRHs could be included in the group of oligonucleotides with therapeutic potential, together with the triplex forming oligonucleotides (TFOs), aODNs, and siRNAs. All of them have in common the silencing of gene expression. It is important to note that although PPRHs share with TFOs the formation of triplex structures, there are differences in their binding properties; while the TFOs bind to the double-stranded DNA by Hoogsteen bonds, PPRHs bind intramolecularly by reverse Hoogsteen bonds and to the double-stranded DNA by Watson and Crick bonds. Previously, we studied the differences of both

PPRHs and TFOs [32] and determined two important features: (1) PPRHs have a higher binding affinity to the dsDNA target and (2) PPRHs have a higher biological activity than TFOs. Therefore, for the purpose of inhibiting gene expression, we showed that PPRHs offer advantages over TFOs. Moreover, previous results [6] indicate that PPRHs, while working at a similar range of concentrations [7], have advantages over siRNAs in terms of stability, lack of immunogenicity, and economy and no off-target effects were found for PPRHs [8,9]. Another silencing approach is based on pyrrole-imidazole polyamides, oligomers that bind to the minor groove of the DNA targeting short sequences of DNA of around 6 bp [33,34]. In comparison, PPRHs cover a 19–25 nucleotide region, which would confer a greater specificity.

Regarding the potential target sites for PPRHs, triplex target sites are generally found in regulatory regions, specifically in promoters, introns, and to a lesser extent in exons. It has been described that these regions are overrepresented in promoters, although they are not necessarily the binding sites for transcription factors [35], PPRHs not only bind to transcription factors binding sites but also other regions in the promoter and within both intronic and exonic sequences. Moreover, PPRHs have the ability to bind to transcribed mRNA.

Other approaches are protein based with different degrees of complexity; these include ZFN, TALENs, and CRISPR-Cas9, and their initial goal was the editing of the genome. Their

mechanism of action is based on the introduction of double-strand breaks and its subsequent repair through homology-directed repair or nonhomologous end joining, where the latter can cause unwanted insertions or deletions [36]. Even if these methods are considered very robust platforms for genome editing, they present several drawbacks, including potential off-target DNA cleavage and unwanted cytotoxic activity [37], which are labor- and time-consuming [38,39], and they face the additional complications linked to viral gene therapy [40].

Another concern for these strategies could be the immune response triggered by the peptides from editing nucleases or by the large amounts of virus necessary for the *in vivo* delivery. In contrast, PPRHs are easy to design and to synthesize, since they are just like a regular unmodified oligonucleotide of about 50 bases and can be directly used without further manipulation, avoiding engineering issues. PPRHs can be labeled in their primary synthesis with fluorophores or biotin and can also be fused to targeting or delivering agents, such as aptamers and antibodies. Moreover, several PPRH-binding sites can be found per targeted gene allowing for combination therapy. Finally, PPRHs can bind not only to DNA but also to RNA.

We have previously studied the *in vivo* efficiency of the PPRHs [9] using a subcutaneous xenograft tumor model of prostate cancer. Using two different types of administration, intratumoral and intravenous, a PPRH against survivin promoter (HpsPr-C) was able to delay the tumor growth, without affecting mice weight. We determined the decrease in the levels of survivin and a lower degree of blood vessel formation. Altogether, PPRHs constitute an innovative and promising technology in the area of gene silencing.

Conclusions

The results presented in this work confirm that the PPRH technology is broadly useful to silence the expression of genes with a special emphasis in genes related to cancer. Regardless of the gene or cell line tested, PPRHs were able to decrease cell survival, mRNA expression levels, and apoptosis to a greater or lesser extent. Thus, we have extended the number of PPRHs used in cancer therapy, now spanning metabolism (DHFR [7]), proliferation (mTOR), DNA-topology (TOP1), lifespan and senescence (Telomerase [7]), apoptosis (Survivin [9], BCL2), transcription factors (MYC), and proto-oncogenes (MDM2).

Acknowledgments

This work was supported by grant SAF2011-23582 and SAF2014-51843 from Plan Nacional de Investigación Científica (Spain). Our group holds the Quality Mention from the Generalitat de Catalunya 2014SGR96. X.V. is the recipient of an APIF fellowship from the University of Barcelona. L.R. and A.S. are the recipients of a fellowship Formació d'Investigadors (FI) from the Generalitat de Catalunya.

Author Disclosure Statement

No competing financial interests exist.

References

1. Beerli RR, DJ Segal, B Dreier and CF Barbas, 3rd. (1998). Toward controlling gene expression at will: specific regulation of the *erbB-2/HER-2* promoter by using polydactyl zinc finger proteins constructed from modular building blocks. *Proc Natl Acad Sci U S A* 95:14628–14633.
2. Christian M, T Cermak, EL Doyle, C Schmidt, F Zhang, A Hummel, AJ Bogdanove and DF Voytas. (2010). Targeting DNA double-strand breaks with TAL effector nucleases. *Genetics* 186:757–761.
3. Mali P, L Yang, KM Esvelt, J Aach, M Guell, JE DiCarlo, JE Norville and GM Church. (2013). RNA-guided human genome engineering via Cas9. *Science* 339:823–826.
4. Wiedenheft B, SH Sternberg and JA Doudna. (2012). RNA-guided genetic silencing systems in bacteria and archaea. *Nature* 482:331–338.
5. Gaj T, CA Gersbach and CF Barbas, 3rd. (2013). ZFN, TALEN, and CRISPR/Cas-based methods for genome engineering. *Trends Biotechnol* 31:397–405.
6. Villalobos X, L Rodriguez, J Prevot, C Oleaga, CJ Ciudad and V Noe. (2013). Stability and immunogenicity properties of the gene-silencing polypurine reverse Hoogsteen hairpins. *Mol Pharm* 11:254–264.
7. de Almagro MC SC, V Noé and CJ Ciudad. (2009). Polypurine hairpins directed against the template strand of DNA knock down the expression of mammalian genes. *J Biol Chem* 284:11.
8. de Almagro MC, N Mencia, V Noe and CJ Ciudad. (2011). Coding polypurine hairpins cause target-induced cell death in breast cancer cells. *Hum Gene Ther* 22:451–463.
9. Rodriguez L, X Villalobos, S Dakhel, L Padilla, R Hervas, JL Hernandez, CJ Ciudad and V Noe. (2013). Polypurine reverse Hoogsteen hairpins as a gene therapy tool against survivin in human prostate cancer PC3 cells *in vitro* and *in vivo*. *Biochem Pharmacol* 86:1541–1554.
10. Alitalo K, G Ramsay, JM Bishop, SO Pfeifer, WW Colby and AD Levinson. (1983). Identification of nuclear proteins encoded by viral and cellular *myc* oncogenes. *Nature* 306:274–277.
11. Haines DS. (1997). The *mdm2* proto-oncogene. *Leuk Lymphoma* 26:227–238.
12. Hall C, SM Troutman, DK Price, WD Figg and MH Kang. (2013). Bcl-2 family of proteins as therapeutic targets in genitourinary neoplasms. *Clin Genitourin Cancer* 11:10–19.
13. Meyer N and LZ Penn. (2008). Reflecting on 25 years with MYC. *Nat Rev Cancer* 8:976–990.
14. Oliner JD, KW Kinzler, PS Meltzer, DL George and B Vogelstein. (1992). Amplification of a gene encoding a p53-associated protein in human sarcomas. *Nature* 358:80–83.
15. Samuels Y, Z Wang, A Bardelli, N Silliman, J Ptak, S Szabo, H Yan, A Gazdar, SM Powell, *et al.* (2004). High frequency of mutations of the *PIK3CA* gene in human cancers. *Science* 304:554.
16. Tsujimoto Y, J Cossman, E Jaffe and CM Croce. (1985). Involvement of the *bcl-2* gene in human follicular lymphoma. *Science* 228:1440–1443.
17. Azmi AS, Z Wang, PA Philip, RM Mohammad and FH Sarkar. (2011). Emerging Bcl-2 inhibitors for the treatment of cancer. *Expert Opin Emerg Drugs* 30:10.
18. Bold RJ, J Chandra and DJ McConkey. (1999). Gemcitabine-induced programmed cell death (apoptosis) of human pancreatic carcinoma is determined by Bcl-2 content. *Ann Surg Oncol* 6:279–285.
19. Zhang X, CG Koh, B Yu, S Liu, L Piao, G Marcucci, RJ Lee and LJ Lee. (2009). Transferrin receptor targeted lipopolyplexes for delivery of antisense oligonucleotide

- g3139 in a murine k562 xenograft model. *Pharm Res* 26:1516–1524.
20. Giovannella BC, JS Stehlin, ME Wall, MC Wani, AW Nicholas, LF Liu, R Silber and M Potmesil. (1989). DNA topoisomerase I—targeted chemotherapy of human colon cancer in xenografts. *Science* 246:1046–1048.
 21. Goldwasser F, T Shimizu, J Jackman, Y Hoki, PM O'Connor, KW Kohn and Y Pommier. (1996). Correlations between S and G2 arrest and the cytotoxicity of camptothecin in human colon carcinoma cells. *Cancer Res* 56:4430–4437.
 22. Mross K, H Richly, N Schleucher, S Korfee, M Tewes, ME Scheulen, S Seeber, T Beinert, M Schweigert, *et al.* (2004). A phase I clinical and pharmacokinetic study of the camptothecin glycoconjugate, BAY 38–3441, as a daily infusion in patients with advanced solid tumors. *Ann Oncol* 15:1284–1294.
 23. Mita MM, A Mita and EK Rowinsky. (2003). Mammalian target of rapamycin: a new molecular target for breast cancer. *Clin Breast Cancer* 4:126–137.
 24. Tokunaga E, E Oki, A Egashira, N Sadanaga, M Morita, Y Kakeji and Y Maehara. (2008). Deregulation of the Akt pathway in human cancer. *Curr Cancer Drug Targets* 8:27–36.
 25. Vogelstein B, D Lane and AJ Levine. (2000). Surfing the p53 network. *Nature* 408:307–310.
 26. Lane DP, CF Cheok and S Lain. (2010). p53-based cancer therapy. *Cold Spring Harb Perspect Biol* 2:a001222.
 27. Vassilev LT, BT Vu, B Graves, D Carvajal, F Podlaski, Z Filipovic, N Kong, U Kammlott, C Lukacs, *et al.* (2004). In vivo activation of the p53 pathway by small-molecule antagonists of MDM2. *Science* 303:844–848.
 28. Wang H, L Nan, D Yu, S Agrawal and R Zhang. (2001). Antisense anti-MDM2 oligonucleotides as a novel therapeutic approach to human breast cancer: in vitro and in vivo activities and mechanisms. *Clin Cancer Res* 7:3613–3624.
 29. Li Y, SC Casey and DW Felsher. (2014). Inactivation of MYC reverses tumorigenesis. *J Intern Med* 276:52–60.
 30. Kang J, CM Sergio, RL Sutherland and EA Musgrove. (2014). Targeting cyclin-dependent kinase 1 (CDK1) but not CDK4/6 or CDK2 is selectively lethal to MYC-dependent human breast cancer cells. *BMC Cancer* 14:32.
 31. Shachaf CM, AJ Gentles, S Elchuri, D Sahoo, Y Soen, O Sharpe, OD Perez, M Chang, D Mitchel, *et al.* (2008). Genomic and proteomic analysis reveals a threshold level of MYC required for tumor maintenance. *Cancer Res* 68:5132–5142.
 32. Rodriguez L, X Villalobos, A Sole, C Lliberos, CJ Ciudad and V Noe. (2015). Improved design of PPRHs for gene silencing. *Mol Pharm* 12:867–877.
 33. Matsuda H, N Fukuda, T Ueno, Y Tahira, H Ayame, W Zhang, T Bando, H Sugiyama, S Saito, *et al.* (2006). Development of gene silencing pyrrole-imidazole polyamide targeting the TGF-beta1 promoter for treatment of progressive renal diseases. *J Am Soc Nephrol* 17:422–432.
 34. Yang F, NG Nickols, BC Li, GK Marinov, JW Said and PB Dervan. (2013). Antitumor activity of a pyrrole-imidazole polyamide. *Proc Natl Acad Sci U S A* 110:1863–1868.
 35. Goni JR, JM Vaquerizas, J Dopazo and M Orozco. (2006). Exploring the reasons for the large density of triplex-forming oligonucleotide target sequences in the human regulatory regions. *BMC Genomics* 7:63.
 36. Lin Y, TJ Cradick, MT Brown, H Deshmukh, P Ranjan, N Sarode, BM Wile, PM Vertino, FJ Stewart and G Bao. (2014). CRISPR/Cas9 systems have off-target activity with insertions or deletions between target DNA and guide RNA sequences. *Nucleic Acids Res* 42:7473–7485.
 37. Fu Y, JA Foden, C Khayter, ML Maeder, D Reyon, JK Joung and JD Sander. (2013). High-frequency off-target mutagenesis induced by CRISPR-Cas nucleases in human cells. *Nat Biotechnol* 31:822–826.
 38. Mussolino C, R Morbitzer, F Lutge, N Dannemann, T Lahaye and T Cathomen. (2011). A novel TALE nuclease scaffold enables high genome editing activity in combination with low toxicity. *Nucleic Acids Res* 39:9283–9293.
 39. Wijshake T, DJ Baker and B van de Sluis. (2014). Endonucleases: new tools to edit the mouse genome. *Biochim Biophys Acta* 1842:1942–1950.
 40. Cox DB, RJ Platt and F Zhang. (2015). Therapeutic genome editing: prospects and challenges. *Nat Med* 21:121–131.

Address correspondence to:
 Carlos J. Ciudad, PhD
 Department of Biochemistry and Molecular Biology
 School of Pharmacy
 University of Barcelona
 Av. Diagonal 643
 Barcelona E-08028
 Spain

E-mail: cciudad@ub.edu

Received for publication January 2, 2015; accepted after revision May 1, 2015.